ISSN 0021-9673

VOL. 410 NO. 2 DECEMBER 11, 1987

THIS ISSUE COMPLETES VOL. 410

JOURNAL OF CHROMATOGRAPHY

INTERNATIONAL JOURNAL ON CHROMATOGRAPHY, ELECTROPHORESIS AND RELATED METHODS

ELSEVIER

JOURNAL OF CHROMATOGRAPHY

Scope. The *Journal of Chromatography* publishes papers on all aspects of chromatography, electrophoresis and related methods. Contributions consist mainly of research papers dealing with chromatographic theory, instrumental development and their applications. The section *Biomedical Applications,* which is under separate editorship, deals with the following aspects: developments in and applications of chromatographic and electrophoretic techniques related to clinical diagnosis or alterations during medical treatment; screening and profiling of body fluids or tissues with special reference to metabolic disorders; results from basic medical research with direct consequences in clinical practice; drug level monitoring and pharmacokinetic studies; clinical toxicology; analytical studies in occupational medicine.

Submission of Papers. Papers in English, French and German may be submitted, in three copies. Manuscripts should be submitted to: The Editor of *Journal of Chromatography,* P.O. Box 681, 1000 AR Amsterdam, The Netherlands, or to: The Editor of *Journal of Chromatography, Biomedical Applications,* P.O. Box 681, 1000 AR Amsterdam, The Netherlands. Review articles are invited or proposed by letter to the Editors. An outline of the proposed review should first be forwarded to the Editors for preliminary discussion prior to preparation. Submission of an article is understood to imply that the article is original and unpublished and is not being considered for publication elsewhere. For copyright regulations, see below.

Subscription Orders. Subscription orders should be sent to: Elsevier Science Publishers B.V., P.O. Box 211, 1000 AE Amsterdam, The Netherlands, Tel. 5803 911, Telex 18582 ESPA NL. The *Journal of Chromatography* and the *Biomedical Applications* section can be subscribed to separately.

Publication. The *Journal of Chromatography* (incl. *Biomedical Applications* and *Cumulative Author and Subject Indexes, Vols. 351–400*) has 40 volumes in 1987. The subscription prices for 1987 are:

J. Chromatogr. (incl. *Cum. Indexes, Vols. 351–400*) + *Biomed. Appl.* (Vols. 384–423):
Dfl. 6400.00 plus Dfl. 1000.00 (p.p.h.) (total *ca.* US$ 3609.75)

J. Chromatogr. (incl. *Cum. Indexes, Vols. 351–400*) only (Vols. 384–412):
Dfl. 5365.00 plus Dfl. 725.00 (p.p.h.) (total *ca.* US$ 2970.75)

Biomed. Appl. only (Vols. 413–423):
Dfl. 2035.00 plus Dfl. 275.00 (p.p.h.) (total *ca.* US$ 1126.75).

Our p.p.h. (postage, package and handling) charge includes surface delivery of all issues, except to subscribers in Argentina, Australia, Brasil, Canada, China, Hong Kong, India, Israel, Malaysia, Mexico, New Zealand, Pakistan, Singapore, South Africa, South Korea, Taiwan, Thailand and the U.S.A. who receive all issues by air delivery (S.A.L. — Surface Air Lifted) at no extra cost. For Japan, air delivery requires 50% additional charge; for all other countries airmail and S.A.L. charges are available upon request. Back volumes of the *Journal of Chromatography* (Vols. 1 through 383) are available at Dfl. 248.00 (plus postage). Claims for missing issues will be honoured, free of charge, within three months after publication of the issue. Customers in the U.S.A. and Canada wishing information on this and other Elsevier journals, please contact Journal Information Center, Elsevier Science Publishing Co. Inc., 52 Vanderbilt Avenue, New York, NY 10017. Tel. (212) 916-1250.

Abstracts/Contents Lists published in Analytical Abstracts, ASCA, Biochemical Abstracts, Biological Abstracts, Chemical Abstracts, Chemical Titles, Current Contents/Physical, Chemical & Earth Sciences, Current Contents/Life Sciences, Deep-Sea Research/Part B: Oceanographic Literature Review, Excerpta Medica, Gas & Liquid Chromatography Abstracts, Index Medicus, Mass Spectrometry Bulletin, PASCAL-CNRS, Referativnyi Zhurnal and Science Citation Index.

See inside back cover for Publication Schedule, Information for Authors and information on Advertisements.

0021-9673/87/$03.50

Printed in The Netherlands

CONTENTS

(Abstracts/Contents Lists published in Analytical Abstracts, ASCA, Biochemical Abstracts, Biological Abstracts, Chemical Abstracts, Chemical Titles, Current Contents/Physical, Chemical & Earth Sciences, Current Contents/Life Sciences, Deep-Sea Research/Part B: Oceanographic Literature Review, Excerpta Medica, Gas & Liquid Chromatography Abstracts, Index Medicus, Mass Spectrometry Bulletin, PASCAL-CNRS, Referativnyi Zhurnal and Science Citation Index)

(Continued overleaf)

Notes

In articles with more than one author, the name of the author to whom correspondence should be addressed is indicated in the article heading by a 6-pointed asterisk (*)

ANABIOTEC '88

2nd INTERNATIONAL SYMPOSIUM ON ANALYTICAL METHODS AND PROBLEMS IN BIOTECHNOLOGY

Noordwijkerhout, The Netherlands, 29–31 March, 1988

FIRST ANNOUNCEMENT AND CALL FOR PAPERS

Organized under the auspices of the Royal Netherlands Chemical Society (KNCV), Section for Analytical Chemistry, and the Netherlands Biotechnological Society (NBV)

ANABIOTEC '88

Analytical methods and systems for biotechnological applications are becoming increasingly important. The development of these methods and systems therefore calls for an interdisciplinary approach.

The use of analytical methods in daily practice in biotechnological research, development and industrial production is coming to be seen as essential for progress in biotechnology in general.

Close cooperation is needed between experts in analytical methodology, system development, and biotechnology.

The purpose of this second ANABIOTEC Symposium is to outline the progress already made through interdisciplinary discussion and cooperation and to deal with the rapid developments taking place.

The Symposium is intended for analytical chemists and both industrial and academic biotechnologists.

Topics

Topics covered will include:

- State-of-the-art analytical techniques already successfully applied in biotechnology.
- Strategies for the selection of analytical procedures with regard to optimum process control in industrial biotechnology, for environmental biotechnology and for fundamental and developmental research.
- Development of new analytical techniques for the above-mentioned areas.

Sessions are planned on: Sampling strategies, biosensors, mass spectrometry in process control, application of computers in analysis and process control, prospects for practical application of new analytical techniques, analytical problems in biotechnology.

The programme will consist of invited plenary lectures, invited and submitted papers (both oral and poster presentations) and discussion sessions.

Organizing Committee

Ir. B. te Nijenhuis
(Gist-brocades N.V.)
Dr. Ir. C. van Dijk
(TNO-Biotechnology)
Ir. W. A. Scheffers
(Delft University of Technology)
Dr. J. Kragten
(University of Amsterdam)

Call for Papers

Participants wishing to present a paper should submit an abstract, in English, of about 250 words before 15 October 1987 to the Symposium Secretariat.

In conjunction with the Symposium, an exhibition of instruments within its scope will be held.

For further information contact:

Symposium Secretariat
ANABIOTEC '88
c/o QLT Convention Services
Keizersgracht 792
1017 EC Amsterdam,
The Netherlands
Telephone: (31-20) 261372
Telefax: (31-20) 259574
Telex: 31578 inter nl attn. qlt

11A029 7381

ELSEVIER THE SCIENCE PUBLISHER
P. O. BOX 211 • 1000 AE AMSTERDAM • THE NETHERLANDS
P. O. BOX 1663 • GRAND CENTRAL STATION • NEW YORK • NY 10163

Journal of Chromatography, 410 (1987) 233–248
Elsevier Science Publishers B.V., Amsterdam — Printed in The Netherlands

CHROM. 19 956

STRUCTURE PARAMETERS OF MOLECULES AND MEDIA EVALUATED BY CHROMATOGRAPHIC PARTITION

II. GEOMETRICAL EXCLUSION IN GELS

HENRIK WALDMANN-MEYER
Fysisk-Kemisk Institut, Technical University of Denmark, DK 2800 Copenhagen-Lyngby (Denmark)
(Received June 22nd, 1987)

SUMMARY

In continuation of the geometrical exclusion model for porous glasses [*J. Chromatogr.*, 350 (1985) 1], a gel model based on cavities approaching conical shape is described. The partition coefficient K emerges as a function of the Stokes' radius R_e, polymer volume fraction, chain and cavity radius. The $K(R_e)$ equations were tested in twelve different gels with proteins, dextrans and Ficoll fractions. The model is self-consistent, *inter alia* since calculated chain radii agree with physical measurements. The correlation between gel parameters appears also to be valid for electrophoresis. Conversely, it is seen that the Ogston model does not apply to gels.

From general theory, R_e is expressed as AM^x where A and x are structure-specific constants. The resulting linearized $K(M)$ plots therefore clearly distinguish between random coils, rods and globular molecules. From such plots the effective bond length, degree of ideality and range of axial ratios are directly determined. Moreover, calibration is set on a non-empirical basis and thus greatly simplified.

INTRODUCTION

In a recent paper[1] we described the dependence of the partition coefficient (K_D) on pore shape and size, as well as on molecular radius and weight, for rod-like and random-coiled molecules in controlled pore glasses. On the basis of a straightforward geometrical exclusion model (GEM) for cylindrical pores, it was shown that the pore radii calculated from the linear $\sqrt{K_D}$ *vs.* molecular Stokes' radius (R_e) correlations were practically identical with the values determined by means of mercury-intrusion porosimetry in eleven different glasses. This fact, together with a re-evaluation of Casassa's results[2], emphasized the unique role of the Stokes' radius and thus confirmed the concept of chromatographic partition as a diffusive quasi-equilibrium process[3]. The partition coefficient therefore reflects not only molecular parameters, but structural features of the chromatographic medium as well.

In the case of gels, a precise evaluation of matrix characteristics and their interplay is evidently more complicated than for porous glasses. Two main theoretical

0021-9673/87/$03.50

approaches have been propounded and tested by means of actual experiments, *viz.* Ogston's equation for the free space available to a sphere in a random network of rigid fibres[4], and Porath's expression for a network chiefly constituted by voids that become narrower with depth and thus can be visualized as conical cavities[5]. An equation formulated by Squire[6] for cavities of mixed shapes could not be corroborated[7].

Ogston's formulation describes partition as a function of the molecular radius, the matrix-polymer concentration, and the chain radius, whereas in the Porath equation K_D varies with R_e and the radius of the conical void. The latter approach has been re-formulated and extensively tested by us[8]. The new GEM equation defines K_D as a function of R_e, cavity radius, polymer concentration and chain radius. In the present paper, the relation between the three matrix parameters, as predicted by the equation, is examined by means of fifteen data sets obtained from the literature and our laboratory. The same data are employed for an evaluation of the Ogston theory.

Special emphasis will be given to partition as a function of the molecular weight. In fact, by replacing R_e in the GEM equation by AM^x, where A and x are structure-specific constants, it is possible not only to distinguish between globular, rod-like and random-coiled molecules, but also to calculate a number of fundamental molecular parameters that so far could only be determined by means of more sophisticated techniques. This is entirely analogous to the GEM theory for porous glasses[1], with the advantage that more precise linearizations will be obtained for most types of gels.

THEORY

Consider a random network of polymer chains in a swollen gel bead. The probability of a parallel chain orientation, giving rise to either cylindrical or lamellar cavities, appears as rather remote, even more so when the presence of entanglements and cross-linkages is taken into account. Likewise, the existence of spherical voids is difficult to envisage. In short, the free spaces will assume highly irregular shapes beyond those regions where chains are physically or chemically connected. According to Flodin[9], because of the restricted chain mobility at the connections it is possible to visualize localized polymer density gradients within the gel, with the density highest around the connecting sites and gradually diminishing with distance from the sites.

In our view, possible local gradients would be subordinate to the fact that filaments of hydrophilic polymers swell anisotropically, in such a way that the degree of swelling is highest at the side facing the solution, whence permeability decreases with the distance from the solution boundary[10,11]. The change of the permeability coefficient with film thickness was ascribed by Ito[12,13] to stresses resulting from differential swelling. When considering a spherical gel bead, therefore, it is probable that the approach to swelling equilibrium is concomitant to an overall density gradient within the bead, with the concentration of loops and thus of chains increasing towards the centre. A balance between internal forces and swelling pressure may contribute to maintain the spherical shape.

These findings lend physical support to Porath's conception of an array of voids, which statistically can be regarded as cones. This is, to a first approximation, equivalent to a gel bead in which the free space available to a permeating molecule decreases with the molecular size, as described below.

The geometrical exclusion model for gels

We define the total bed volume as V_t, equal to the sum of V_i (imbibed solvent), V_m (polymer matrix) and V_0 (excluded solvent). V_e denotes the elution volume. Since the volume of a cone is given by $(\pi/3)hR_x^2$ where h is the height and R_x the radius, we represent V_i by N conical cavities as

$$V_i = (N\pi/3)hR_x^2 \tag{1}$$

Assuming a cylindrical shape for the polymer chain and denoting its diameter as $2r_0$, the gel volume is

$$V_i + V_m = (N\pi/3)(h + r_0/\sin\theta)(R_x + r_0/\cos\theta)^2 \tag{2}$$

where θ stands for one-half of the solid angle subtending the cone, and r_0 is used because the polymer chain is shared by two adjacent cavities.

Consider now a molecule within the gel. Since the smallest molecules will be able to permeate the total gel phase ($V_i + V_m$), the volume available to the centre of mass is equal to the reduced elution volume, *viz*:

$$V_e - V_0 = \left(\frac{N\pi}{3}\right)\left(h + \frac{r_0 - R_e}{\sin\theta}\right)\left(R_x + \frac{r_0 - R_e}{\cos\theta}\right)^2 \tag{3}$$

where R_e is the Stokes' radius of the pertinent molecule. Although from theory Stokes' law does not apply to radii smaller than some 0.5 nm, practice has shown that the limit may lie significantly lower.

Since

$$\tan\theta = \frac{R_x}{h} = \frac{R_x + r_0/\cos\theta}{h + r_0/\sin\theta} = \frac{R_x + r_0/\cos\theta - R_e/\cos\theta}{h + r_0/\sin\theta - R_e/\sin\theta} \tag{4}$$

the sine term of eqn. 3 can be replaced, and by combination with eqn. 1 the expression for the classical partition coefficient is obtained as

$$K_D \equiv \frac{V_e - V_0}{V_i} = \left(\frac{R_x\cos\theta + r_0 - R_e}{R_x\cos\theta}\right)^3 \tag{5}$$

Analogously, the partition coefficient K_{AV} is readily calculated from eqns. 2 and 3, and replacing the sine terms by means of eqn. 4 to

$$K_{AV} \equiv \frac{V_e - V_0}{V_t - V_0} = \frac{V_e - V_0}{V_i + V_m} = \left(1 - \frac{R_e}{R_x\cos\theta + r_0}\right)^3 \tag{6}$$

Taking third roots and defining the ordinate intercept in eqn. 5 as $k \equiv 1 + r_0/R_x\cos\theta$, the linearized expressions become

$$K_D^{1/3} = k - R_e/R_x\cos\theta \tag{7}$$

and

$$K_{AV}^{1/3} = 1 - R_e/(kR_x \cos\theta) \tag{8}$$

It can be seen that since $K_D/K_{AV} = 1 + V_m/V_i$ = constant, both coefficients have the same exclusion limit. The experimental maximum is reached at $R_e = r_0$, as distinct from $R_e = 0$ as generally assumed.

The extrapolated ordinate intercepts are of considerable interest. The fact that K_{AV} extrapolates to unity greatly facilitates the analysis of partition as a function of the molecular weight described below. On the other hand, from the intercept k we derive the fundamental relation between cavity radius and polymer concentration as follows.

Let $R_e = 0$ in eqn. 3, whence eqns. 2 and 3 become equivalent and $V_e - V_0 = V_i + V_m$, such that $K_D = 1 + V_m/V_i$. Hence, the intercept value of eqn. 7 is

$$k \equiv 1 + r_0/(R_x \cos\theta) = (1 + V_m/V_i)^{1/3} = (1 - \varphi)^{-1/3} = (1 - c/d)^{-1/3} \tag{9}$$

where φ is the polymer volume fraction $V_m/(V_i + V_m)$, c the polymer concentration in gram per cm^3 of gel and d the density of the dry polymer. It is readily apparent that for a given chain radius r_0 the cavity radius $R_x \cos\theta$ is obtained directly from $\varphi = c/d$.

Thus, the partition coefficient is defined by three parameters, *viz.* the effective hydrodynamic radius R_e, the polymer volume fraction φ and the chain radius r_0. This means that molecules of identical radius, but different molecular weights or structures, cannot be separated by gel permeation chromatography.

The crucial role of the radius R_e has been theoretically and experimentally substantiated in the previous paper dealing with controlled pore glasses[1]. It is precisely this role that establishes the basis for a quantitative, non-empirical, correlation between chromatographic partition and molecular weight as described in the following.

For any molecule subject to Stokes' law,

$$R_e = AM^x \tag{10}$$

where A and x are well-defined constants that reflect fundamental specific properties of molecular structure. This equation is derived from general physico-chemical theory and has been developed in detail for random-coiled and rod-like molecules in the previous article[1]. Here, it will be extended to prolate ellipsoids which represent the great majority of proteins.

Table I summarizes A and x values for different kinds of molecule. For coils[1], eqn. 10 becomes

$$R_e = A_\theta M^{1/2}\alpha \tag{11}$$

where for large M/M_0 values, $A_\theta = 0.2714\ \beta/M_0^{1/2}$ and β denotes the effective bond length, M_0 the monomer molecular weight, and α is the expansion coefficient equal to 1.00 for ideality.

TABLE I

THE RELATION $R_e = AM^x$ BETWEEN RADIUS AND MOLECULAR WEIGHT

See text. The units of A are cm(mol/g)$^{1/2}$ for coils and cm(mol/g)$^{1/3}$ for rods and ellipsoids.

	$M_{max}/10^3$	$A/10^{-8}$	x
Random coils* (ideal solutions)		$A = A_\theta$	
Dextrans	–	0.2	0.50
Polystyrenes	–	0.179	0.50
Rods*		$A = \mu A_0/p^m$	$x = 1/3+m$
SDS-proteins	70	0.022	0.73
	>250		max. 0.82
Prolate ellipsoids		$A = \bar{\mu}A_0$	$x = 1/3+\bar{m}$
Globular proteins**	100	0.423	0.395
	800	0.478	0.383
	9000	0.551	0.370
Fibrous proteins***	1000	0.654	0.393

* Derived in the previous paper[1].
** Calculated from Felgenhauer's critical compilation of 64 proteins[14]. (Correlation $r \simeq 0.99$).
*** Calculated from Sober[15] for 34 proteins ($r = 0.89$).

For ellipsoids and rods[1], on the other hand,

$$R_e = A_0 M^{1/3} f/f_0 \tag{12}$$

where $A_0 \equiv (3\bar{V}/4\pi N_A)^{1/3}$, which for an average partial specific volume for proteins of $\bar{V} = 0.725$ cm^3/g gives $A_0 = 0.66 \cdot 10^{-8}$.

The frictional coefficient can be correlated with the axial ratio as $f/f_0 = \mu(a/b)^m$, equal to $\mu(M/p)^m$ for homologous rods[1], where (a/b) increases linearly with M. Hence, for such rods, $A = \mu A_0/p^m$ and $x = 1/3 + m$.

In contrast, globular proteins evidently have little or no tendency to become more elongated with the molecular weight. Letting $f/f_0 = \mu(a/b)^m = \bar{\mu}(M)^{\bar{m}}$, by combination with eqn. 12, $A = \bar{\mu}A_0$ and $x = 1/3 + \bar{m}$. In spite of significant variation in $\bar{V}$ and the fact that f/f_0 may reflect both asymmetry and hydration, the overall picture emerging for $M < 10^6$ is

$$f/f_0 \simeq 0.724 \cdot M^{0.05} \text{ (globular proteins)}$$

and

$$f/f_0 \simeq M^{0.06} \text{ (fibrous proteins)}$$

Thus, for any molecule whatsoever eqn. 10 can be combined with eqns. 7 or 8 as

$$K_D^{1/3} = k - M^x A/R_x \cos\theta \tag{13}$$

or

$$K_{AV}^{1/3} = 1 - M^x A/k\ R_x \cos\theta \tag{14}$$

where $x \simeq 0.4$ for proteins in the usual range and $x = 0.5$ for random coils in ideal solutions.

When x is unknown it may be determined[1] from

$$-\ln (k - K_D^{1/3}) = -x \ln M - \ln(A/R_x \cos\theta) \tag{15}$$

or

$$-\ln (1 - K_{AV}^{1/3}) = -x \ln M - \ln(A/k\ R_x \cos\theta) \tag{16}$$

Note however, that precise x and A values will be obtained only when the actual ordinate intercepts from eqns. 7 or 8 are used, since a small difference will be greatly magnified in the logarithmic term by the use of k or 1.00.

The GEM equations will be tested by application to data obtained with twelve different gels in this laboratory and from the literature. Special emphasis will be given to an evaluation of the Ogston model[4] by means of the same data, and to the concentration function of the gel cavity radius.

EXPERIMENTAL

Chromatography was performed on a precision-bore column of 1.60 cm I.D. containing 40–60 cm^3 of gel. The column was thermostated to 20.0°C and effluents were measured with a 2138 Uvicord-S (LKB, Bromma, Sweden) monitor at 206 nm. V_e was obtained from the effluent weight at maximum absorbance and the buffer density. The total volume V_t was calculated from the bed height measured by means of a vernier height gauge, and corrected for dead volume. The excluded volume V_0 was determined with tobacco mosaic virus (TMV), kindly donated by the Institute for Plant Pathology, Danish Research Centre for Plant Protection. In Sephadex experiments, blue dextran (Pharmacia, Uppsala, Sweden) was used. The elution volume of glycine was taken as $(V_i + V_0)$. Unless otherwise mentioned, phosphate buffer (pH 7.00, $I = 0.145$ mol/dm^3) was employed because of its low absorbance at 206 nm.

Samples of 100 mm^3 were used at 1–3% (w/w). Proteins were highest grade products (Sigma) and were used without further treatment. Fluorescein-labelled dextrans 3, 20, 40, 70 and 150, as well as Dextran-500 (Batch Nr. FDR 876) were purchased from Pharmacia.

PARTITION AS FUNCTION OF PORE SIZE AND MOLECULAR STRUCTURE

In order to test the model, we began by analysing fifteen sets of experimental data, six of which are taken from the literature. Since the latter are tabulated as K_{AV} values, eqn. 8 is applied throughout the compilation given in Table II. The analysed substances were proteins and fluorescent dextrans, the radii of which are listed in

TABLE II

PARTITION AS FUNCTION OF RADIUS

N = number of permeants; r = linear correlation coefficient; R_{ex} = abscissa intercept (*cf.* eqn. 17); b = ordinate intercept; c = g polymer per cm³ gel. Densities used in calculating c: agarose, 1.695; Sephacryl, 1.38; Sephadex, 1.64; hyaluronic acid, 1.45 g/cm³.

Gel	*N*	*GEM theory (eqn. 8)*			*Ogston model (eqn. 21)*		*Ref.*
		$-r$	R_{ex}/Å	b	r_0/Å	$c \cdot 10^2$	
Agarose, 2%	4*	0.990	950.50	1.006	26.37	2.90	16
4%	10	0.966	362.73	1.006	22.7	7.28	16
4B-CL	8	0.997	412.60	0.983	54.03	19.65	**
6%	7	0.991	186.34	1.021	23.18	14.92	16
6B	3	1.000	208.66	1.012	16.94	9.37	**
6B-CL	13	1.000	208.88	0.986	39.32	27.52	**
8%	10	0.994	173.92	0.998	26.48	21.00	16
(Agar) 9%	6	0.992	134.88	1.006	17.45	15.10	17
Sephacryl S-200	11	0.999	101.62	0.989	20.58	24.43	**
Sephadex G50-f	5	0.997	44.10	1.077	5.08	11.20	**
G50-f	4	1.000	43.04	1.110	3.88	6.77	**
G100-M	6	1.000	80.15	1.090	6.81	6.33	**
G100-M	10***	0.999	74.38	1.067	7.72	9.30	**
G100-Sf	5	0.998	71.09	1.077	7.54	9.34	**
Hyaluronic acid (CL)	10	0.988	113.61	1.008	8.74	5.44	18

* $K_{AV} < 0.94$ computed.
** This investigation.
*** $I = 0.445$ mol/dm³.

Table III, as well as Ficoll fractions. Radii of the latter, determined by gel permeation chromatography, were taken from Laurent[16].

In Table II, R_{ex} denotes the exclusion radius given by the abscissa intercept in eqns. 7 or 8, *i.e.*:

$$R_{ex} \equiv kR_x \cos\theta = R_x \cos\theta + r_0 \tag{17}$$

and b is the ordinate intersection (eqn. 8).

Table II shows that the linear correlation required by eqn. 8 is satisfied since, in all but one case, $r \geqslant 0.99$. Moreover, for all gels except Sephadex,

$$b = 1.0015 \pm 0.012$$

compared with 1.00 predicted by eqn. 8. The Sephadex anomaly is ascribed to hydration and adsorption effects, and will be treated elsewhere[19].

Molecular weight limits were calculated from the R_e values for $K_{AV} = 0.05$, considered to be the smallest K_{AV} measurable with precision, and the $R_e(M)$ functions given in Table I. The limits are in good agreement with the manufacturer's values. Cross-linking does not affect the exclusion limit of agarose gels, as also noted by

TABLE III

MOLECULAR PARAMETERS OF PROTEINS AND DEXTRANS

	R_e/Å	M
Cytochrome *c*	16.5	12 700
Myoglobin (sperm whale)	18.5	17 800
Soya bean trypsin inhibitor	21.64	21 500
Carbonic anhydrase	23	29 800
Haemoglobin	31	67 400
Serum albumin (bovine)	35.5	66 500
Transferrin (human)	39.1	90 000
Alcohol dehydrogenase (yeast)	45.7	151 000
		$\bar{M}_{S,D}$
FITC–dextran 3	15.74	4 540
dextran 20	31.61	18 500
dextran 40	44.01	35 800
dextran 70	56.46	58 900
dextran 150	81.81	123 800
Dextran 500	106	209 900

Hjertén[20], whereas an increase of ionic strength lowers the limiting value of Sephadex 100-M. This effect is the subject of a separate study[19].

The well-known fact that the smaller Sephadex 100-Sf beads yield lower limits than larger beads (100-M) supports our concept of an overall swelling gradient, since for the same gel a decrease in size leads to a steeper gradient and thus to a lower exclusion limit. The swelling gradient is most probably also the reason why the irregular gel particles, used in the early 1960s, were replaced by beads to obtain better separations.

The experimental data obtained in this laboratory, summarized in Table II, are plotted as K_D functions (eqns. 7, 13, 15) in Figs. 1–4. K_D was employed because its determination does not require measurements of dead volume, solvent density and total volume, whereas V_i is easily obtained at low wavelengths.

Fig. 1 illustrates the basic conclusion of the GEM theory, *i.e.* the fact that all molecules give the same straight line when their $K_D^{1/3}$ values are plotted against R_e. The slope and intercepts of the line are functions of gel concentration and pore size only. The same is of course true for $K_{AV}^{1/3}$ *vs.* R_e, since $K_D/K_{AV} = k^3$ (*cf.* eqn. 9). R_{ex} and r values are therefore identical. Thus, the ordinate intercept of eqn. 7 plots is $b' = bk$, where b is given in Table II. Further correlations of this kind have previously been described[8].

In Figs. 2–3 the same data are plotted according to eqn. 13. The numerical results appear in Table IV. In all but one gel, $r \geqslant 0.99$. The $\bar{\mu}A_0$ average of 0.43 ($\pm$ 0.03) $\cdot$ 10^{-8} (proteins) is in excellent agreement with the value in Table I for this molecular weight range. For dextrans, from Fig. 3, $\langle A_\theta \rangle \simeq 0.229 \cdot 10^{-8}$ which, by eqn. 11 and M_0 162.2, results in an effective bond length β of 10.7 Å. This is *ca.* 1 Å higher than calculated from chromatography in controlled-pore glasses[1] and within the range of 8.2–11.2 Å estimated from Granath's data[21].

When the material is analysed as in Fig. 4 (eqn. 15), it is seen from Table IV

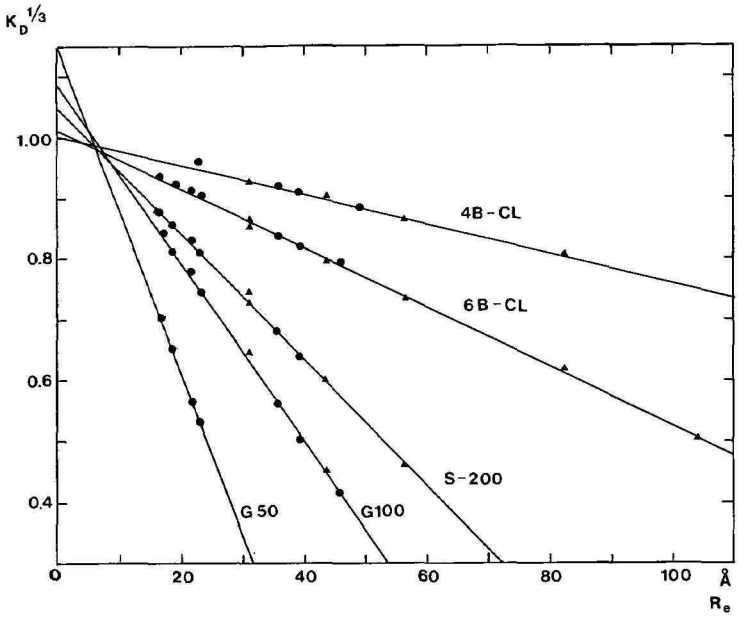

Fig. 1. Partition as function of Stokes' radius in five gels according to GEM eqn. 7. (●) Proteins; (▲) dextrans. Exclusion radii and correlation coefficients as given in Table II.

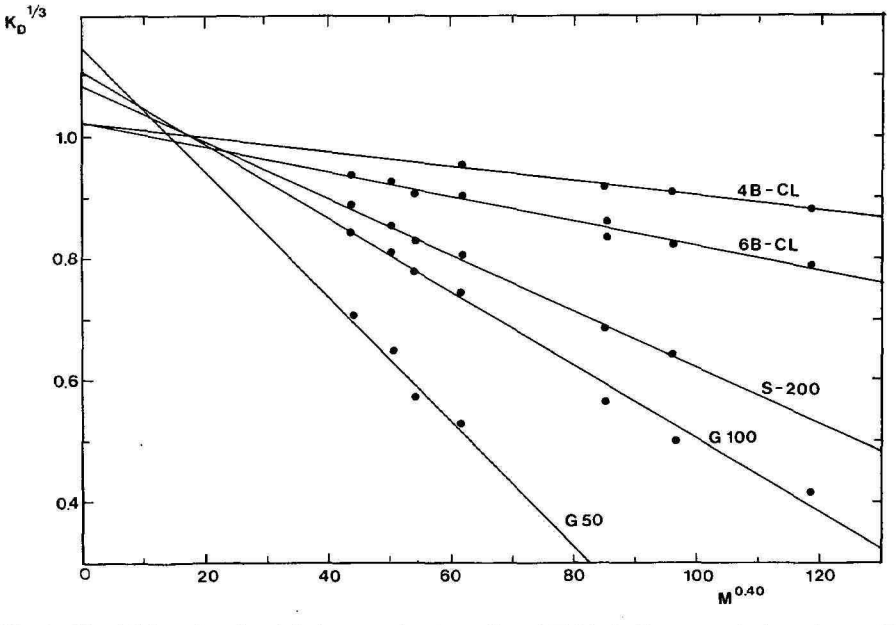

Fig. 2. The M^x function for globular proteins (eqn. 13 and Table I). For numerical results, see Table IV.

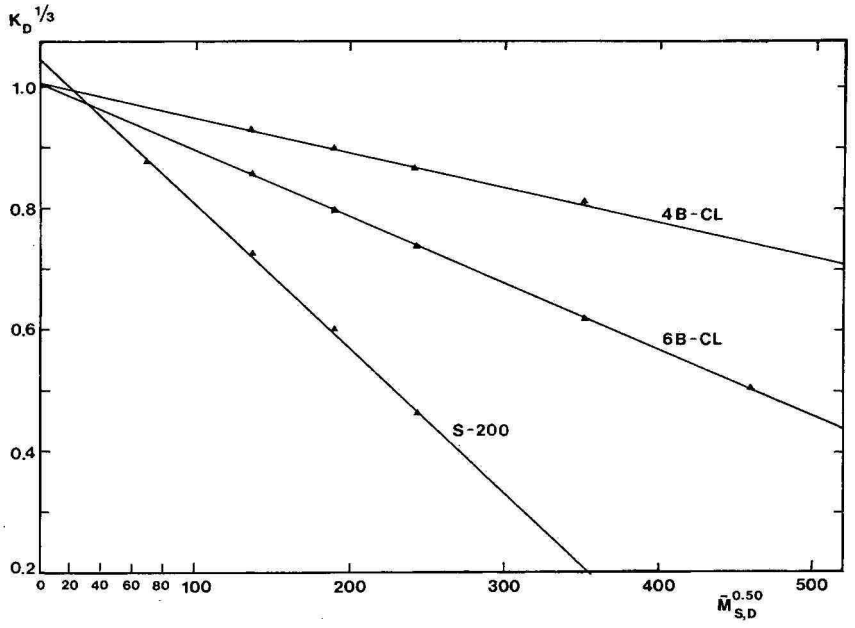

Fig. 3. Random-coiled dextrans in ideal solution (eqn. 13 and Table I). The results are given in Table IV.

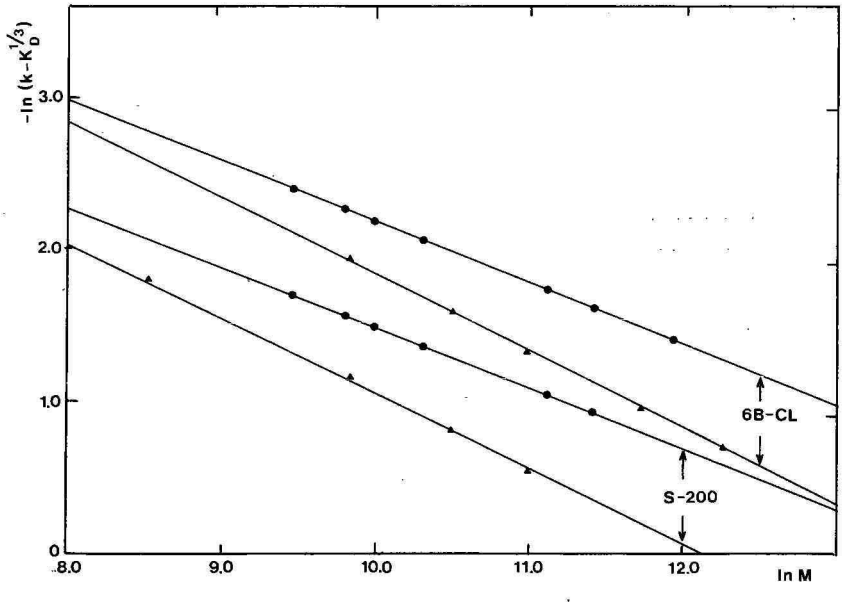

Fig. 4. The double logarithmic GEM plot (eqn. 15) for proteins (●) and dextrans (▲) in two gels. $M = \bar{M}_{S,D}$ for dextrans as required. The resulting molecular parameters x and A appear in Table IV.

TABLE IV

PARTITION AS FUNCTION OF MOLECULAR WEIGHT

$\bar{\mu}A_0$ values are given in cm(mol/g)$^{1/3}$ and A_θ in cm(mol/g)$^{1/2}$

Eqn.	*Fig.*	*Gel*	$-r$	*Intercept*	*|Slope|*	$\bar{\mu}A_0 \cdot 10^9$
Proteins						
13	2	4B-Cl	0.991	1.0226	$1.1899 \cdot 10^{-3}$	4.888
		6B-Cl	0.987	1.0217	$2.0009 \cdot 10^{-3}$	4.128
		S-200	0.997	1.084	$4.6288 \cdot 10^{-3}$	4.480
		G-100M	0.994	1.1109	$6.1273 \cdot 10^{-3}$	4.197
		G-50f	0.967	1.147	$10.1709 \cdot 10^{-3}$	3.831
15	4	6B-Cl	0.993	6.1656	0.3997	4.333
		S-200	0.979	5.4301	0.3951	4.242
Dextrans						$A_\theta \cdot 10^9$
13	3	4B-Cl	0.996	1.0051	$0.5673 \cdot 10^{-3}$	2.331
		6B-Cl	1.000	1.0034	$1.0878 \cdot 10^{-3}$	2.244
		S-200	0.999	1.0455	$2.3740 \cdot 10^{-3}$	2.298
15	4	6B-Cl	1.000	6.8669	0.5038	2.149
		S-200	0.999	5.9143	0.4874	2.614

that $\langle \bar{\mu}A_0^* \rangle$ remains unchanged, whereas $\langle A_\theta \rangle$ shows a slight increase. The fundamental feature, however, is the precision with which the structure-specific slope can be determined. In fact, the average slope is 0.397 for proteins, which is identical with the value for low-molecular-weight specimens in Table I, and 0.496 for dextrans as compared with 0.500. In contrast to the intercepts, slopes are independent of the gel, as required by eqn. 15.

This type of linear correlation may prove to be extremely useful inasmuch as different hydrodynamic structures can readily be distinguished. While prolate proteins in, for example, Sephadex 6B-CL give $f(K_D) \simeq 6.17 - 0.4 \ln M$ (*cf.* Table IV), the same light proteins would yield $f(K_D) \simeq 9.16 - 0.73 \ln M$ when brought into rod-like form by denaturation since, as previously derived[1], A changes to $0.0218 \cdot 10^{-8}$ and x to 0.73. Analogously, if random coils such as dextrans were analysed under non-ideal conditions, both the slope and the intercept would increase[1].

The consequences for calibration of gel media will be discussed in the last section.

PORE SIZE AS FUNCTION OF POLYMER CONCENTRATION AND CHAIN RADIUS

We have previously shown that in porous glasses the chromatographically determined R_x values are practically identical with the pore radii measured by means of mercury-intrusion porosimetry[1]. No such test is feasible in gels. However, the GEM theory predicts a stringent relation between R_x and the polymer concentration. This relation is given by eqn. 9, which in the limit $\varphi = c/d = 0$ gives $k = 1$ and $R_x \cos\theta \to \infty$, while for $c = d$, $k \to \infty$ and $R_x \cos\theta = 0$. By combination with eqn. 7, for all molecules $K_D = 1$ or zero, respectively, as expected.

TABLE V

AGAROSE EXCLUSION RADII — ADDITIONAL DATA

% Agarose	R_{ex}/Å	*Determination*	*Ref.*
1.98*	974.9	Electroosmotic migration of unlabelled dextrans	22
2.95*	668	Electroosmotic migration of unlabelled dextrans	22
3.91*	509	Electroosmotic migration of unlabelled dextrans	22
9**	75.7	$M(K_D = 0) \simeq 5.61 \cdot 10^5$ (proteins). Chromatography	20
12**	67.9	$M(K_D = 0) \simeq 4.22 \cdot 10^5$ (proteins). Chromatography	20

* Litex LSL-agarose.

** Beads prepared from Reactifs IBF agarose.

Table II lists R_{ex} values for agarose of different concentrations. Since $R_{ex} \equiv R_x \cos\theta + r_0 = kR_x \cos\theta$ (eqn. 17), and from eqn. 9, $R_x \cos\theta/r_0 = 1/(k - 1)$, it is seen that

$$R_{ex} = r_0[k/(k - 1)] \tag{18}$$

A more tangible expression is obtained by expanding eqn. 9 in various ways and taking the mean as

$$R_{ex} \simeq r_0(3d/c - 1) \tag{19}$$

The error introduced by this approximation is 0.08% for $\varphi = 0.1$ ($\approx$ 17% agarose) and 0.02% for $\varphi = 0.05$. The equation was applied to the seven gels for which $r \geqslant 0.99$ (Table II), together with the results given in Table V.

Fig. 5 depicts R_{ex} *vs.* $1/c$ according to eqn. 19. The linear correlation is surprisingly good in view of the fact that the exclusion radii were determined from both chromatography and electrophoresis and that four different gels are covered, *viz.* beads and compact gels from three sources, and agar particles. Moreover the polymer concentration of Sepharose was taken directly from the rather approximate w/v percentage given by the gel number. On the other hand, the effect of small differences in pH and temperature may be neglected. Also, an ionic strength variation from 0.02 to 0.08 mol/dm^3 does not seem to affect the value of R_{ex} as measured by electrophoresis[22].

As can be seen, R_{ex} becomes zero at $c \simeq 0.17$. Though beads of $c = 0.2$ have been described[20], most types of agarose apparently lose their gel properties in this region. Note that exactly the same concentration limit is obtained by application of eqn. 18. In a recent investigation by two-dimensional electrophoresis[23] the linear R_{ex} *vs.* $1/c$ relationship is substantiated for $c \geqslant 0.013$, whereas $R_{ex} \to 0$ for $c \to \infty$. As also observed from another electrophoretic study[24], at concentrations below 0.01 the slope decreases. Evidently, the geometrical exclusion model is no longer valid at higher dilutions, as the polymer chains become increasingly more mobile. In fact, chromatography can apparently not be carried out in media containing less than 1–2% agarose.

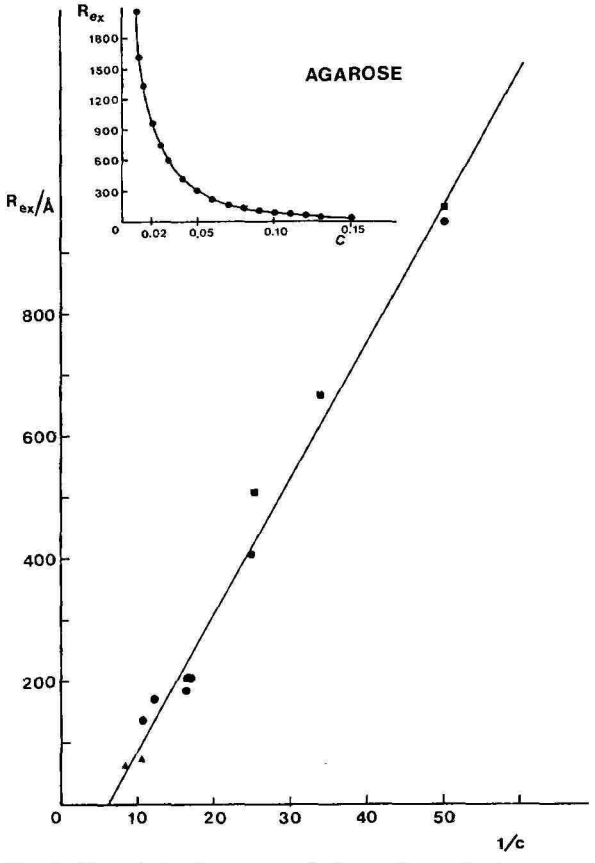

Fig. 5. The relation between exclusion radius and gel concentration as given by eqn. 19. R_{ex} determined by chromatography: ● (Table II) and ▲ (Table V). R_{ex} determined by electrophoresis: ■ (Table V). $R_{ex} = 22.157/c - 132.86$ ($r = 0.9932$), shown in the inset as R_{ex}:c, where c is grams of polymer per cm^3 of gel.

Polymer chain radii and the Ogston model

A fundamental result of eqn. 19 is the size of the chain radius r_0. For the data illustrated in Fig. 5 the slope is 22.157 Å g/cm^3 which for $d = 1.695$ g/cm^3 gives $r_0 = 4.36$ Å. From both physico-chemical measurements and the chemical structure, Hickson and Polson[25] found values of $r_0 \simeq 5.8$ Å, whereas they obtained $\simeq 7.8$ Å from electron microscopy. By X-ray diffraction, optical rotation and molecular building, Arnott *et al.*[26] arrived at a helix diameter of $\simeq 15$ Å (ref. 27) and a cross-section of the intrahelical cavity extending along the axis of $\geqslant 4.5$ Å. It seems therefore reasonable to assign $\simeq 5$ Å to the agarose chain radius.

This value is in sharp contradiction to r_0 calculated from Ogston's model[4] and given in Table II, namely $\langle r_0 \rangle \simeq 24.6 \pm 7.5$ Å for seven agarose gels. The situation is identical for hyaluronic acid, since a chain radius of 8.7 Å is obtained from eqn.

21 (*cf.* Table II), as compared with 3.3 Å given by Ogston and Phelps[29]. According to Ogston

$$K_{AV} = \exp[-\pi L(R_e + r_0)^2] \tag{20}$$

where L is the polymer chain length per cm^3 of gel. For a chain of cylindrical shape, as assumed in his model, the mass/length ratio is $c/L = d\pi r_0^2$. We therefore replace the adjustable parameter πL in eqn. 20 by c/dr_0^2, and obtain the plotting expression

$$(-\ln K_{AV})^{1/2} = (c/d)^{1/2} + (c/d)^{1/2} R_e/r_0 \tag{21}$$

A correlation of the logarithmic term *vs.* R_e should therefore intersect the ordinate at $(c/d)^{1/2}$ and the abscissa at $-r_0$.

Agarose radii of 25 Å were explained by Laurent[16] on ground of strong hydration. However, NMR analysis[28] has proven that the amount of irreversibly bound water does not exceed 3–8 mg/g agarose. Significant hydration would also lead to b values greatly differing from unity[19]. Table II shows that this is not the case with agarose.

Table II shows that agarose concentrations calculated by means of eqn. 21 may be up to four times higher than the real values and bear no relation to them. The same difference is found for cross-linked hyaluronic acid of c 0.0145 when using Ogston and Phelps' d 1.45 (ref. 29). These discrepancies have not been observed before, since eqn. 21 appears in terms of πL throughout the literature. The differences with Sephadex concentrations calculated from solvent regain values are much smaller, although these values appear to be highly overestimated[19]. Also, plots according to eqn. 21 give in all cases linear correlations identical with those obtained from eqns. 7 and 8. On the other hand, the equation does not lead to a reasonable expression of $f(K_{AV})$ as log M. Since the radii of the only gel parameter that can be assessed are incorrect, it is concluded that the Ogston model does not apply to gels.

CONCLUSIONS

It is evident that any expression involving partition coefficients will be strictly valid only in absence of adsorption. In principle, solute adsorption could be a function of the molecular size, affect the excluded or the fully included test substance alone, or be present as a combination thereof. Simulation shows that these effects produce anomalous intercepts in the GEM plots and can therefore be elucidated. The problem will be treated in connection with Sephadex gels[19].

As shown by the relation between gel concentration, exclusion and polymer chain radii, the clearly simplified model from which the theory derives appears to be entirely self-consistent. Partition is a function of molecular size as expressed by the effective hydrodynamic radius R_e, and of cavity shape and size. When R_e is substituted by the frictional factor $f = 6\pi\eta_0 R_e$ obtained from diffusion or sedimentation, all molecules, whatever their structure, still give the same correlation with the partition coefficient. For random coils[1] R_e can be replaced by $R_e/\chi = K([\eta]M)^{1/3}$, as shown by Bénoit *et al.*[30]. When R_e is expressed in terms of molecular weight the linearized $K(M)$ functions make it possible not only to distinguish between different

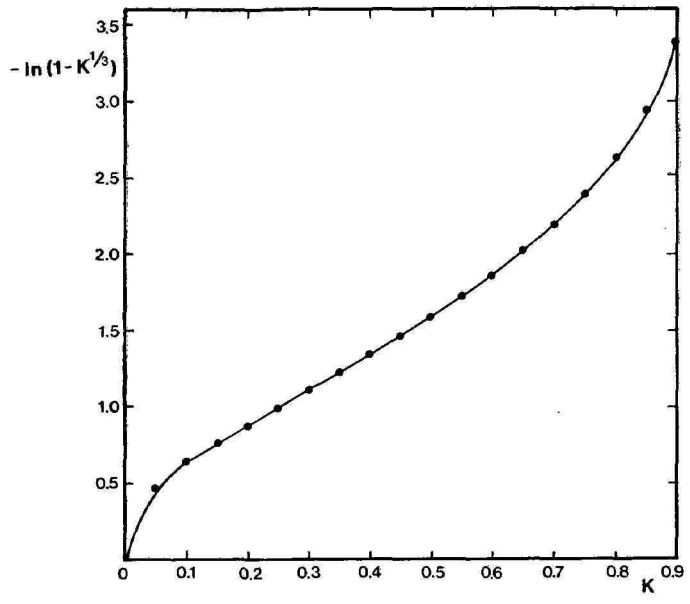

Fig. 6. The sigmoidal curve, known from empirical K *vs.* log M plots, as a result of replacing $-\ln(1 - K^{1/3})$ in eqn. 16 by K.

molecular structures, but also to determine effective bond lengths, radii of gyration, degrees of ideality and approximate axial ratios.

The advantage of linear expressions that contain well-defined physical parameters seems quite considerable. Thus, if the exclusion radius for a given gel has been determined once for all, calibration only requires a minimum of samples and may, in principle, even be unnecessary when the molecular parameters A and x are known, as in the case of globular proteins.

It is revealing that the empirical K *vs.* log M plots derive directly from the double logarithmic equations 15 and 16. This is illustrated in Fig. 6, where the well-known sigmoidal curve, characterized by a long quasi-linear portion, results from a $-\log(1 - K^{1/3})$ *vs.* K correlation. An analogous curve was obtained from $-\log(1 - K^{1/2})$, required for cylindrical pores[1].

In view of the information obtained from the geometrical exclusion model for gels, it appears that separations achieved with non-porous glass spheres[31,32] may be ascribed to a similar process. These and other chromatographic media are being investigated.

ACKNOWLEDGEMENTS

I am indebted to Dr. F. Yssing Hansen for most valuable discussions and to Mrs. H. Birch for her expert technical assistance.

REFERENCES

1 H. Waldmann-Meyer, *J. Chromatogr.*, 350 (1985) 1.
2 E. F. Casassa, *J. Polym. Sci., Part B*, 5 (1967) 773.
3 E. F. Casassa and Y. Tagami, *Macromolecules*, 2 (1969) 14.
4 A. G. Ogston, *Trans. Faraday Soc.*, 54 (1958) 1754.
5 J. Porath, *Pure Appl. Chem.*, 6 (1963) 233.
6 P. G. Squire, *Arch. Biochem. Biophys.*, 107 (1964) 471.
7 L. M. Siegel and K. J. Monty, *Biochim. Biophys. Acta*, 112 (1966) 346.
8 H. Waldmann-Meyer, in R. Epton (Editor), *Chromatography of Synthetic and Biological Polymers*, Vol. 1, Ellis Horwood, Chichester, 1978, Ch. 19, p. 289.
9 P. Flodin, *Dissertation*, Uppsala University, 1962.
10 F. L. Warburton, *Trans. Faraday Soc.*, 42B (1946) 151.
11 J. A. Barrie, in J. Crank and G. S. Park (Editors), *Diffusion in Polymers*, Academic Press, London and New York, 1968, Ch. 8.
12 Y. Ito, *J. Soc. High Polym. Jpn.*, 17 (1960) 397.
13 Y. Ito, *J. Soc. High Polym. Jpn.*, 17 (1960) 489.
14 K. Felgenhauer, *Hoppe-Seyler's Z. Physiol. Chem.*, 355 (1974) 1281.
15 H. A. Sober (Editor), *Handbook of Biochemistry*, CRC Press, Cleveland, OH, 1968.
16 T. C. Laurent, *Biochim. Biophys. Acta*, 136 (1967) 199.
17 P. Andrews, *Biochem. J.*, 91 (1964) 222.
18 T. C. Laurent, *Biochem. J.*, 93 (1964) 106.
19 H. Waldmann-Meyer, in preparation.
20 S. Hjertén and K. O. Eriksson, *Anal. Biochem.*, 137 (1984) 313.
21 K. A. Granath, *J. Colloid Sci.*, 13 (1958) 308.
22 H. Waldmann-Meyer and T. Jacobsen, in M. J. Dunn (Editor), *Electrophoresis '86*, VCH Verlagsges., Weinheim, 1986, p. 259.
23 P. Serwer and S. J. Hayes, *Anal. Biochem.*, 158 (1986) 72.
24 P. G. Righetti, B. C. W. Brost and R. S. Snyder, *J. Biochem. Biophys. Meth.*, 4 (1982) 347.
25 T. G. L. Hickson and A. Polson, *Biochim. Biophys. Acta*, 165 (1968) 43.
26 S. Arnott, A. Fulmer, W. E. Scott, I. C. M. Dea, R. Moorhouse and D. A. Rees, *J. Mol. Biol.*, 90 (1974) 269.
27 A. Amsterdam, Z. Er-El and S. Shaltiel, *Arch. Biochim. Biophys.*, 171 (1975) 673.
28 J. Andrasko, *Biophys. J.*, 15 (1975) 1235.
29 A. G. Ogston and C. F. Phelps, *Biochem. J.*, 78 (1960) 827.
30 H. Bénoit, Z. Grubisic, P. Rempp, D. Decker and J. G. Zilliox, *J. Chim. Phys.*, 63 (1966) 1507.
31 K. O. Pedersen, *Arch. Biochem. Biophys.*, Suppl. 1 (1962) 157.
32 H. Small, *J. Colloid Interface Sci.*, 48 (1974) 147.

Journal of Chromatography, 410 (1987) 249–265
Elsevier Science Publishers B.V., Amsterdam — Printed in The Netherlands

CHROM. 19 966

RETENTION AND SELECTIVITY IN AMINO, CYANO AND DIOL NORMAL BONDED PHASE HIGH-PERFORMANCE LIQUID CHROMATOGRAPHIC COLUMNS

P. L. SMITH* and W. T. COOPER*

Department of Chemistry and Center for Biomedical and Toxicological Research, Florida State University, Tallahassee, FL 32306-3006 (U.S.A.)

(First received June 16th, 1987; revised manuscript received August 17th, 1987)

SUMMARY

Selectivity matrices have been used to characterize the retention of polar solutes in amino-, diol- and cyano-silica normal bonded phase high-performance liquid chromatographic (HPLC) columns. Three solutes and three solvents were chosen to represent the apices of the Snyder selectivity triangle. Mobile phases consisted of binary mixtures of polar solvent modifiers and hexane. The selectivity matrices, derived from the adsorption–displacement model of retention, provide not only a quantitative measure of the impact of localization and secondary solvent effects, but also give insight into the mechanisms responsible for observed behaviour. Detailed discussions of localization phenomena (site-competition and restricted-access delocalization) and secondary solvent effects, both in the mobile and stationary phases, are included for all three bonded phases as are comparisons of the impact of residual silanols on retention. One important result to emerge from these studies is the potential for isocratic, multi-stage HPLC separations when these columns are coupled and used with the appropriate mobile phase.

INTRODUCTION

Although reversed-phase applications currently outnumber those of normal phase, researchers are increasingly recognizing the distinct advantages of normal bonded phase liquid chromatography[1]. Because of the variety of bonded phases now available for normal phase use, the potential for unique separations via multi-stage operation is much greater than for the reversed phase. Also, the number of separations unique to the single stage, normal phase mode are substantial and continually growing. The realization of these potentials is, however, tempered by more complicated and less predictable retention mechanisms. Unlike reversed-phase high-performance liquid chromatography (HPLC), in which retention is determined primarily

* Current address: Chemical and Agricultural Products Division, Abbott Laboratories, 14th Street & Sheridan Drive, North Chicago, IL 60034, U.S.A.

0021-9673/87/$03.50

by solvophobic interactions, solute–solvent, solute–stationary phase and solvent–stationary phase interactions must be considered[2,3]. Any predictive model of retention must therefore consider all of these effects together.

We have demonstrated in a previous paper[4] that single-valued solvent strengths do not sufficiently describe the retention of polar probes in a cyano column. It is the combined effects of stationary and mobile phase selectivities on solute retention which must be considered. A selectivity matrix based on the Snyder adsorption–displacement model which accounts for both localization of solutes and solvents and secondary effects in either the adsorbed or bulk phases has been proposed. This matrix not only provides information regarding the relative retention of specially chosen probes, but also gives insight into the retention mechanism responsible for observed behaviour. In the present study, matrices have been generated for amino and diol bonded phases and compared with the previously determined cyano matrix.

Various characterizations of the amino phase have been published, as well as a large number of applications[5–9]. Majors[7] has compiled a wide variety of applications for both the cyano and amino phases. On the other hand, characterizations and applications of the diol phase are very rare at this time. We expect, however, that as multi-stage chromatography becomes more popular, this phase will find much more widespread use, since it is uniquely different from either the cyano or amino phases. Also, by virtue of the fact that the diol phase has not been well characterized, it has not been brought to the forefront of bonded phases commonly used in single-stage separations. This phase has been used primarily as a high-performance size-exclusion packing[10], although Huber *et al.*[11] have used a multi-stage coupling of a diol and cyano column to separate a herbicide and its metabolite from a complex matrix.

The three solutes and solvents used to generate each selectivity matrix were chosen from different apices of the selectivity triangle, where each apex represents a solute or solvent whose primary interaction is either dipolar, proton accepting or proton donating. By choosing solutes and solvents in this fashion, the retention information from each solute–solvent pair (nine pairs per matrix; one stationary phase per matrix) is unique. This approach allows coverage of a large experimental space while keeping the interpretation of non-unique combinations to a minimum. In this way, important retention mechanisms and effects are readily identified and should provide insight for the practicing chromatographer who wishes to design a more complex separation.

The present discussions will include comparisons of selectivity and retention mechanisms for cyano-, amino- and diol-silica phases. Also included is a detailed discussion of the impact of secondary solvent effects, various localization phenomena and the role of residual silanols.

THEORY

The Snyder adsorption–displacement model, from which the selectivity matrix is derived, has been discussed in detail elsewhere[2,3,12–14] and thus only a brief review will be presented here. Detailed discussion, when appropriate, will be offered in the Results and discussion section.

The original model was based on the premise that solute and solvent molecules

compete for positions in a monolayer adjacent to the stationary phase. It was assumed that this surface is energetically homogeneous (*i.e.* no solute or solvent localization) and that solute–solvent interactions in the mobile phase were cancelled by corresponding interactions in the adsorbed phase. This model led to an expression that related changes in the retention of a solute to a change in mobile phase composition:

$$\log(k'_2/k'_1) = \alpha' A_s(\varepsilon_1 - \varepsilon_2) \quad (1)$$

where the k's represent capacity factors, A_s the calculated cross-sectional area of the solute, α' the adsorbent activity coefficient (defined as one in this study), and the ε's the solvent strengths of the two mobile phases.

It has been observed in practice that retention typically violates one or both of the two underlying assumptions of the model; stationary phases are energetically not homogeneous and solute–solvent interactions often do not cancel. The model and eqn. 1 were therefore modified to account for these effects by using increased values of A_s and adding secondary solvent terms:

$$\log(k'_2/k'_1) = \alpha' A_s(\varepsilon_1 - \varepsilon_2) + (\Delta_2 - \Delta_1) \quad (2)$$

The secondary solvent terms, Δ_1 and Δ_2, are necessary because, as solutes and solvents increase in polarity, their interactions with one another become stronger and more specific. The likelihood that such interactions will be the same in both the mobile and stationary phases diminishes greatly in such cases. It is the dissimilarity of such interactions which often account for large and useful changes in the selectivity of a given system.

Increased values of A_s are necessary not only to account for solute localization, but site-competition delocalization as well[5,15]. This important phenomenon occurs when polar solvent molecules are able to interact laterally with an adsorption site on which solute molecules are localized. This disturbance of localization is manifested as an apparent increase in the value of the cross-sectional area, A_s, but is in reality due to an underestimation of the solvent strength that results from a solvent's ability to interact laterally with an adsorption site on a surface. This will be discussed in detail later.

Eqn. 2 can be simplified if one of the mobile phases is hexane. In this case, it is assumed that hexane does not induce a secondary solvent effect with any solute (*i.e.* $\Delta_h = 0$), and, being the weakest solvent available, is assigned a solvent strength of 0. Rearrangement yields:

$$\log(k'_2) = -A_s\varepsilon_2 + \log(k'_h + \Delta_2) \quad (3)$$

It is this form of the Snyder equation which is the basis of our studies. When the capacity factors of solutes are plotted against corresponding binary solvent strengths, a slope, A_s, and an intercept, ($\log k'_h + \Delta_2$), are generated, providing the experimenter with quantitative assessments of the impact of localization and secondary solvent effects. Also, because retention data is plotted against solvent strengths, differences in solvent selectivity rather than solvent strength will be apparent.

$$r_{ij} = -(a_{ij} \times \varepsilon_{ij}) + \Delta_{ij}$$

i: (1) phenol, (2) aniline, (3) nitrobenzene

j: (1) chloroform, (2) MTBE, (3) dichloromethane

A. Cyano

$$r_{ij} = -\begin{pmatrix} 2.25 & 6.13 & 2.35 \\ 2.49 & 4.61 & 2.01 \\ 1.18 & 1.64 & 1.58 \end{pmatrix} \times \begin{pmatrix} 0.106 & 0 & 0 \\ 0 & 0.049 & 0 \\ 0 & 0 & 0.120 \end{pmatrix} + \begin{pmatrix} 1.41 & 1.00 & 1.44 \\ 0.93 & 0.97 & 0.75 \\ -0.04 & -0.03 & 0.02 \end{pmatrix} = \begin{pmatrix} 1.17 & 0.70 & 1.16 \\ 0.67 & 0.74 & 0.51 \\ -0.17 & -0.11 & -0.17 \end{pmatrix}$$

B. Amino

$$r_{ij} = -\begin{pmatrix} 2.53 & 1.50 & 2.27 \\ 2.26 & 1.52 & 1.41 \\ 1.31 & 1.51 & 1.39 \end{pmatrix} \times \begin{pmatrix} 0.143 & 0 & 0 \\ 0 & 0.124 & 0 \\ 0 & 0 & 0.141 \end{pmatrix} + \begin{pmatrix} 3.40 & 1.25 & 3.15 \\ 1.46 & 0.75 & 0.74 \\ 0.24 & 0.19 & 0.22 \end{pmatrix} = \begin{pmatrix} 3.04 & 1.05 & 2.83 \\ 1.14 & 0.66 & 0.66 \\ 0.05 & 0.00 & 0.02 \end{pmatrix}$$

C. Diol

$$r_{ij} = -\begin{pmatrix} 2.92 & 2.72 & 3.49 \\ - & - & - \\ 1.35 & 1.51 & 1.18 \end{pmatrix} \times \begin{pmatrix} 0.097 & 0 & 0 \\ 0 & 0.071 & 0 \\ 0 & 0 & 0.096 \end{pmatrix} + \begin{pmatrix} 2.09 & 0.62 & 2.26 \\ - & - & - \\ -0.10 & -0.12 & -0.12 \end{pmatrix} = \begin{pmatrix} 1.81 & 0.43 & 1.93 \\ - & - & - \\ -0.23 & -0.23 & -0.23 \end{pmatrix}$$

Fig. 1. Selectivity matrices for (A) cyano (B) amino and (C) diol normal bonded phases.

The selectivity matrix[4] (Fig. 1) is a compilation of slopes, intercepts and solvent strengths which describe the retention of the nine solute–solvent pairs for each bonded phase (six pairs for the diol phase). The selectivity matrix, r_{ij}, is generated by adding the product of the localization, $a_{ij}[A_s(\text{exp})/A_s(\text{calc})]$, and solvent strength elements, ε_{ij}, to that of the corresponding intercept element, Δ_{ij}. In effect, retention and solvent strength data for each solute–solvent pair, fit to eqn. 3, are compiled in matrix form.

The selectivity matrix has many practical uses which have been described previously[4]. These include the ready identification of optimal binary mixtures for maximum resolution of solutes with different selectivities and assessment of the relative importance of a solute's proton donor, proton acceptor and dipolar character on retention by a particular bonded phase. Two applications of particular importance, discussed in detail in the present work, include the use of the selectivity matrix as a guide to changing the selectivity of a bonded phase through changes in mobile phase selectivity and the development of stationary phase programming.

EXPERIMENTAL

Equipment

All measurements were obtained with an HPLC system consisting of a Varian LC 5000 ternary liquid chromatograph, Varian Vari-Chrom UV–VIS detector and a Shimadzu C-R3A Chromatopac integrator. Each solute was detected at the wavelength corresponding to its UV absorption maximum.

Columns

The diol (1,2-dihydroxypropyl propyl ether), cyano (cyanopropyl) and amino (aminopropyl) columns used in these studies were Hibar-RT, 5-μm LiChrosorb (25

cm × 4.6 mm I.D.) manufactured by Merck (Darmstadt, F.R.G.) and purchased from E.M. Science (Cherry Hill, NJ, U.S.A.). Bonded phase coverage was 6.8% or 3.1 mol/m^2. The cyano column was endcapped, the amino and diol phases were used as received.

Solutes and solvents

Hexane and methyl *tert.*-butyl ether (MTBE), each pesticide grade, were obtained from Burdick & Jackson (Muskegon, MI, U.S.A.) while chloroform and dichloromethane (ChromAr grade) were obtained from Mallincrodt (St. Louis, MO, U.S.A.). Phenol, nitrobenzene and aniline (reagent grade) were obtained from Mallincrodt. Aniline and nitrobenzene were purified by distillation, while phenol was used without further purification. Aromatic hydrocarbons (phenanthrene, chrysene and perylene) and 1,2-dinitrobenzene were obtained from Aldrich (Milwaukee, WI, U.S.A.) and used as received.

Procedures

Repeated injections of perylene and phenanthrene were used to measure the reproducibility of retention times. Relative standard deviations were no greater than 3%. Reported solute capacity factors were replicated at least twice.

Column void volumes were determined by repeated injections of hexane with a chloroform mobile phase. The first baseline disturbance was taken as the void volume.

The flow-rate was maintained at 1.0 ml/min during the course of these studies. No less than fifteen column volumes was allowed for column equilibration upon a change of the mobile phase.

RESULTS AND DISCUSSION

Solvent strengths

Binary solvent strengths were calculated in two different ways. In the direct method, capacity factors of polycyclic aromatic hydrocarbons (PAHs) were determined in the binary mixture of interest and in pure hexane ($\varepsilon_1 = 0$). The expression relating these measurements to the binary solvent strength of a mixture of solvents a and b is:

$$\varepsilon_{ab} = -\frac{\log(k'_{ab}/k'_h)}{A_s} \tag{4}$$

where ε_{ab} is the binary solvent strength, k'_{ab} the capacity factor of the PAH with that binary mixture, and k'_h the capacity factor of the PAH in hexane. PAH retention data for the amino, diol and cyano phases is summarized in Table I. The cyano data has been published previously[4], but is included here for the sake of completeness. To assess the applicability of generating binary solvent strengths in this fashion, we fit ε_{ab} *versus* log k'_{ab} data for each of the nine PAH data sets for each column to a straight line via a linear, least squares regression. The data of Table I indicate good adherence to eqn. 1 as evidenced by the agreement between experimental and calculated A_s values.

TABLE I

RETENTION DATA FOR NONLOCALIZING AROMATIC HYDROCARBONS USED TO CALCULATE SOLVENT STRENGTHS FOR THREE BONDED PHASES

	Log k' and corresponding ε_{ab} value for indicated volume percent of modifier (ε_{ab} in parentheses)							*A_s (Exp./Calc.)*	*Correlation coefficient*
	0%	*5%*	*8%*	*10%*	*15%*	*20%*	*25%*		
Cyano									
Hexane–chloroform									
	(0.000)	(0.013)		(0.028)	(0.040)	(0.048)			
Phenanthrene	−0.271	−0.406		−0.558	−0.777	−0.753		1.01	0.998
Chrysene	−0.067	−0.243		−0.406	−0.572	−0.649		0.98	0.999
Perylene	−0.002	−0.163		−0.342	−0.493	−0.643		1.02	0.997
Hexane–MTBE									
	(0.000)	(0.017)		(0.023)	(0.027)	(0.032)	(0.035)		
Phenanthrene	−0.271	−0.447		−0.493	−0.493	−0.613		1.02	0.997
Chrysene	−0.067	−0.271		−0.368	−0.406	−0.447		0.99	0.997
Perylene	0.002	−0.217		−0.271	−0.346	−0.407	−0.459	1.01	0.999
Hexane–dichloromethane									
	(0.000)	(0.020)		(0.036)	(0.046)				
Phenanthrene	−0.271	−0.470		−0.636	−0.748			1.01	0.999
Chrysene	−0.067	−0.301		−0.544	−0.634			1.03	0.997
Perylene	0.002	−0.256		−0.448	−0.573			0.97	0.999
Amino									
Hexane–chloroform									
	(0.000)	(0.027)		(0.044)	(0.053)				
Phenanthrene	−0.0490	−0.333		−0.493	−0.602			1.01	0.999
Chrysene	0.269	−0.067		−0.271	−0.379			0.96	0.999
Perylene	0.422	0.078		−0.146	−0.257			1.00	1.000

Hexane–MTBE								
	(0.000)	(0.013)		(0.023)	(0.035)	(0.045)		
Phenanthrene	−0.049	−0.180		−0.286	−0.406	−0.493	0.98	0.999
Chrysene	0.269	0.109		−0.008	−0.168	−0.286	1.01	0.999
Perylene	0.422	0.260		0.121	−0.032	−0.157	1.01	1.000
Hexane–dichloromethane								
	(0.000)	(0.030)		(0.044)	(0.059)			
Phenanthrene	−0.049	−0.333		−0.481	−0.634		0.97	1.000
Chrysene	0.269	−0.115		−0.286	−0.456		1.00	1.000
Perylene	0.422	0.030		−0.157	−0.368		1.04	1.000
Diol								
Hexane–chloroform								
	(0.000)	(0.013)	(0.020)	(0.024)	(0.033)			
Phenanthrene	−0.321	−0.460	−0.522	−0.533	−0.656		0.98	0.999
Chrysene	−0.049	−0.211	−0.274	−0.344	−0.469		1.02	0.997
Perylene	0.114	−0.056	−0.177	−0.202	−0.329		1.05	0.998
Hexane–MTBE								
	(0.000)	(0.006)	(0.009)	(0.011)	(0.013)			
Phenanthrene	−0.321	−0.377	−0.404	−0.422	−0.458		0.89	0.999
Chrysene	−0.049	−0.124	−0.166	−0.191	−0.229		0.99	0.998
Perylene	0.114	0.035	−0.008	−0.035	−0.089		1.06	0.999
Hexane–dichloromethane								
	(0.000)	(0.013)	(0.022)	(0.027)	(0.037)			
Phenanthrene	−0.321	−0.436	−0.529	−0.580	−0.688		0.97	0.999
Chrysene	−0.049	−0.211	−0.320	−0.382	−0.491		0.98	0.999
Perylene	0.114	−0.062	−0.178	−0.251	−0.367		1.02	0.999

TABLE II

POLAR MODIFIER PURE SOLVENT STRENGTHS

Column	*Modifier*		
	Chloroform	*MTBE*	*Dichloromethane*
Amino	0.143 ± 0.006	0.124 ± 0.004	0.141 ± 0.004
Diol	0.097 ± 0.004	0.071 ± 0.004	0.096 ± 0.007
Cyano	0.106 ± 0.007	0.049*	0.120 ± 0.007

* See text for description of how this value was calculated.

Unfortunately, this empirical measurement of binary solvent strengths is limited to low polar modifier concentrations because of the inaccuracy of using capacity factors of less than 0.2 and the low solubility of PAHs larger than perylene in the reference solvent hexane. Therefore, solvent strengths of more polar binary mixtures were generated indirectly. First, pure solvent strengths of polar modifiers were calculated from experimental binary solvent strengths with:

$$\varepsilon_b = \varepsilon_a + \frac{\log\left(\frac{10^{\alpha' n_b(\varepsilon_{ab} - \varepsilon_a)} - 1 + N_b}{N_b}\right)}{\alpha' n_b} \tag{5}$$

where N_b is the mol fraction of the polar modifier, ε_a the pure solvent strength of hexane (equal to zero), and n_b the modifier solvent cross-sectional area. Values used for n_b were 5.0, 4.5, and 4.1 for chloroform, MTBE and dichloromethane respectively[2,12]. Pure solvent strengths of the modifiers when used with cyano, diol and amino phases are displayed in Table II. Once the pure solvent strength of a modifier is determined, rearrangement of eqn. 5 allows calculation of solvent strength for any binary mixture of the modifier with hexane:

$$\varepsilon_{ab} = \varepsilon_a + \frac{\log(N_b 10^{\alpha' n_b(\varepsilon_b - \varepsilon_a)} + 1 - N_b)}{\alpha' n_b} \tag{6}$$

In general, pure solvent strengths calculated from experimental binary solvent strengths remain constant over the entire range of concentrations except when restricted-access delocalization occurs. This is manifested as high pure solvent strengths at low modifier concentrations followed by a leveling off at anywhere from several percent for some localizing solvents to 50% or more for solvents such as ethers which are capable of semi-localization past a monolayer[2,14]. This behaviour has been observed by us previously for a cyano phase with MTBE as the polar modifier. Bonded phases, because of their mobility and low surface coverage, are not likely candidates for restricted-access delocalization as are silanols which are rigid[5]. The observation of this phenomenon is therefore an indication of the presence of accessible residual silanols. A more detailed discussion of restricted-access delocalization will be offered in later sections. For purposes of the present study, the MTBE solvent strength for

the cyano-silica phase was obtained by fitting available binary strengths to a logarithmic function and extrapolating to MTBE concentrations corresponding to complete delocalization (pure solvent strength remains constant). At these concentrations, MTBE molecules are interacting primarily with cyano groups.

The pure solvent strengths we report for the amino phase (chloroform = 0.143 ± 0.006; dichloromethane = 0.141 ± 0.004) are in good agreement with those reported by Snyder and Schunk[5] (chloroform = 0.134; dichloromethane = 0.130) but not in agreement with those of Hennion *et al.*[16] (chloroform = 0.15; dichloromethane = 0.19). Pure solvent strengths for the diol phase have not yet appeared in the literature.

Localization effects

Inspection of the localization matrices for the three columns studied (Fig. 1) indicates that localization effects, manifested as $a_{ij} > 1$, are present in varying degrees for all solute–solvent–bonded phase combinations. This is attributable to localization effects involving the bonded phase and, in all likelihood, residual silanols. The impact of residual silanols on retention by a cyano phase has been discussed previously[4] and will be elaborated on here as well as compared to their impact in both the amino and diol phases.

The descriptor "localization effects" actually refers to three specific, related effects: solute localization, site-competition delocalization (solute and/or solvent) and restricted-access delocalization (solvent localization). These have been discussed in the theory section and elsewhere[15,17]. We will show in the following discussion that all three are important when describing retention mechanisms for the three bonded phases.

First, it is important to note that of the nine nitrobenzene–solvent–bonded phase combinations, the three with MTBE appear to have the largest deviations of experimental A_s values from the theoretical value of 7.3. Also, from Table III it appears that for all three columns the intracolumn retention ordering of nitrobenzene is always (chloroform ≈ dichloromethane > MTBE), despite the fact that MTBE has the lowest solvent strength when used with these phases. For the purposes of a more thorough study, 1,2-dinitrobenzene was substituted for nitrobenzene so that retention and slope differences would be more pronounced and therefore more accurately measured. This data, along with statistical evaluations, appear in Table III.

Because it is unlikely that the seemingly preferential elution of dinitrobenzene in MTBE is a mobile phase effect, we began to consider retention phenomena in which the solvent strength of MTBE would be underestimated. To begin with, we will discuss the cyano–MTBE–dinitrobenzene combination.

The high localization element (2.17) associated with MTBE is recognized in theory as a localization effect, and specifically, should be attributable to site-competition delocalization. Why, however, would this solvent be more likely than either chloroform (1.51) or dichloromethane (1.98) to interact laterally with cyano groups on which dinitrobenzene molecules are localized? Again, the pure solvent strength of MTBE (0.049) is significantly less than that of the other two modifiers. This behaviour can be rationalized if we assume that residual silanols are involved in retention. Recalling earlier discussions, MTBE exhibits strong interactions with residual silanols (Fig. 2). It therefore seems appropriate to suggest that it is lateral interactions of

TABLE III

ANALYSIS OF POLAR SOLUTE RETENTION DATA

	Vol. % modifier	*Slope* (A_s)	*Intercept* ($\log k'_h + \Delta_2$)	*Correlation coefficient*
Nitrobenzene				
Cyano				
Chloroform	3–17	8.65 ± 0.46	−0.044 ± 0.012	0.996
MTBE	2–20	12.01 ± 0.33	−0.031 ± 0.010	0.998
Dichloromethane	2–13	11.54 ± 0.22	0.019 ± 0.006	0.999
Amino				
Chloroform	2–17	9.58 ± 0.22	0.242 ± 0.009	0.999
MTBE	2–30	11.02 ± 0.08	0.194 ± 0.010	0.998
Dichloromethane	2–17	10.12 ± 0.17	0.225 ± 0.007	0.999
Diol				
Chloroform	2–15	9.87 ± 0.18	−0.097 ± 0.004	0.999
MTBE	3–17	11.01 ± 0.23	−0.117 ± 0.002	0.999
Dichloromethane	2–15	8.61 ± 0.36	−0.121 ± 0.008	0.998
1,2-Dinitrobenzene				
Cyano				
Chloroform	3–17	13.03 ± 0.51	0.576 ± 0.013	0.998
MTBE	2–20	18.70 ± 0.70	0.609 ± 0.015	0.999
Dichloromethane	2–13	17.12 ± 0.50	0.670 ± 0.012	0.999
Amino				
Chloroform	5–17	14.32 ± 0.78	1.120 ± 0.037	0.997
MTBE	10–30	18.78 ± 0.51	1.186 ± 0.018	0.999
Dichloromethane	5–17	15.95 ± 0.60	1.147 ± 0.029	0.999
Diol				
Chloroform	2–20	14.08 ± 0.52	0.541 ± 0.013	0.997
MTBE	3–17	20.47 ± 0.98	0.574 ± 0.010	0.998
Dichloromethane	2–15	15.10 ± 0.59	0.545 ± 0.014	0.998
Phenol				
Cyano				
Chloroform	10–60	14.43 ± 2.80	1.408 ± 0.017	0.999
MTBE	5–50	39.41 ± 1.67	1.003 ± 0.053	0.996
Dichloromethane	10–60	15.06 ± 0.39	1.438 ± 0.029	0.999
Amino				
Chloroform	65–100	16.21 ± 0.11	3.396 ± 0.015	0.999
MTBE	40–100	9.61 ± 0.20	1.237 ± 0.020	0.999
Dichloromethane	65–100	14.51 ± 0.21	3.155 ± 0.028	0.999
Diol				
Chloroform	60–100	18.71 ± 0.40	2.090 ± 0.035	0.999
MTBE	40–100	17.40 ± 0.41	0.619 ± 0.028	0.999
Dichloromethane	50–100	22.36 ± 1.41	2.262 ± 0.124	0.995
Aniline				
Cyano				
Chloroform	10–60	16.47 ± 0.84	0.929 ± 0.049	0.995
MTBE	5–60	30.40 ± 1.17	0.996 ± 0.039	0.996
Dichloromethane	10–60	13.24 ± 0.44	0.755 ± 0.033	0.998
Amino				
Chloroform	25–65	14.95 ± 0.38	1.463 ± 0.040	0.999
MTBE	30–65	10.04 ± 0.20	0.750 ± 0.016	0.999
Dichloromethane	10–45	9.33 ± 0.52	0.739 ± 0.043	0.997
Diol				
Data not available, see text				

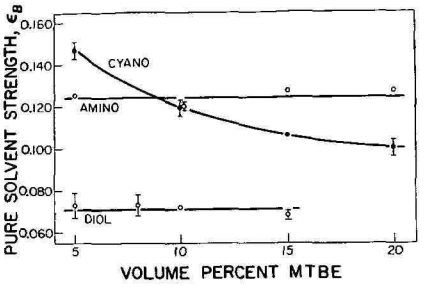

Fig. 2. Pure solvent strengths of MTBE plotted as a function of modifier content for cyano, amino and diol normal bonded phases. Indicated ranges represent one standard deviation (ranges less than 0.002 not shown).

MTBE with silanols which disrupts 1,2-dinitrobenzene localization on these silanols and possibly cyano groups as well. That is, restricted-access delocalization rather than site-competition delocalization at cyano sites is apparently responsible for the preferential elution of dinitrobenzene by MTBE. How this results in the dual observations of apparent reduced retention and increased slope can be more readily understood by rearranging eqn. 1:

$$A_s(\text{exptl}) = \log(k'_1/k'_2)/(\varepsilon_2 - \varepsilon_1) \tag{7}$$

It is apparent from inspection of this relationship that underestimation of a change in solvent strength, $(\varepsilon_2 - \varepsilon_1)$, responsible for a change in solute retention, $(\log k'_1 - \log k'_2)$, will result in an increased slope. Also, any solvent strength determined using nonlocalizing solutes will result in low calculated capacity factors for localizing solutes, and the plot will shift to the left (indicating preferential elution relative to the other two solvents). Also, at higher concentrations of MTBE, when molecules of MTBE and dinitrobenzene are competing for adsorption on the MTBE monolayer (discussed in the selectivity section), site-competition delocalization of the dinitrobenzene molecules could occur as well.

The large dinitrobenzene–MTBE slope (relative to chloroform and dichloromethane) and the intracolumn retention order for dinitrobenzene (chloroform $\approx$ dichloromethane > MTBE) observed for the amino and diol phases are indicative of restricted-access delocalization in these columns as well. However, plots of pure solvent strength *vs.* MTBE content (Fig. 2) give contradictory information, since there is no change in the MTBE solvent strength. We believe this apparent contradiction is due to the relative accessibility of residual silanols in these columns. It must be remembered that restricted-access delocalization (and the nonlinearity of MTBE plots) only occurs when solute and solvent molecules compete for the same adsorption sites. It appears that in these columns residual silanols are not accessible to the large, non-polar PAHs (*i.e.* perylene) used to generate solvent strength values, but they are accessible to the smaller, more polar solute probes. Therefore, because interactions of MTBE with silanols are unaccounted for, the MTBE solvent strength will be underestimated. Also, it is very likely that, in addition to this type of underestimation, the site-competition delocalization effect describerd for the cyano phase occurs as well.

Unfortunately, aniline retention data for the diol phase with all three solvents is not available. In each case, the aniline peak exhibited a very pronounced and unreproducible nonlinearity, making it impossible to accurately measure retention times. Careful control of the amount of aniline injected did not alleviate this problem. Increasing the concentration of aniline in an attempt to find an adsorption isotherm plateau was also ineffective. It was apparent that the diol phase is extremely heterogeneous when probed with a strong base such as aniline. This heterogeneity can be attributed to the presence of three different functionalities: the hydroxyl groups of the diol phase, the ether linkage in the diol, and residual silanols.

Secondary solvent effects

Manipulation of secondary solvent effects is the most effective means of altering selectivity but it can also be the most unpredictable[3,15]. We have observed secondary solvent effects in all three columns studied. In two solute–solvent–bonded phase combinations, (phenol–MTBE–cyano, aniline–chloroform–amino) we have found that when accessibility and changes in acidity/basicity of solvent molecules in the stationary phase are considered, the effects are understandable but unfortunately not predictable. Another type of secondary effect was observed with two different combinations (phenol–MTBE–diol, phenol–MTBE–amino). This type of effect occurs in the mobile phase and does not appear to be significantly altered by interactions in the adsorbed solvent layer.

Our use of the terms "positive" and "negative" secondary solvent effects differs from their use in the adsorption–displacement model, in that they usually refer to effects which either increase (positive) or decrease (negative) retention relative to hexane. We find it more meaningful in the present work to compare the intercepts of log k' *vs.* solvent strength plots (eqn. 3) for each solute–solvent pair to one another rather than to the measured log k' in pure hexane. Although all three intercepts for a particular solute may be less than log k' in hexane (negative effect in the classical sense), the effects may be due to very different processes, and it is much easier to interpret these processes in each bonded phase column by comparing the relative behaviour of solute–solvent combinations. Measuring the retention of a solute in pure hexane also ignores any alteration of the stationary phase resulting from sorption of the modifier itself.

Previously we discussed a negative secondary solvent effect in the mobile phase for the phenol–MTBE–cyano combination which is enhanced by steric hinderance and restricted-access delocalization in the stationary phase. One might have expected increased retention of phenol with such a combination due to a stationary phase much richer in MTBE than the mobile phase[18]. However, the cyano selectivity matrix indicates that there is a strong negative secondary solvent effect in the mobile phase (Δ_{ij} MTBE = 1.00 *vs.* Δ_{ij} chloroform = 1.41 and Δ_{ij} dichloromethane = 1.44). Apparently, interaction of phenol with the basic oxygen of adsorbed MTBE is not very favorable at higher MTBE contents. At low modifier concentrations (<6%) phenol interacts strongly with the adsorbed molecules while at higher concentrations the phenol–MTBE interaction in the mobile phase is much more favorable, even though there is still in all likelihood a greater concentration of MTBE in the stationary phase. Also, the localization element corresponding to phenol–MTBE is extremely large (6.13) indicating that adsorbed MTBE disrupts phenol localization on basic cyano groups (site-competition delocalization).

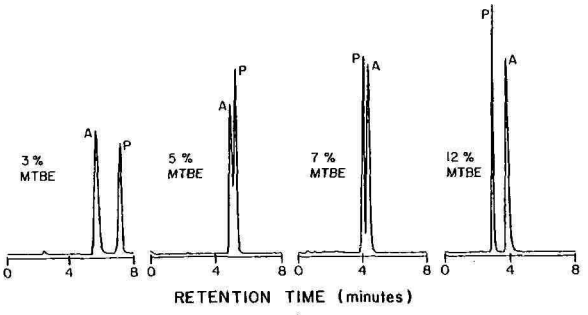

Fig. 3. Retention reversal of phenol (P) and aniline (A). Cyano stationary phase, hexane–MTBE mobile phase.

A retention reversal of phenol and aniline with the cyano phase has been observed (Fig. 3). At low modifier concentrations, adsorption sites are probably cyano groups and adsorbed MTBE. Aniline is less retained than phenol, probably due to the blocking of silanol sites by MTBE and the weaker interaction of aniline with cyano groups and adsorbed MTBE relative to phenol. At concentrations greater than 6%, aniline is retained longer due to an absence of the acid–base interactions in the mobile phase that are experienced by phenol. These observations are consistent with data provided by the retention matrices; the phenol–MTBE intercept element (1.00) is much less than those of either dichloromethane (1.44) or chloroform (1.41), while the MTBE–aniline intercept element (0.97) does not differ significantly from those of chloroform (0.93) or dichloromethane (0.75).

Aratskova *et al.*[19] have also observed a retention reversal of phenol and aniline on a silica and an octadecyl surface with isopropanol and hexane as the mobile phase. At low modifier concentrations ($< 1.5\%$), phenol is retained longer than aniline while at modifier contents greater than 1.5%, a retention order reversal is observed. These researchers did not consider the possibility of phenol interacting with adsorbed isopropanol at low modifier concentrations. Instead they suggested that phenol interacts with silanols to a greater extent than aniline. This certainly differs from our observations and those of other researchers. In fact, compounds containing amino groups are often employed as remedies for tailing caused by residual silanols and as probes of silanol activity in packings[20].

A secondary solvent effect in the adsorbed phase (a positive effect) is observed for the amino column. The chloroform–aniline element (1.46) differs radically from the corresponding elements of MTBE (0.75) and dichloromethane (0.74). Apparently, there is an interaction of aniline and chloroform in the adsorbed phase which is not balanced in the mobile phase. This interaction is the source of a very large change in selectivity relative to dichloromethane or MTBE. The difference in selectivity between chloroform and MTBE is not unexpected and assessment of the other matrices indicate that this is also the case for the other two bonded phases. Also, in almost every solute–solvent–bonded phase combination, differences in selectivity between chloroform and dichloromethane are minimal, except in the amino column where a secondary effect results in a large difference in selectivity. This supports Snyder's contention that secondary effects can dramatically alter selectivity and our obser-

vations that it is the combination of solute, solvent and stationary phases which must be characterized.

The origin of this secondary effect is more difficult to pinpoint than the effect we have observed with the phenol–MTBE–cyano combination. It is certain, however, that this effect is occurring in the stationary phase. Apparently, due to adsorption geometry, the chloroform is adsorbed such that it is extremely susceptible to hydrogen bonding with aniline. Also, it is interesting to note that the localization element associated with this combination is very large. This element, (2.26) is significantly different from that of MTBE (1.52) and dichloromethane (1.41). It is reasonable to suggest that, because it is known that there is a specific interaction between the amino groups and chloroform[9], it is the solvent most capable of disturbing aniline localized on amino groups. It is therefore appropriate to attribute this high localization element to site-competition delocalization.

We have observed another type of secondary solvent effect with a phenol–MTBE–diol combination. The intercept element of this combination (0.62) is significantly different from those of dichloromethane (2.26) or chloroform (2.09). However, unlike the other two secondary solvent effects we have discussed, the localization element of the MTBE combination (2.72) is not significantly different from those of chloroform (2.92) or dichloromethane (3.49). This data implies that a negative mobile phase effect is occurring but that interactions of phenol with adsorbed solvent do not significantly influence retention behaviour. This type of secondary mobile phase effect also occurs with a phenol–MTBE–amino combination where the intercept element (1.24) is markedly different from those of chloroform or dichloromethane (3.40 and 3.15, respectively). Interestingly, the localization element of the MTBE combination (1.50) is somewhat less than those of chloroform (2.53) and dichloromethane (2.27), indicating again that MTBE molecules in the stationary phase are chemically different from those in the mobile phase.

In conclusion, three very different secondary solvent effects have been observed in our studies. In the first, a negative mobile phase effect is exacerbated by steric effects in the stationary phase that prevent specific solute–adsorbed solvent interactions. The second type is a positive stationary phase effect resulting from an increase in acidity of solvent molecules upon adsorption relative to their acidity in the mobile phase. The third type, observed in the amino and diol phases, is primarily a negative

TABLE IV

SUMMARY OF STATIONARY MOBILE PHASE COMBINATIONS THAT RESULT IN NON-CORRELATED RETENTION BEHAVIOUR

N = Nitrobenzene; P = phenol; A = aniline.

Solvent	*Column*	*Retention order*
MTBE	Cyano	N < P < A
	Amino	N < A < P
Chloroform	Diol	N < P < A
	Cyano	N < A < P
Chloroform	Amino	N < A < P
	Diol	N < P < A

mobile phase effect which is not significantly influenced by solute–solvent interactions in the stationary phase.

Selectivity

The previous discussions of localization and secondary solvent effects have addressed the retention mechanisms responsible for observed behaviour. The following discussion addresses, in a more general way, the result of these mechanisms; the relative selectivity of different solvent–bonded phase combinations. In this discussion, we refer to selectivity as the relative importance of proton donor, proton acceptor and dipole characteristics of a combination.

The selectivities of the solvent–bonded phase combinations we have tested vary widely with respect to proton donor and acceptor tendencies. The amino phase is such a strong proton donor that the retention order is always aniline < phenol regardless of the solvent. Even though there is a strong interaction of phenol and MTBE in the mobile phase, this is not sufficient to change the retention order (*i.e.* aniline > phenol). This is also the case for the diol phase where the retention order is always phenol < aniline. As we have discussed previously, the cyano phase may have an acidic *or* basic character depending on the mobile phase.

The dipolar selectivity of the solvent–bonded phase combinations (nitrobenzene or 1,2-dinitrobenzene) do not appear to vary significantly from one bonded phase to another. Nitrobenzene is always the least retained of the three probes and the intracolumn order is always chloroform ≈ dichloromethane > MTBE. The intracolumn character does, however, change with the solvent. For example, with a chloroform–cyano combination, the dipolar character (retention of nitrobenzene) relative to proton donor character (retention of phenol) is much different from that of a MTBE–cyano combination. This and other examples from the other matrices again illustrate dramatically the importance of assessing solvent–bonded phase combinations.

As we mentioned earlier, one use of the selectivity matrix which we believe holds great promise is in the area of multi-stage chromatography. Because very different selectivities have been observed with different columns while using the same mobile phase, it is reasonable to expect that efficient, isocratic, multi-stage chromatography may have significant potential. It is this potential which will attract chromatographers to normal phase use since it has been demonstrated that there are many complex separations which cannot be carried out with a single stage[11]. Giddings[21] has shown that maximum resolving power occurs when two columns with different selectivities are coupled. In the best case, separation will approach $R_1 \times R_2$, where R_1 and R_2 refer to the resolution of columns 1 and 2, respectively. When retention in columns 1 and 2 is similar, separation can only approach $R_1 + R_2$. Table IV lists examples of pairs of bonded phases which have very different selectivities (poorly correlated mechanisms) while using the same mobile phase.

Typically, solvent optimization proceeds by choosing polar modifiers from different apices of the the Snyder selectivity triangle[22]. Indeed, this is how the solutes, solvents and bonded phases were chosen for this study. One solvent is usually chosen from Groups I, V and VIII. It is important to note that a Group I solvent such as MTBE will exhibit strong interactions with residual silanols. It must therefore be recognized that use of a strongly localizing solvent such as MTBE will have more

significant effects on retention and selectivity in a column with residual silanols than a nonlocalizing solvent such as chloroform or dichloromethane would. This has been noted by Mourey *et al.*[23] with a silica phase used to separate polystyrene oligomers. These researchers have found that stereospecific retention of polystyrene isomers is possible when nonlocalizing solvents such as dichloromethane or chloroform are used. However, when localizing solvents such as tetrahydrofuran (THF) or ethyl acetate are used, these isomeric separations do not occur. A similar effect has been observed by Snyder[24] in the separation of *threo/erythro* diastereomers. Also, Snyder *et al.*[17] have discussed the theoretical possibilities of using localizing and nonlocalizing solvents to alter the character of a stationary phase.

Because we have shown that residual silanols are accessible in the normal bonded phases we have studied and that solute and solvent compete for adsorption sites, it is probable that the use of localizing and nonlocalizing solvents represents another dimension in the optimization of separations via changes in mobile phase selectivity. Indeed, the presence of residual silanols should not necessarily be viewed in a negative sense, and we believe that future characterizations of bonded phases should include the identification of unique separations possible with these heterogeneous stationary phases.

CONCLUSIONS

It is apparent that the retention of polar solutes by amino-, diol- and cyano-silica bonded phases cannot be described apart from the unique selectivity of a solvent–bonded phase combination. The use of the adsorption–displacement model in the expanded selectivity matrix form provides a powerful tool for quantifying localization and secondary solvent effects responsible for the selectivities we have observed.

The localization effects observed in these studies indicate that solutes and solvents may adsorb on silanol as well as bonded phase sites and that competition for these sites has a pronounced effect on retention. The relative importance of silanols in retention and selectivity will vary as a function of their accessibility and the nature of solute, solvent and bonded phase. In any case, the characterization of a bonded phase must include the role of residual silanols whose presence should not necessarily be viewed in a negative sense. In another paper we discuss in more detail the role of residual silanols in normal bonded phases[25].

We have also concluded that cyano-silica may represent a "universal" phase, as has been suggested by others. In our earlier work[4], we found that cyano-silica exhibited either acidic or basic character, depending on the polar modifier used. In the present work we have seen that this behaviour is unique to the cyano phase. In addition, the accessibility of residual silanols can be controlled through the use of localizing or nonlocalizing solvents, further enhancing the versatility of cyano-silica.

Finally, we believe there is great potential for the development of isocratic, multi-stage separations using these phases. The diol and amino phases seem well suited for this because their selectivities are so different. The cyano phase is attractive for either single- or multi-stage column separations because its character can be so drastically altered by the mobile phase composition.

REFERENCES

1 S. R. Abbott, *J. Chromatogr. Sci.*, 18 (1980) 540.
2 L. R. Snyder, *Principles of Adsorption Chromatography*, Marcel Dekker, New York, 1968.
3 L. R. Snyder, *Anal. Chem.*, 46 (1974) 1384.
4 W. T. Cooper and P. L. Smith, *J. Chromatogr.*, 355 (1986) 57.
5 L. R. Snyder and T. C. Schunk, *Anal. Chem.*, 54 (1982) 1764.
6 S. Hara and S. Ohnishi, *J. Liq. Chromatogr.*, 7 (1984) 69.
7 R. E. Majors, *J. Chromatogr. Sci.*, 18 (1980) 488.
8 R. J. Hurtubise, A. Hussain and H. F. Silver, *Anal. Chem.*, 53 (1981) 1993.
9 W. E. Hammers, M. C. Spanjer and C. L. de Ligny, *J. Chromatogr.*, 174 (1979) 291.
10 D. E. Schmidt, R. W. Giese, D. Conron and B. L. Karger, *Anal. Chem.*, 52 (1980) 177.
11 J. F. K. Huber, I. Fogy and C. Fioresi, *Chromatographia*, 13 (1980) 408.
12 L. R. Snyder and J. L. Glajch, *J. Chromatogr.*, 248 (1982) 165.
13 L. R. Snyder and H. Poppe, *J. Chromatogr.*, 184 (1980) 363.
14 L. R. Snyder and J. L. Glajch, *J. Chromatogr.*, 214 (1981) 1.
15 L. R. Snyder, *J. Chromatogr.*, 255 (1983) 3.
16 M. C. Hennion, C. Picard, C. Combellas, M. Caude and R. Rosset, *J. Chromatogr.*, 210 (1981) 211.
17 L. R. Snyder, J. L. Glajch and J. J. Kirkland, *J. Chromatogr.*, 218 (1981) 299.
18 L. R. Snyder, *J. Chromatogr.*, 16 (1964) 55.
19 A. A. Aratskova, A. V. Kiselev and Y. I. Yashin, *Chromatographia*, 17 (1983) 312.
20 R. Gill, S. P. Alexander and A. C. Moffat, *J. Chromatogr.*, 247 (1982) 39.
21 J. C. Giddings, *Anal. Chem.*, 56 (1984) 1258A.
22 L. R. Snyder, in Cs. Horváth (Editor), *High Performance Liquid Chromatography*, Vol. 3, Academic Press, New York, 1983.
23 T. H. Mourey, G. A. Smith and L. R. Snyder, *Anal. Chem.*, 56 (1984) 1773.
24 L. R. Snyder, *J. Chromatogr.*, 245 (1982) 165.
25 S. P. Boudreau, P. L. Smith and W. T. Cooper, *Chromatography*, 2(5) (1987) 31.

Journal of Chromatography, 410 (1987) 267–278
Elsevier Science Publishers B.V., Amsterdam — Printed in The Netherlands

CHROM. 19 980

INVERSGASCHROMATOGRAPHISCHE UNTERSUCHUNGEN VON POLYETHERALKOHOLEN

HANS BECKER* und ROLAND GNAUCK
Akademie der Wissenschaften der D.D.R., Zentralinstitut für Organische Chemie, Bereich Makromolekulare Verbindungen, Rudower Chaussee 5, 1199 Berlin (D.D.R.)
(Eingegangen am 23. Juni, 1987; geänderte Fassung eingegangen am 21. August, 1987)

SUMMARY

Inverse gas chromatographic study of polyether alcohols

Mono- and bifunctional polyethers consisting of ethylene and propylene oxides were used as stationary phases and were investigated by inverse gas chromatography with several solutes at temperatures ranging from 80 to 150°C. The enthalpy, free energy, and entropy of mixing as well as the Flory-Huggings-parameters were calculated based on the obtained retention data and correlated with the structure of the polyethers used. The polyethers varied in their molecular masses, functionalities, monomer compositions, and distributions.

EINLEITUNG

Im Verlauf der letzten 10–15 Jahre hat sich die auf Guillet[1] zurückgehende inverse Gaschromatographie als eine erfolgreiche Methode zur Charakterisierung von Polymersystemen, aber vor allem zur Gewinnung thermodynamischer Daten entwickelt. Neuere zusammenfassende Darstellungen zu diesem Gebiet liegen u.a. von Aspler[2], Gilbert[3] und von Berezkin *et al.*[4] vor. Seltener sind dagegen Publikationen, in denen mittels der inversen Gaschromatographie erhaltene thermodynamischen Daten der Wechselwirkungen mit der Struktur der als stationäre Phasen eingesetzten Polymeren korreliert wurden. Klein und Jeberien[5] und Alishoyev *et al.*[6] untersuchten den Einfluss der Molmasse von Polyoxyethylenglykolen (PEG) und Polyoxypropylenglykolen (PPG) auf das Retentionsverhalten. Ito *et al.*[7] verglichen statistische und Pfropfcopolymere aus Styren und 2-Hydroxymethylmethacrylat.

In der vorliegenden Arbeit wurden mono- und bifunktionelle Polyetheralkohole aus Ethylen- (EO) und Propylenoxid (PO) mit unterschiedlicher Molmasse, Monomerzusammensetzung und -verteilung als stationäre Phasen eingesetzt und mit verschiedenen Lösungsmitteln inversgaschromatographisch untersucht.

0021-9673/87/$03.50

EXPERIMENTELLES

Polymere

Die Polyether wurden durch anionische Polymerisation von EO und/oder PO bei 110°C unter Schutzgasatmosphäre bei Normaldruck mit den Kaliumalkoholaten des *n*-Butanols, des Ethylenglykols bzw. des 1,2-Propandiols als Initiator hergestellt. Zur Synthese der Blockcopolymeren wurde nach der Monomerwechselmethode gearbeitet. Die synthetisierten Produkte lassen sich durch folgende allgemeine Strukturformeln beschreiben:

$$H\text{-}(O\text{-}CH_2\text{-}CH_2)_n\text{-}OH$$

$$\begin{array}{l} \qquad\quad CH_3 \\ \qquad\quad | \\ H\text{-}(O\text{-}CH_2\text{-}CH)_n\text{-}OH \end{array} \qquad n = 8,\ 20,\ 40,\ 80$$

$$\begin{array}{l} \qquad\qquad\quad CH_3 \\ \qquad\qquad\quad | \\ C_4H_9\text{-}[(O\text{-}CH_2\text{-}CH)_x\text{-}(O\text{-}CH_2\text{-}CH_2)_y]_z\text{-}OH \end{array} \qquad (x+y)z = 40$$

Im folgenden steht PEG für die erste und PPG für die zweite Strukturformel. PEA und PPA stehen für die homopolymeren Varianten der monofunktionellen Polyetheralkohole (dritte Formel) mit $x=0$ bzw. $y=0$. Die copolymeren Produkte werden mit der Abkürzung CPA bezeichnet.

Säulenpräparierung

Etwa 0,5 g des jeweiligen Polyetheralkohols wurden in 50–100 ml Chloroform gelöst. Nach Zugabe von 5 g Chromosorb W AW (60–80 mesh) wurde das Lösungsmittel langsam am Rotationsverdampfer abgezogen und der beschichtete Träger 8 h bei 100°C vakuumgetrocknet. Noch anhaftendes Restlösungsmittel wurde durch 12-stündige Konditionierung der gefüllten Trennsäule (Stahlsäule, 2 m × 2 mm I.D.) bei 100°C entfernt. Der tatsächliche Beladungsgrad wurde nach der Konditionierung bzw. nach den Messungen durch Veraschung bestimmt.

Geräte

Die Messungen wurden mit einem Varian 3700 Gaschromatographen, ausgerüstet mit einem Flammenionisationsdetektor, durchgeführt. Die Retentionszeiterfassung erfolgte mit dem Varian CDS-111. Zur Totzeitbestimmung wurde Methan verwendet[8]. Als Trägergas diente Reinststickstoff. Der Säulenvordruck und der Ausgangsdruck (= atmosphärischer Druck) wurden mit Präzisionsquecksilbermanometern bestimmt. Der Trägergasmengenstrom wurde mit einem temperierten Seifenblasenflowmeter gemessen. Die Genauigkeit der Temperaturregulierung des Säulenofens betrug ±0,1°C. Die Injektionen von jeweils 0,01 µl Lösungmittel erfolgten mit einer 1-µl Hamiltonspritze. Diese Menge Lösungsmittel gewährleistete die für die Berechnungen vorausgesetzte ideale Verdünnung der Probe im Polymeren. Durch Messungen an Säulen, die mit unterschiedlich beladenem Träger (2–20 Masse%

PPG-2000 bzw. PEG-2000) gefüllt waren, ergaben, dass eine etwa 10%ige Beladung ausreichend ist, um Adsorptionen des Lösungsmittels am Träger ausschliessen zu können.

DATENBEHANDLUNG

Das spezifische Retentionsvolumen, V_g', als Grundgrösse aller weiteren Berechnungen wurde gemäss Gleichung 1 erhalten:

$$V_g' = \frac{(t_R - t_M)Fj}{W_l} \tag{1}$$

mit

$$F = F_M \frac{(P_0 - P_w)}{P_0} \cdot \frac{273{,}2}{T_F} \tag{2}$$

Hierbei sind F_M der gemessene Trägergasmengenstrom bei der absoluten Temperatur des Flowmeters, T_F; P_0 der Atmosphärendruck; P_w der Sättigungsdampfdruck des Wassers bei T_F; t_R und t_M sind die Gesamtretentionszeit bzw. die Totzeit; W_l ist die Masse des Polymeren in der Säule; und j der James-Martin-Faktor zur Korrektur der Kompressibilität des Trägergases zwischen dem Eingangsdruck P_i und dem Ausgangsdruck P_0.

Zur Aufstellung der Retentionsdiagramme und für die weiteren Berechnungen wurden die Logarithmen der Retentionsvolumina sowohl einer linearen, als auch einer binomischen Regression nach der Methode der kleinsten Fehlerquadrate unterworfen. Neben der Eliminierung zufälliger Fehler wird dadurch die Vergleichbarkeit der Daten unterschiedlicher Messungen gewährleistet, unabhängig davon, ob die jeweiligen Messtemperaturen tatsächlich identisch waren. Die Beziehungen zwischen dem spezifischen Retentionsvolumen und der Temperatur kann demnach durch die folgenden Gleichungen wiedergegeben werden:

$$\ln V_g' = A_0 + A_1/T \quad \text{(linear)} \tag{3}$$

beziehungsweise

$$\ln V_g' = A_0 + A_1/T + A_2/T^2 \qquad \text{(binomisch)} \tag{4}$$

Hierbei sind A_0, A_1 und A_2 die Regressionskoeffizienten.

In beiden Fällen wurden Korrelationskoeffizienten > 0.99 erhalten. In den folgenden Gleichungen ist je nach gewünschter Berechnungsbasis für $\ln V_g'$ der gemessene Originalwert oder einer der Regressionswerte nach Gleichung 3 bzw. 4 einzusetzen. Alle Grössen, die in einer proportionalen Beziehung zum Retentionsvolumen stehen, zeigen, im Einklang mit den für beide Regressionen erhaltenen hohen Korrelationskoeffizienten, keine signifikante Abhängigkeit von der Berechnungsbasis. Dagegen besteht bei den abgeleiteten Werten zum Beispiel der Mischungsenthalpie insbeson-

dere in den Temperaturbereichen, die am Rande des Regressionsbereiches liegen, die Gefahr einer Überinterpretation der aufgezwungenen Krümmung.

Der gewichtsbezogene Aktivitätskoeffizient $(a_1/w_1)^\infty$ der Wechselwirkung zwischen dem injizierten Lösungsmittel und dem Polymeren ergibt sich nach Gleichung 5:

$$\ln (a_1/w_1)^\infty = \ln \left(\frac{273{,}2R}{V_g' P_1^{0\prime} M_1} \right) - \left(\frac{P_1^0}{RT} \right) (B_{11} - V_1) \tag{5}$$

P_1^0 ist der Sättigungsdampfdruck, V_1 das Molvolumen und B_{11} der zweite Virialkoeffizient des Lösungsmittels mit der Molmasse M_1 bei der Säulentemperatur T. Aus den Aktivitätskoeffizienten ergeben sich die Zustandsfunktionen der Mischung nach:

$$\Delta G_m = -RT \ln (a_1/w_1)^\infty \tag{6}$$

$$\Delta S_m = -\mathrm{d}\,(\Delta G_m)/\mathrm{d}T \tag{7}$$

$$\Delta H_m = \mathrm{d}[\ln(a_1/w_1)^\infty]/\mathrm{d}(1/T) = \Delta G_m + T\Delta S_m \tag{8}$$

Hierbei sind ΔG_m die freie Energie; ΔS_m die Entropie und ΔH_m die Enthalpie der Mischung.

Die sich aus der Mischungs- und der Verdampfungsenthalpie zusammensetzende Lösungsenthalpie, ΔH_l, ergibt sich aus den Retentionsdaten nach Gleichung 9:

$$\Delta H_l = -R\mathrm{d}(\ln V_g')/\mathrm{d}(1/T) \tag{9}$$

oder unter Verwendung von Gleichung 3 bzw. 4

$$\Delta H_l = -RA_1 \quad \text{(linear)} \tag{10}$$

$$\Delta H_l = -R(A_1 + 2A_2/T) \quad \text{(binomisch)} \tag{11}$$

Eine analoge Beziehungen kann auf Basis der binomisch regressierten Werte auch für die Änderung der Wärmekapazität, ΔC_P, des Lösungsmittels mit der Temperatur angegeben werden:

$$\Delta C_P = \mathrm{d}(\Delta H_l)/\mathrm{d}T \tag{12}$$

bzw. wieder unter Verwendung von Gleichung 4:

$$\Delta C_P = R2A_2/T^2 \tag{13}$$

Die Flory-Huggins-Parameter der Wechselwirkung des Lösungsmittels mit der stationären Phase, X_{12}, ergeben sich schliesslich zu:

$$X_{12} = \ln\left(\frac{273{,}2Rv_2}{V_g' V_1 P_1^{0\prime}}\right) - \left(1 - \frac{V_1}{M_2 v_2}\right) - \left(\frac{P_1^{0\prime}}{RT}\right)(B_{11} - V_1) \qquad (14)$$

beziehungsweise unter Verwendung der Aktivitätskoeffizienten:

$$X_{12} = \ln (a_1/w_1)^{\infty} - \ln\left(\frac{v_1}{v_2}\right) - \left(1 - \frac{V_1}{M_2 v_2}\right) \qquad (15)$$

v_1 und v_2 sind die spezifischen Volumina des Lösungsmittels bzw. des Polymeren mit der Molmasse M_2 bei der Säulentemperatur T.

ERGEBNISSE UND DISKUSSION

Alle im Temperaturbereich von 80–150°C erhaltenen Retentionsdiagramme zeigen, entsprechend der sehr guten Übereinstimmung der linear und der binomisch regressierten Werte (vergl. Tabelle I) und abgesehen von der im Zusammenhang mit der Temperaturabhängigkeit von ΔC_P stehenden, graphisch praktisch nicht erfassbaren Krümmung, einen quasi linearen Verlauf, so dass selbst bei den bei Raumtemperatur kristallinen PEG und PEA keine Beeinflussung der Retentionsdiagramme durch Phasenübergänge berücksichtigt werden mussten (Fig. 1).

Mit den Tabellen I und II wird eine Zusammenstellung der V_g'-, ΔG_m-, ΔH_m- und ΔS_m-Werte bei 100°C für verschiedene Polyether mit veriierter Molmasse und Nonan bzw. *n*-Propanol gegeben. Gleichzeitig wird in der Tabelle I die sehr gute Übereinstimmung der linear und der binomisch regressierten Retentionsvolumina demonstriert.

Am Beispiel der Mischungsenthalpie ΔH_m wird im folgenden der Einfluss der Polyethermolmasse auf thermodynamische Zustandsgrössen betrachtet. Prinzipiell gleiche Korrelationen ergeben sich für die anderen Zustandsfunktionen. Die Mischungsenthalpie erscheint uns für Korrelationen am geeignetsten, da aufgrund der

TABELLE I

RETENTIONSVOLUMINA UND ZUSTANDSFUNKTIONEN DER MISCHUNG VON POLYETHERN MIT NONAN BEI 100°C

Polyol	M_n	V_g'		ΔG_m	ΔH_m	ΔS_m
		Bin.	*Lin.*			
PEG	400	16,68	16,70	−12,22	11,2	0,063
	1000	17,75	17,74	−12,03	11,6	0,066
	2000	17,07	17,10	−12,15	11,4	0,063
	4000	17,51	17,55	−12,06	12,1	0,065
PEA	1800	37,87	38,15	− 9,70	11,4	0,056
PPG	425	113,5	113,2	− 6,27	5,4	0,034
	1000	111,8	112,3	− 6,31	5,3	0,031
	2000	118,2	118,7	− 6,15	5,4	0,031
	4000	117,9	118,7	− 6,16	5,2	0,030

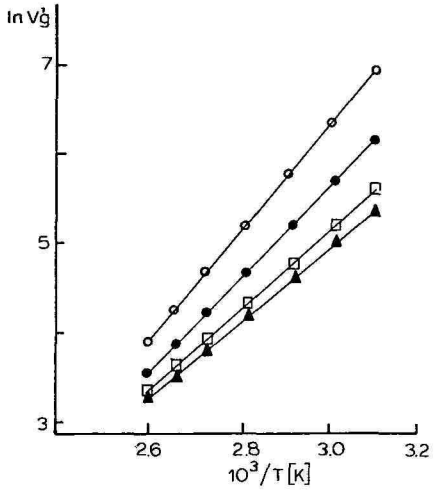

Fig. 1. Retentionsdiagramme von *n*-Propanol an Polyoxyethylenglykolen (PEG) unterschiedlicher Molmasse. ○ = PEG-400; ● = PEG-1000; □ = PEG-2000; ▲ = PEG-4000.

unterschiedlichen Vorzeichen von ΔH_m und ΔS_m hier die Effekte deutlicher in Erscheinung treten, als bei der freien Energie, ΔG_m, obwohl die Genauigkeit der Werte für die Mischungsenthalpie geringer ist, da es sich bei ihr um eine abgeleitete Grösse handelt[9].

Ein Vergleich der Figs. 2 und 3 veranschaulicht, dass diese Abhängigkeit wesentlich durch das als Probe verwendete Lösungsmittel geprägt wird. Während beim Nonan keine signifikante Abhängigkeit von der Polyethermolmasse beobachtet werden kann, ist sie beim Propanol gegenüber den PEG deutlich ausgeprägt. Mit steigender Molmasse des PEG nähert sich beim Propanol die Mischungsenthalpie einem Grenzwert. Aus diesen beiden Beobachtungen folgt, dass im Falle der untersuchten Polyether weniger die Molmasse der Polymeren, als vielmehr die Konzentration der

TABELLE II

RETENTIONSVOLUMINA UND ZUSTANDSFUNKTIONEN DER MISCHUNG VON POLYETHERN MIT *n*-PROPANOL BEI 100°C

Polyol	M_n	V_g'	ΔG_m	ΔH_m	ΔS_m
PEG	400	70,03	−4,96	3,4	0,022
	1000	56,58	−5,62	4,5	0,027
	2000	50,16	−6,00	5,5	0,031
	4000	54,25	−5,75	6,7	0,033
PEA	1800	62,18	−5,33	6,4	0,032
PPG	425	78,98	−4,59	4,8	0,024
	1000	57,35	−5,58	4,2	0,031
	2000	54,44	−5,74	4,1	0,026
	4000	57,59	−5,57	4,2	0,026

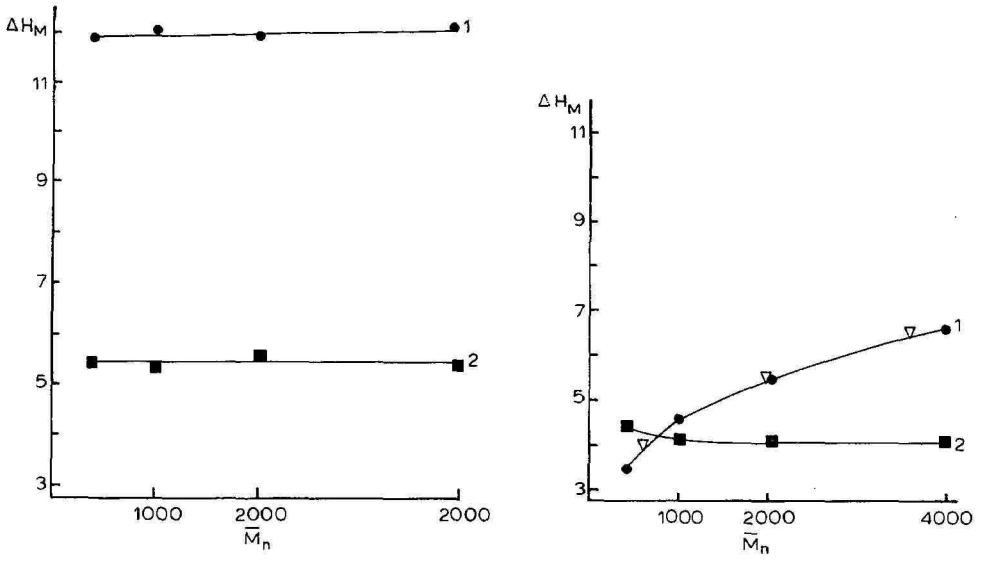

Fig. 2. Mischungsenthalpie, ΔH_m, von Nonan mit Polyoxyethylenglykolen (●) und mit Polyoxypropylenglykolen (■) in Abhängigkeit von der Molmasse.

Fig. 3. Mischungsenthalpie, ΔH_m, von *n*-Propanol mit Polyoxyethylenglykolen (●) und mit Polyoxypropylenglykolen (■) in Abhängigkeit von der Molmasse (▽ = PEA bei verdoppelter Molmasse).

Endgruppen und deren spezifische Wechselwirkung mit dem Probenmolekül die ausschlaggebende Grösse ist. So ergeben die ΔH_m-Werte der monofunktionellen PEA auch mit denen der bifunktionellen PEG einen gemeinsamen Kurvenverlauf, wenn sie bei der doppelten Molmasse, also bei der gleichen OH-Endgruppenkonzentration, eingetragen werden. (Fig. 3, Kurve 1). Die Kurve 2 der gleichen Abbildung, die den Verlauf von ΔH_m als Funktion der Polyethermolmasse beim System PPG–Propanol wiedergibt, zeigt diese Abhängigkeit nicht. Hier wird offenbar der Einfluss der Molmasse, genauer gesagt der Konzentration der OH-Endgruppen, von einem gegenläufigen Effekt überlagert, nämlich von der zunehmenden Wechselwirkung des Propylrestes des Alkohols mit der methylsubstituierten PPG-Kette. Für eine Korrelation inversgaschromatographischer Daten mit der Molmasse der untersuchten stationären Phase, besonders wenn es sich hierbei um funktionelle Polymere mit Molmassen $< 10\,000$ handelt, müssen also solche Lösungsmittel ausgewählt werden, die einerseits spezifische Wechselwirkungen mit den Endgruppen eingehen und deren Wechselwirkung mit der Polymerkette dagegen andererseits vernachlässigt werden kann.

In den Tabellen III und IV sind die Retentionsvolumina und die Werte der Zustandsfunktionen der Mischung für copolymere Polyetheralkohole (CPA) zusammengestellt. Bei ihrer Betrachtung zeigt sich, dass andere Kriterien bei der Auswahl eines geeigneten Lösungsmittels heranzuziehen sind, wenn die Zusammensetzung von Copolymeren mit der Mischungsenthalpie korreliert werden soll. Die Figs. 4 und 5 zeigen die Mischungsenthalpien des Nonans und des Propanols mit CPA gleichen Polymerisationsgrades, aber unterschiedlicher Bruttozusammensetzung und auch unterschiedlicher Monomerverteilung. Es wird augenfällig, dass die Mischungsenthalpie

TABELLE III

RETENTIONSVOLUMINA UND ZUSTANDSFUNKTIONEN DER MISCHUNG VON COPOLYETHERN MIT NONAN BEI 100°C

Mol% EO	*Struktur**	V_g'	ΔG_m	ΔH_m	ΔS_m	X_{12}
100	H	38,15	−9,66	12,7	0,060	1,82
75	S	63,27	−8,09	9,9	0,048	1,30
50	B	91,06	−7,00	8,4	0,041	0,69
50	S	87,59	−7,08	9,3	0,044	1,03
25	B	121,48	−6,06	7,3	0,036	0,66
25	S	129,13	−5,87	7,4	0,037	0,59
0	H	128,08	−5,90	6,4	0,033	0,61

* H = Homopolyether; B = Blockstruktur; S = Stat. Verteilung.

bei Verwendung von Propanol nur geringfügig von der Monomerzusammensetzung abhängig ist. Dies kann nicht überraschen, da sich die Werte der beiden Homopolymeren ebenfalls nicht unterscheiden.

Beim Nonan, das zwar den PPA, jedoch nicht den PEA zu lösen vermag, unterscheiden sich die Werte der Mischungsenthalpie dagegen signifikant. Die Werte für die Copolymeren mit statistischer Monomerverteilung liegen im Prinzip erwartungsgemäss auf der Verbindungsgeraden der beiden Eckwerte. Bei den Blockcopolymeren sind dagegen erhebliche Abweichungen von dieser Geraden zu beobachten. Dieses Verhalten lässt sich wie folgt interpretieren.

Zunächst ist darauf zu verweisen, dass entsprechend der Löslichkeit aller untersuchten Polyether im Propanol sowie der Polyether mit hohem Propylenoxidgehalt auch im Nonan, in diesen Fällen keine Abhängigkeit des Retentionsvolumens vom Beladungsgrad festgestellt wurde. Dagegen wird beim Nonan und Polyethern mit höherem Ethylenoxidgehalt diese Abhängigkeit zunehmend deutlich. Der Effekt tritt sowohl bei statistischen, als auch bei Blockcopolyethern in Erscheinung. Er korreliert mit der abnehmenden Löslichkeit dieser Produkte im Nonan und findet seine Erklärung in einer Änderung des Retentionsmechanismus infolge zunehmender Adsorption des Nonans an der Gas–Flüssig-Grenzfläche.

TABELLE IV

RETENTIONSVOLUMINA UND ZUSTANDSFUNKTIONEN DER MISCHUNG VON COPOLYETHERN MIT *n*-PROPANOL BEI 100°C

Mol% EO	*Struktur**	V_g'	ΔG_m	ΔH_m	ΔS_m	X_{12}
100	H	63,46	−5,27	8,2	0,036	0,44
75	S	68,02	−5,05	7,9	0,035	0,36
50	B	66,87	−5,11	8,0	0,035	0,40
50	S	65,03	−5,19	8,3	0,036	0,46
25	B	60,82	−5,40	8,1	0,038	0,51
25	S	67,17	−5,09	8,1	0,035	0,38
0	H	63,26	−6,03	8,3	0,038	0,70

* H = Homopolymer; B = Blockstruktur; S = Stat. Verteilung.

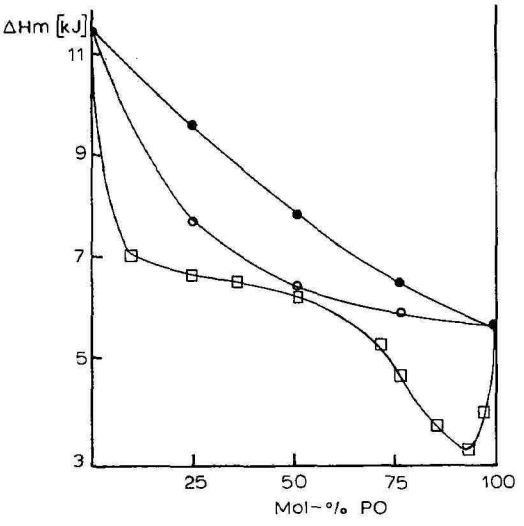

Fig. 4. Mischungsenthalpie, ΔH_m, von Nonan mit Copolyetheralkoholen unterschiedlicher Monomerzusammensetzung und -verteilung. ○ = Block-CPA; ● = statistische CPA; □ = PEA–PPA-Gemische.

Das unterschiedliche Verhalten in Abhängigkeit von der Monomerverteilung hat darüber hinausgehende Ursachen. Wie im experimentellen Teil beschrieben, wurden die Polyetheralkohole aus einer Lösung auf eine Kieselgeloberfläche aufgebracht. Dabei kommt es zu einer Vorzugsadsorption der die Hydroxylgruppen tragenden Kettenenden der Polymermoleküle. Das hat zur Folge, dass bei den untersuchten monofunktionellen Blockcopolyethern, die am hydrophilen Ethylenoxidblock OH-terminiert sind, dieser Block an der Fest–Flüssig-Grenzfläche und der hydrophobe Propylenoxidblock in der die Retention beeinflussenden Grenzfläche zur Dampfphase angereichert vorliegt. Dementsprechend können die tabellierten Werte der Zustandsfunktionen des Nonans und der Polyether mit Ethylenoxidgehalten über 30 Mol% auch nur als scheinbare Grössen betrachtet werden. Dass es im Falle des Propanols trotz Vorzugsadsorption keine Unterschiede im Verlauf der Mischungsenthalpien in Abhängigkeit von der Struktur gibt, resultiert aus dem hier wirkenden,

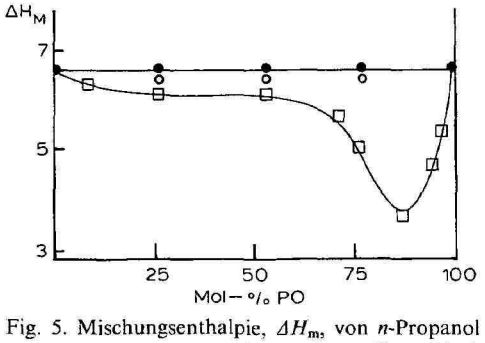

Fig. 5. Mischungsenthalpie, ΔH_m, von *n*-Propanol mit Copolyetheralkoholen unterschiedlicher Monomerzusammensetzung und -verteilung. ○ = Block-CPA; ● = statistische CPA; □ = PEA–PPA-Gemische.

TABELLE V

RETENTIONSVOLUMINA UND ZUSTANDSFUNKTIONEN DER MISCHUNG VON HOMOPOLYETHERGEMISCHEN MIT NONAN BEI 100°C

Mol% EO	*Beladung**	V_g'	ΔG_m	ΔH_m	ΔS_m	X_{12}
100	H	38,15	−9,66	12,7	0,060	1,82
90	A	48,75	−8,90	7,9	0,045	1,57
75	A	70,09	−7,77	7,7	0,041	1,21
75	B	58,28	−8,34	6,4	0,038	1,39
60	B	70,88	−7,73	6,5	0,038	1,20
50	A	95,47	−6,86	7,8	0,039	0,90
40	B	84,95	−7,17	4,9	0,032	1,02
40	C	87,00	−7,10	6,5	0,036	0,99
30	A	109,77	−6,38	5,4	0,031	0,76
30	B	90,59	−6,97	4,7	0,031	0,96
25	A	110,65	−6,35	5,8	0,033	0,76
15	A	123,68	−6,00	4,5	0,028	0,64
10	A	127,39	−5,94	3,8	0,026	0,61
5	A	133,13	−5,78	4,5	0,028	0,57
0	H	128,08	−5,90	6,4	0,033	0,61

* A = Mischung in Lösung; B = Mischung der beschichteten Träger; C = Getrennte Säulenbereiche; H = Homopolymer.

einheitlichen Retentionsmechanismus, verbunden mit der praktisch gleichen Löslichkeit der Homopolymeren im Propanol.

Zur Stützung dieser Hypothese wurden Messungen mit Nonan an Mischungen der beiden Homopolymeren durchgeführt. Hierfür wurden Säulen mit zwei Varianten der Mischung eingesetzt. Zum einen wurde das Polymergemisch aus einer Lösung

TABELLE VI

RETENTIONSVOLUMINA UND ZUSTANDSFUNKTIONEN DER MISCHUNG VON HOMOPOLYETHERGEMISCHEN MIT *n*-PROPANOL BEI 100°C

Mol% EO	*Beladung**	V_g'	ΔG_m	ΔH_m	ΔS_m	X_{12}
100	H	63,46	−5,27	8,2	0,036	0,44
90	A	60,13	−5,44	7,6	0,035	0,49
75	A	65,94	−5,15	7,1	0,033	0,40
75	B	53,26	−5,81	6,3	0,032	0,62
60	B	56,29	−5,64	5,7	0,030	0,55
50	A	62,41	−5,37	8,5	0,037	0,46
40	B	52,99	−5,83	5,7	0,031	0,62
40	C	56,52	−5,63	5,9	0,031	0,55
30	A	60,56	−5,41	5,4	0,029	0,49
30	B	51,54	−5,91	7,2	0,035	0,64
25	A	55,94	−5,66	5,4	0,030	0,57
15	A	57,79	−5,56	4,0	0,026	0,53
10	A	54,33	−5,75	6,2	0,032	0,60
5	A	54,81	−5,82	7,2	0,032	0,63
0	H	63,26	−6,03	8,3	0,032	0,71

* A = Mischung in Lösung; B = Mischung der beschichteten Träger; C = Getrennte Säulenbereiche; H = Homopolymer.

desselben auf das Trägermaterial aufgebracht und zum anderen wurde eine Mischung der mit den Homopolymeren getrennt beladenen Träger hergestellt. Die hierzu gehörigen Daten sind in den Tabellen V und VI zusammengestellt.

Wie aus der Fig. 6 ersichtlich, liegen die Retentionsvolumina des Nonans bei den mit getrennt beschichteten Trägern gefüllten Säulen auf der Verbindungsgeraden zwischen den Eckpunkten der beiden Homopolymeren und zwar unabhängig davon, ob vor der Säulenfüllung eine innige mechanische Durchmischung der beiden unterschiedlich beschichteten Träger erfolgte oder diese auf zwei getrennte Bereiche der Säule verteilt wurden. Bei den mit den Polymergemischen beschichteten Trägern ist dagegen ein signifikant grösseres Retentionsvolumen gemessen worden.

Der Verlauf der Mischungsenthalpien in Abhängigkeit von der Zusammensetzung der Mischung geht ebenfalls aus den Figs. 4 und 5 hervor. Hier sind zwei Phänomene auffällig. Zum einen ist das 'Durchhängen' der Kurve infolge der beschriebenen Vorzugsadsorption und der daraus resultierenden Konzentrationsgradienten noch stärker als bei den Blockcopolymeren ausgeprägt. Dies kann auch erwartet werden, da sich die Vorzugsadsorption von hydrophilen Molekülen am Kieselgel stärker manifestieren sollte als die von hydrophilen Molekülsegmenten.

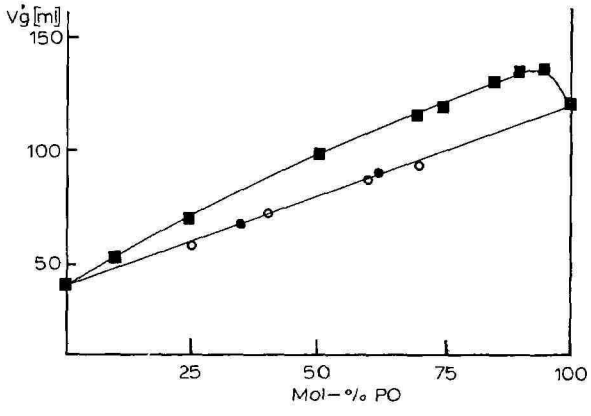

Fig. 6. Retentionsvolumina des Nonans an Gemischen homopolymerer Polyetheralkohole unterschiedlicher Zusammensetzung und Verteilung auf dem Träger und in der Trennsäule. ■ = als Mischung auf den Träger aufgebracht; ○ = getrennt beladene Träger mechanisch gemischt; ● = getrennt beladene Träger in separaten Säulenbereichen.

Hinzu kommt aber noch, dass im Bereich der geringeren Masseanteile des PPA in der Mischung Mischungsenthalpien berechnet wurden, die noch unterhalb der des reinen PPA lagen. Dieser Effekt ist unabhängig von dem als Probe verwendeten Lösungsmittel. Er wurde auch bei anderen Lösungsmitteln gefunden und muss deshalb mit Wechselwirkungen der beiden Polymeren untereinander in Verbindung gebracht werden. Hierüber wird gesondert berichtet.

ZUSAMMENFASSUNG

Mono- und bifunktionelle Polyetheralkohole aus Ethylenoxid (EO) und Propylenoxid (PO) mit varierter Molmasse, Monomerzusammensetzung und -verteilung wurden als stationäre Phasen eingesetzt und mit verschiedenen Lösungsmitteln inversgaschromatographisch untersucht. Aus den im Temperaturbereich von 80–150°C erhaltenen Retentionsdaten wurden die Enthalpie, die freie Energie, die Entropie der Mischung und die Flory-Huggins-Parameter berechnet und mit der Struktur der eingesetzten Polyether korreliert.

LITERATUR

1 J. E. Guillet, in J. H. Purnell (Herausgeber), *New Developments in Gas Chromatography*, Wiley, New York, 1973, p. 187.
2 J. S. Aspler, in S. A. Liebmann (Herausgeber), *Pyrolysis and GC in Polymer Analysis* (*Chromatographic Science Series*, Vol. 29), Marcel Dekker, Basle, New York, 1985, p. 399.
3 S. G. Gilbert, *Adv. Chromatogr.*, 23 (1984) 199.
4 V. G. Berezkin, V. R. Alishoyev und I. B. Nemirovskaya, *Gas Chromatography of Polymers* (*Journal of Chromatography Library Series*, Vol. 10), Elsevier, Amsterdam, 1977.
5 J. Klein und H.-E. Jeberien, *Makromol. Chem.*, 181 (1980) 1237.
6 V. R. Alishoyev, V. G. Berezkin und G. A. Mirzabayev, *Dokl. Akad. Nauk. SSSR*, 190 (1970) 1365.
7 K. Ito, Y. Masuda, T. Shintani, T. Kitano und Y. Yamashita, *Polymer J.*, 15 (1983) 577.
8 H. Becker und R. Gnauck, *J. Chromatogr.*, 366 (1986) 378.
9 B. W. Gainey und C. L. Young, *Trans. Faraday Soc.*, 64 (1968) 349.

Journal of Chromatography, 410 (1987) 279–295
Elsevier Science Publishers B.V., Amsterdam — Printed in The Netherlands

CHROM. 19 925

COMPLEX-FORMING EQUILIBRIA IN ISOTACHOPHORESIS

VII*. EVALUATION OF THE ION-PAIR FORMATION CONSTANTS OF PHOSPHORUS OXO ACIDS WITH HISTIDINE AND ASSESSMENT OF THEIR SEPARABILITY

TAKESHI HIROKAWA*, SHINJI KOBAYASHI** and YOSHIYUKI KISO
Applied Physics and Chemistry, Faculty of Engineering, Hiroshima University, Shitami, Saijo, Higashi-hiroshima 724 (Japan)
(First received July 1st, 1987; revised manuscript received August 3rd, 1987)

SUMMARY

The qualitative indices (R_E) of six phosphorus oxo acids (phosphorous, orthophosphoric, pyrophosphoric, triphosphoric, trimetaphosphoric and tetrametaphosphoric acids) were observed using histidine-buffered electrolyte systems. The ion-pair formation constants of the phosphorus oxo acids with histidine (1:1) were evaluated by the least-squares method utilizing a simulation of the isotachophoretic steady state. The separability of the six oxo acids and hypophosphorous acid was assessed using the evaluated constants. The separation of the seven oxo acids with a histidine-buffered electrolyte system as reported by Yagi *et al.* could be elucidated as the result of the decrease in the effective mobilities accompanied by ion-pair formation.

INTRODUCTION

The seven phosphorus oxo acids (POA) hypophosphorous ($H_3P^{I}O_2$), phosphorous ($H_3P^{III}O_3$), orthophosphoric ($H_3P^{V}O_4$), pyrophosphoric ($H_4P^{V}{}_2O_7$), triphosphoric ($H_5P^{V}{}_3O_{10}$), trimetaphosphoric ($H_3P^{V}{}_3O_9$) and tetrametaphosphoric acids ($H_4P^{V}{}_4O_{12}$)*** have been separated isotachophoretically using a leading electrolyte buffered by histidine at pH 5.5[1]. According to our simulational assessment of the separability using the previously evaluated mobilities and pK_a values[2], as detailed later, the simulated effective mobilities of $P^{V}{}_3O_9$ and $P^{V}{}_4O_{12}$ were very similar to each other. However, the complete separation of $P^{V}{}_3O_9$ and $P^{V}{}_4O_{12}$ was observed on the isotachopherogram[1]. This result suggests that there might be other factors

* For Part VI, see *J. Chromatogr.*, 312 (1984) 11.
** Present address: Seitetsu Kagaku Kogyo Co., Research Centre, Imanishi-cho 1, Shikama-ku, Himeji, Japan.
*** When an accurate ionic charge is not necessary, the anions of these POAs are designated as $P^{V}{}_4O_{12}$, $P^{III}O_3$, etc.

0021-9673/87/$03.50

affecting the effective mobilities of $P^{V}_{3}O_{9}$, $P^{V}_{4}O_{12}$, etc., in addition to the effect of the pH and the ionic strength of the separated zones.

In isotachophoresis, the interaction of sample ions with the counter ions to form kinetically labile complexes and ion pairs results in a decrease in the effective mobility of the samples. Examples can be found in previous papers (*e.g.*, refs. 3 and 4). In the present case the reported separation was considered to be the result of ion-pair formation between the oxo acids and histidine. The qualitative indices (R_E) of the POAs, except $P^{I}O_2$, were observed under several different electrolyte conditions forming ion pairs, and the ion-pair formation constants were evaluated by the least-squares method utilizing a simulation of the isotachophoretic steady state. Using the evaluated constants, the separability of the POAs was simulated to elucidate the separation of the POAs by the use of histidine buffer.

THEORETICAL

Table I gives the m_0 and pK_a values of electrolyte constituents used in the following simulations and Table II gives the m_0 and pK_a values of the seven POAs evaluated previously[2]. Most of the values in Tables I and II were evaluated by our isotachophoretic method and some were taken from the literature[5–7]. In Table II m_0 and pK_a values are not given for several ionic species as their abundances are negligibly small in the isotachophoretically "safe" pH range of *ca.* 3–11 and therefore the m_0 and pK_a values could not be evaluated by the isotachophoretic method.

Fig. 1A shows the pH dependence of the effective mobilities of the seven POAs in the pH range 4–8 at ionic strength zero. The curves were plotted using the m_0 and pK_a values listed in Table II and are not for the isotachophoretic steady state. The predominant ionic species in the pH range 4–8 are $H_2P^{I}O_2^-$, $H_2P^{III}O_3^-$, $HP^{III}O_3^{2-}$, $H_2P^{V}O_4^-$, $HP^{V}O_4^{2-}$, $H_2P^{V}{}_2O_7^{2-}$, $HP^{V}{}_2O_7^{3-}$, $HP^{V}{}_3O_{10}^{3-}$, $P^{V}{}_3O_{10}^{4-}$, $HP^{V}{}_3O_9^{3-}$ and $P^{V}{}_4O_{12}^{4-}$.

From the large differences in the effective mobilities among the POAs in Fig. 1A, it seems that these POAs might be separated easily by isotachophoresis in the pH range 4–5.5.

Fig. 1B shows the pH_L (pH of leading electrolyte) dependence of the simulated effective mobilities of the POAs at the isotachophoretically steady state in the pH

TABLE I

PHYSICO-CHEMICAL CONSTANTS USED IN SIMULATION (25°C)

m_0 = Absolute mobility ($cm^2\ V^{-1}\ s^{-1}$) · 10^5; pK_a = thermodynamic acid dissociation constants, assumed values being used for Cl^-; AMC = ε-aminocaproic acid; CRE = creatinine; MP = 3-methylpyridine; IM = imidazole; MOR = morpholine.

Cation	m_0*	pK_a	*Anion*	m_0	pK_a
AMC^+	29.8	4.373	Cl^-	79.08	−3
CRE^+	36.8	4.848	Acetate	42.4	4.756
MP^+	42.8	6.08	Propionate	37.1	4.874
IM^+	50.4	7.15	Butyrate	33.8	4.82
MOR^+	42.5	8.33	Caproate	30.2	4.857

* Obtained by the present isotachophoretic method.

TABLE II

ABSOLUTE MOBILITIES AND pK_a VALUES OF SEVEN PHOSPHORUS OXO ACIDS (25°C)

m_1–m_5 = Absolute mobilities ($cm^2\ V^{-1}\ s^{-1}$) · 10^5 of monovalent–pentavalent ions; pK_1–pK_5 = thermodynamic acid dissociation constants.

Sample	m_1	m_2	m_3	m_4	m_5	pK_1	pK_2	pK_3	pK_4	pK_5
$P^{I}O_2$	45.1					1.1				
$P^{III}O_3$	40.0	65.9				1.3	7.086			
$P^{V}O_4$	34.2	59.1	71.5			2.161	7.207	12.325		
$P^{V}{}_2O_7$	29	57.9	76.4	89.4		1	1.9	6.6	9.6	
$P^{V}{}_3O_{10}$	–	48	74.7	89.3	113.0	–	1.1	2.3	6.5	9.24
$P^{V}{}_3O_9$	–	–	87.7*			–	–	2.05		
$P^{V}{}_4O_{12}$	–	–	75.6	94.7		–	–	–	2.74	

* In ref. 2, the value was erroneously cited as 83.7.

range 4–8. The leading ion was 10 m*M* chloride and the buffers used were ε-aminocaproic acid (pH_L = 4–4.6), creatinine (4.2–5.4), 3-methylpyridine (5.0–6.5), imidazole (6.2–7.5) and morpholine (7.2–8.0). The discontinuities of the curves in Fig. 1B are due to the different buffers.

As the effect of the ionic strength of electrolyte on the effective mobility was taken into account in the simulation, the effective mobilities of all POAs in Fig. 1B were smaller than those in Fig. 1A. Also, it was suggested by the simulation that the effective mobilities of $P^{V}{}_3O_9$ and $P^{V}{}_4O_{12}$ at the steady state were very similar in the

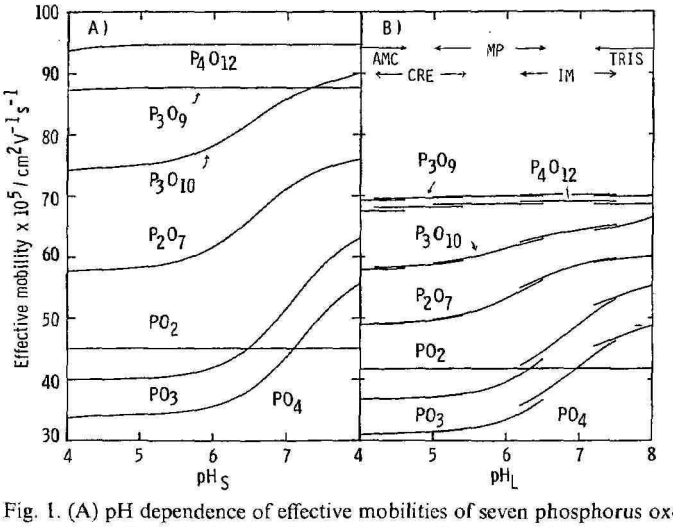

Fig. 1. (A) pH dependence of effective mobilities of seven phosphorus oxo acids (POAs) at ionic strength zero, not for the isotachophoretic steady state. The oxo acids are hypophosphorous ($P^{I}O_2$), phosphorous ($P^{III}O_3$), orthophosphoric ($P^{V}O_4$), pyrophosphoric ($P^{V}{}_2O_7$), triphosphoric ($P^{V}{}_3O_{10}$), trimetaphosphoric ($P^{V}{}_3O_9$) and tetrametaphosphoric acids ($P^{V}{}_4O_{12}$). pH_S = pH of samples. (B) pH_L dependence of effective mobilities of the seven POAs at the isotachophoretically steady state. pH_L = pH of leading electrolyte. Leading ion, 10 m*M* chloride. Buffers: ε-aminocaproic acid (AMC), creatinine (CRE), 3-methylpyridine (MP), imidazole (IM) and tris(hydroxymethyl)aminomethane (Tris).

pH_L range 4–8. Therefore, their separation may be difficult, contrary to the expectations from Fig. 1A, if there were no other factor affecting to the effective mobilities except the pH and the ionic strength.

To confirm this simulation, an isotachopherogram of the seven POAs was obtained. The leading ion was 10 m*M* chloride, the terminator was 10 m*M* caproic acid and pH_L was adjusted to 5.5 by adding 3-methylpyridine. The buffer used was the same as that used in the evaluation of the m_0 and pK_a values of POAs[2]. The ion-pair interaction between POAs and 3-methylpyridine was negligibly small. Fig. 2 shows the observed and simulated isotachopherograms of the seven POAs. Apparently the separation of $P^V_3O_9$ and $P^V_4O_{12}$ was incomplete in spite of the small amount of sample (*ca.* 2 nmol). This experimental result was consistent with the simulation shown in Fig. 1B.

The seven POAs were separated isotachophoretically using a histidine-buffered leading electrolyte (pH_L = 5.5). The isotachopherogram is shown later in Fig. 9. The sample zones were detected in the order $P^V_3O_9$, $P^V_4O_{12}$, $P^V_3O_{10}$, $P^V_2O_7$, P^IO_2, $P^{III}O_3$ and P^VO_4.

Although the order of appearance was the same as that observed with the use of the 3-methylpyridine system, the separability of $P^V_3O_9$ and $P^V_4O_{12}$ was considerably improved by the use of histidine. As the pH_L value was the same as that of the 3-methylpyridine system used, such a difference in the separability strongly suggests that the degree of interaction between POAs and the buffers may be different. The most probable explanation may be that ion-pair forming interactions occurred between histidine and $P^V_3O_9$, $P^V_4O_{12}$, etc., and under the selected electrolyte conditions the decrease in the effective mobilities was optimal for separation.

On the assumption that 1:1 ion-pair species are formed between POAs and

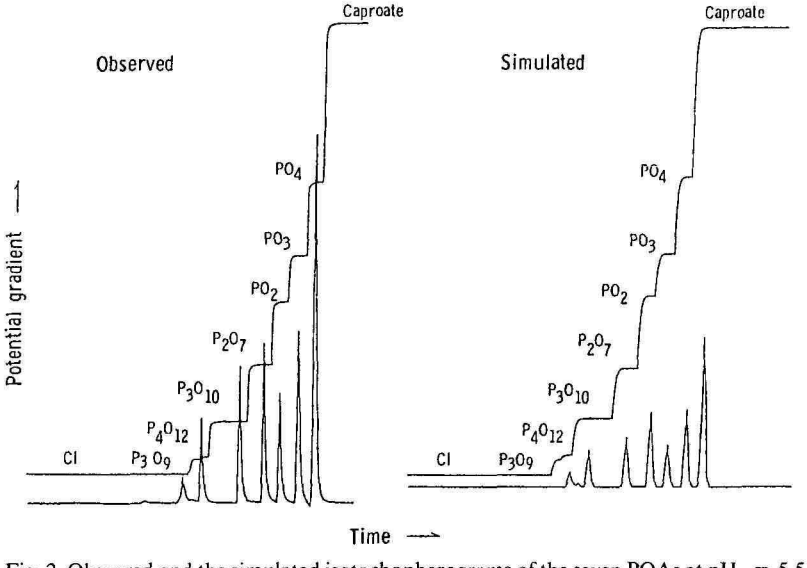

Fig. 2. Observed and the simulated isotachopherograms of the seven POAs at pH_L = 5.5 (3-methylpyridine buffer). Leading ion, 10 m*M* chloride. For abbreviations, see Fig. 1.

histidine in the separated zones, the proton dissociation and the ion-pair formation equilibria in the zone of phosphorous acid, for example, can be expressed by

$$\begin{aligned}
&H_3PO_3 \overset{K_1}{\rightleftharpoons} H_2PO_3^- + H^+ \\
&H_2PO_3^- \overset{K_2}{\rightleftharpoons} HPO_3^{2-} + H^+ \\
&H_2PO_3^- + HisH^+ \overset{K_{1,i}}{\rightleftharpoons} (H_2PO_3\text{–}HisH)^0 \\
&HPO_3^{2-} + HisH^+ \overset{K_{2,i}}{\rightleftharpoons} (HPO_3\text{–}HisH)^- \\
&HisH^+ \overset{K_Q}{\rightleftharpoons} His + H^+
\end{aligned} \tag{1}$$

where K_1, K_2 and K_Q are the acid dissociation constants of phosphorous acid and histidine, and $K_{1,i}$ and $K_{2,i}$ are the ion-pair formation constants, respectively. Then the effective mobility ($\bar{m}$) of phosphorous acid coexisting with histidine can be expressed as follows:

$$\bar{m}_{PO_3} = \frac{(m_1[H_2PO_3^-] + m_2[HPO_3^{2-}] + m_{1,i}[H_2PO_3\text{–}HisH^0] + m_{2,i}[HPO_3\text{–}HisH^-])}{([H_3PO_3] + [H_2PO_3^-] + [HPO_3^{2-}] + [H_2PO_3\text{–}HisH^0] + [HPO_3\text{–}HisH^-])}$$

$$= \frac{\{K_1/[H^+](m_1 + m_{1,i}K_{1,i}[HisH^+]) + K_1K_2/[H^+]^2(m_2 + m_{2,i}K_{2,i}[HisH^+])\}}{\{1 + K_1/[H^+](1 + K_{1,i}[HisH^+]) + K_1K_2/[H^+]^2(1 + K_{2,i}[HisH^+])\}} \tag{2}$$

where $[H_2PO_3^-]$, etc., designate the concentrations, m_1 and m_2 the mobilities of $H_2P^{III}O_3^-$ and $HP^{III}O_3^{2-}$ corrected for the ionic strength of the separated zones using Onsager's equation and $m_{1,i}$ and $m_{2,i}$ the mobilities of the ion-pair species formed. The mobilities of the ion pairs are necessarily smaller than those of the non-interacting POAs, as not only do the ionic charges decrease but also the Stokes' radii increase on ion-pair formation. Therefore, the effective mobility of POA decreases with increase in the abundance of the ion-pair species formed.

In order to evaluate the ion-pair formation constants by the least-squares method, the qualitative index of POAs should be measured under several different electrolyte conditions in order to vary the abundance of ion-pair species. As shown by eqn. 2, the effective mobility is determined by the acid dissociation constants, the ion-pair formation constants, the pH of the POA zone and the concentration of the interacting histidine cation ($HisH^+$) in the zone. When the effective mobility could be measured under certain pH conditions varying the concentration of $HisH^+$ of the POA zone, the ion-pair formation constants can be evaluated by analysing the dependence. The concentration of $HisH^+$ can be expressed as

$$[HisH^+] = C^t_{B,S} / (1 + K_Q/[H^+]) \tag{3}$$

where $C^t_{B,S}$ is the total concentration of histidine free from ion-pair formation in the separated zones. As the sum of $C^t_{B,S}$ and the concentration of ion-paired histidine is

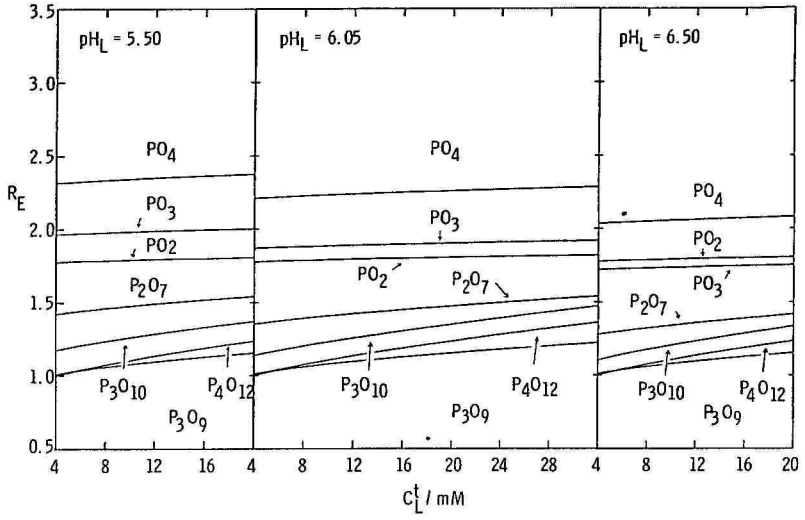

Fig. 3. C_L^t dependence of the R_E values of the seven POAs at the isotachophoretic steady state on the assumption that no ion-pair interaction occurred. For abbreviations, see Fig. 1. C_L^t = Total concentration of leading ion.

determined by the mass balance of the counter ions[3]* (buffer ions in the present situation), $C_{B,S}^t$ is closely related to the concentration of the buffers in the leading electrolyte ($C_{B,L}^t$). The $C_{B,L}^t$ values can be expressed by the total concentration of the leading ion (C_L^t) and the pH of the leading zone:

$$C_{B,L}^t = (1 + K_Q/[H^+])\, C_L^t \tag{4}$$

Under several different C_L^t conditions in order to vary the abundance of ion-pair species, the qualitative index of isotachophoresis (R_E) was measured. The R_E value is the ratio of the potential gradient (E/V cm^{-1}) of a sample zone (E_S) to that of a leading zone (E_L). It is equal to the ratio of the effective mobility ($\bar{m}$) of the leading ion to that of the sample ion in its zone from the equality of velocities of migrating zones ($v = \bar{m}E$):

$$R_E = E_S/E_L = \bar{m}_L/\bar{m}_S = h_S/h_L \tag{5}$$

where h_S and h_L are the step heights of the sample and the leading zones, respectively, in the isotachopherograms obtained. Apparently from eqn. 5, when the effective mobility decreases accompanied by ion-pair formation, the R_E value of POAs increases.

However, it should be noted that even if no ion-pair interaction occurred, when the R_E values are measured with varying C_L^t, the R_E values increase with the increase in C_L^t because the ionic strength of the isotachophoretically separated zones increases with increase in C_L^t, and the effective mobility decreases.

* The total amount of the counter ions that flows into the sample zone from the leading electrolyte is equal to the amount that flows out from the sample zone.

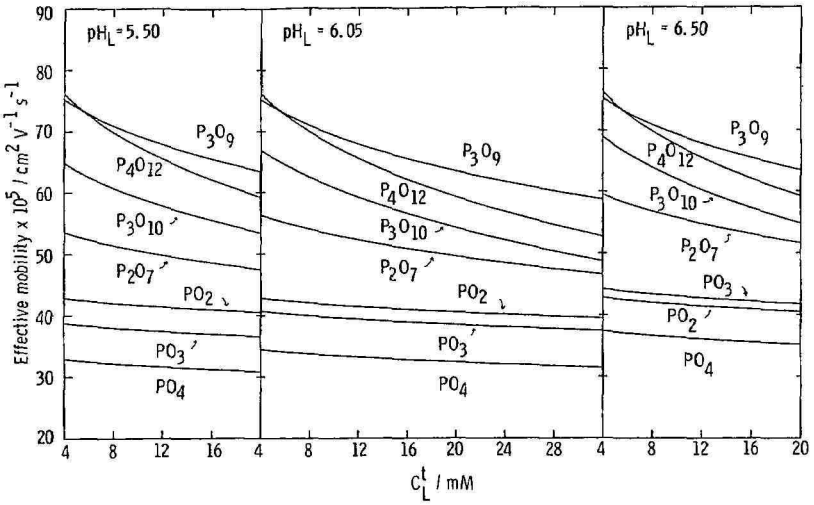

Fig. 4. C_L^t dependence of the simulated effective mobilities of the seven POAs at the isotachophoretic steady state on the assumption that no ion-pair interaction occurred. For abbreviations, see Fig. 1. C_L^t = Total concentration of leading ion.

Fig. 3 shows the C_L^t dependence of the R_E values of seven POAs on the assumption that ion-pair interaction does not occur between POAs and histidine; pH_L was 5.5–6.5 and C_L^t was 4–32 m*M*. The selected ranges included the present experimental conditions considered in the following section. The C_L^t dependence of the simulated effective mobilities of seven POAs is also plotted in Fig. 4 using the same assumption. In the C_L^t range 4–32 m*M* (pH_L = 6.05), the ionic strength of the $P^{III}O_3$ zone varied from 0.0062 to 0.0268 according to the simulation. The R_E values and the effective mobilities varied from 1.87 to 1.92 and from $40.7 \cdot 10^{-5}$ to $37.5 \cdot 10^{-5}$ cm^2 V^{-1} s^{-1}, respectively, in the C_L^t range 4–32 m*M*. For the $P^V{}_4O_{12}$ zone, the values varied from 1.00 to 1.36 and from $76.2 \cdot 10^{-5}$ to $52.7 \cdot 10^{-5}$ cm^2 V^{-1} s^{-1} in the same C_L^t range. The ionic strength of the $P^{III}O_3$ zone varied from 0.015 to 0.057. If the observed degree of variations exceeded the above values, the difference can be attributed to the result of ion-pair formation between POA anions and $HisH^+$.

Details of the computational procedures for the evaluation of the formation constants have been described previously[3,4].

EXPERIMENTAL

The sodium salts of hypophosphorous, phosphorous, pyrophosphoric and triphosphoric acids were purchased from Tokyo Kasei Kogyo in the purest form, together with orthophosphoric acid. Synthesized and purified sodium salts of trimetaphosphoric and tetrametaphosphoric acids were provided by Dr. Ohashi of Kyushu University. Stock sample solutions (10 m*M*) were prepared by dissolving these samples in distilled water. The evaluation of the ion-pair formation constant of hypophosphite ion ($H_2P^IO_2^-$) with histidine was not considered, as it became apparent from preliminary experiments that the formation constant was too small for isotacho-

TABLE III

OPERATIONAL SYSTEMS, INTERNAL STANDARD SAMPLES AND EFFECTIVE MOBILITIES AND CONCENTRATIONS OF ZONE CONSTITUENTS (25°C)

Leading ion, chloride; terminating ion, *n*-caproate; migration current, 50–200 μA. pH_L = pH of leading electrolyte; C_L^t = total concentration of leading ion (m*M*); $\bar{m}_L$ = effective mobility of leading ion ($cm^2 V^{-1} s^{-1}$) · 10^5; $C_{B.L}^t$ = total concentration (m*M*) of buffer ion; $\bar{m}_{B.L}$ = effective mobility of buffer ion ($cm^2 V^{-1} s^{-1}$) · 10^5; Std. = internal standards used for corrections; R_E = ratio of potential gradients, E_S/E_L.

No.	pH_L	C_L^t	$\bar{m}_L$	$C_{B.L}^t$	$\bar{m}_{B.L}$	*Std. (R_E)*
1	5.50	6.11	75.56	7.73	21.25	Butyrate (2.648)
2	5.50	10.18	74.66	12.82	20.79	Butyrate (2.663)
3	5.50	18.32	73.38	22.94	20.13	Butyrate (2.684)
4	6.05	7.13	75.31	13.80	13.78	Acetate (1.970), propionate (2.281)
5	6.05	10.37	74.63	19.92	13.62	Acetate (1.977), propionate (2.292), butyrate (2.520)
6	6.05	12.22	74.29	23.39	13.54	Acetate (1.980), propionate (2.297)
7	6.05	14.60	73.91	27.82	13.44	Acetate (1.984), propionate (2.303)
8	6.05	17.31	73.52	32.84	13.34	Acetate (1.989), propionate (2.309)
9	6.05	19.46	73.23	36.80	13.27	Acetate (1.992), propionate (2.314)
10	6.05	22.40	72.88	42.19	13.18	Acetate (1.996), propionate (2.320)
11	6.05	26.47	72.43	49.62	13.06	Acetate (2.001), propionate (2.328)
12	6.05	30.54	72.03	56.99	12.95	Acetate (2.006), propionate (2.335)
13	6.50	6.11	75.56	22.33	7.36	Butyrate (2.440)
14	6.50	10.18	74.66	36.63	7.28	Butyrate (2.459)
15	6.50	18.32	73.38	64.50	7.16	Propionate (2.256), butyrate (2.487)

phoretic determination, *i.e.*, the abundance of the ion-pair species was negligibly small. However, hypophosphorous acid was included in the assessment of the separability of POAs.

The R_E values of the six POAs were measured using fifteen kinds of leading electrolytes buffered by histidine. The leading ion was chloride and the C_L^t values were in the range 6.1–30.5 m*M*. For $P^{III}O_3$, P^VO_4, $P^V{}_2O_7$ and $P^V{}_3O_{10}$, at least two ionic species coexist at $pH_L \approx 6$. To change the abundance of the interacting ionic species for the determination of predominant ion-pair species, the pH_L values were also varied in the range 5.5–6.5. The terminator was 10 m*M* caproic acid. The pH measurements were carried using a Horiba Model F7ss expanded pH meter. Table III summarizes the leading electrolyte conditions, the calculated concentrations and the effective mobilities of the electrolyte constituents.

The isotachopherograms were obtained using a Shimadzu IP-2A isotachophoretic analyser equipped with a potential gradient detector. The temperature was thermostated at 25°C. The separating tube used was *ca.* 40 cm × 0.5 mm I.D. The driving current applied was 50 μA when C_L^t was 10 m*M*, 100 μA for 20 m*M*, etc. A single run took *ca.* 35 min under these conditions. To correct the asymmetric potential of the potential gradient detector used for the precise R_E measurements, one of acetic, propionic and butyric acids was used selectively as the internal standard to avoid the formation of mixed zones with the samples. The simulated R_E values are given in Table III; the method of correction has been detailed elsewhere[8].

The R_E measurement was repeated three times and the averages were used for

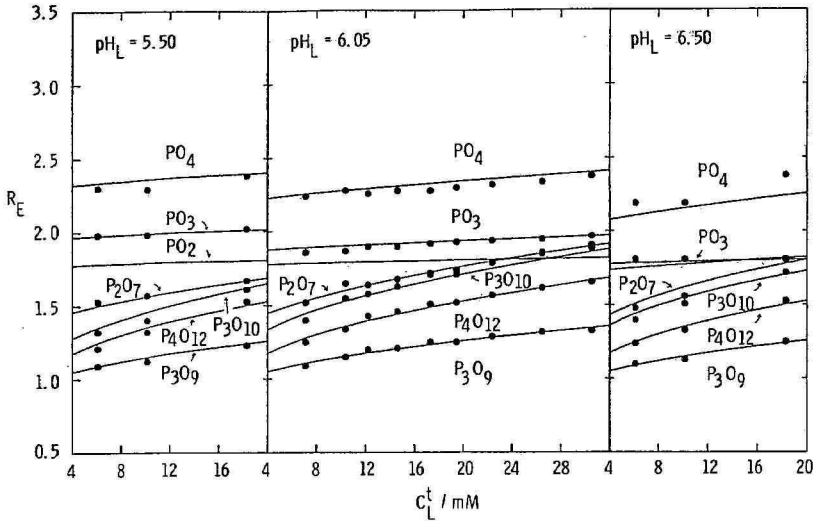

Fig. 5. C_L^t dependence of the observed R_E values (●) of six POAs. pH buffer, histidine. The curves show the C_L^t dependence of simulated R_E values using best-fitted formation constants. For abbreviations, see Fig. 1.

the least-squares method. The experimental errors of the corrected R_E values were less than $0.05R_E$ unit at most.

For data processing and simulation, SIPS programs on SORD M223 MkIII and NEC PC9801E microcomputers were used[9]. For the least-squares method a SIPS-LSQ program on an NEC MS120 minicomputer was used. For plotting the figures, Watanabe Model WX4671 X–Y and Roland DG Model DXY-980 plotters were used.

RESULTS AND DISCUSSION

Fig. 5 shows the C_L^t dependence of the observed R_E values of the six POAs (black circles). The curves were plotted using the best-fitted constants discussed below. The simulated curve for $P^{I}O_2$, which was plotted considering no ion-pair, is also shown. In Fig. 5 the R_E values of $P^{V}{}_2O_7$, $P^{V}{}_3O_{10}$, $P^{V}{}_3O_9$ and $P^{V}{}_4O_{12}$ increase significantly with the increase in C_L^t and the increments of the R_E values are apparently larger than those in Fig. 3, confirming the formation of ion pairs at least for these POAs. The increments were different among the POAs, suggesting that the ion-pair formation constants may differ. In contrast to these POAs, the differences in the R_E values of both $P^{III}O_3$ and $P^{V}O_4$ between Figs. 3 and 5 are slight, suggesting that the abundances of the ion-pair species, *i.e.*, the formation constants, are small.

For the evaluation of the formation constants, the mobilities of the ion-pair species formed are necessary. Although the mobilities might be evaluated together with the formation constants by the least-squares method, the use of reasonably assumed mobilities may be more practical in order to reduce the number of different R_E values necessary. To obtain the mobilities, we previously used the correlation between the mobilities and the formula weights. It has become apparent that this

method can be utilized for given samples with similar chain molecular structure, such as normal carboxylic acids[10], but among the POAs considered, $P^{V}_3O_9$ and $P^{V}_4O_{12}$ have ring structures. Therefore, in this work the mobilities were determined on the basis of a simple relationship between the Stokes' radii of the ion-pair constituents and the ion pair itself, by analogy with the determination of the mobility of dipeptides from the constituent amino acids[11]. On the assumption that the ions are spherical and the ionic volume of the ion-pair species is equal to the sum of the volumes of the constituent POAs and histidine, the absolute mobilities of ion-pair species can be expressed as

$$m_i = (m_f^{-3} + m_{His}^{-3})^{-1/3} \cdot (Z + 1) \quad (6)$$

where m_f is the absolute mobility of free POA anions with ionic charge $-Z$ and m_{His} is the absolute mobility of histidine. Although the assumption used seemed to be rough, the mobilities of dipeptides obtained agreed with the observed values within 5% error[11]. For POA–histidine ion pairs the calculated values are given later in Table V.

Using the observed R_E values in Fig. 5, the ion-pair formation constants were evaluated by the least-squares method utilizing a simulation of the isotachophoretic steady state. The interacting POA anions could be limited considering the abundance of them in the pH range 5.5–6.5. Apparently, from Fig. 1A and from the pK_a values in Table II, the anions interacting with $P^{V}_3O_9$ and $P^{V}_4O_{12}$ are $P^{V}_3O_9^{3-}$ and $P^{V}_4O_{12}^{4-}$. However, for other POAs points of inflection are seen in the mobility–pH_L curves, suggesting that at least two anionic species of POA may interact with $HisH^+$. Therefore, in the evaluation of the formation constants the coexistence of some different ion-pair species was considered. For example, the possible ion pairs of $P^{V}_2O_7$ may

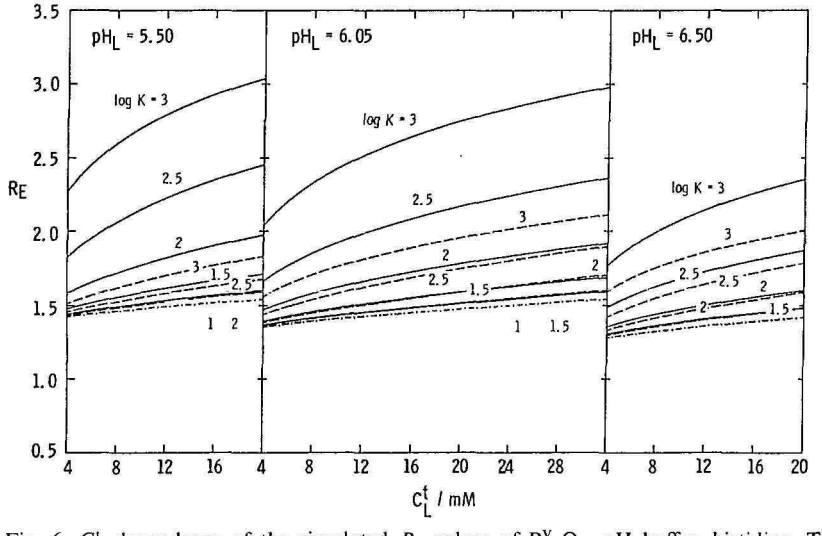

Fig. 6. C^t_L dependence of the simulated R_E values of $P^{V}_2O_7$. pH buffer, histidine. The formation of $(P^{V}_2O_7^{2-}\text{–}HisH^+)^-$ (solid curves) and $(P^{V}_2O_7^{3-}\text{–}HisH^+)^{2-}$ (broken curves) was assumed independently. . – . – . –, C^t_L dependence of simulated R_E values of $P^{V}_2O_7$ if no ion-pair interaction occurred.

be $(H_2P^V_2O_7^{2-}\text{–}HisH^+)^-$, $(HP^V_2O_7^{3-}\text{–}HisH^+)^{2-}$ and $(P^V_2O_7^{4-}\text{–}HisH^+)^{3-}$ considering the pK_a values of $H_4P^V_2O_7$ ions (1.9, 6.6, 9.6 for the 2−, 3− and 4− ions, respectively) and the pH_L values of 5.5–6.5. The abundance of $(P^V_2O_7^{4-}\text{–}HisH^+)^{3-}$ might be very small considering the abundance of $P^V_2O_7^{4-}$. For simplicity these three types of ion-pair species are abbreviated to type I, II and III, respectively.

Fig. 6 shows the C^t_L dependence of the simulated R_E values of $P^V_2O_7$ when the formation constants were varied in the range log K = 1–3. The pH_L values were 5.5, 6.05 and 6.50 and C^t_L was varied in the ranges 4–18, 4–30 and 4–20 mM, respectively. In Fig. 6 it is assumed that the type I $(H_2P^V_2O_7^{2-}\text{–}HisH^+)^-$ and type II $(HP^V_2O_7^{3-}\text{–}HisH^+)^{2-}$ ion-pair species are formed independently. The solid and broken curves show type I and II, respectively. Apparently from Fig. 6, for the type I ion pair, the increments of the R_E values decrease with increase in pH_L. In contrast, for the type II ion pair, the increments of the R_E values increase with increase in pH_L. These effects are due to the fact that the abundance of type I ion pairs decreases and those of type II ion pairs increases with increasing pH_L, suggesting that the predominant ion pairs may be determined by the observation of the C^t_L dependence of R_E values. As the experimental errors of the R_E values are less than $0.05R_E$ unit when appropriate internal standards are used, the lower limit of the formation constant that can be evaluated by the present method is log K = 1–1.5. For the type III ion pairs, the C^t_L dependence of the R_E values is very similar to that of type II ion pairs.

When the least-squares method was applied on the assumption that one of three types was selectively formed in the sample zone, the mean deviations of the R_E values in the least-squares method were 4.78%, 1.08% and 1.95%, respectively. The evaluated formation constants (log K) were 1.906, 2.544 and 6.451 for type I, II and III ion-pair species, respectively. Fig. 7 shows the C^t_L dependence of the simulated R_E values using the evaluated constants for these models, together with the observed

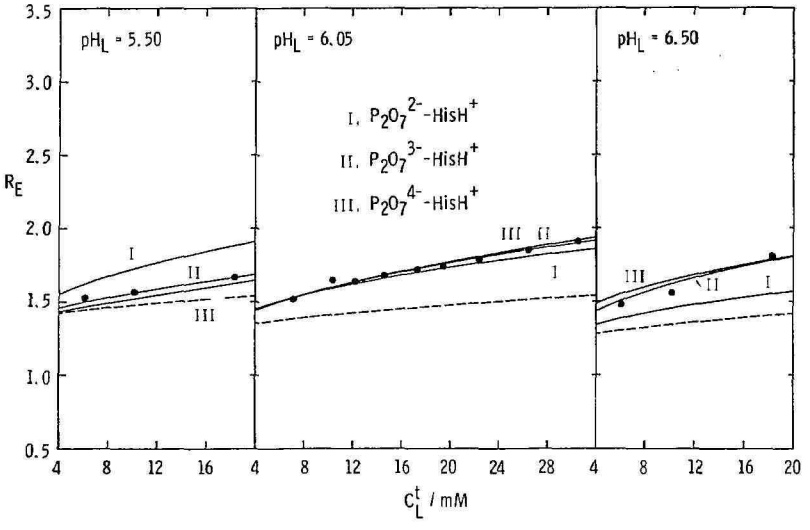

Fig. 7. C^t_L dependence of the observed R_E values of $P^V_2O_7$. pH buffer, histidine. The curves were plotted using the best-fitted formation constants on different assumptions concerning the ion-pair species: type 1, $(H_2P^V_2O_7^{2-}\text{–}HisH^+)^-$; type 2, $(HP^V_2O_7^{3-}\text{–}HisH^+)^{2-}$; and type 3, $(P^V_2O_7^{4-}\text{–}HisH^+)^{3-}$. The broken curves show the simulated effective mobility on the assumption that no ion-pair interaction occurred.

TABLE IV

OBSERVED AND BEST-FITTED R_E VALUES OF PHOSPHOROUS, PYROPHOSPHORIC AND TETRAMETAPHOSPHORIC ACIDS FORMING ION PAIRS WITH HISTIDINE, EFFECTIVE MOBILITIES AND CONCENTRATIONS OF ZONE CONSTITUENTS (25°C)

No. = Number of electrolyte system (see Table II); R_E = observed and best-fitted ratio of potential gradients, E_S/E_L; $\bar{m}_S$ = effective mobility of sample ion ($cm^2\ V^{-1}\ s^{-1}$) · 10^5; pH_S = pH of sample zone; C'_S = total concentration of sample ion (mM); P_f = abundance (%) of non-complexing POA; P_i = abundance (%) of ion-pair species, POA–$HisH^+$; $C'_{B,S}$ = total concentration (mM) of complexing agent (buffer); $\bar{m}_{B,S}$ = effective mobility of complexing ion ($cm^2\ V^{-1}\ s^{-1}$) · 10^5; I = ionic strength · 10^3.

Ion pair	*No.*	R_E			$\bar{m}_S$	pH_S	C'_S	P_f	P_i	$C'_{B,S}$	$\bar{m}_{B,S}$	I
		Observed	*Fitted*	*%*								
$(HP^{III}O_3^{2-}$–$HisH^+)^-$	1	1.98	1.98	0.24	38.3	5.63	4.59	4.20	0.43	6.50	19.8	4.97
	2	1.98	1.99	−0.42	37.5	5.63	7.61	4.42	0.69	10.8	19.4	8.29
	3	2.02	2.01	0.51	36.5	5.63	13.6	4.76	1.19	19.2	18.7	14.9
	4	1.86	1.89	−1.68	39.8	6.17	4.92	13.4	1.53	12.5	11.7	6.23
	5	1.87	1.90	−1.81	39.2	6.17	7.11	13.8	2.16	18.0	11.5	9.08
	6	1.90	1.91	−0.55	38.9	6.17	8.35	14.0	2.51	21.2	11.4	10.7
	7	1.90	1.92	−0.98	38.5	6.17	9.94	14.3	2.95	25.1	11.3	12.8
		Mean error 0.88%										
	8	1.92	1.93	−0.40	38.1	6.17	11.7	14.6	3.43	29.6	11.2	15.2
	9	1.93	1.93	−0.24	37.9	6.17	13.2	14.7	3.80	33.1	11.1	17.1
	10	1.94	1.94	−0.19	37.5	6.17	15.1	15.0	4.29	37.9	10.9	19.6
	11	1.95	1.96	−0.30	37.0	6.17	17.8	15.2	4.95	44.5	10.8	23.2
	12	1.97	1.97	0.12	36.6	6.17	20.4	15.5	5.59	51.0	10.6	26.8
	13	1.81	1.75	3.27	43.2	6.61	3.76	29.0	2.92	21.4	5.95	5.94
	14	1.81	1.77	1.98	42.1	6.61	6.20	29.9	4.58	35.0	5.80	9.90
	15	1.81	1.82	−0.32	40.4	6.61	11.0	30.9	7.50	61.4	5.56	17.8
		Mean error 0.87%										

$(HP^{V}_{2}O_{7}^{3-}–HisH^{+})^{2-}$	1	1.53	1.50	2.09	50.4	5.56	2.54	11.4	11.9	7.00	18.0	8.48
	2	1.57	1.56	0.50	47.8	5.56	4.18	11.7	17.6	11.4	16.6	14.0
	3	1.67	1.67	0.17	44.0	5.56	7.36	12.1	26.1	20.0	14.7	24.7
	4	1.52	1.53	−0.61	49.2	6.12	2.74	25.4	29.1	12.8	9.77	10.3
	5	1.65	1.60	3.01	46.6	6.12	3.94	24.4	36.0	18.3	8.98	14.7
	6	1.64	1.64	0.22	45.4	6.13	4.62	23.9	39.2	21.4	8.63	17.2
	7	1.68	1.68	0.07	44.0	6.13	5.49	23.3	42.7	25.3	8.25	20.3
	8	1.72	1.72	−0.17	42.7	6.13	6.47	22.6	46.0	29.8	7.90	23.8
	9	1.74	1.76	−0.88	41.7	6.14	7.24	22.2	48.3	33.2	7.66	26.6
	10	1.79	1.80	−0.37	40.6	6.14	8.29	21.6	51.1	37.9	7.38	30.3
	11	1.85	1.85	0.05	39.2	6.14	9.74	20.9	54.3	44.3	7.06	35.3
	12	1.91	1.90	0.67	38.0	6.15	11.2	20.3	56.9	50.7	6.79	40.3
	13	1.48	1.51	−1.83	50.1	6.57	2.22	37.6	37.9	21.5	4.86	9.17
	14	1.56	1.62	−3.74	46.1	6.58	3.68	33.4	47.7	35.0	4.32	14.7
	15	1.81	1.78	1.83	41.3	6.60	6.55	28.3	58.4	61.0	3.76	25.3
		Mean error 1.08%										
$(P^{V}_{4}O_{12}^{4-}–HisH^{+})^{3-}$	1	1.21	1.25	−3.09	60.6	5.55	1.63	46.8	53.2	7.30	12.8	12.9
	2	1.32	1.35	−2.47	55.2	5.56	2.73	39.9	60.1	11.9	11.6	20.7
	3	1.53	1.50	1.86	48.9	5.57	4.86	33.5	66.5	20.8	10.5	35.7
	4	1.25	1.28	−2.18	59.0	6.10	1.91	44.6	55.4	13.3	8.25	14.9
	5	1.34	1.36	−1.26	55.0	6.11	2.78	39.7	60.3	19.0	7.71	21.1
	6	1.43	1.40	2.43	53.2	6.11	3.27	37.7	62.3	22.2	7.50	24.5
	7	1.46	1.44	1.38	51.3	6.12	3.89	35.8	64.2	26.3	7.29	28.9
	8	1.51	1.49	1.61	49.5	6.12	4.60	34.1	65.9	30.9	7.10	33.9
	9	1.52	1.52	0.05	48.2	6.12	5.16	33.0	67.0	34.5	6.99	37.7
	10	1.57	1.56	0.51	46.7	6.13	5.91	31.7	68.3	39.4	6.85	43.0
	11	1.62	1.62	0.20	44.8	6.13	6.95	30.4	69.6	46.1	6.71	50.1
	12	1.66	1.67	−0.44	43.2	6.14	7.97	29.3	70.7	52.7	6.59	57.2
	13	1.24	1.25	−0.60	60.6	6.55	1.64	46.8	53.2	21.9	4.59	12.9
	14	1.33	1.35	−1.71	55.2	6.56	2.73	39.9	60.1	35.7	4.20	20.7
	15	1.53	1.50	1.85	48.9	6.57	4.86	33.5	66.5	62.4	3.85	35.7
		Mean error 1.44%										

R_E values. The broken curve indicates the C_L^i dependence of R_E values on the assumption that no ion-pair formation occurred. Apparently, even if any type of ion-pair species was assumed, the deviations for the nine R_E values observed at pH_L 6.05 were similar and the values for type I, II and III species were 1.71%, 0.67% and 0.85%, respectively. However, there were small but significant differences in the deviations for the three R_E values at pH_L 5.5 and 6.5. The deviations were 9.61% (type I), 0.89% (II) and 3.31% (III) for pH_L = 5.5 and 9.15% (I), 2.48% (II) and 3.90% (III) for pH_L = 6.5. These deviations suggest that the selective formation of type I ion pairs was not probable. However, no significant difference was found to support the selective formation of type II or III ion pairs, although the deviation for type II was slightly smaller than that for type III. The least-squares method was then applied on the assumption that the type II and III ion-pair species coexist in the sample zone. The mean deviation between the observed and best-fitted R_E values was 1.09% and was comparable to that for type II species. The evaluated formation constants were 2.540 and 3.583. The abundances of type II and III ion-pair species were 11.9 and 0.02% for electrolyte system No. 1 and 57.5 and 1.36% for No. 15, suggesting that the ion-pair species formed under the present electrolyte conditions can be consequently limited to type II, $(HP^{V}_2O_7^{3-}\text{–}HisH^+)^{2-}$. The formation constants were evaluated similarly for the other POAs, assuming several different ion pairs. The observed increase in the R_E values of $P^{III}O_3$, $P^{V}O_4$, $P^{V}_3O_{10}$, $P^{V}_3O_9$ and $P^{V}_4O_{12}$ could be elucidated by ion-pair formation, and the probable chemical forms were $(HP^{III}O_3^{2-}\text{–}$

TABLE V

ABSOLUTE MOBILITIES AND STABILITY CONSTANTS OF ION-PAIRS AMONG SIX PHOSPHORUS OXO ACIDS AND HISTIDINE (25°C)

$m_{2,i}$–$m_{5,i}$ = Absolute mobilities ($cm^2\ V^{-1}\ s^{-1}$) · 10^5 of monovalent–tetravalent ions; for all ion-pair species, $m_{1,i}$ = 0; log $K_{1,i}$–log $K_{5,i}$ = thermodynamic ion-pair formation constants.

Sample	$m_{2,i}$	$m_{3,i}$	$m_{4,i}$	$m_{5,i}$	*Log* $K_{1,i}$	*Log* $K_{2,i}$	*Log* $K_{3,i}$	*Log* $K_{4,i}$	*Log* $K_{5,i}$
$P^{I}O_2$					−1.5				
$P^{III}O_3$	24.7				*	1.459			
					−1.251	1.450			
$P^{V}O_4$	23.5	41.4			*	1.966	*		
					−1.572	1.972	*		
					*	1.488	8.963		
					−1.150	1.540	8.960		
$P^{V}_2O_7$	23.2	43.2	59.5		*	*	2.544	*	
					*	0.913	2.495	*	
					*	*	2.540	3.583	
					*	0.932	2.484	4.730	
$P^{V}_3O_{10}$	20.8	42.6	59.5	80.0	*	*	*	3.241	*
					*	*	−1.938	3.240	*
					*	*	−0.417	3.244	2.458
$P^{V}_3O_9$	–	46.7			*	*	1.591		
$P^{V}_4O_{12}$	–	42.9	61.9		*	*	*	2.704	

* Corresponding ion pairs are not considered. The dominant ion-pair species are $(HP^{III}O_3^{2-}\text{–}HisH^+)^-$, $(HP^{V}O_4^{2-}\text{–}HisH^+)^-$, $(HP^{V}_2O_7^{3-}\text{–}HisH^+)^{2-}$, $(P^{V}_3O_{10}^{4-}\text{–}HisH^+)^{3-}$, $(P^{V}_3O_9^{3-}\text{–}HisH^+)^{2-}$ and $(P^{V}_4O_{12}^{4-}\text{–}HisH^+)^{3-}$, respectively.

$HisH^+)^-$, $(HP^VO_4^{2-}–HisH^+)^-$, $(P^V_3O_{10}^{4-}–HisH^+)^{3-}$, $(P^V_3O_9^{3-}–HisH^+)^{2-}$ and $(P^V_4O_{12}^{4-}– HisH^+)^{3-}$, respectively.

Table IV gives the observed and the best-fitted R_E values, the effective mobilities and the concentrations of the zone constituents of $P^{III}O_3$, $P^V_2O_7$ and $P^V_4O_{12}$. The abundances of the ion-pair species are also given. Good agreement was obtained between the observed and the best-fitted R_E values. The largest mean error was 1.9% for $P^V_3O_{10}$. In Table IV the ion-pair species considered were unique, as discussed above. Table V also summarizes the formation constants evaluated for several different combinations of ion-pair species.

The accuracy of the evaluated formation constants was determined by the errors of both the calculated mobilities of the ion-pair species and the observed effective mobilities. The former is apparent from eqn. 2, as the products of the mobilities and the formation constants are closely related to the effective mobilities of POAs.

Assessment of separability

As discussed before, the separation of $P^V_3O_9$ and $P^V_4O_{12}$ was incomplete under the electrolyte conditions C^t_L = 10 m*M* and pH_L = 5.5 when 3-methylpyridine buffer was used. For the separation of these POAs using the 3-methylpyridine system, the use of a leading electrolyte with a higher C^t_L, *e.g.*, 20 m*M* at pH_L 5.5, may be suitable. However, from the viewpoint of sensitivity of detection the use of a leading ion at a high concentration is not desirable, as the zone length become shorter with increase in C^t_L.

Fig. 8 shows the C^t_L dependence of the simulated effective mobilities of the seven POAs coexisting with histidine. As mentioned before, the seven POAs have been separated using a leading electrolyte (C^t_L = 10 m*M*) at pH 5.5[1]. By comparison with Figs. 4 and 8, it was apparent that the selected pH_L and C^t_L conditions[1] were suitable for the separation of the seven POAs, especially $P^V_3O_9$ and $P^V_4O_{12}$.

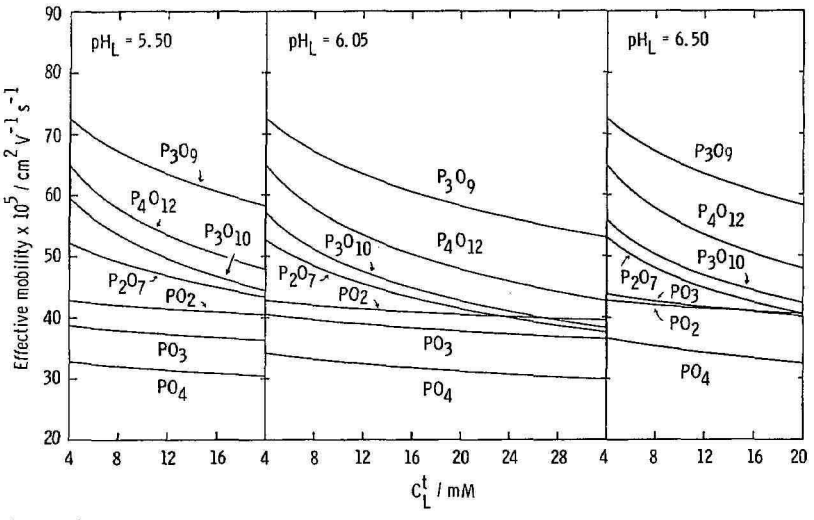

Fig. 8. C^t_L dependence of the simulated effective mobilities of seven POAs forming ion pairs with histidine. For abbreviations, see Fig. 1.

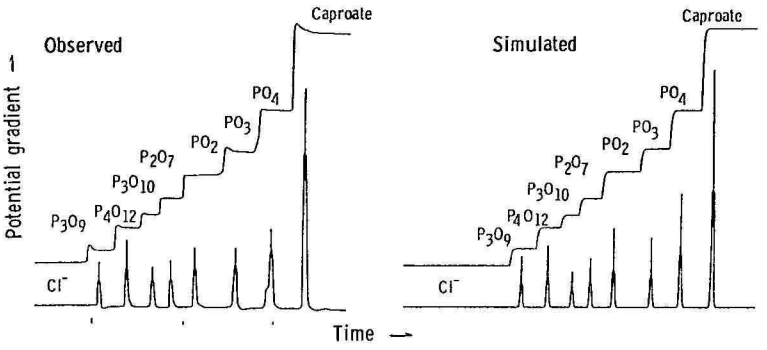

Fig. 9. Simulated and observed isotachopherograms of seven POAs at pH_L = 5.5 (histidine buffer). Leading ion, 10 m*M* chloride; terminator, caproic acid. The observed isotachopherogram is the linear trace as reported by Yagi *et al.*[1]. Current, 50 μA.

Fig. 9 shows the simulated isotachopherograms of the seven POAs under the above electrolyte conditions using the evaluated formation constants, together with the observed isotachopherogram. The observed isotachopherogram is that reported by Yagi *et al.*[1]. Good agreement was obtained. The *PU* values of $P^{V}{}_3O_9$, $P^{V}{}_4O_{12}$, $P^{V}{}_3O_{10}$, $P^{V}{}_2O_7$, $P^{I}O_2$, $P^{III}O_3$ and $P^{V}O_4$ given by Yagi *et al.* were converted into R_E values using the following equation:

$$R_E = PU[R_E(T) - 1] + 1 \tag{7}$$

where $R_E(T)$ is the R_E value of the terminating caproic acid. The results are summarized in Table VI together with the simulated R_E values. The agreement was good when ion-pair formation was considered.

In conclusion, the separation of the seven oxo acids with the histidine system could be elucidated as the result of a decrease in the effective mobilities accompanied by ion-pair formation, suggesting that the choice of buffer ions and the concentration adjustment are very important in isotachophoresis, in addition to the pH of the leading electrolyte.

TABLE VI

OBSERVED AND SIMULATED QUALITATIVE INDICES AT pH_L = 5.5 BUFFERED BY HISTIDINE AND 3-METHYLPYRIDINE

System	*Indices*	P_3O_9	P_4O_{12}	P_3O_{10}	P_2O_7	PO_2	PO_3	PO_4
Histidine (ion pair)	Reported *PU**	0.074	0.170	0.233	0.305	0.394	0.498	0.661
	Converted R_E	1.15	1.34	1.47	1.61	1.79	2.00	–
	Simulated R_E	1.14	1.35	1.42	1.56	1.79	1.99	2.31
3-Methylpyridine (no ion pair)	Observed R_E	1.09	1.11	1.25	1.48	1.76	1.98	2.28
	Simulated R_E	1.08	1.12	1.24	1.47	1.79	1.98	2.32

* Ref. 1.

ACKNOWLEDGEMENT

The authors thank Dr. Ohashi at Kyushu University for providing the samples of sodium tri- and tetrametaphosphates.

REFERENCES

1 T. Yagi, K. Kojima, H. Nariai and K. Motooka, *Bull. Chem. Soc. Jpn.*, 55 (1982) 1831.
2 T. Hirokawa, S. Kobayashi and Y. Kiso, *J. Chromatogr.*, 318 (1985) 195.
3 T. Hirokawa and Y. Kiso, *J. Chromatogr.*, 257 (1983) 197.
4 T. Hirokawa and Y. Kiso, *J. Chromatogr.*, 260 (1983) 225.
5 *Landolt-Bornstein, Zahlenwerte und Funktionen*, 6 Aufl., Bd. II, Teil 7, Springer-Verlag, Berlin, 1960.
6 R. A. Robinson and R.H. Stokes, *Electrolyte Solutions*, Butterworths, London, 1959.
7 C. Long (Editor), *Biochemist's Handbook*, Spon, London, 1961.
8 T. Hirokawa, M. Nishino and Y. Kiso, *J. Chromatogr.*, 252 (1982) 49.
9 T. Hirokawa and Y. Kiso, *Shimadzu Kagaku Kikai News*, 25 (1984) 24.
10 Y. Kiso and T. Hirokawa, *Chem. Lett.*, (1984) 24.
11 T. Hirokawa, T. Gojo and Y. Kiso, *J. Chromatogr.*, 390 (1987) 201.

Journal of Chromatography, 410 (1987) 297–318
Elsevier Science Publishers B.V., Amsterdam — Printed in The Netherlands

CHROM. 20 006

CAPILLARY GAS CHROMATOGRAPHIC–ELECTRON CAPTURE DETECTION OF COCA-LEAF-RELATED IMPURITIES IN ILLICIT COCAINE: 2,4-DIPHENYLCYCLOBUTANE-1,3-DICARBOXYLIC ACIDS, 1,4-DIPHENYLCYCLOBUTANE-2,3-DICARBOXYLIC ACIDS AND THEIR ALKALOIDAL PRECURSORS, THE TRUXILLINES

JAMES M. MOORE*, DONALD A. COOPER, IRA S. LURIE, THEODORE C. KRAM, SUSAN CARR, CHARLES HARPER and JOANNE YEH*

Special Testing and Research Laboratory, Drug Enforcement Administration, 7704 Old Springhouse Road, McLean, VA 22102-3494 (U.S.A.)

(First received August 3rd, 1987; revised manuscript received August 31st, 1987)

SUMMARY

A method has been developed that allows for the detection of the eleven stereoisomers of diphenylcyclobutanedicarboxylic acid in illicit cocaine samples, including α-, γ-, and ε-truxillic acids and β- and δ-truxinic acids. These, and other carboxylic acids, were also detected as ester moieties of alkaloidal impurities in illicit cocaine as well as in alkaloids of the South American coca leaf, *e.g.*, α- and β-truxilline. After lithium aluminum hydride reduction of the acidic and basic extracts of a prepared sample, the reduced species were derivatized with heptafluorobutyric anhydride in the presence of pyridine. The heptafluorobutyryl derivatives of the reduced diphenylcyclobutanedicarboxylic compounds were easily detected on-column at low picogram levels using a moderately polar fused-silica capillary column in the splitless mode and interfaced with a ^{63}Ni electron-capture detector.

INTRODUCTION

We report the sensitive gas chromatographic (GC) detection of five stereoisomers of diphenylcyclobutanedicarboxylic (truxillic and truxinic) acid and their alkaloidal precursors, the truxillines, in illicit cocaine samples. We have also detected these truxilline alkaloids, namely, α-, β-, γ-, δ- and ε-truxilline, in a sample of Bolivian coca leaves. We also offer strong presumptive evidence for the presence of the remaining possible truxillines, namely, *epi*-, *peri*-, *neo*-, μ-, ω- and ζ-truxilline, in coca leaves and illicit cocaine samples (Figs. 1–3). This was accomplished by the application of a capillary gas chromatographic–electron capture detection (CGC–ECD)

* Cooperative student, Department of Chemistry, Rochester Institute of Technology, Rochester, New York, NY 14623-0877, U.S.A.

0021-9673/87/$03.50

method, used previously for the determination of acidic and neutral manufacturing impurities in illicit heroin[1], and modified for this study. When using the modified methodology, it was noted that all illicit cocaine samples examined yielded peak-enriched chromatograms when acidic extracts of these samples were subjected to lithium aluminum hydride ($LiAlH_4$) reduction, derivatization with heptafluorobutyric anhydride (HFBA) and CGC–ECD analyses. Furthermore, when the basic extracts of these samples were treated by the same methodology, a significant increase in the chromatographic response for the same peaks was noted, when compared to the acidic extracts. After subjecting the basic extract of a cocaine sample to acid hydrolysis and methyl esterification, analysis using capillary gas chromatography–mass spectrometry (CGC–MS) yielded a series of closely eluting compounds, all having an apparent molecular weight of 324. A cursory examination of the mass spectra suggested that these compounds were stereoisomers of diphenylcyclobutanedicarboxylic (DPCBDC) acid dimethyl ester. The foregoing evidence suggested that the basic extracts of the cocaine samples contained coca alkaloids consisting, in part, of esters of isomeric DPCBDC acids. It followed, then, that the acid extracts of these samples were comprised, in part, of "free" isomeric DPCBDC acids, the probable result of hydrolysis of the respective precursor alkaloidal compounds during the manufacturing process.

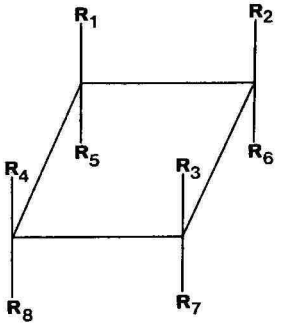

Fig. 1. Structures of the truxillic and truxinic acids and the truxillines. Truxillic and truxinic acids: (1) α-truxillic, $R_1=R_7=$ COOH, $R_4=R_6=$ phenyl, $R_2=R_3=R_5=R_8=$ H; (2) β-truxinic, $R_5=R_6=$ COOH, $R_3=R_4=$ phenyl, $R_1=R_2=R_7=R_8=$ H; (3) δ-truxinic, $R_2=R_5=$ COOH, $R_4=R_7=$ phenyl, $R_1=R_3=R_6=R_8=$ H; (4) ε-truxillic , $R_5=R_7=$ COOH, $R_2=R_4=$ phenyl, $R_1=R_3=R_6=R_8=$ H; (5) μ-truxinic, $R_1=R_6=$ COOH, $R_4=R_7=$ phenyl, $R_2=R_3=R_5=R_8=$ H; (6) γ-truxillic, $R_1=R_3=$ COOH, $R_4=R_6=$ phenyl, $R_2=R_5=R_7=R_8=$ H; (7) *neo*-truxinic, $R_2=R_5=$ COOH, $R_3=R_4=$ phenyl, $R_1=R_6=R_7=R_8=$ H; (8) ζ-truxinic, $R_5=R_6=$ COOH, $R_4=R_7=$ phenyl, $R_1=R_2=R_3=R_8=$ H; (9) *epi*-truxillic, $R_1=R_7=$ COOH, $R_2=R_4=$ phenyl, $R_3=R_5=R_6=R_8=$ H; (10) *peri*-truxillic, $R_1=R_3=$ COOH, $R_2=R_4=$ phenyl, $R_5=R_6=R_7=R_8=$ H; (11) ω-truxinic, $R_1=R_2=$ COOH, $R_3=R_4=$ phenyl, $R_5=R_6=R_7=R_8=$ H. Truxillines (see Scheme I for structure of representative truxilline): (1) α-, $R_1=R_7=$ methyl ecgonine ester, $R_4=R_6=$ phenyl, $R_2=R_3=R_5=R_8=$ H; (2) β-, $R_5=R_6=$ methyl ecgonine ester, $R_3=R_4=$ phenyl, $R_1=R_2=R_7=R_8=$ H; (3) δ-, $R_2=R_5=$ methyl ecgonine ester, $R_4=R_7=$ phenyl, $R_1=R_3=R_6=R_8=$ H; (4) ε-, $R_5=R_7=$ methyl ecgonine ester, $R_2=R_4=$ phenyl, $R_1=R_3=R_6=R_8=$ H; (5) μ-, $R_1=R_6=$ methyl ecgonine ester, $R_4=R_7=$ phenyl, $R_2=R_3=R_5=R_8=$ H; (6) γ-, $R_1=R_3=$ methyl ecgonine ester, $R_4=R_6=$ phenyl, $R_2=R_5=R_7=R_8=$ H: (7) *neo*-, $R_2=R_5=$ methyl ecgonine ester, $R_3=R_4=$ phenyl, $R_1=R_6=R_7=R_8=$ H; (8) ζ-, $R_5=R_6=$ methyl ecgonine ester, $R_4=R_7=$ phenyl, $R_1=R_2=R_3=R_8=$ H; (9) *epi*-, $R_1=R_7=$ methyl ecgonine ester, $R_2=R_4=$ phenyl, $R_3=R_5=R_6=R_8=$ H; (10) *peri*-, $R_1=R_3=$ methyl ecgonine ester, $R_2=R_4=$ phenyl, $R_5=R_6=R_7=R_8=$ H; (11) ω-, $R_1=R_2=$ methyl ecgonine ester, $R_3=R_4=$ phenyl, $R_5=R_6=R_7=R_8=$ H.

The configurations of the eleven possible isomeric DPCBDC acids, *i.e.*, truxillic (2,4-diphenylcyclobutane-1,3-dicarboxylic) and truxinic (1,4-diphenylcyclobutane-2,3-dicarboxylic) acids, have been well-elucidated[2]. Acids of this structure were first reported by Hesse[3] and Liebermann[4] in the late nineteenth century. They reported the presence of α-truxillic and β-isotruxillic (β-truxinic) acids as constituents of the alkaloids accompanying cocaine in the coca leaf. These alkaloids were named α- and β-truxilline. As is the case with the DPCBDC acids, there are theoretically eleven possible truxilline-type alkaloids comprised of esters of methyl ecgonine and the DPCBDC acids. The structures of the isomeric DPCBDC acids and truxillines are illustrated in Fig. 1. As seen in Fig. 1, each truxilline is comprised of two methyl ecgonine moieties present as esters of a DPCBDC acid. For the purpose of consistency and clarity, we have adopted the terminology used by Uff[2] to describe the configurations of the DPCBDC moiety.

Since the early investigations of Hesse and Liebermann, little has been reported on the presence of additional DPCBDC acids or truxillines in either coca leaves or illicit cocaine samples. Recent comprehensive reviews and studies[5–9] have discussed the presence in coca leaves of well-known alkaloids such as α- and β-truxilline, *cis*- and *trans*-cinnamoylcocaine, tropacocaine, hygrine and cuscohygrine as well as more recently identified alkaloids such as 3β-benzoyloxynortropane, 3α-benzoyloxytropan-6β-ol, 3-phenylacetoxynortropan-6-ol and alkaloidal esters involving trimethoxybenzoic acid. The lack of literature relating to the characterization of DPCBDC acids and truxillines in illicit cocaine and coca leaves is not entirely surprising. The combination of low levels of individual truxillines (<0.01–1%, relative to cocaine) in cocaine samples and the difficulty associated with the chromatographic resolution of these isomers have precluded their characterization until now.

In this study, the truxillines and truxillic and truxinic acids were reduced with $LiAlH_4$ to their respective alcohols, which were derivatized with HFBA to yield electrophiles that were suitable for chromatography on a moderately polar, fused-silica capillary column and sensitive detection using an electron capture detector. We report quantitative data for α-, β-, γ- and ε-truxilline in Bolivian coca leaves and approximate quantitative results for the remaining truxillines. This investigation also reports on the approximate levels of truxillines in 35 illicit cocaine hydrochloride samples. The extraction efficiencies of various methodologies for the isolation of truxillines in coca leaves is determined and the possibility of artifact formation discussed. The presence of other alkaloids in coca leaves and illicit cocaine hydrochloride samples is reported. Characterization of the truxillic and truxinic acids and their precursor truxillines was accomplished by CGC–ECD, high-performance liquid chromatography–photodiode array (HPLC–PDA) detection, ^1H nuclear magnetic resonance (^1H NMR) spectrometry, MS, including CGC–negative/positive chemical ionization (CGC–NPCI) and CGC–electron ionization (CGC–EI) and high-resolution MS (HR-MS) and by comparison to reference standards.

EXPERIMENTAL

Instrumentation

Low-resolution electron ionization (EI) and chemical ionization (CI) mass spectra were acquired on a Finnigan MAT Model 4630 (San Jose, CA, U.S.A.) qua-

drupole mass spectrometer. The GC–MS system was fitted with a 15 m × 0.25 mm I.D. fused-silica capillary column coated with DB-1701 (J & W Scientific, Rancho Cordova, CA, U.S.A.) at a film thickness of 1.0 μm. Sample injection was accomplished with an on-column injector (J & W Scientific) at a helium carrier velocity of 40 cm/s. All EI data were acquired at an ionization potential of 60 eV and with the source temperature at 120°C. Negative chemical ionization (NCI) data were acquired via CGC introduction of sample with methane containing trace levels of water as the reagent gas. Positive chemical ionization (PCI) data were acquired using reagent gases of methane–water, isobutane and ammonia at source pressures of 0.35, 0.50 and 0.30 Torr, respectively (uncorrected). Under PCI operation the methane–water reagent gas was adjusted to give a H_3O^+ to CH_5^+ ratio of one and the source pressure was maintained at 0.35 Torr. Source temperatures were set to 80°C for NCI and to 140°C for PCI operation. Sample introduction under PCI operation was either CGC or desorption probe. Desorption probe parameters were 0.1 A for 90 s and then increased to 0.5 A at 0.05 A/s.

HR-MS data were obtained with a Finnigan MAT Model 8230 (Bremen, F.R.G.) double-focusing GC–MS system operating at an ionization potential of 70 eV. Sample introduction was accomplished with a solids probe. Source temperature was 175°C and data were acquired at a resolution of 10000 (5% valley).

^{1}H NMR spectra were collected as 32K transforms at 200 MHz using an NT-200 spectrometer (General Electric) equipped with a 293A′ pulse programmer and 1180 data system. Compounds were examined as 0.01–0.03 *M* solutions in deuterochloroform, with tetramethylsilane as internal reference standard. Chemical shifts and coupling constants were calculated with the aid of the GE ITRCAL 1180 (spectrum simulation) program, an adaption of LAOCN3[10,11].

For the analytical HPLC separations, a Series 4 liquid chromatograph (Perkin Elmer, Norwalk, CO, U.S.A.), an ISS 100 autosampler fitted with a 150-μl loop (Perkin Elmer), an HS-5 C_{18} column (12.5 cm × 4.6 mm I.D.), a Model 1040A photodiode array HPLC detection system (Hewlett-Packard, Waldbronn, F.R.G.) and two Model LCI-100 laboratory computing integrators interfaced to a Model 7500 data station, equipped with Chromatographics 3 and solvent optimization software (SOS) (Perkin-Elmer), were used.

For the preparative HPLC separations, a Model 8800 four-solvent gradient system fitted with a preparative head, and equipped with an oven, was used. Also used were an injector valve fitted with a 40-ml loop (Valco, Houston, TX, U.S.A.), a preparative C_{18} column (25 cm × 22 mm I.D.) (Perkin-Elmer), a Model LC85 variable-wavelength UV detector containing an 8.0-μl flow cell (Perkin-Elmer) in series with a Model 401 differential refractometer (Waters Assoc., Milford, MA, U.S.A.), a Model FC 100 fraction collector (Gilson, Middletown, WI, U.S.A.) and an Omniscribe dual-pen recorder (Houston, TX, U.S.A.). For the isolation of *cis*-cinnamoylcocaine a mobile phase of acetonitrile–phosphate buffer (30:70) was used at ambient temperature at a flow-rate of 25.0 ml/min. The phosphate buffer consisted of 870 parts water, 30 parts 2 *M* sodium hydroxide and 10 parts 85% phosphoric acid. The preparative separation of the DPCBDC acid dimethyl esters was accomplished using a mobile phase of acetonitrile–tetrahydrofuran–water (21:14.6:63.6) at a flow-rate of 25.0 ml/min and a temperature of 50°C.

For the analytical preparative HPLC separations, a Series 4 liquid chromato-

graph was used with an injector valve fitted with a 2-ml loop (Rheodyne, Cotati, CA, U.S.A.), an HS-5 C_{18} column (12.5 cm × 4.6 cm I.D.), a Model LC 85B variable-wavelength UV detector containing a 1.5-μl flow cell (Perkin-Elmer) and a Model 56 recorder (Perkin-Elmer). The mobile phase consisted of acetonitrile–tetrahydrofuran–water (21.8:14.6:63.6) at a flow-rate of 1.5 ml/min and at ambient temperature.

CGC-flame ionization detection (CGC–FID) analysis was done on a Hewlett-Packard 5880A gas chromatograph fitted with a 30 m × 0.25 mm I.D. fused-silica capillary column coated with DB-1 (J & W Scientific) at a film thickness of 0.25 μm. The oven temperature was multilevel programmed as follows: (level 1) initial temperature, 180°C, initial hold, 1.0 min; temperature program rate, 4°C/min; final temperature, 280°C; final hold, 1.0 min; (level 2) temperature program rate, 20°C/min; final temperature, 320°C. A split injection of 40:1 was used at a hydrogen carrier velocity of 55 cm/s.

Gas chromatography–electron capture detection

All chromatograms were generated in the splitless mode with a Hewlett-Packard 5880A gas chromatograph fitted with a 30 m × 0.25 mm I.D. fused-silica capillary column coated with DB-1701 (J & W Scientific) at a film thickness of 0.25 μm. The gas chromatograph was equipped with a ^{63}Ni electron-capture detector (15 mCi) and interfaced with a Hewlett-Packard Level IV data processor. The oven temperature was multilevel programmed as follows: (level 1) initial temperature, 90°C, initial hold, 1.6 min; temperature program rate, 25°C/min; final temperature, 160°C; final hold, 1.0 min; (level 2) temperature program rate, 4.0°C/min; final temperature, 275°C; final hold, 5.0 min. Injector and detector temperatures were maintained at 275°C and 300°C, respectively. Hydrogen (Zero Grade, Air Products, Tamaqua, PA, U.S.A.) was used as the carrier gas at a velocity of about 40–45 cm/s and measured for isooctane at an oven temperature of 90°C. An argon–methane (95:5) mixture (Air Products) was used as the detector make-up gas at a flow-rate of about 35 ml/min. The septa used were Thermogreen LB-2 (Supelco, Bellefonte, PA, U.S.A.). The illustrated chromatograms were recorded at a chart speed of 1.0 cm/min and at an attenuation of 2^6. During the splitless injection the solvent was vented after a 1.0-min hold.

Reagents and solvents

All solvents, including pyridine, were distilled-in-glass products of Burdick & Jackson Labs. (Muskegon, MI, U.S.A.) and were peroxide- and preservative-free. HFBA, supplied in 1-ml sealed glass ampuls, was obtained from Pierce (Rockford, IL, U.S.A.). $LiAlH_4$ in diethyl ether (1.0 *M*) was a product of Aldrich (Milwaukee, WI, U.S.A.). Aluminum oxide, activated, basic, Brockmann 1 (standard grade, *ca.* 150 mesh) was supplied by Aldrich. Methyl-8 and Methyl-8 (deuterated) were products of Pierce. Boron trifluoride–methanol was obtained from Aldrich. All other chemicals were reagent grade quality.

Glassware

Unless otherwise noted, all extractions were carried out in 15-ml graduated, conical, glass-stoppered centrifuge tubes.

Standards

The instrumental internal standard, aldrin, was supplied by Supelco. The methodology internal standards, C_{13}, C_{15}, C_{17}, C_{19} and C_{21} straight-chain fatty acids and their methyl esters, were obtained from Alltech Assoc. (Deerfield, IL, U.S.A.). *trans*-Cinnamic acid was a product of Aldrich. All drug standards were obtained from this laboratory and were part of an authenticated reference collection.

The truxillic and truxinic acid standards were prepared in our laboratory using modifications of existing procedures[12–17]. When necessary the dimethyl ester of the DPCBDC acid was prepared using either methanol–hydrochloric acid, boron trifluoride–methanol or Methyl-8. See Fig. 1 for the structures of the truxillic and truxinic acids and their corresponding truxillines. All DPCBDC standards were subjected to ^{1}H NMR and/or CGC–MS for verification of structure. Tables III and IV list ^{1}H NMR and low- and high-resolution mass spectral data for some of the DPCBDC acid dimethyl esters.

Internal standards solutions

Methodology internal standards solutions were prepared as follows. (a) Solution A: an acetone solution containing the methyl esters of C_{13}, C_{15}, C_{17}, C_{19} and C_{21} straight-chain fatty acids, each at a concentration of 0.80 mg/ml, was prepared. (b) Solution B: a four-fold dilution of solution A with acetone was prepared. (c) Solution C: an acetone solution containing C_{13}, C_{15}, C_{17}, C_{19} and C_{21} straight-chain fatty acids, each at a concentration of 0.20 mg/ml, was prepared. The instrumental internal standard, aldrin, was prepared at a concentration of 200 pg/μl in isooctane.

Truxillic and truxinic acids and their dimethyl esters standard solutions

Individual methanolic solutions of the DPCBDC acids and/or their dimethyl esters, each at a concentration of 1.0 mg/ml, were prepared. Further serial dilutions with methanol were prepared as needed.

Determination of truxillic and truxinic acids and truxillines in illicit cocaine hydrochloride and base samples

Truxillic and truxinic acids. An amount of unadulterated sample equivalent to about 50 mg of cocaine was dissolved in 5 ml of 0.1 *N* sulfuric acid in a centrifuge tube. To the tube was added 50 μl of internal standards solution C. After vortex mixing, the solution was extracted with three 5-ml aliquots of diethyl ether, passing each extract through anhydrous sodium sulfate into a centrifuge tube and evaporating to dryness. To the residue was added 200 μl of chloroform and, with occasional vortex mixing, heated at 75°C for 3 min to dissolve the residue. To the tube was added 4.0 ml of anhydrous diethyl ether (kept over 5 Å molecular sieve) and the contents vortexed thoroughly. After mixing, 0.20 ml of an ethereal solution of $LiAlH_4$ (1 *M*) was added to the tube. The contents of the tube were vortexed and the volume reduced to about 0.5 ml at 50 ± 2°C without the aid of air or nitrogen stream. To the tube was added 3 ml of diethyl ether that had been saturated with water. After vortex mixing, the solution was evaporated just to dryness at 75–85°C under a nitrogen stream. The residue was dissolved in 1 *N* sulfuric acid and the solution extracted with two 5-ml aliquots of diethyl ether, passing each extract through anhydrous sodium sulfate into a centrifuge tube. The combined ether extracts were evaporated

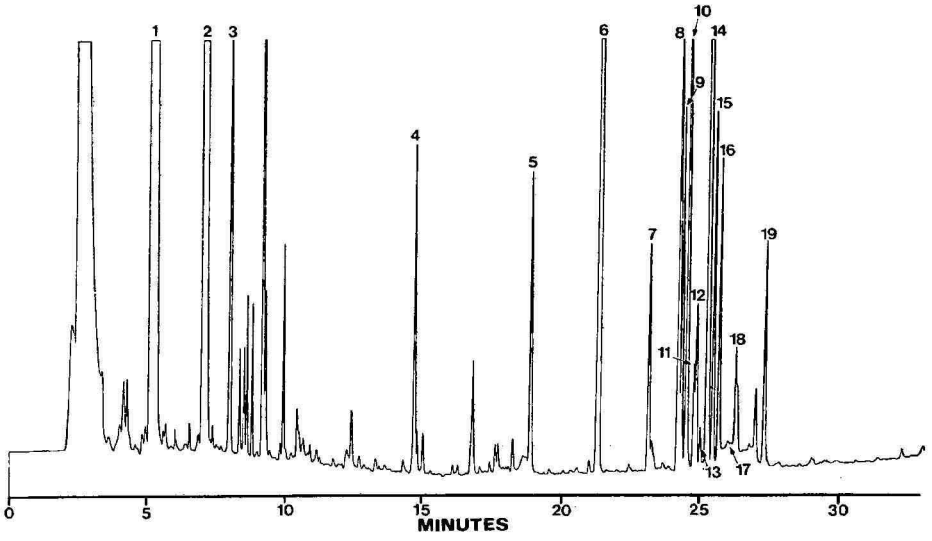

Fig. 2. CGC–ECD chromatogram of an illicit cocaine hydrochloride sample, illustrating the O-HFB derivatives of the $LiAlH_4$-reduced truxillines, cocaine, cinnamoylcocaines and internal standards. See Table II for retention times. All illustrated peaks (except internal standards) represent alkaloids isolated from the basic extract of an illicit cocaine hydrochloride sample and subjected to $LiAlH_4$ reduction, HFB derivatization and chromatography as either O-HFB or di-O-HFB derivatives. Identity of the peaks is as follows (Table II): 1 = cocaine; 2 = *cis*-cinnamoylcocaine + large amount of unidentified component; 3 = *trans*-cinnamoylcocaine; 4 = C_{15} internal standard (IS); 5 = C_{17} IS; 6 = aldrin IS; 7 = C_{19} IS; 8 = ε-; 9 = δ-; 10 = β-; 11 = *peri*-; 12 = *neo*-; 13 = *epi*-; 14 = α-; 15 = ω-; 16 = γ-; 17 = μ-; 18 = ζ- and 19 = C_{21} IS. The identification of peaks 11, 12, 13, 15, 17 and 18 is based on presumptive evidence. C_{13} is not illustrated. Final cocaine concentration = 0.067 mg/ml.

at 50–55°C under a nitrogen stream to a volume of about 1 ml. The 1 *N* sulfuric acid solution was extracted again with an additional 5-ml aliquot of diethyl ether, passing through sodium sulfate as before into the centrifuge tube. The combined ether extracts were evaporated as before but just to dryness (note: prolonged heating of the tube when dry may result in the loss of the more volatile, reduced species).

Without delay, to the residue in the tube was added 1.0 ml of acetonitrile and 50 μl of HFBA. After vortex mixing, the solution was heated at about 75°C for 10 min. To the tube was added 10 μl of pyridine and the heating continued for an additional 2 min. After cooling, 5.0 ml of isooctane (containing aldrin at 200 pg/μl) and 5 ml of a saturated aqueous solution of sodium bicarbonate were added to the tube. Without delay, the tube was shaken vigorously for 5–10 s and then centrifuged. About 2–3 μl of the isooctane layer was injected into the CGC–ECD system under conditions described previously.

Truxillines. After extraction of the truxillic and truxinic acids as described above, 250 μl of internal standards solution A was added to the 0.1 *N* sulfuric acid solution. After mixing, the solution was made basic by the addition of 3 ml of a saturated aqueous solution of sodium bicarbonate. After careful mixing, the alkaloids were extracted with four 5-ml aliquots of diethyl ether, filtering each extract through anhydrous sodium sulfate into a 25-ml volumetric flask and then diluting to volume

with diethyl ether. A 2-ml aliquot of the ethereal extracts was transferred to a centrifuge tube and evaporated to dryness. The residue was dissolved in 200 μl of chloroform and, after heating and vortex mixing, the sample was treated as described above for the truxillic and truxinic acids, beginning with "To the tube was added 4.0 ml of anhydrous diethyl ether ...", except an additional 3 × dilution with isooctane (containing aldrin) was made prior to injection. Fig. 2 illustrates a CGC–ECD chromatogram of an illicit South American cocaine hydrochloride sample subjected to analysis for truxillines and other alkaloids.

Determination of truxillines in coca leaves

Ten coca leaf samples, about 500–1000 g each, were collected in late October/early November, 1985, in four different cultivation areas of Bolivia. After drying, the leaves were reduced in size, using a mill, to pass a 10-mesh sieve, and then a portion of each used for a composite. The composite was further reduced to a powder with mortar and pestle.

About 5 g of the powdered coca leaf composite was accurately weighed, placed in a flask and heated at about 65°C with 50 ml of dimelthylsulfoxide (DMSO) for 1 h, with frequent mixing. The contents of the flask were filtered through paper in a Buchner funnel under vacuum. The coca leaf residue in the funnel was treated with additional aliquots of warm DMSO until a total of 100.0 ml of DMSO filtrate was collected. After cooling, and thorough mixing, a 6.0-ml aliquot of the coca leaf extract was transferred to a 50-ml centrifuge tube. After cooling the tube in ice water, 25 ml of 0.1 *N* sulfuric acid was added and the solution extracted with four 10-ml aliquots of diethyl ether, which were discarded. Sodium bicarbonate was added carefully to the solution to render it basic. The coca alkaloids were extracted with four 10-ml aliquots of diethyl ether, transferring the aliquots to a separatory funnel. To the

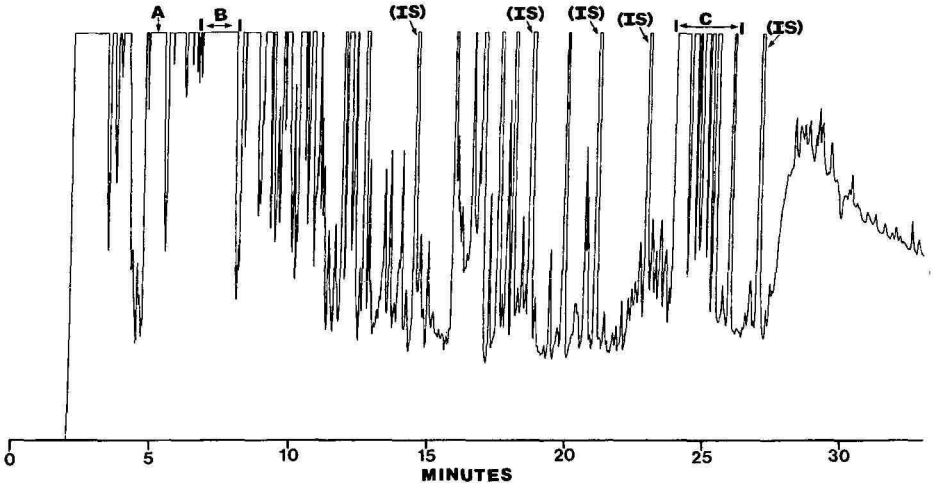

Fig. 3. CGC–ECD chromatogram of a concentrated alkaloidal extract of Bolivian coca leaves, illustrating the O-HFB derivatives of the $LiAlH_4$-reduced truxillines (C), the cinnamoylcocaines (B), cocaine (A), internal standards (IS) and unidentified alkaloids. Final cocaine concentration = 2.0 mg/ml. Most unlabeled peaks represent suspected, unknown coca alkaloids.

funnel was added 5.0 ml of 0.1 *N* sulfuric acid and the alkaloids extracted into the acid layer by mixing vigorously for 5–10 s. The acid layer was transferred to a centrifuge tube and the ether extracted with an additional 2 ml of 0.1 *N* sulfuric acid, transferring the latter extract to the same centrifuge tube. The combined acid extracts were extracted with a 5-ml aliquot of diethyl ether, which was discarded. To the acid solution was added 100 μl of internal standards solution B and then sodium bicarbonate was added carefully to render the solution basic. The coca alkaloids and internal standards were extracted with four 10-ml aliquots of diethyl ether, passing each extract through anhydrous sodium sulfate into a centrifuge tube and evaporating at 50–55°C under a nitrogen stream to dryness.

The residue in the centrifuge tube was dissolved in 200 μl of chloroform and, after heating and vortex mixing, the sample was treated as described previously for the truxillic and truxinic acids, beginning with "To the tube was added 4.0 ml of anhydrous diethyl ether ...", except an additional 5 × dilution with isooctane (containing aldrin) was made prior to injection. Fig. 3 illustrates a CGC–ECD chromatogram of Bolivian coca leaves subjected to analyses for truxillines and other alkaloids, except final 5 × dilution with isooctane is omitted.

Reduction and derivatization of truxillic and truxinic acids and/or their dimethyl ester standards

In order to optimize quantitative results for the truxillines in coca leaves reported in this study a technique of successive approximations was used. Based upon the results of an initial quantitative analysis, the quantities of DPCBDC standards subjected to reduction and derivatization were adjusted to more closely approximate the levels found in the cocaine sample. This was repeated until the CGC–ECD response of the standards were within 25% of the corresponding DPCBDC compounds found in the sample. For the quantitation of truxillines in coca leaves, aliquots of the appropriate DPCBDC acid or dimethyl ester standards were transferred to a centrifuge tube containing 80 μl of internal standards solution B. After evaporation to dryness, to the tube was added 200 μl of chloroform containing 4 mg of standard cocaine base. After heating and vortex mixing, the sample was treated as described previously for the analysis of truxillic and truxinic acids in illicit cocaine hydrochloride samples, beginning with "To the tube was added 4.0 ml of anhydrous diethyl ether ...", except a 3 × dilution with isooctane (containing aldrin) was made prior to CGC–ECD injection. Because the DPCBDC acid standards have lesser solubility in chloroform than their dimethyl ester counterparts, they were heated in chloroform (75°C), prior to the addition of anhydrous diethyl ether and $LiAlH_4$ reduction, for several minutes longer than the dimethyl ester standards.

For quantitative purposes, the C_{21} internal standard areas were used in all calculations. A multiplication factor of 2.2 was used to convert the DPCBDC acids to their respective truxillines.

Isolation of the truxillines from the bulk cocaine matrix

In order to isolate the truxillines from cocaine for further study, the following was done. An amount (0.5 g) of an unadulterated, illicit cocaine hydrochloride sample (cocaine content, 85–90%) was placed in a centrifuge tube, dissolved in 5 ml of 0.1 *N* sulfuric acid and then extracted with three 5-ml aliquots of diethyl ether to remove

the DPCBDC acids as well as other carboxylic acids. The solution was then made basic by the careful addition of 3 ml of a saturated aqueous solution of sodium bicarbonate. The cocaine, cinnamoylcocaine and truxilline alkaloids were extracted with four 5-ml aliquots of diethyl ether, passing each extract through anhydrous sodium sulfate into a centrifuge tube and evaporating to dryness. The residue was reconstituted in about 3 ml of diethyl ether–methylene chloride (60:40) and saved for chromatographic analysis described below.

A chromatographic column was prepared by packing 5.0 g of basic alumina (used directly from bottle without further treatment) into a 10-ml Mohr pipette (*ca.* 350 mm × 8 mm I.D.). The diethyl ether–methylene chloride from above was transferred to the head of the column. The column was then eluted with diethyl ether–methylene chloride (60:40), discarding the first 12 ml of eluate (contains bulk of cocaine and cinnamoylcocaines). The elution was continued with chloroform–acetone (60:40), collecting the next 32 ml of eluate (contains the truxillines and small amounts of cocaine and the cinnamoylcocaines). To further purify the truxilline fraction a second pass through the alumina column may be desirable. When a second pass was done, more than 99.9% of the cocaine was removed. The eluate containing the truxillines was saved for further study.

RESULTS AND DISCUSSION

Truxillines in coca leaves

During this study a number of extraction methods were evaluated to determine their suitability for the analysis of truxillines in coca leaves. The methods were: (a) Soxhlet extraction of coca leaves–sodium bicarbonate with chloroform for 20 h, (b) Soxhlet extraction of coca leaves–sodium bicarbonate–water (cakey consistency) with chloroform for 20 h, (3) Soxhlet extraction of coca leaves–sodium carbonate–water (cakey consistency) with chloroform for 20 h, (d) methanol extraction of leaves over-

TABLE I

QUANTITATIVE AND REPRODUCIBILITY DATA FOR THE DETERMINATION OF TRUXILLINES IN BOLIVIAN COCA LEAVES USING CGC–ECD

Cocaine content of coca leaves = 0.80%; *cis*- and *trans*-cinnamoylcocaine content of coca leaves = 6.8% and 5.9%, respectively, relative to the cocaine content. Numerical values given are % truxillines relative to the cocaine content. The data for α-, β-, ε-, and γ- are quantitative, whereas the data for the remaining truxillines are an approximation and are as follows: δ- = 0.8%, ω- = 0.2%, *neo*- = 0.2%, ζ- = 0.07%, *peri*- = 0.07%, *epi*- = 0.06% and μ- < 0.01%. The presence of *peri*-, *neo*-, *epi*-, ω-, μ- and ζ-truxilline is based on presumptive data.

Compound	*Replicate analysis**				
	1	*2*	*3*	*4*	*Average*
α-	1.33	1.46	1.29	1.43	1.38
β-	1.22	1.34	1.11	1.33	1.25
ε-	–	0.59	0.65	0.62	0.62
γ-	0.17	0.20	0.18	0.20	0.19

* Analysis was repeated four times over the period of one week.

night at ambient temperature, (e) DMSO extraction of leaves overnight at ambient temperature, (f) treatment of leaves with refluxing ethanol for 1 h and (g) treatment of leaves with warm (65°C) DMSO for 1 h. Methods d and e used continuous stirring overnight. All extractions were done on a Bolivian coca leaf composite whose individual members had been reduced in size to pass a 10-mesh sieve.

All of the above methods yielded at least ten of the eleven possible truxillines in similar ratios. However, they differed significantly in the total amounts of truxillines extracted. Methods f and g were found to be superior in terms of quantitative extraction, with method g being somewhat more efficient than method f. Furthermore, we believe the possibility of artifact formation is reduced when using DMSO *in lieu* of ethanol and the methods described above. For these reasons method g was selected as the procedure of choice for the extraction of the truxillines, as well as other alkaloids, from coca leaves.

The DMSO method was used to quantitate α-, β-. γ- and ε-truxilline in Bolivian coca leaves and to provide approximate quantitative data for the remaining truxillines, namely, δ-, μ-, *epi*-, *peri*-, *neo*-, ζ- and ω-, for which no standards were available at the time of quantitation. The analysis was repeated four times over the period of one week. The results are given in Table I. The approximate quantitative results were based upon the β-truxinic and γ-truxillic acid standards and assumed equal molar ECD response and linearity. As mentioned previously, to optimize the quantitative results, standard concentrations were adjusted, prior to analysis, to approximate closely the amounts of the corresponding truxillines in the sample. All sample extracts and standards were injected in triplicate and all results are relative to the cocaine content of the coca leaves. Fig. 3 illustrates the CGC–ECD chromatogram of an enriched alkaloidal extract of Bolivian coca leaves.

Truxillic and truxinic acids and truxillines in illicit cocaine hydrochloride samples

A total of 35 unadulterated, illicit cocaine hydrochloride samples were selected at random for truxillic and truxinic acids and truxilline analyses. The samples were seized from various countries of South, Central and North America. In all 35 samples the presence of truxillic and truxinic acids was easily determined. The presence of these DPCBDC acids in samples is believed due primarily to the hydrolysis of truxillines during the manufacturing process. A review of the chromatograms revealed that the ratios of some of the DPCBDC acids to one another did not correlate with the ratios of their parent truxillines. This indicated that some of the truxillines were more readily hydrolyzed than others. This was not surprising, given the fact that some truxilline configurations possesses more crowded steric conditions than others.

In the basic extracts of all samples, ten of the eleven possible truxillines were easily detected. In some samples the eleventh truxilline was seen. This truxilline, assigned the μ-configuration was, by far, the truxilline of least abundance in all samples (Fig. 2). This was rather surprising in that it possesses a configuration which appears to be thermodynamically more preferable when compared to other truxillines, *e.g.*, the ω-isomer. A review of all truxilline chromatograms revealed some variation in the ratio of the truxillines to one another. On the other hand, the total truxilline content varied significantly from sample to sample. It is not known at this time whether variations in truxilline ratios or in total truxilline content in these samples is due to the chemotaxonomic properties of the coca leaves used in the manu-

facture of the refined cocaine or due to the manufacturing process itself. We do believe it would be difficult indeed to remove significant quantities of truxillines from the cocaine using established clandestine South American cocaine manufacturing procedures. The levels and ratios of total truxillines in some samples were similar to that found in the sample of Bolivian coca leaves (Table I). Other cocaine hydrochloride samples had significantly lower total truxilline content, in some cases as much as 50 × lower. In all samples, α- and β-truxilline were the two isomers of greatest abundance. On the other hand, the μ-isomer was the truxilline of least abundance in all samples examined. Fig. 2 illustrates a typical cocaine chromatographic profile.

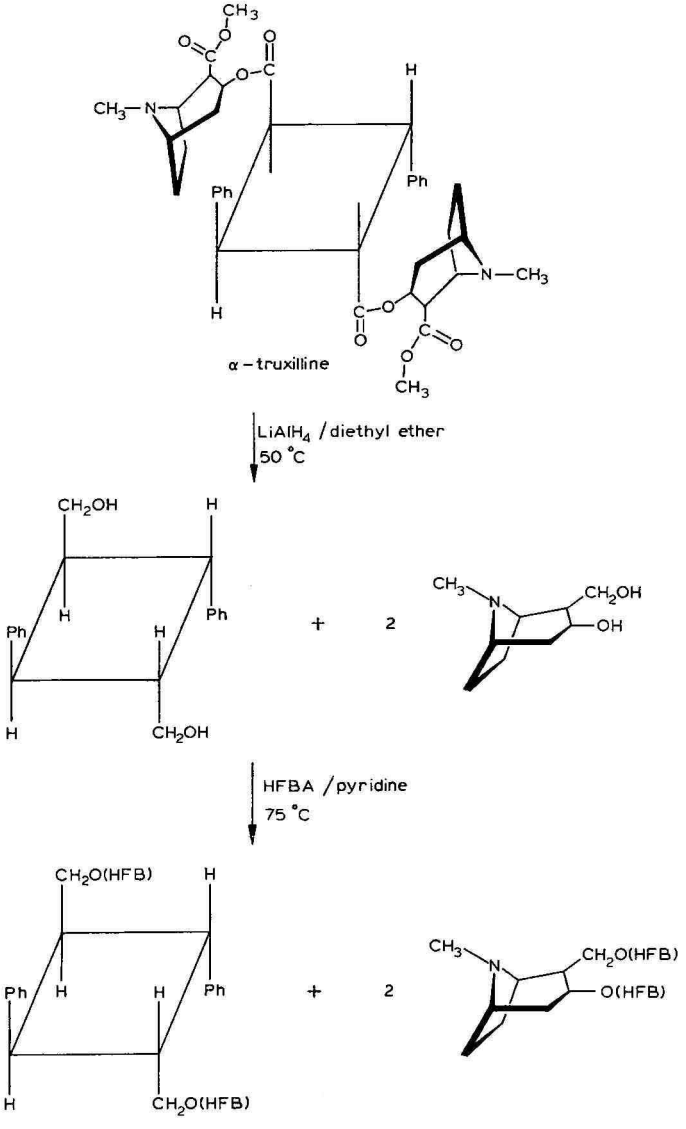

Scheme 1. α-Truxilline subjected to $LiAlH_4$ reduction and HFBA derivatization. Ph represents a phenyl group.

Reduction, derivatization and chromatography of the truxillines

We were unsuccessful in chromatographing the intact truxillines, isolated from the alumina column described previously, using CGC systems. Subsequent work using on-column injection into a CGC–MS system indicated that the truxillines were being degraded into their respective DPCBDC acids and methyl ecgonidine. This may explain, in part, why previous studies using GC systems did not report the presence of truxillines in coca leaf extracts. In our study we first reduced the truxillines, and DPCBDC acids, with $LiAlH_4$ to their respective diols, which were rendered ECD-sensitive by derivatization with HFBA (Scheme 1). The reduction and derivatization proceeded smoothly and in high yield. All HFB electrophiles exhibited good chromatography and could be easily detected on-column at low picogram levels. We investigated both a nonpolar column, namely, DB-1 and the moderately polar DB-1701. Using DB-1, only five major peaks representing the truxillines were apparent, whereas all eleven truxillines were detected on DB-1701, though not achieving baseline resolution for some of them (Fig. 2). Table II lists retention times for the truxillines, other coca alkaloids and the internal standards. The listed retention times are for the HFB or di-HFB derivative for the corresponding alcohol (Scheme 1).

TABLE II

CGC–ECD RETENTION TIMES FOR THE TRUXILLINES, OTHER COCA ALKALOIDS AND INTERNAL STANDARDS

All compounds, except aldrin, were subjected to $LiAlH_4$ reduction and HFBA derivatization followed by chromatography on DB-1701; retention times given are for the O-HFB or di-O-HFB derivatives of the corresponding alcohol.

Compound	*Retention time (min)*	*Compound*	*Retention time (min)*
Cocaine*	5.11	δ-Truxilline†	23.94
Tropacocaine**	6.78	β-Truxilline†	24.11
cis-Cinnamoylcocaine***	7.00	*peri*-Truxilline†,††	24.38
trans-Cinnamoylcocaine***	7.97	*neo*-Truxilline†,††	24.45
Ecgonine§	9.94	*epi*-Truxilline†,††	24.61
Methyl tridecanoate (C_{13})§§	10.84	α-Truxilline†	24.83
Methyl pentadecanoate (C_{15})§§	14.52	ω-Truxilline†,††	25.04
Methyl heptadecanoate (C_{17})§§	18.64	γ-Truxilline†	25.25
Aldrin§§§	21.01	μ-Truxilline†,††	25.51
Methyl nonadecanoate (C_{19})§§	22.82	ζ-Truxilline†,††	25.81
ε-Truxilline†	23.82	Methyl heneicosonoate (C_{21})§§	26.85

* Chromatographed as the O-HFB derivative of benzyl alcohol and the di-O-HFB derivative of $LiAlH_4$-reduced ecgonine (Scheme 1).

** Chromatographed as the O-HFB derivative of tropine.

*** Cinnamoylcocaines chromatographed as the O-HFB derivative of the corresponding cinnamyl alcohol.

§ Chromatographed as the di-O-HFB derivative of $LiAlH_4$-reduced ecgonine (Scheme 1).

§§ Fatty acids and their methyl esters used as methodology internal standards and chromatographed as the O-HFB derivative of the corresponding alcohol.

§§§ Instrumental internal standard.

† Chromatographed as the di-O-HFB derivative of the corresponding $LiAlH_4$-reduced truxilline (Scheme 1).

†† Identification based upon presumptive evidence.

Other coca alkaloids

In addition to the truxillines, we were able to detect other alkaloids, such as *cis*- and *trans*-cinnamoylcocaine, which elute early in the same chromatogram (Figs. 2 and 3). A review of all sample chromatograms revealed that the cinnamoylcocaine content varied widely. This was not surprising, given the fact that the South American process often includes a step which partially or fully oxidizes these species. This oxidation is believed to have less effect on the truxillines. When a concentrated coca leaf or illicit cocaine alkaloidal extract known to be enriched in truxillines was subjected to reduction and derivatization, the resultant CGC–ECD chromatogram revealed an additional 30–40 alkaloidal species. This is illustrated in Fig. 3 for a concentrated coca leaf alkaloidal extract. That these compounds were basic was supported by the fact that after their extraction from a basic solution into diethyl ether they could be quantitatively extracted into dilute sulfuric acid in a one-step extraction. Furthermore, it is believed that these alkaloids contained different carboxylic acid moieties, present as ester linkages, such as that found in cocaine, cinnamoylcocaine and the truxillines. This was supported by first subjecting a concentrated coca leaf alkaloidal extract to hydrolysis with refluxing 1 *M* hydrochloric acid (30 min) and then extraction of the liberated carboxylic acids into diethyl ether. A one-step extraction of the diethyl ether with an aqueous sodium bicarbonate solution removed the suspected carboxylic acids quantitatively. It is believed, therefore, that the majority of peaks illustrated in the CGC–ECD chromatogram in Fig. 3 represent HFB derivatives of alcohols that were derived from carboxylic acids that were present as ester linkages of individual coca alkaloids.

Derivatization of neutral and basic alcohols

It should be noted that in this methodology the reduction of the coca alkaloids yields two major products, namely, neutral alcohols and alcohols containing a basic function, *e.g.*, the diol of ecgonine (Scheme 1). In this procedure the products of primary interest are the neutral alcohols, so they are isolated from the basic alcohols by extraction from 1 *N* sulfuric acid prior to derivatization. In order to generate a CGC–ECD chromatogram illustrating both groups of alcohols, the step involving the extraction of the DPCBDC alcohols from 1 *N* sulfuric acid into diethyl ether is eliminated, and the HFBA derivatization is carried out immediately after the reduction of the DPCBDC compounds and evaporation of the diethyl ether. When this was done, the chromatogram revealed, not surprisingly, the major basic moiety of the coca alkaloids was ecgonine. Generating chromatograms of both neutral and basic alcohols is useful only for the detection of basic moieties other than ecgonine, *e.g.*, such as that found in tropacocaine, namely, tropine (Table II). It should be emphasized, however, that HFBA derivatization in the presence of lithium and aluminum salts resulted in reduced HFB derivative yield. It was for this reason that derivatization of the neutral alcohols was carried out only after their removal from the lithium–aluminum salts.

Artifact formation

In the analyses of trace impurities in refined drugs or the characterization of trace levels of alkaloids in plant extracts, the chemist must be vigilant in recognizing possible artifact formation. In this study we concerned ourselves with the possibility

that some, if not all, of the truxillines were artifacts resulting from manipulations associated with the clandestine manufacture or our own methodology. Rivier[8] and Plowman and Rivier[9] raised the same concerns during their investigations. To insure that the truxillines reported in this study were indeed bonafide components of the coca leaf–refined cocaine hydrochloride samples, and not artifactual, a number of steps were taken. (a) Standard cocaine (Mallinkrodt) was subjected to the coca leaf methodology in its entirety. Additionally, standard cocaine hydrochloride was subjected to truxilline analysis as described in this paper for illicit cocaine hydrochloride samples. No chromatographic peaks representing truxillines were noted in either case. (b) *trans*- And *cis*-cinnamoylcocaine (isolated from a cocaine sample using HPLC) were subjected to our methodololgy. Furthermore, both of these alkaloids were subjected to 1 *M* hydrochloric acid hydrolysis, followed by $LiAlH_4$ reduction and HFBA derivatization. No truxillic or truxinic acids or truxillines were found to be generated in either case. (c) The truxillines were detected in coca leaves regardless of variations in extraction solvents, extraction temperatures, pH or the length of extraction. (d) The truxillines (with the exception of μ-) were detected in all 35 illicit cocaine hydrochloride samples examined. This is significant, because these samples were seized in diverse geographical areas and the manufacture of these samples probably involved clandestine South American procedures, believed to be quite unlike the extraction methods used in our study. (e) The truxillines and DPCBDC acids and their dimethyl esters were not observed to interconvert, despite subjecting them to varied manipulations, thus discounting interconversion as a possible explanation to account for some of the DPCBDC compounds. These manipulations included (i) variations in the extraction methodology for the truxillines in a given coca leaf sample, (ii) storage of coca leaf extracts in different solvents, namely, methanol, diethyl ether and DMSO, for extended periods of time, (iii) subjecting DPCBDC acids and their dimethyl esters to varied analytical procedures, (iv) isolation of a truxilline mixture from an illicit cocaine sample by means of alumina column chromatography, and (v) HPLC fraction collection of individual truxillines from a purified truxilline mixture and fraction collection of a mixture of DPCBDC acid dimethyl esters. Any interconversion during these fraction collections would have been noted by the appearance of significant amounts of other DPCBDC compounds.

Characterization of the truxillic and truxinic acids and the truxillines

Used in the characterization of the DPCBDC compounds were CGC–ECD, HPLC, CGC–MS used under electron ionization and positive and negative chemical ionization conditions, MS using desorption probe, HR-MS and ^1H NMR. Much of the characterization was accomplished by studying the dimethyl esters of the DPCBDC acids isolated by HPLC and the O-HFB derivatives of the truxillines subjected to $LiAlH_4$ reduction. The terms "head-to-tail" and "head-to-head" were used in ^1H NMR study to describe truxillic and truxinic acids, respectively.

Because of extraction characteristics, hydrolysis experiments, dimethyl esterification of the hydrolyzed species and HFBA derivatization of the $LiAlH_4$-reduced species, it was relatively straightforward to conclude that the impurities in question detected in illicit cocaine samples were carboxylic acids and alkaloidal species containing carboxyl moieties present as ester functions, the latter hydrolyzing to the former during the cocaine manufacturing process. That the alkaloidal impurities were

TABLE III

CHEMICAL SHIFT AND COUPLING CONSTANT DATA FOR SOME DPCBDC ACID DIMETHYL ESTERS

Isomer	*Chemical shift (ppm)*				*Coupling constants (Hz)*						
	A	*A'*	*B*	*B'*	*AA'*	*AB*	*A'B'*	*AB'*	*A'B*	*BB'*	*K**
α-	3.99		4.46		0.5	10.8	10.8	6.7	6.7	1.0	1.5
β-	3.86		4.40		11.2	7.5	7.5	−1.3	−1.3	11.9	23.1
δ-	3.50		3.74		8.0	9.4	9.4	0.26	0.26	8.0	16.0
γ	3.69	4.79		4.21	0.0	10.1	10.7	10.7	10.1	0.0	0.0
ε-	3.29		4.00		0.0	9.7	9.7	9.7	9.7	0.0	0.0
μ-	3.91		4.60		10.6	10.5	10.5	−1.1	−1.1	3.4	14.0

* $K = J_{AA'} + J_{BB'}$.

suspected truxillines was provided by the fact that acid hydrolysis of a basic cocaine extract followed by methyl esterification yielded, among others, closely eluting compounds all having a molecular weight of 324, as determined by mass spectral examination. Their electron ionization spectra were consistent with compounds containing a DPCBDC moiety. Subsequent high-resolution MS examination confirmed the DPCBDC dimethyl ester moiety as $C_{20}H_{20}O_4^{\cdot +}$. That the acidic impurities in the cocaine samples were truxillic and truxinic acids was provided by the fact that they were generated when the suspected truxillines were subjected to acid hydrolysis.

When the nine DPCBDC acid standards and/or their dimethyl ester reference standards, prepared as described previously, were subjected to the methodology described herein, their CGC retention times were virtually identical with nine of the eleven suspected DPCBDC compounds isolated from Bolivian coca leaves and illicit cocaine hydrochloride samples (Table II). These DPCBDC standards were prepared using referenced methodology [12–17] and had been previously characterized. These included the α-, β-, γ-, ε-, δ-, μ-, *neo-*, *peri-* and ζ-isomers. Tables III and IV provide ^{1}H NMR and MS data for some of the DPCBDC standard compounds.

Evidence for the presence of five of the eleven possible DPCBDC isomers in cocaine samples and additional presumptive evidence for the remaining six was provided as follows: An illicit cocaine hydrochloride sample (5–10 g) with a cocaine content of 85–90% was subjected to 1 *M* hydrochloric acid hydrolysis followed by isolation of the liberated DPCBDC, benzoic, cinnamic and other carboxylic acids by extraction with diethyl ether. After evaporation of the ether, the residue was heated (75–80°C) overnight in a vacuum oven to effect the sublimation of benzoic and cinnamic acids. The carboxylic acids that remained, the bulk being DPCBDC isomers, were dimethyl esterified using 4% hydrochloric acid in methanol. The DPCBDC dimethyl esters were then subjected to preparative HPLC. The mobile phase used for this separation was ascertained using a solvent optimization scheme. Various binary, tertiary and quaternary mixtures of methanol, acetonitrile, tetrahydrofuran and water were investigated at different solvent strengths. For the preparative HPLC separation and collection of the truxillic/truxinic acid dimethyl esters, the sample was dissolved in the mobile phase at 50°C in order to solubilize the esters. Fraction collection took place at a flow-rate of 26.0 ml/min and at a temperature of 50°C. The

isolated fractions were monitored for single component purity by analytical HPLC and CGC–ECD. In some cases it was necessary to further purify the fractions by using analytical, preparative HPLC techniques. A total of eight DPCBDC dimethyl ester isomers were isolated in this manner. The HPLC–UV spectra of all eight isomers were consisent with a DPCBDC moiety. The HPLC retention times of three of these isomers correlated well with three of the standards available at the time of analysis, namely, the dimethyl esters of α- and ε-truxillic acids and β-truxinic acid. The eight isolated DPCBDC acid dimethyl esters were subjected to ^{1}H NMR and/or MS analyses as described below.

^{1}H NMR characterization of some of the sample DPCBDC acid dimethyl esters, isolated by HPLC, was accomplished by comparison with reference compounds, evaluating chemical shift and coupling constant data and the review of literature values for the same or similar compounds[18–20]. ^{1}H NMR evaluation of some HPLC fractions was not possible due to coeluting species or insufficient material. However, our investigations revealed that the eleven DPCBDC acid dimethyl esters would be expected to yield, for the most part, distinguishable ^{1}H NMR spectra. Based, in part, upon this reasoning, we were able to confirm the identities of three DPCBDC acid dimethyl esters by direct comparison of their ^{1}H NMR patterns with three corresponding reference standards. The DPCBDC compounds identified were the α-, β- and ε-isomers (Table III). Based upon gross spectral characteristics and the coupling constants and chemical shifts of five known DPCBDC acid dimethyl esters (Table III) and reported literature values for similar compounds, we were able to confirm the structure of a fourth DPCBDC compound isolated by HPLC, namely, the δ-isomer. Inspection of the chemical shift data (Table III) for this isomer, in light of stereochemical considerations, suggested the following:

(a) The AA'BB' patterns produced by the cyclobutane protons in situations of planar or biaxial symmetry may be expected to be more nearly of a first order A_2B_2 type for the truxillic (head-to-tail) isomers as contrasted with those of the truxinic (head-to-head) series. Because the magnetically equivalent nuclei in isomers of the former type are not vicinal, coupling between them may be expected to be of negligible magnitude. In contrast, those of the latter, being vicinal, would be significantly greater. Expressed otherwise, $K(J_{AA'} + J_{BB'})$ is very small for the head-to-tail isomers but large for the head-to-head variety[19] (Table III). This would be reflected in the patterns of these compounds (Fig. 4).

(b) Chemical shifts of the CHs are influenced, in an upfield direction, by a vicinal phenyl or a C=O in the *cis* position. Although our data base was insufficient to quantify these influences, it was apparent from inspection of the data that phenyl groups in the *cis*-vicinal position exerted a markedly greater influence than C=O in effecting these shifts.

(c) The CHs are deshielded by phenyl and C=O in the *cis*-diagonal position. Here, the influence of C=O appears to be greater than that of phenyl.

(d) Of greatest significance is the effect of vicinal-*cis* phenyl groups on the chemical shifts of the methyl protons. Based upon the chemical shift data for the reference compounds, a substituent effect of about 0.4–0.45 ppm was assumed for each vicinal-*cis* phenyl. It should be noted that the resulting shifts of about 3.7 ppm found in the β- and ε-isomers (Table IV), where there are no vicinal-*cis* phenyls, are close to the values consistently observed for methyl esters of straight chain fatty acids

TABLE IV

EI MASS SPECTROMETRIC DATA FOR TRUXINIC AND TRUXILLIC ACID DIMETHYL ESTERS

Emperical structure	*Actual measure*	*Theoretical value*	*Relative abundance*								
			α-	*γ-*	*ε-*	*β-*	*δ-*	*μ-*	*neo-*	*ζ-*	*peri-*
C_4H_3	51.0220	51.0237	3.0	4.0	5.0	2.0	2.0	4.0	2.0	3.0	0.7
$C_2H_3O_2$	59.0141	59.0135	1.0	3.0	3.0	1.0	3.0	5.0	0.1	3.0	1.0
C_6H_5	77.0393	77.0395	12.0	17.0	15.0	7.0	7.0	7.0	6.0	5.0	0.9
C_7H_7	91.0545	91.0548	5.0	10.0	9.0	3.0	6.0	6.0	3.0	4.0	4.0
C_8H_7	103.0551	103.0548	21.0	28.0	27.0	13.0	13.0	9.0	7.0	8.0	0.2
$C_5H_5O_3$	113.0237	113.0239	0.0	0.0	0.0	9.0	16.0	25.0	7.0	13.0	0.0
C_9H_7	115.0536	115.0548	3.0	6.0	6.0	1.0	3.0	4.0	1.0	2.0	0.4
C_9H_7O	131.0493	131.0497	70.0	97.0	95.0	57.0	55.0	41.0	94.0	59.0	2.0
$C_7H_{11}O_3$	143.0741	143.0709	0.0	0.0	0.3	0.0	0.0	0.1	0.0	0.0	0.0
$C_{10}H_8O$	144.0589	144.0575	2.0	3.0	3.0	0.5	2.0	2.0	1.0	0.6	0.0
$C_{10}H_{10}O_2$	162.0679	162.0681	100.0	100.0	100.0	100.0	100.0	77.0	100.0	100.0	0.2
$C_{13}H_9$	165.0702	165.0704	0.8	1.0	2.0	0.5	6.0	23.0	3.0	6.0	1.0
$C_{14}H_{10}$	178.0796	178.0783	0.9	2.0	2.0	2.0	10.0	35.0	3.0	12.0	4.0
$C_{14}H_{11}$	179.0824	179.0861	0.2	0.1	0.7	1.0	10.0	52.0	3.0	13.0	1.0
$C_{14}H_{12}$	180.0927	180.0939	0.0	0.0	0.0	0.5	6.0	69.0	2.0	8.0	0.0
$C_{15}H_{10}$	190.0784	190.0783	1.0	2.0	2.0	0.2	1.0	2.0	0.2	0.2	2.0
$C_{15}H_{11}$	191.0866	191.0861	1.0	3.0	3.0	0.3	2.0	2.0	2.0	0.3	1.0
$C_{16}H_{12}$	204.0934	204.0939	4.0	17.0	15.0	1.0	5.0	13.0	2.0	4.0	15.0
$C_{16}H_{13}$	205.1015	205.1017	8.0	31.0	27.0	10.0	18.0	45.0	31.0	15.0	100.0
$C_{17}H_{12}O$	232.0901	232.0889	1.0	3.0	3.0	0.1	0.2	3.0	0.5	0.0	0.1
$C_{17}H_{13}O$	233.0960	233.0968	3.0	7.0	6.0	0.1	0.4	2.0	0.5	0.1	0.0
$C_{18}H_{16}O_2$	264.1142	264.1150	22.0	29.0	22.0	26.0	51.0	100.0	68.0	34.0	78.0
$C_{19}H_{16}O_3$	292.1087	292.1099	1.0	18.0	11.0	0.2	0.3	1.0	0.5	0.0	0.0
$C_{19}H_{17}O_3$	293.1171	293.1177	0.2	2.0	2.0	0.3	2.0	2.0	0.2	0.1	0.0
$C_{20}H_{20}O_4$	324.1350	324.1356	0.3	27.0	20.0	0.4	0.0	0.3	0.0	0.0	3.0

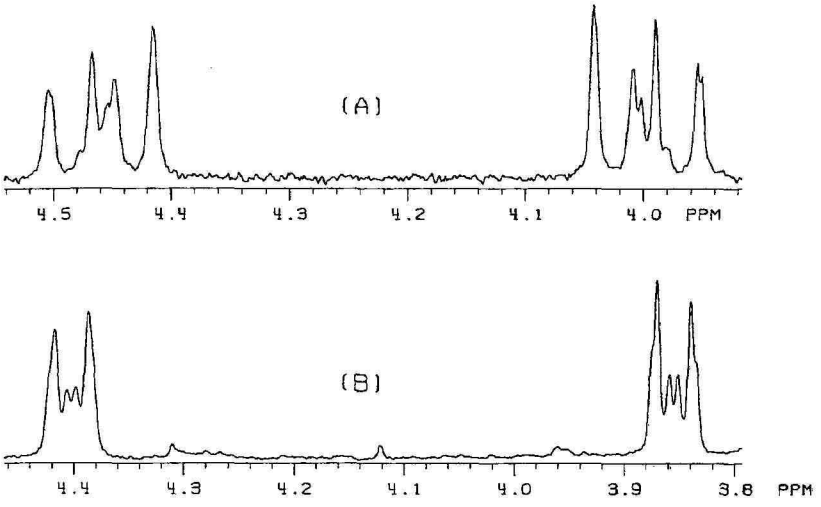

Fig. 4. 200 MHz ^{1}H spectra (CH region) of dimethyl esters of (A) α-truxillic acid and (B) β-truxinic acid.

where shielding or deshielding influences may be deemed to be negligible. Therefore, in view of the structural differences of these isomers, it is highly unlikely that offsetting influences of any sort contribute, in any significant way, to these shifts and that the vicinal-*cis* phenyl may be deemed as the only significant consideration to be made in predicting shifts for the methyl groups of unknown DPCBDC acid dimethyl esters.

The shielding effect of *cis*-vicinal phenyl on protons and carbomethoxy methyl protons in 3–5 membered rings has been well-documented and determined to be reliably predictable [21–27]. No such consistency has been observed, however, with respect to such influence by carboxyl groups. It seems plausible that this is due to the wider range of conformations feasible for this smaller group among different families of compounds and its more restricted anisotropic geometry.

On the basis of the foregoing considerations, particularly as regards the methyl group, the fourth DPCBDC acid dimethyl ester isolated as a single HPLC component was characterized as the δ-isomer. This was supported by favorable comparison with a literature spectrum[28].

Structural confirmation for the DPCBDC acid dimethyl esters for which ^{1}H NMR data was obtained (Table III) was provided by MS analysis. Furthermore, the presence of all eleven in a cocaine sample was supported using CGC–MS under EI and negative ion chemical ionization (NICI) conditions. Eight DPCBDC acid dimethyl esters which were isolated using preparative HPLC were subjected to CGC–MS analysis. Under EI conditions, mass spectra consistent with either a truxillic or truxinic moiety were obtained. The mass spectra for five of these compounds for which ^{1}H NMR data was obtained (Table III) were virtually identical with five of the standard reference compounds. These were the α-, β-, γ-. ε- and δ-isomers, thus confirming, unequivocally, their presence in illicit cocaine. Table IV lists low- and high-resolution EI data for these and other DPCBDC acid dimethyl esters. The three remaining DPCBDC isomers isolated by HPLC and characterized by CGC–MS were the *neo-*, *epi-* and *peri*-acid dimethyl esters. The *neo*-isomer isolated by HPLC gave an EI mass spectra that was virtually identical to the *neo*-reference standard. MS

examination of the two remaining isomers isolated by HPLC revealed the presence of a truxillic moiety (as opposed to a truxinic moiety). This necessitated the assignments of *peri-* and *epi*-configurations for these isomers. That this was so was based upon the following rationale. A review of the EI mass spectra of the eight DPCBDC acid dimethyl esters isolated by HPLC, as well as the mass spectra for the μ- and ζ-reference standards, revealed the presence of a fragment ion, *m/z* 113, which was present in the isomers assigned the truxinic configuration, but not found in the truxillic isomers. When standard β-truxinic acid was subjected to deutero-dimethyl esterification, the *m/z* 113 ion shifted to *m/z* 116. Given the fact that the structural difference between truxillic and truxinic acids is the sequence of substitution in the cyclobutane ring and the fact that the *m/z* 113 ion must contain one intact methyl ester function, a structure for this ion was postulated as

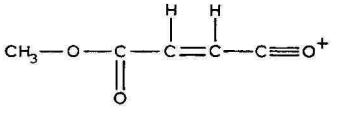

The structure of this ion was confirmed by high resolution EI–MS as $C_5H_5O_3^+$. Based upon the spectral absence of this diagnostic ion, we were able to account for all five of the possible truxillic acids, namely, α-, γ-, ε-, *epi-* and *peri-*. The three other DPCBDC acid dimethyl esters isolated by HPLC all contained the *m/z* 113 ion. These were assigned the truxinic configurations of β-, δ- and *neo-*, based upon comparison to reference standards.

Although CGC–ECD analysis of cocaine samples suggested the presence of at least ten, and possibly eleven, of the DPCBDC isomers, the most compelling evidence for the presence of all eleven isomers was provided by CGC–NICI–MS analysis. An illicit cocaine sample (cocaine content, 85–90%) was subjected to $LiAlH_4$ reduction and HFBA derivatization as described in the body of the text. Using chromatographic conditions similar to those for the CGC–ECD method, the isolated di-O-HFB derivatives were subjected to CGC–NICI–MS analysis. The resultant chromatographic pattern was similar to that illustrated in Fig. 2. A review of the chromatogram and mass spectral data revealed that ten of the eleven peaks gave the expected $M^{\cdot -}$ ion of *m/z* 660, representing $C_{26}H_{18}O_4F_{14}$. The eleventh peak did not yield an $M^{\cdot -}$ ion but did provide an ($M^{\cdot -}$ – HF) fragment ion.

Most of the characterization studies described thus far were associated with the DPCBDC moiety of the truxillines. In the earlier studies of Hesse[3] and Liebermann[4], it was reported that the alkaloidal moiety associated with α- and β-truxilline was methyl ecgonine. It was our intention to confirm their findings and demonstrate that this was the case for the remaining truxillines. This was done in the following manner. A cocaine sample (cocaine content, 85–90%) was subjected to alumina column chromatography as described previously. The truxilline fraction isolated from the column was subjected to an additional two "passes" through the alumina column. Using this technique, we were able to remove more than 99.9% of the cocaine and cinnamoylcocaines from the mixed truxillines fraction. The enriched truxilline fraction was subjected to $LiAlH_4$ reduction, derivatization with HFBA and CGC–ECD analysis of the HFB derivatives of both the neutral and basic alcohols (Scheme 1).

The generated chromatogram revealed the expected presence of the DPCBDC isomers between 23 and 26 min (Table II) and an off-scale peak at 9.95 min (Table II). The 9.95 min peak was due to the di-O-HFB derivative of the alkaloidal moiety of the truxillines after their reduction and derivatization. As there were no other significant peaks in the chromatogram representing basic alcohols, this species had to be the alkaloidal moiety associated with the DPCBDC isomers. Furthermore, when the alumina column was monitored by CGC–ECD in 4-ml fractions, it was noted that the 9.95 min CGC–ECD peak appeared and disappeared with the appearance and disappearance of the DPCBDC peaks, thus lending support to their relationship. It is noted that coca alkaloids possessing the methyl ecgonine moiety, *e.g.*, cocaine, cinnamoylcocaines and the truxillines, will generate this peak upon reduction, derivatization and CGC–ECD analysis. Coca alkaloids possessing different alkaloidal moieties, *e.g.*, the tropine moiety in tropacocaine, will generate a peak(s) of different retention time(s) (Table II).

When the enriched truxilline fraction from the alumina column was subjected to hydrolysis with hydrochloric acid followed by trimethylsilyl derivatization and EI–MS analysis, a mass spectrum was generated which was consistent with that of the di-O-TMS derivative of ecgonine. When the same truxilline fraction was subjected to $LiAlH_4$ reduction, HFBA derivatization and NICI–CGC–MS analysis, an early eluting peak appeared that yielded a molecular ion of *m/z* 563, consistent with the di-O-HFB derivative of reduced ecgonine (Scheme 1). As described previously, when the truxilline fraction was subjected directly to CGC–MS analysis decomposition occurred, yielding the "free" DPCBDC acids and methyl ecgonidine.

The truxilline mixture was also subjected to desorption probe MS analysis using PCI. The resultant mass spectrum yielded a very intense *m/z* 659 ion, which was the expected protonated molecule ion of the truxillines, thus confirming their molecular weight of 658. A weaker ion at *m/z* 478 was accounted for by the elimination of methyl ecgonidine from the truxilline molecule ion, a process consistent with the presence of a methyl ecgonine moiety. When an illicit cocaine sample was dissolved in methanol and taken directly to the desorption probe, and when using conditions identical to those used previously, a response was observed for $MH^+ = 659$, thus supporting the presence of the truxillines in cocaine.

CONCLUSIONS

CGC–ECD methodology has been developed that allows for the sensitive detection of the eleven stereoisomers of diphenylcyclobutanedicarboxylic acid (truxillic and truxinic acids) and their alkaloidal precursors, the truxillines, in illicit cocaine samples. Methodology is also described for the detection of the truxillines in South American coca leaves.

ACKNOWLEDGEMENTS

We extend our appreciation to Thomas Cantrell for providing α-truxillic acid and to Frederick D. Lewis for the dimethyl esters of *μ*- and *neo*-truxinic acids. We would also like to acknowledge Gabor Fodor for useful discussions. We are grateful to Joyce Jones for the typing of the manuscript.

REFERENCES

1 J. M. Moore, A. C. Allen and D. A. Cooper, *Anal. Chem.*, 58 (1986) 1003.
2 B. C. Uff, in S. Coffey (Editor), *Rodd's Chemistry of Carbon Compounds*, Vol. II, Part A, Elsevier, Amsterdam, 1967, p. 72.
3 O. Hesse, *Justus Liebigs Ann. Chem.*, 271 (1892) 180.
4 C. Liebermann, *Ber. Dtsch. Chem. Ges.*, 22 (1889) 782.
5 H. L. Schlesinger, *Bull. Narc.*, 37 (1984) 67.
6 W. C. Evans, *J. Ethnopharmacol.*, 3 (1981) 1981.
7 Y. M. A. El-Imam, W. C. Evans and T. Plowman, *Phytochemistry*, 24 (1985) 2285.
8 L. Rivier, *J. Ethnopharmacol.*, 3 (1981) 313.
9 T. Plowman and L. Rivier, *Ann. Bot. (London)*, 51 (1983) 641.
10 S. Castellano and A. A. Bothner-By, *J. Chem. Phys.*, 41 (1964) 3863.
11 S. M. Castellano, in D. F. DeTar (Editor), *Computer Programs for Chemistry*, Vol. I, Benjamin, New York, 1968, p. 10.
12 *Merck Index*, Merck, Rahway, NJ, 10th ed., 1983, 9591.
13 H. I. Berstein and W. C. Quimby, *J. Am. Chem. Soc.*, 65 (1943) 1845.
14 A. W. K. DeJong, *Chem. Ber.*, 55 (1922) 463.
15 B. S. Green and M. Rejto, *J. Org. Chem.*, 39 (1974) 3284.
16 B. S. Green, Y. Rabinsohn and M. Rejto, *J. Chem. Soc., Chem. Commun.*, (1975) 313.
17 R. Stoermer and Fr. Moller, *Ber. Dtsch. Chem. Ges.*, 68 (1935) 2130.
18 G. Montaudo and S. Caccamese, *J. Org. Chem.*, 38 (1973) 710.
19 S. Montaudo, S. Caccamese and V. Librando, *Org. Magn. Reson.*, 6 (1974) 1934.
20 F. D. Lewis and R. J. DeVoe, *J. Org. Chem.*, 45 (1980) 948.
21 N. S. Bhacca, D. P. Hollis, L. F. Johnson and E. A. Pier, *N.M.R. Spectra Catalog*, Vol. 2, Varian, Palo Alto, CA, 1963, No. 528.
22 L. A. Caprino, *J. Am. Chem. Soc.*, 84 (1962) 2196.
23 H. Schechter, W. J. Link and G. V. D. Tiers, *J. Am. Chem. Soc.*, 85 (1963) 1601.
24 P. Scribe, *C.R. Acad. Sci., Ser. B*, 261 (1965) 160.
25 C. G. Overberger and A. Drucker, *J. Org. Chem.*, 29 (1964) 360.
26 G. L. Kreuger, F. Kaplan, M. Orchin and W. H. Faul, *Tetrahedron Lett.*, 45 (1965) 3979.
27 R. M. Dodson and A. G. Zielske, *J. Org. Chem.*, 32 (1967) 28.
28 D. A. Ben-Efraim and B. S. Green, *Tetrahedron*, 30 (1974) 2357.

Journal of Chromatography, 410 (1987) 319–328
Elsevier Science Publishers B.V., Amsterdam — Printed in The Netherlands

CHROM. 19 923

CAPILLARY COLUMN GAS CHROMATOGRAPHIC IDENTIFICATION OF SUGARS IN HONEY AS TRIMETHYLSILYL DERIVATIVES

RUFINO MATEO*, FRANCISCO BOSCH and AGUSTÍN PASTOR
Department of Analytical Chemistry, Faculty of Chemistry, University of Valencia, Dr. Moliner 50, 46100-Burjassot, Valencia (Spain)
and
MISERICORDIA JIMENEZ
Department of Biotechnology, Polytechnic University of Valencia, Camino de Vera 14, 46022-Valencia (Spain)
(First received April 8th, 1987; revised manuscript received August 4th, 1987)

SUMMARY

A method for identifying carbohydrates (mono-, di- and trisaccharides) in honey is presented. It is based on the separate preparation of both trimethylsilyl ethers and oxime trimethylsilyl ethers of the sugars followed by their gas chromatographic separation on a fused-silica capillary column coated with OV-101 using temperature programming. From the two chromatograms, the number of peaks given by each derivatized sugar, their relative retention times and peak-area ratios are used for identification. The identities of two unidentified trisaccharide peaks are considered. Quantitative applications to honey sugar analysis are discussed.

INTRODUCTION

Honey is composed mainly of carbohydrates and water. Fructose and glucose are the major components and di- and trisaccharides form a complex mixture[1].

Several chromatographic techniques have been used in the study of honey sugars. Separation on a carbon–Celite column followed by paper chromatography and infrared spectroscopy led to the identification of sucrose, turanose, maltulose, maltose and nigerose[2]. Kojibiose was further reported in this product[3]. Siddiqui and Furgala[4,5] characterized the disaccharides cited above and also α,β-trehalose, palatinose (tentatively), gentiobiose and laminaribiose; the trisaccharides melezitose, erlose, 1-kestose, theanderose, maltotriose and other oligosaccharides. Their method, involving carbon–Celite, paper and thin-layer chromatography, paper electrophoresis and physico-chemical assays, is very reliable but very time consuming, and is not appropriate for the routine analysis of honey sugars.

Gas–liquid chromatography (GLC) with packed columns has been used for the separation and determination of honey carbohydrates as trimethylsilyl (TMS) ethers[6–10] and oxime TMS ethers[11]. Isomerism of reducing sugars often led to several

0021-9673/87/$03.50

peaks for a single compound and poor resolution was generally obtained, especially with disaccharides. α,α-Trehalose[6–8], melibiose[6] and raffinose[6–9] have been found in honey by GLC.

High-performance liquid chromatography (HPLC) has also been applied[12,13], but problems of resolution and sensitivity occurred in the separation of complex mixtures of low-concentration sugars. In such a case, capillary column gas chromatography (capillary GC) appears to be an advantageous technique[13] and has been used in the separation of some disaccharides as TMS-O-methyl oximes[14] and TMS ethers[15]. A concentration procedure for TMS derivatives of sugars prior to their separation by capillary GC was applied to honey[16], although the origin of the peaks was not studied in detail. Carbohydrates in nectar[17], industrial sugar products[18,19] and royal jelly[20] have also been determined by this technique. However, a study of the identification and quantitation of honey sugars by means of capillary GC has not been reported.

This paper describes the identification of honey sugars by capillary GC of the TMS ethers and TMS oximes. Some aspects of quantitative applications are discussed.

EXPERIMENTAL

Reagents

D-Glucose, sucrose, melibiose, maltose and α,α-trehalose were purchased from E. Merck (Darmstadt, F.R.G.), D-fructose and raffinose from Carlo Erba (Milan, Italy), β-gentiobiose and melezitose from Fluka (Buchs, Switzerland), turanose, palatinose, isomaltose and maltotriose from Sigma (St. Louis, MO, U.S.A.) and α-kojibiose from Koch-Light (Colnbrook, U.K.). Maltulose, nigerose and 1-kestose were gifts.

Hexamethyldisilazane (HMDS), trifluoroacetic acid (TFA), hydroxylamine hydrochloride and magnesium sulphate were obtained from E. Merck, anhydrous pyridine solvent from F.E.R.O.S.A. (Barcelona, Spain) and triphenylethylene standard from Fluka.

Apparatus

A Perkin-Elmer Sigma 115 gas chromatograph equipped with a split–splitless injector, a flame ionization detector and a 25 m × 0.23 mm I.D. OV-101 fused-silica capillary column was used.

The injector and detector temperatures were 280 and 300°C, respectively. The following oven temperature programme was generally employed: 180°C immediately increased at 3°C/min to 280°C, held for 4 min, programmed at 2°C/min to 290°C and held at 290°C until elution of trisaccharides. The carrier gas was hydrogen at a flow-rate of 0.35 ml/min measured at the initial oven temperature, the inlet pressure was 60 kPa and the splitting ratio was 1:75.

Derivatization

Preparation of standard and sample solutions. Sugar standards were solved in a minimal amount of water and anomerized for 48 h. Pyridine was then added to give solutions of the following concentrations: fructose *ca.* 15 mg/ml, glucose *ca.* 12

mg/ml and other carbohydrates 1–3 mg/ml. Honey samples were dissolved in anhydrous pyridine (40 mg/ml).

Preparation of TMS ethers. Volumes of 2.5 ml of the pyridine standard solutions were diluted with 2.5 ml of anhydrous pyridine in a test-tube, 2 g of anhydrous magnesium sulphate (desiccant) were added and the tightly sealed tube was kept horizontal for about 20 h at 25°C. Then 1 ml of the decanted solution was silylated with 1 ml of HMDS and 0.1 ml of TFA in a Reacti-vial (Pierce, Rockford, IL, U.S.A.) for 1 h at 80°C with stirring. A 5-μl volume of the resulting solution was injected into the gas chromatograph. Honey solutions were derivatized in the same way as standards.

Preparation of TMS oximes. The procedure described for preparing TMS ethers was followed, but dilution of solutions was carried out with the same volume of a solution of hydroxylamine hydrochloride in anhydrous pyridine (100 mg/ml). The white precipitate formed was easily decanted and did not interfere in the analysis. this procedure is based on the Pourtallier and Rognone technique[11].

Gas chromatographic analysis

The number of peaks and their ratio were obtained for the TMS ethers and TMS oximes of every sugar standard. Relative retention times (RRTs) of each peak were then calculated with respect to sucrose and isomaltose. These disaccharides give characteristic peaks in the middle of the chromatograms, they are always present in honey and do not give interference problems. Sucrose gave a peak with the same retention time (t_R) in the chromatograms of both types of derivatives and was chosen as a reference when its peak was not too small. In such a case, the main peak given by the TMS oximated isomaltose or the peak of TMS β-isomaltose were more suitable references for identifying sugars in TMS oximated or trimethylsilylated honey, respectively.

Identification of carbohydrates in honey was carried out by comparison of the RRTs of the different peaks with those obtained from standards, taking into account the number of isomeric peaks produced by each sugar and their area ratio.

For quantitative analysis triphenylethylene was used as the internal standard. It was added to sugar standards and honey samples dissolved in the pyridine solution used in the dilution step (5 mg/ml).

RESULTS AND DISCUSSION

Any fluctuation of the carrier gas flow-rate produced accidentally in the chromatographic system affected the repeatability of the RRTs when temperature programming was used, so corrections were introduced. Fig. 1 shows linear relationships between the retention times of several disaccharides relative to TMS-sucrose and the t_R of this sugar peak. These linear plots with small slopes were useful for compensating RRT deviations, making strict carrier gas flow control unnecessary for identification purposes. In this way, RRT deviations of ± 0.002 to ± 0.005 were obtained for disaccharides. Similar plots to those shown in Fig. 1 were used to correct the RRTs of other sugar peaks.

Table I shows the number of significant peaks, their RRTs in relation to reference standards and the peak-area ratio between isomers for a series of saccharides as TMS oximes and/or TMS ethers.

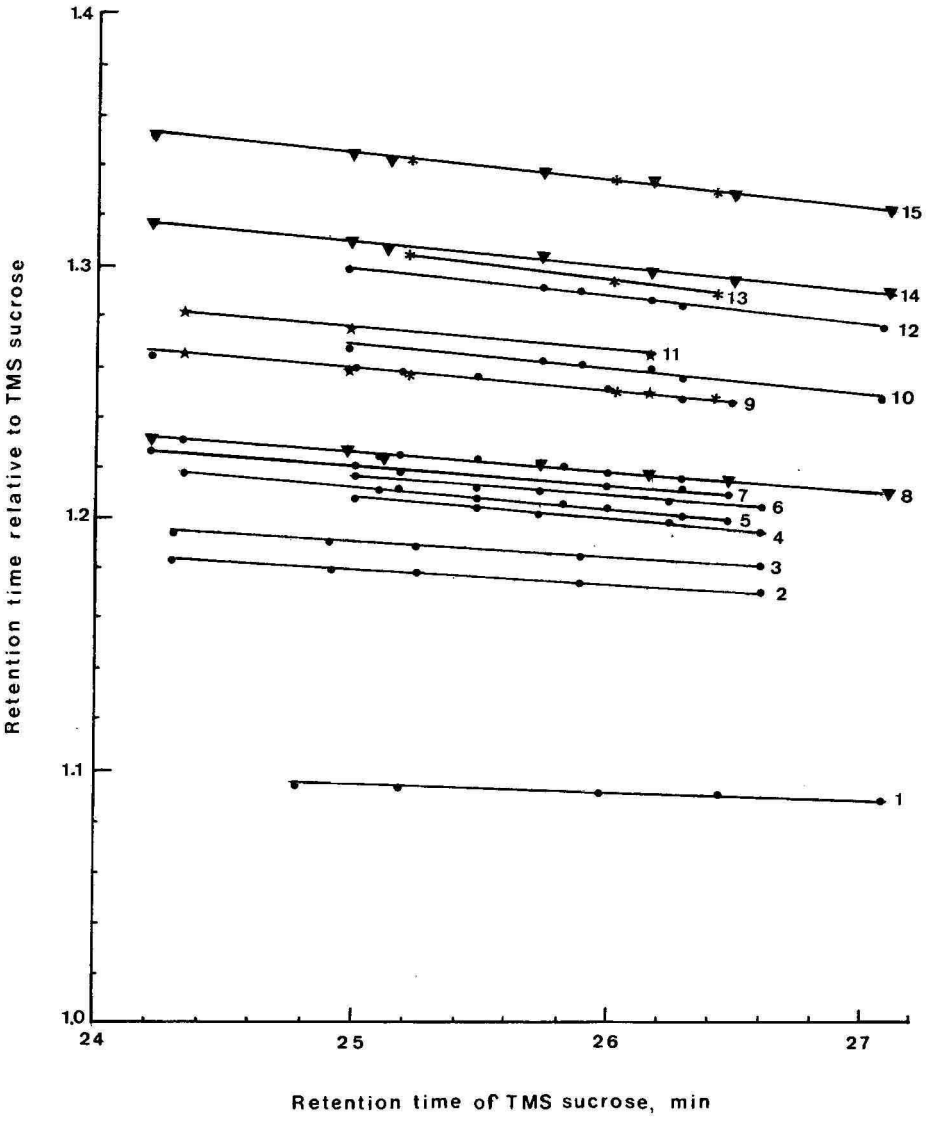

Fig. 1. Retention time relative to TMS-sucrose *versus* retention time of TMS-sucrose for TMS-α,α-trehalose and some TMS oximated disaccharide peaks. 1, α,α-Trehalose; 2 and 3, maltulose; 4, turanose; 5, maltose; 6, turanose; 7, kojibiose; 8, maltose (⬙) and isomaltose (▼); 9, kojibiose (●), palatinose (★) and melibiose (✳); 10, gentiobiose; 11, palatinose; 12, gentiobiose; 13, melibiose; 14, isomaltose; 15, isomaltose (▼) and melibiose (✳).

Oxime TMS ethers

Both fructose and glucose produced two peaks, in agreement with data obtained by other workers[21–23]. Petersson[24] related the two peaks to *syn* and *anti* isomers of the derivatized oximes, the first, being more stable, causing the major peak. Results obtained with disaccharides correspond well with data from packed col-

TABLE I

NUMBER OF ISOMERIC PEAKS, RELATIVE RETENTION TIMES AND ISOMER PEAK-AREA RATIOS OF SOME CARBOHYDRATES AS TMS OXIMES AND TMS ETHERS

Carbohydrate	*Oxime TMS ether*				*TMS ether*			
	Isomer peak	*Retention time relative to*		*Area ratio*	*Isomer peak*	*Retention time relative to*		*Area ratio*
		*TMS-sucrose**	*Isomaltose TMS oxime (peak 2)***			*TMS-sucrose**	*TMS-β-isomaltose****	
Fructose	1	0.343	0.273	8	1	0.242	0.193	8
	2	0.352	0.282	10	2	0.248	0.197	8
					3	0.254	0.202	10
					4	0.269	0.214	4
Glucose	1	0.378	0.309	10	1(α)	0.297	0.236	8
	2	0.400	0.319	3	2(β)	0.363	0.289	10
Sucrose§	1	1.000	0.767	–	1	1.000	0.796	–
α,α-Trehalose§	1	1.092	0.837	–	1	1.092	0.869	–
Maltulose	1	1.177	0.903	9	1	1.059	0.843	7
	2	1.188	0.905	10	2	1.063	0.846	10
					3	1.079	0.859	1
Nigerose	1	1.143	0.877		1	1.073	0.854	10
	2	1.204	0.923	10	2	1.092	0.869	7
	3	1.233	0.946	3				
Turanose	1	1.206	0.925	8	1	1.072	0.853	8
	2	1.214	0.931	10	2	1.075	0.856	10
Maltose	1	1.209	0.927	10	1(α)	1.035	0.824	5
	2	1.224	0.939	3	2(β)	1.080	0.860	10
Kojibiose	1	1.218	0.934	10	1(β)	1.093	0.870	10
	2	1.224	0.963	2	2(α)	1.153	0.918	6
Palatinose	1	1.256	0.963	9	1	1.090	0.868	§§
	2	1.272	0.976	10	2	1.108	0.882	10
Melibiose	1	1.256	0.963	1	1(α)	1.201	0.956	9
	2	1.300	0.997	10	2(β)	1.220	0.971	10
	3	1.340	1.028	2				
Gentiobiose	1	1.171	0.898	1	1§§§	1.245	0.991	–
	2	1.264	0.969	10				
	3	1.293	0.992	2				
Isomaltose	1	1.224	0.939	1	1(α)	1.208	0.962	9
	2	1.305	1.000	10	2(β)	1.256	1.000	10
	3	1.340	1.028	3				
Raffinose§	1	1.800	1.381	–	1	1.800	1.433	–
1-Kestose§	1	1.824	1.399	–	1	1.824	1.452	–
Melezitose§	1	1.918	1.471	–	1	1.918	1.527	–
Maltotriose	1	2.023	1.552	1	1(α)†	1.960	1.560	
	2	2.270	1.741	10	2(α)†	1.969	1.567	–
	3	2.333	1.789	3				

* Retention time (t_R) of TMS-sucrose peak: 25.40 min.
** t_R of isomaltose TMS oxime (peak 2): 33.12 min.
*** t_R of TMS β-isomaltose: 31.90 min.
§ Non-reducing sugar. Retention data are referred to TMS ether.
§§ Broad peak whose area cannot be measured accurately.
§§§ Anomers are not resolved, giving a single peak.
† Anomers are very poorly resolved and their areas are measured inaccurately.

umns[25], except for maltose, turanose and gentiobiose, for which only one peak for the first two and a 10:5 peak-area ratio for the third were reported. Although the TMS-methyl oxime of palatinose gave one peak[14], no comparative data for TMS oximes of maltulose, palatinose and maltotriose were found. Isomaltose also gives three peaks on an OV-17 packed column[26]. Non-reducing sugars produced a single peak from their TMS ethers.

Some overlapping was observed with disaccharides. The overlapped peaks, following the notation "name–number"[27], were nigerose–2 with turanose–1, maltose–1 with turanose–1 (sometimes also with turanose–2), maltose–2 with isomaltose–1, kojibiose–2 and palatinose–1 with melibiose–1, melibiose–2 with isomaltose–2 (only with very different concentrations) and melibiose–3 with isomaltose–3.

TMS ethers

Assignment of the anomeric configuration (α- or β-) to peaks originating from every reducing sugar TMS ether was carried out on the basis of available data[15,28,29] and Table I shows only the elution order by correlative numbers when the relevant information was not found.

Fructose gave seven peaks under our conditions but only the four most relevant ones appear in Table I. This has been discussed by others[30,31]. However, glucose produced two well separated peaks[28], although the first of them overlapped with a fructose peak. Reducing aldo-disaccharides generally gave rise to two peaks (except

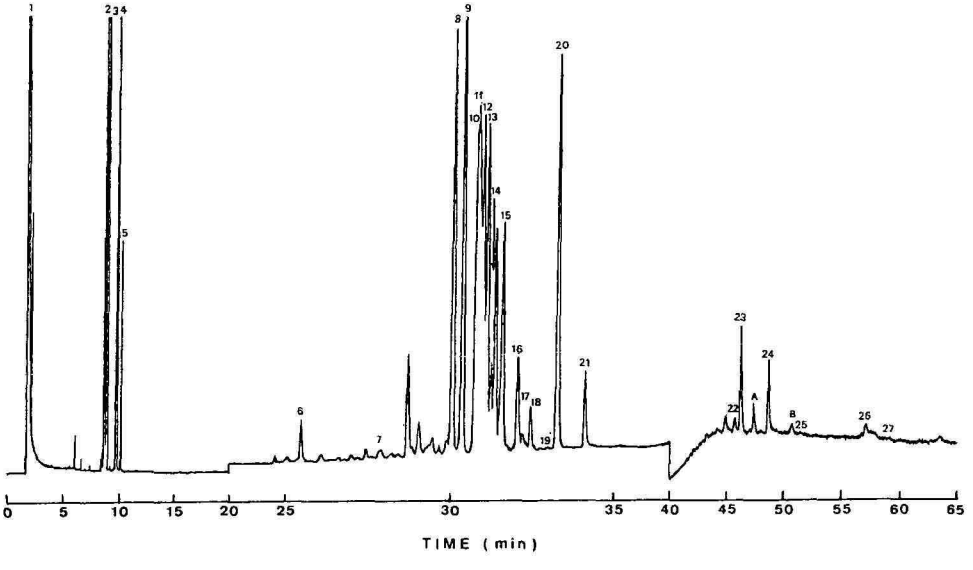

Fig. 2. Gas chromatogram of the sugars of a TMS oximated honeydew honey. Peaks: 1, solvent; 2 and 3, fructose; 4 and 5, glucose; 6, sucrose; 7, α,α-trehalose; 8 and 9, maltulose; 10, nigerose; 11, turanose and maltose; 12, turanose; 13, kojibiose; 14, maltose and isomaltose; 15, nigerose and an unidentified compound; 16, kojibiose and palatinose; 17, gentiobiose; 18, palatinose; 19, gentiobiose; 20 and 21, isomaltose; 22, raffinose; 23, 1-kestose; 24, melezitose; 25, 26 and 27, maltotriose. A, B and non-labelled peaks correspond to unidentified components. Chromatographic conditions: see under *Apparatus*.

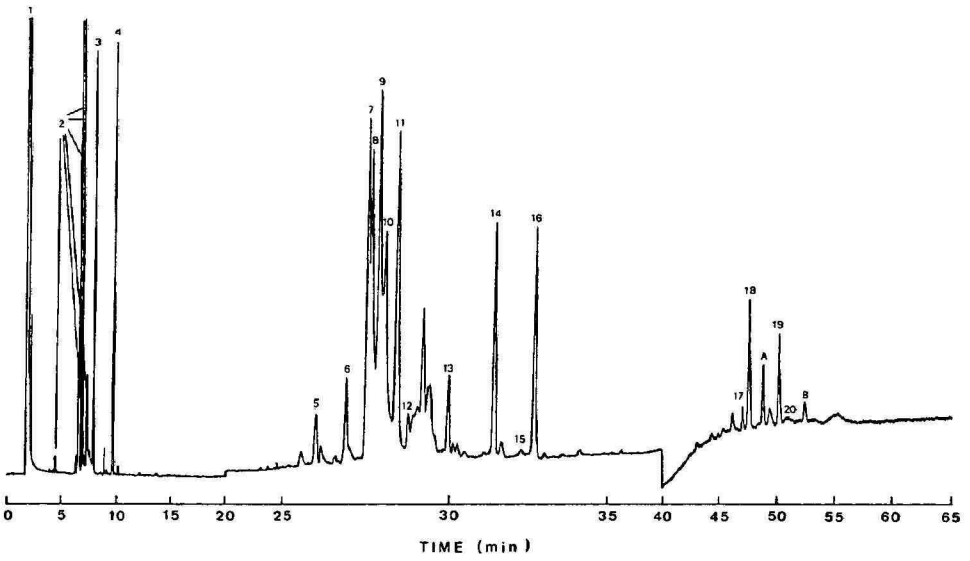

Fig. 3. Gas chromatogram of the sugars of a trimethylsilylated honeydew honey. Peaks: 1, solvent; 2, fructose (several isomeric forms); 3, α-glucose; 4, β-glucose; 5, sucrose; 6, α-maltose; 7 and 8, maltulose; 9, turanose and nigerose; 10, β-maltose; 11, β-kojibiose, nigerose and α,α-trehalose; 12, palatinose; 13, α-kojibiose; 14, α-isomaltose; 15, gentiobiose; 16, β-isomaltose; 17, raffinose; 18, 1-kestose; 19, melezitose; 20, maltotriose. A, B and non-labelled peaks correspond to unidentified components. Chromatographic conditions as in Fig. 2.

for gentiobiose), but the resolution decreased for keto-disaccharides. The anomer ratio tended to reach a stable value corresponding to mutarotational equilibrium which may be accelerated by catalysts[15,32]. Serious overlapping occurred between turanose and nigerose–1 and between trehalose, β-kojibiose and nigerose–2.

Honey samples

A *Quercus* sp. honeydew honey sample was derivatized by the two procedures and then chromatographed. The chromatogram of the TMS oximated sample (Fig. 2) shows at least one peak for each of the carbohydrates listed in Table I, with the exception of melibiose. Peaks of turanose and isomaltose hinder the identification of maltose. The nigerose–2 peak is still detectable on the ascending limb of the turanose–1 peak, whereas an unidentified component overlaps with the nigerose–3 peak. Some signals remain unidentified; A and B may be attributed to trisaccharides.

The chromatogram in Fig. 3 corresponds to the separation of sugar TMS ethers of the same honey sample. The location of the sucrose peak is more difficult than in Fig. 2, but both peaks of α- and β-maltose are easily observed. Signals from other sugars appearing in Fig. 2 are detected, which may be considered as a confirmation of their identity. Trehalose and nigerose are exceptions owing to presence of turanose and kojibiose. Melibiose is not detected and a peak coinciding with its β-anomer may arise from an unidentified compound[9]. Peaks A and B might be related to trisaccharides erlose and theanderose, respectively, on the basis of the following facts: (a) neither peak changes its RRT from one chromatogram to another, so they

must correspond to non-reducing trisaccharides; (b) hydrolysis with β-D-fructosidase (Boehringer, Manheim, F.R.G) carried out on the sample[33], followed by derivatization and separation of sugar derivatives, resulted in the disappearance of peaks A and B, and also those from sucrose, raffinose and 1-kestose, whereas the fructose peaks were increased; this result indicates that residual fructose β-linked to hexose was present in the substrate; a slight increase in maltose peaks attributable to erlose hydrolysis and the appearance of very small peaks of melibiose due to raffinose breakage were noticeable; (c) these two compounds, in addition to raffinose, 1-kestose and melezitose, are the only non-reducing trisaccharides reported in relation to honey composition[1,5] and the order of elution given for their TMS ethers is taken from data obtained with packed columns[34].

Quantitative analysis

The quantitative application of this technique to honey sugar analysis was studied. A problem relating especially to disaccharides arises from the poor resolution obtained with these compounds. From this viewpoint, the oxime-TMS procedure seems more suitable for determining fructose, glucose, sucrose, trehalose, kojibiose, palatinose and melibiose. Quantification of maltose may be achieved by the separation of the TMS ethers. Turanose and nigerose cannot be determined separately by any of these methods whereas maltulose, isomaltose, gentiobiose and trisaccharides may be determined by the two procedures. Response factors of sugars in relation to the internal standard were calculated taking into account only slightly or non-overlapping peaks.

TABLE II

SUGAR CONCENTRATION OF A *QUERCUS* SP. HONEYDEW HONEY CALCULATED BY INTERNAL STANDARDIZATION OF THE TMS DERIVATIVES SEPARATED BY OV-101 CAPILLARY COLUMN GAS CHROMATOGRAPHY

Internal standard: triphenylethylene (retention time relative to TMS-sucrose = 0.420).

Sugar	*Type of derivative*							
	TMS oximes				*TMS ethers*			
	Peak(s) used for calculation	$\bar{x}^*$ *(%)*	*s*	*C.V. (%)*	*Peak(s) used for calculation*	$\bar{x}^*$ *(%)*	*s*	*C.V. (%)*
Fructose	1 + 2	35.1	0.60	1.7				
Glucose	1 + 2	25.8	0.52	2.0	α + β	26.1	0.66	2.5
Sucrose	1	0.21	0.020	9.9	1	0.24	0.028	11.7
Trehalose	1	0.06	0.006	10.0				
Maltulose	1 + 2	3.1	0.26	8.4	1 + 2	2.8	0.30	10.7
Maltose					α + β	2.4	0.35	14.6
Kojibiose	1	2.7	0.28	10.4				
Palatinose	2	0.41	0.048	11.7				
Gentiobiose	2	0.30	0.045	15.0	1	0.25	0.03	12.0
Isomaltose	2	1.9	0.22	11.6	α + β	2.1	0.18	8.6
Raffinose	1	0.10	0.02	20.0	1	0.13	0.023	17.6
Melezitose	1	0.35	0.05	14.3	1	0.37	0.045	12.1

* Mean of five replicate injections.

Table II gives sugar concentration and precision data found in the analysis of honeydew honey. They were obtained by replicate injections of the sample derivatized by the two procedures. The precision was better for monosaccharides [coefficient of variation (C.V.) range 1.7–2.5%] than for disaccharides (C.V. 8.4–15.0%) or trisaccharides (C.V. 12–20%). Discriminatory effects between the three groups of carbohydrates were noticeable with split injection and could not be avoided either by raising the inlet temperature to 300°C or increasing the splitting ratio to 1:100. In any case, the precision of the results is similar to or better than reported values given by other capillary GC methods[18,20], and quantification of several disaccharides in honey is possible.

CONCLUSIONS

The separation of the TMS ethers and TMS oximes of honey sugars by fused-silica capillary column GC is very useful for identifying these compounds in this complex matrix, owing to the low detection limit and high efficiency of the chromatographic system and also to the complementary information obtained from chromatograms of both types of derivatives.

Some sugars are best recognized in honey by one of the two procedures. Thus, maltose gives two well resolved peaks as the TMS ether but suffers from severe interfering from turanose and isomaltose as the TMS oxime. In contrast, trehalose cannot be identified in a trimethylsilylated honey because of overlapping with kojibiose and nigerose, but it is readily detected if oximation is effected prior to silylation.

By application of this methodology to a *Quercus* sp. honeydew honey, the following sugars were identified: fructose, glucose, sucrose, α,α-trehalose, maltulose, turanose, maltose, nigerose (tentatively), kojibiose, palatinose, gentiobiose, isomaltose, raffinose, 1-kestose, melezitose and maltotriose. Two trisaccharide peaks might come from erlose and theanderose.

The proposed method appears acceptable for quantifying honey disaccharides, except turanose and nigerose, with regard to reproducibility of replicate injection data.

ACKNOWLEDGEMENTS

The authors are grateful to Dr. D. Dualde, Director of the Laboratory of Animal Health and Production, Valencia, for facilities for the use of the gas chromatograph. Prof. P. J. Reilly (University of Ames, IA, U.S.A.), Dr. H. D. Scobell (A. E. Staley Mfg., Decatur, IL, U.S.A.) and Dr. K. Sayama (Nippon Beet Sugar Mfg. Inada-cho, Hokkaido, Japan), who supplied samples of nigerose, maltulose and 1-kestose, respectively, are also thanked.

REFERENCES

1 I. R. Siddiqui, *Adv. Carbohydr. Chem. Biochem.*, 25 (1970) 285.
2 J. W. White, Jr. and N. Hoban, *Arch. Biochem. Biophys.*, 8 (1959) 386.
3 T. Watanabe and K. Aso, *Tohoku J. Agric. Res.*, 11 (1960) 109.
4 I. R. Siddiqui and B. Furgala, *J. Apic. Res.*, 6 (1967) 139.

5 I. R. Siddiqui and B. Furgala, *J. Apic. Res.*, 7 (1968) 51.
6 J. Pourtallier, *Z. Bienenforsch.*, 9 (1968) 217.
7 M. B. Battaglini and G. Bosi, *Apiata*, 7 (1972) 5.
8 M. B. Battaglini and G. Bosi, *Sci. Technol. Aliment.*, 4 (1973) 217.
9 H. Hadorn, K. Zürcher and Ch. Strack, *Mitt. Geb. Lebensmittelunters. Hyg.*, 65 (1974) 198.
10 A. Grandi, *Rass. Chim.*, 2 (1973) 73.
11 J. Pourtallier and C. Rognone, in *Les Directives Pratiques, Basées sur des Critères Fondamentaux, Technologiques et Scientifiques pour Assurer au Miel son Intégrité Naturelle, Symp. Int. Technol. Apicol., Bologne, 25–27 Janvier 1977*, Apimondia, Bucarest, 1977, pp. 74–84.
12 J. E. Thean and W. C. Funderburk, Jr., *J. Assoc. Off. Anal. Chem.*, 60 (1977) 338.
13 Z. L. Nikolov, J. B. Jakovljevic and Z. M. Boskov, *Starch/Stärke*, 36 (1984) 9.
14 S. Adam and W. G. Jennings, *J. Chromatogr.*, 115 (1975) 218.
15 Z. Nikolov and P. J. Reilly, *J. Chromatogr.*, 254 (1983) 157.
16 M. Martinez, D. Nurok and A. Zlatkis, *Anal. Chem.*, 50 (1978) 1226.
17 M. S. S. Pais and H. J. Chaves das Neves, *Apidologie*, 11 (1980) 39.
18 K. J. Schäffler and P. G. Morel du Boil, *J. Chromatogr.*, 207 (1981) 221.
19 A. Preuss, E. Schulte and H. P. Thier, *Lebensm. Wiss. Technol.*, 17 (1984) 163.
20 G. Lercker, S. Savioli, M. A. Vecchi, A. G. Sabatini, A. Nanetti and L. Piana, *Food Chem.*, 19 (1986) 225.
21 B. S. Mason and H. T. Slover, *J. Agric. Food Chem.*, 19 (1971) 551.
22 M. Demaimay, *Ann. Technol. Agric.*, 27 (1978) 455.
23 B. W. Li and K. W. Andrews, *Chromatographia*, 21 (1986) 596.
24 G. Petersson, *Carbohydr. Res.*, 33 (1974) 47.
25 T. Toba and S. Adachi, *J. Chromatogr.*, 135 (1977) 411.
26 R. Mateo and F. Bosch, *Estudio Comparativo de Algunos Patrones Internos e la Determinación de Carbohidratos en Miel por Cromatografía de Gases, XX Reun. Bien. Real Soc. Esp. Quim., Castellón, 24–28 Sept., 1984*, Com. No. 8–194.
27 K. Tesařík, *J. Chromatogr.*, 65 (1972) 295.
28 C. C. Sweeley, R. Bentley, M. Makita and W. W. Wells, *J. Am. Chem. Soc.*, 85 (1963) 2497.
29 L. Gruchala and E. Wasowicz, *Chem. Anal. (Warsaw)*, 28 (1983) 275.
30 H.-Ch. Curtius, M. Müller and J. A. Völlmin, *J. Chromatogr.*, 37 (1968) 216.
31 P. J. Wood, I. R. Siddiqui and J. Weisz, *Carbohydr. Res.*, 42 (1975) 1.
32 P. E. Reid, B. Donaldson, P. W. Secret and B. Bradford, *J. Chromatogr.*, 47 (1970) 199.
33 A. Lombard, M. Buffa, A. Manino and A. Patetta, *Experientia*, 40 (1984) 178.
34 A. Deifel, *Dtsch. Lebensm. Rundsch.*, 81 (1985) 209.

Journal of Chromatography, 410 (1987) 329–342
Elsevier Science Publishers B.V., Amsterdam — Printed in The Netherlands

CHROM. 19 921

SESQUITERPENE LACTONES FROM *ARNICA CHAMISSONIS* LESS.

VI*. IDENTIFICATION AND QUANTITATIVE DETERMINATION BY HIGH-PERFORMANCE LIQUID AND GAS CHROMATOGRAPHY

WALTER LEVEN*,** and GÜNTER WILLUHN
Institut für Pharmazeutische Biologie der Universität Düsseldorf, Universitätsstr. 1, D-4000 Düsseldorf 1 (F.R.G.)
(Received July 27th, 1987)

SUMMARY

Sesquiterpene lactones are pharmacologically interesting compounds of the flowerheads of *Arnica chamissonis* Less. spp. *foliosa* (Nutt.) Maguire, officinal as Arnicae Flos (DAB 9 and 2.AB-DDR). For the qualitative and quantitative determination of these compounds, high-performance liquid chromatographic (HPLC) and gas chromatographic (GC) methods, have been developed using Hypersil-ODS columns with a water–methanol elution gradient and UV detection at 225 nm in the HPLC system and an OV-01-CB capillary column with flame ionization detection in the GC system. The procedure includes the extraction of the sesquiterpene lactones from the plant material and a rapid sample clean-up on Extrelut columns. Based on different reference substances and different methods of calculation, the sesquiterpene lactone contents varied from 0.6 to 1.7% [relative standard deviation 4.40% by GC and 4.59% by HPLC system (n = 8)].

INTRODUCTION

Flowerheads of *Arnica chamissonis* contain sesquiterpene lactones of the pseudoguaianolide type. Recently, in addition to the known compound arnifolin (11)[1,2], several new helenanolides were isolated and identified (Fig. 1)[3–6]. Owing to their antiphlogistic and antibacterial properties[7], sesquiterpene lactones are the pharmacologically active compounds of the officinal Arnicae Flos listed in the 2.AB-DDR and DAB 9 (F.R.G.). Up to now, no standardization method for these plant components have been established in a pharmacopoeia.

In a previous paper[8], we described a colour reaction based on *m*-dinitrobenzene for the determination of sesquiterpene lactones with cyclopenten-4-one and 2-α-hydroxy-cyclopentan-4-one structures in Arnica flowerheads. In order to obtain

* For Parts IV and V, see refs. 3 and 6.
** Part of a Dissertation by W. Leven, Universität Düsseldorf, in preparation.

0021-9673/87/$03.50

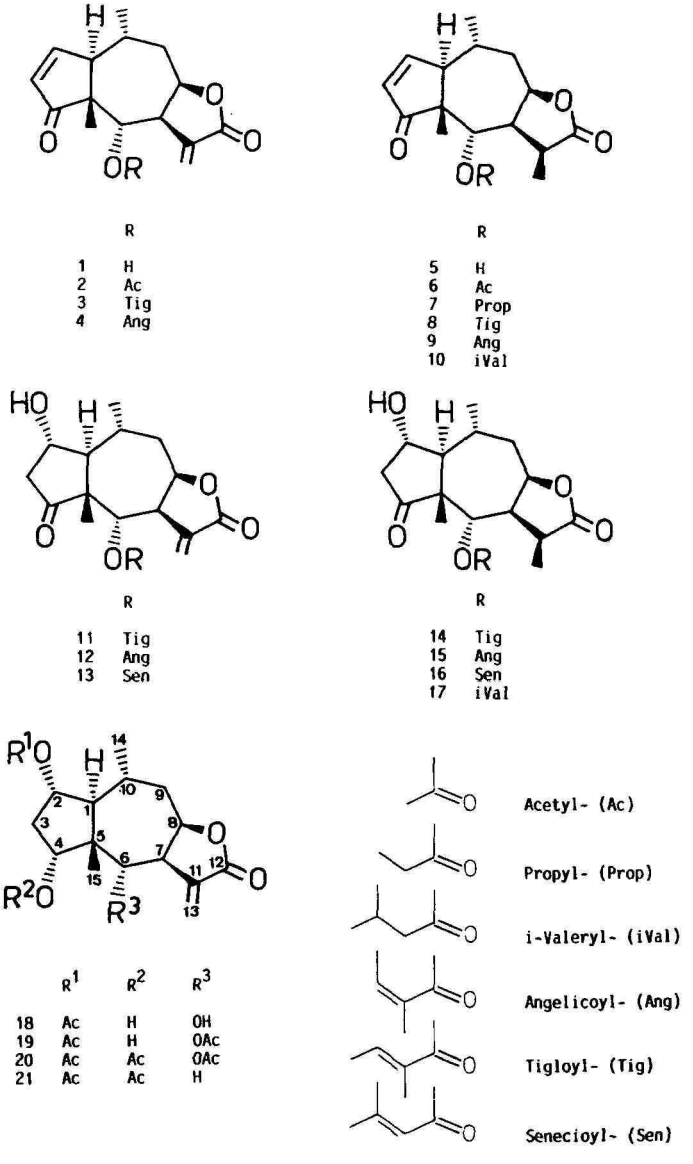

Fig. 1. Structures of sesquiterpene lactones from flowerheads of *Arnica chamissonis* ssp. *foliosa*.

more information about the amounts of individual sesquiterpene lactones in flowerheads of *A. chamissonis* ssp. *foliosa*, we have developed high-performance liquid chromatographic (HPLC) and gas chromatographic (GC) methods. Both systems had been already used for studying sesquiterpene lactones on an analytical scale[9–14]. The efficiency of reversed-phase HPLC columns and an OV-01-CB GC capillary column are reported in this paper.

EXPERIMENTAL

Extraction

The following simple and rapid sample preparation method was found to give the best results for extracting and concentrating the neutral, amphilic Arnica sesquiterpene lactones.

A 1.000-g amount of powdered flowers of Arnica were extracted twice with 50 ml of water–methanol (1:1, v/v) at 50°C using a reflux condenser and stirrer for 30 min. Santonin (1.50 mg) in methanolic solution was added to the combined and filtered crude extract as an internal standard. The extract was concentrated under reduced pressure to nearly 20 g and applied to a Extrelut 20 column (Merck, Darmstadt, F.R.G.) to separate the sample from interfering, hydrophilic compounds. After 15 min, the sesquiterpene lactones were eluted with 100 ml of methylene chloride–ethyl acetate (1:1, v/v). The eluate was evaporated under vacuum and the residue dissolved in 20 ml of methylene chloride. The methylene chloride extract was filtered and the filtrate evaporated to dryness. The sesquiterpene lactone concentrate obtained was dissolved in 10 ml of methanol and diluted with an equal volume of water. After adding 7 g of aluminium oxide, the suspension was shaken well, centrifuged and filtered. A 10-ml volume was evaporated to dryness, the residue dissolved in 2.00 ml of water–methanol (1:1, v/v), and, to avoid plugging of the HPLC column by precipitated waxes, filtered through a membrane filter (Sartorius).

HPLC equipment and experimental conditions

The HPLC system consisted of a Series 2 liquid chromatograph, an LC 75 variable-wavelength UV detector operated at 225 nm, a Model 561 recorder, a Model M-1 integrator (Perkin-Elmer, Überlingen, F.R.G.) and a sample injection valve, fitted with a 0.175-ml loop (Rheodyne, Cotati, CA, U.S.A.). The chromatographic columns were a 5-μm Hypersil-ODS (125 × 4.6 mm I.D.) (system 1) and a 5-μm Hypersil-ODS (250 × 4.6 mm I.D.) (system 2) (Shandon, filled by Bischoff, Leonberg, F.R.G.). All analyses were performed at ambient temperature with the mobile phase delivered at a flow-rate of 2.0 ml/min (system 1) or 1.0 ml/min (system 2).

Elution

Two solvents were used: (A) methanol and (B) water. The elution profile for the 125-mm column (system 1) was 0–260 s, 45% A; 260–380 s, 45–50% A (linear gradient); and 380–900 s, 50% A. The system was slightly modified in the 250-mm column (system 2): 0–600 s, 50% A; 600–720 s, 50–55% A (linear gradient); and 720–1900 s, 55% A.

HPLC solutions

Standard solutions of several Arnica sesquiterpene lactones (Table IV) were prepared in methanol–water (1:1, v/v) to contain 1 mg/ml. To determine the linearity of the detector response to these compounds, different concentrations were injected. A linear relationship between concentration and detector response (peak area) was obtained in the range 0.15–7.5 μg.

GC equipment and experimental conditions

GC analyses were carried out with an F-22 gas chromatograph (Perkin-Elmer), equipped with a capillary injection system and a flame ionization detector, using nitrogen as carrier gas in the split mode. A 25 m × 0.25 mm I.D. fused-silica capillary column coated with 0.24-μm OV-01-CB-0.25 (Macherey, Nagel & Co., Düren, F.R.G.) was used for analytical separation. The initial column temperature was 180°C, programmed from 180 to 250°C at 4°C/min and held at 250°C for 8 min. The injector and detector temperatures were 300°C. The carrier gas pressure was 1.0 bar with a 1:10 splitting ratio. A 0.5-ml volume of the sample solution was evaporated to dryness and the residue dissolved in 0.25 ml of ethyl acetate. The injection volume was 1.0 μl.

Internal standardization

Santonin, a commercial available, pure sesquiterpene lactone, was added as an internal standard for the chromatographic procedures. It could be placed near the peaks of interest and separated from other compounds of the sample in the GC and HPLC systems.

To establish the HPLC calibration factors, f(sl), relative to the standard substance, f(st) = 1, solutions of mixed sesquiterpene lactones (sl), listed in Table IV, and santonin were prepared in methanol–water (1:1, v/v) to contain 1 mg/ml of each compound. The peak area of the sesquiterpene lactone, A(sl), multiplied by the content of santonin, c(st), was divided by the peak area of santonin, A(st), multiplied by the content of the sesquiterpene lactone, c(sl), to give the individual HPLC calibration factor, f(sl/st):

$$f(\text{sl/st}) = \frac{A(\text{sl})c(\text{st})}{A(\text{st})c(\text{sl})} = \frac{f(\text{sl})}{f(\text{st})} \tag{1}$$

where c is amount in mg.

The content of each sesquiterpene lactone, c(sl), in the sample (s) was calculated by the equation

$$c(\text{sl}) = \frac{A(\text{sl})c(\text{st})}{A(\text{st})} \cdot \frac{1}{f(\text{sl})} \tag{2}$$

where c(st) is the amount of santonin (mg) added to the crude extract of the sample.

The peak areas in GC were measured by multiplying the peak width at half-height by the total peak height.

The GC calibration factors were determined by the following equations with f(st) = 1:

$$f(\text{sl/st}) = \frac{Z(\text{st})M(\text{sl})}{Z(\text{sl})M(\text{st})} = \frac{f(\text{sl})}{f(\text{st})} \tag{3}$$

where Z = number of hydrogen-bearing carbon atoms in the molecule (santonin = 10) and M = molecular weight (santonin = 246), and

$$f(\text{sl}) = \frac{0.04065M(\text{sl})}{Z(\text{sl})} \tag{4}$$

The content of each sesquiterpene lactone, $c(\mathrm{sl})$, in the sample (s) was calculated by the equation

$$c(\mathrm{sl}) = \frac{A(\mathrm{sl})c(\mathrm{st})f(\mathrm{sl})}{A(\mathrm{st})} \quad (5)$$

where $c(\mathrm{st})$ is the amount of santonin (mg) added to the crude extract of the sample.

Chemicals and plant material

Mobile phases were prepared using HPLC-grade methanol (Roth, Karlsruhe, F.R.G.) and water (Merck, Darmstadt, F.R.G.). Santonin of analytical-reagent grade was obtained from Roth (No. 2-7150).

Flowerheads of *A. chamissonis* Less. spp. *foliosa* (Nutt.) Maguire (= *A. foliosa* Nutt.) were collected from fields in Düsseldorf, Christophstrasse, during June–August 1986. The plant material was carefully dried at 40°C.

RESULTS AND DISCUSSION

HPLC separation

In order to compare the selectivity of reversed-phase (RP) packing materials we tested several different columns filled with Nucleosil 300 C_{18} (5 μm) (125 × 4.1 mm I.D. and 250 × 4.1 mm I.D.), LiChrosorb RP-18 (5 μm)(150 × 4 mm I.D.), Zorbax C_8 (5 μm) (250 × 4.1 mm I.D.) and Hypersil-ODS (5 and 3 μm) (125 × 4.1 mm I.D.). The RP materials showed considerable differences in their physical and chemical properties. Sufficient resolutions, combined with good batch stability and low working pressures, were obtained by using 5-μm Hypersil-ODS. We tried two different column sizes and, as shown in Fig. 2, the 250-mm column gave a better resolution than the 125-mm column (Fig. 3) of "critical pairs" such as arnifolin (11) and arnifolin B (12) or the corresponding 11α,13-dihydro analogues (14 and 15).

The retention times (t_r) and k' values, defined as $(t_r - t_0)/t_0$, are given in Table I. Dead times (t_0) were measured as the first distortion of the baseline following the injection of methanol. As the analysed sesquiterpene lactones cover à wide range of polarity, the mobile phase composition (mixtures of methanol–water) has to be changed slightly during the separation run. In general, adequate resolutions were obtained by varying isocratic and gradient elution with a mobile phase containing methanol at concentrations between 45 and 50% (system 1) and 50 and 55% (system 2), respectively.

The relationship between chemical structure and chromatographic behaviour of pseudoguaianolides was previously investigated by gradient elution RP-HPLC with water–acetonitrile mixtures by Marchand *et al.*[10]. In agreement with their so-called general "rules" for the structure–chromatographic behavior correlation, we noted that helenanolides containing an α,β-unsaturated cyclopentenone ring eluted later then the chemically closely related compounds with a hydroxy group in the C-2 position.

A lack of a C-6 oxygenated function causes a considerable decrease in polarity, which explains the significantly higher retention time of 4-acetyl-6-desoxychamissonolide (21) compared with chamissonolide (18), 6-acetylchamissonolide (19) or 4,6-diacetylchamissonolide (20).

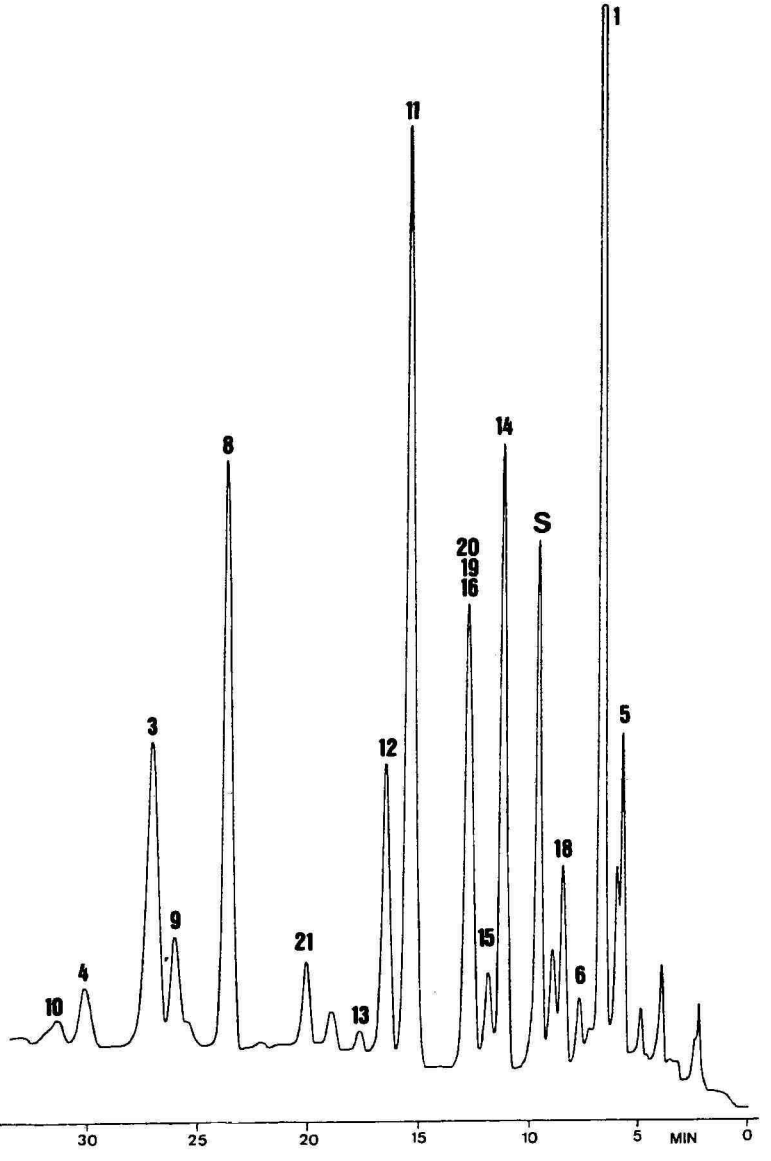

Fig. 2. HPLC separation of sesquiterpene lactones from flowerheads of *A. chamissonis* ssp. *foliosa*. 250 mm Hypersil-ODS column, system 2 (see Experimental section).

As would be expected in RP-HPLC, the polar alcohols helenalin (1) and 11α,13-dihydrohelenalin (5) have a shorter retention time than the homologous esterified derivatives (3, 4, 6, 8 and 9), but unexpectedly the 11α,13-dihydro derivatives consistently eluted before the corresponding compounds with an *exo*-methylene group. This elution sequence might be attributed to an internal hydrogen bond formed between the oxygen in the C-6 position and a C-13 hydrogen or to interac-

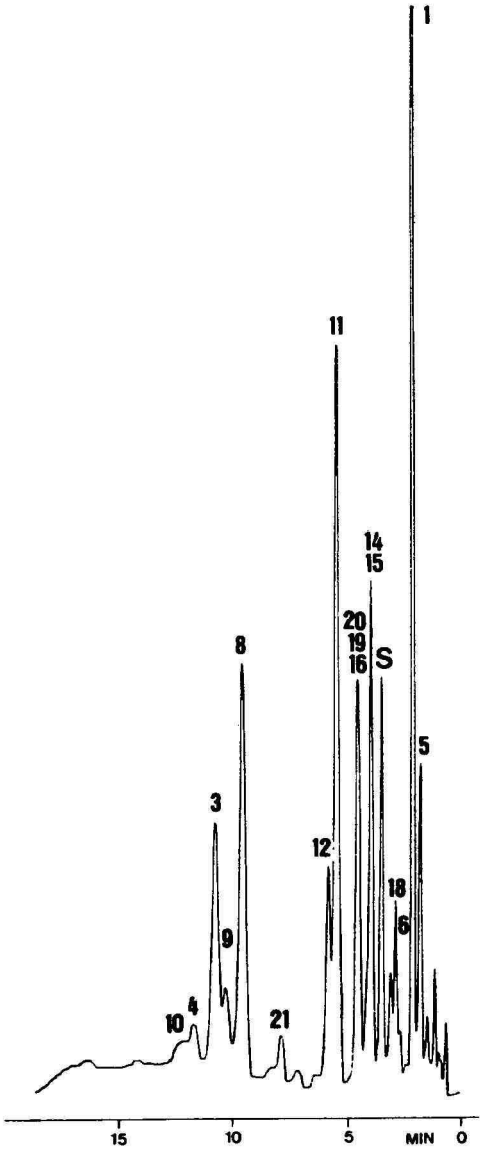

Fig. 3. HPLC separation of sesquiterpene lactones from flowerheads of *A. chamissonis* ssp. *foliosa*. 125 mm Hypersil-ODS column, system I (see Experimental section).

tions with underivatized silanol groups. The structural dependence of retention is also illustrated by the three pairs of *E,Z* isomers with an angelicoyl (*Z*-isomer) or tigloyl (*E*-isomer) group attached at C-6. Although their relative retention values, given in Table II, differ only slightly, the double bond configuration effect on separation increases with decrease in polarity.

The explanation of the similar retention times of 6-O-acetylchamissonolide

TABLE I

HPLC RETENTION TIMES, t_R (min), AND CAPACITY FACTORS, k' $[(t_R - t_0)/t_0]$, OF ARNICA SESQUITERPENE LACTONES

Stationary phase, 5-μm Hypersil-ODS; mobile phase, methanol–water.

No.	*Substance*	*HPLC Column**			
		125 mm (system 1), t_0 = 0:35		*250 mm (system 2), t_0 = 2:15*	
		t_R	k'	t_R	k'
S	Santonin	3:30	5.00	10:00	3.44
5	11α,13-Dihydrohelenalin (DH)	1:46	2.03	5:42	1.57
1	Helenalin (H)	2:10	2.71	6:38	1.99
6	6-O-Acetyl-DH	2:51	3.89	7:44	2.49
18	Chamissonolide	3:04	4.26	8:28	2.82
14	11α,13-Dihydroarnifolin	4:11	6.17	11:14	4.07
15	11α,13-Dihydroarnifolin B			11:57	4.39
16	Flexuosin B	4:48	7.23	12:50	4.79
19	6-O-Acetylchamissonolide	4:48	7.23	12:50	4.79
20	4,6-O-Diacetylchamissonolide	4:48	7.23	12:50	4.79
11	Arnifolin	5:48	8.94	15:30	5.99
12	Arnifolin B	6:11	9.60	16:37	6.50
13	11,13-Anhydroflexuosin B			17:42	6.87
21	4-O-Acetyl-6-desoxychamissonolide	8:17	13.20	20:14	8.13
8	6-O-Tigloyl-DH	9:54	15.97	23:45	9.71
9	6-O-Angelicoyl-DH	10:40	17.29	26:13	10.83
3	6-O-Tigloyl-H	11:08	18.09	27:12	11.21
4	6-O-Angelicoyl-H	12:05	19.71	30:17	12.66

* Times 3:30 etc. represent minutes and seconds.

TABLE II

RELATIVE RETENTION (k'_2/k'_1) VALUES CALCULATED FOR THE *E,Z* ISOMERS

No.	*Substance*	*125 mm column (system 1)*	*250 mm column (system 2)*
14	11α,13-Dihydroarnifolin		
15	11α,13-Dihydroarnifolin B		1.079
11	Arnifolin		
12	Arnifolin B	1.074	1.085
8	6-O-Tigloyl-11α,13-dihydrohelenalin		
9	6-O-Angelicoyl-11α,13-dihydrohelenalin	1.083	1.115
3	6-O-Tigloylhelenalin		
4	6-O-Angelicoylhelenalin	1.089	1.123

(19) and 4,6-O-diacetylchamissonolide (20), which are co-eluted in combination with flexuosin B (16), is difficult. Even under optimal chromatographic conditions neither of the compounds could be separated. The chromatographic behaviour of these two compounds might be explicable as a complex retention mechanism influenced by several effects, such as configuration, hydration and interactions.

Based on the above results, it may be concluded that the retention of the Arnica sesquiterpene lactones with an α,β-unsaturated ketone moiety generally increases with increasing length of the acyl substituent on C-6, but decreases significantly with a β-hydroxy ketone structure on the cyclopentane ring. Concerning the chamissonolide derivatives (18–21), it is evident that a C-6 oxygenated function, in contrast to unsubstituted C-6, affects the retention time in a similar manner to that for C-2. Finally, compounds with an *exo*-methylene group are retained longer than the dihydro homologues.

GC separation

In spite of the uncontested utility of RP-HPLC, problems arise in measuring compounds such as 11α,13-dihydroarnifolin C (17) that have very low UV absorption in the range of the wavelength of measurement, or that are co-eluted in all HPLC systems, *e.g.*, flexuosin B (16), 6-O-acetylchamissonolide (19) and 4,6-O-diacetylchamissonolide (20). Therefore, we investigated the capillary GC separation of Arnica sesquiterpene lactones using a relatively non-polar dimethylsilicone column connected to a flame ionization detector. Columns with a normal OV-01 phase showed substantial wastage of helenalin and dihydrohelenalin and considerable peak tailing of compounds with a β-hydroxy ketone moiety in the cyclopentane ring. Excellent resolution was obtained with an OV-01 chemically bonded phase. The adsorption effects on the normal-phase columns may be attributed to the silanol groups on the surface of the fused-silica material, which are capped on the chemically modified column.

Fig. 4 demonstrates the GC separation of the sesquiterpene lactones extracted from *A. chamissonis* ssp. *foliosa*. Retention times, k' values and relative retention values, calculated with santonin as an internal standard, and by a comparison of the analogues 11α,13-dihydro- and 11,13-anhydro derivatives, are given in Table III.

It is evident that although in both the liquid and gas chromatographic systems a reversed-phased material was used as the stationary phase, the effect of structure on the chromatographic behaviour of the sesquiterpene lactones differed and was nearly reversed in GC. As illustrated in Fig. 4, compounds with a 2-α-hydroxycyclopentanone structure are retained longer than the analogous compounds with an α,β-unsaturated ketone structure. Owing to the higher resolving power of the GC system, the *E,Z*-isomers are well separated. As a result of the lower polarity, the 11α,13-dihydro derivatives eluted after the corresponding compounds with an *exo*-methylene group.

Nevertheless, the GC system does not solve all the separation problems. For example, 11α,13-dihydroarnifolin C (17) appears together with 6-O-acetylchamissonolide (19) in a badly resolved peak, and the corresponding tiglin- (11,14) and senecio acid esters (13,16) are separated by HPLC but co-elute in the GC system.

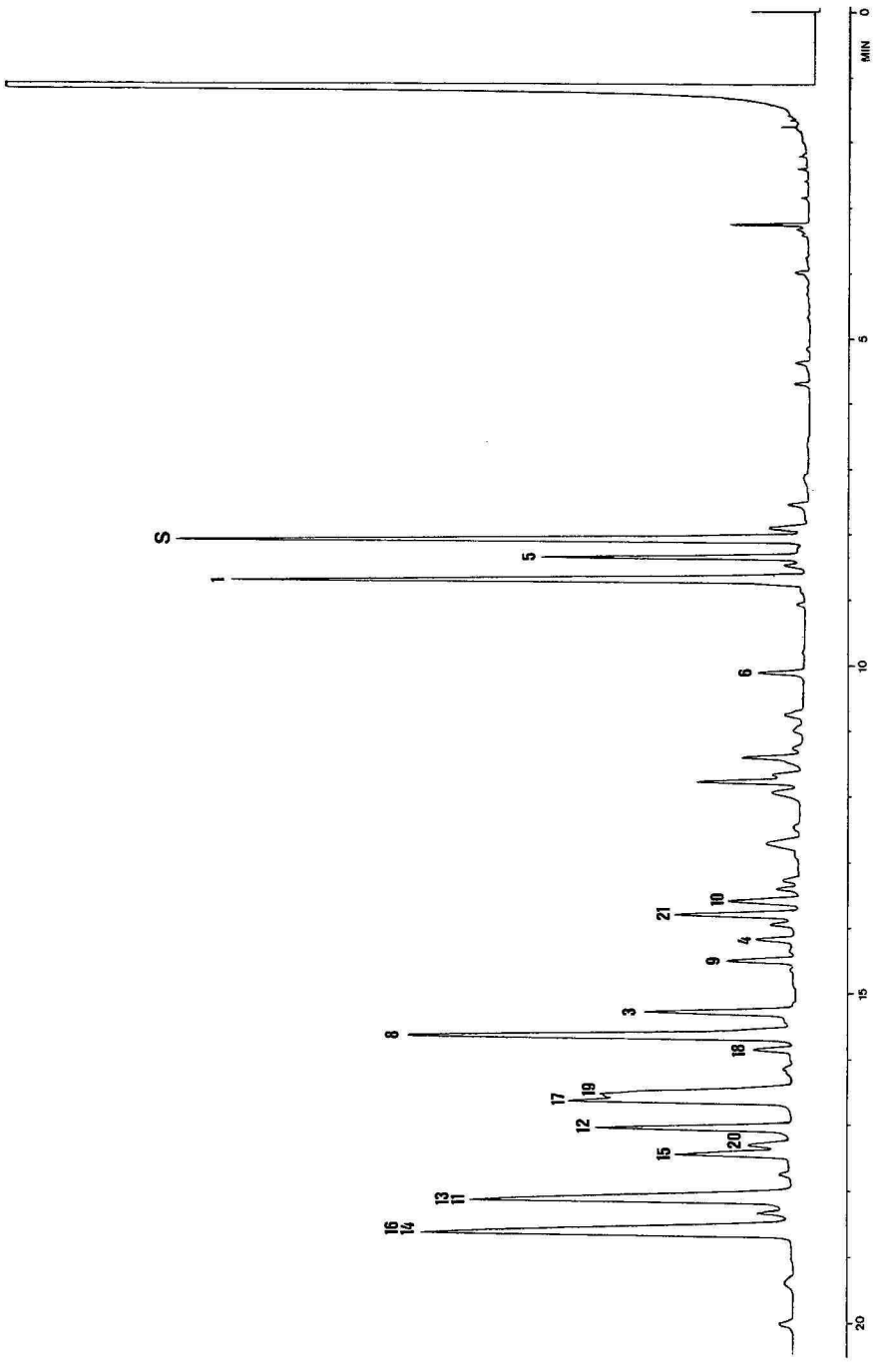

Fig. 4. GC separation of sesquiterpene lactones from flowerheads of *A. chamissonis* ssp. *foliosa*. OV-01-CB capillary column (see Experimental section).

TABLE III

GC RETENTION TIMES, t_R (min), AND CAPACITY FACTORS, $k'[(t_R - t_0)/t_0$; t_0 = 72 s], OF ARNICA SESQUITERPENE LACTONES

Stationary phase: OV-01-CB.

No.	*Substance*	t_R*	k'**
S	Santonin	8:06	5.75
5	11α,13-Dihydrohelenalin (DH)	8:24	6.00
1	Helenalin (H)	8:47	6.31
6	6-O-Acetyl-DH	11:45	8.79
10	6-O-Isovaleryl-DH	13:39	10.38
21	4-O-Acetyl-6-desoxychamissonolide	13:53	10.56
4	6-O-Angelicoyl-H	14:17	10.90
9	6-O-Angelicoyl-DH	14:39	11.21
3	6-O-Tigloyl-H	15:21	11.79
8	6-O-Tigloyl-DH	15:45	12.12
18	Chamissonolide	16:00	12.33
19	6-O-Acetylchamissonolide	16:39	12.87
17	11α,13-Dihydroarnifolin C	16:47	12.98
12	Arnifolin B	17:09	13.29
15	11α,13-Dihydroarnifolin B	17:36	13.67
20	4,6-O-Diacetylchamissonolide	17:27	13.54
13	11,13-Anhydroflexuosin B/		
11	Arnifolin	18:15	14.21
14	11α,13-Dihydroarnifolin/		
16	Flexuosin B	18:45	14.62

* Times 8:06 etc. represent minutes and seconds.

** Relative retention (α) of 11α,13-dihydro compounds relative to the corresponding compounds with an *exo*-methylene group, *i.e.*, $k'(8)/k'(3)$, $k'(9)k'(4)$, $k'(15)k'(14)$ and $k'(12)/k'(11)$: $\alpha = 1.028$.

TABLE IV

HPLC AND GC CALIBRATION FACTORS, MOLAR ABSORPTIVITIES (ε), AND λ_{max} OF SESQUITERPENE LACTONES FROM *A. CHAMISSONIS* LESS. SSP. *FOLIOSA*

No.	*Substance*	*f(sl)*		ε ($l\ mol^{-1}\ cm^{-1}$)	λ_{max} (*nm*)
		GC	*HPLC*		
1	Helenalin (H)	0.968	2.20	12 090	225*
2	11α,13-Dihydrohelenalin (DH)	0.894	0.80	4480	227**
3	6-O-Tigloyl-H	1.000	1.15	14 361	218**
8	6-O-Tigloyl-DH	0.938	0.88	10 414	222**
18	Chamissonolide	1.013	1.00	7708	214**
11	Arnifolin	1.051	2.14	16 958	216**
14	11α,13-Dihydroarnifolin	0.986	1.00	7780	218**

* In 50% methanol.

** In methanol.

TABLE V

TOTAL AMOUNT OF SESQUITERPENE LACTONES IN FLOWERHEADS OF *A. CHAMISSONIS* SSP. *FOLIOSA*

No.	*Calculated as*	*mg/g dry weight*	
		GC	*HPLC*
1	Helenalin (H)	8.16	6.31
5	Dihydrohelenalin (DH)	9.00	17.35
3	6-O-Tigloyl-H	8.10	12.09
8	6-O-Tigloyl-DH	7.61	15.80
11	Arnifolin	8.57	6.49
14	11α,13-Dihydroarnifolin	8.01	13.90
18	Chamissonolide	8.21	13.90

* Relative standard deviation calculated from measurements on eight sample solutions = 4.40% in the GC and 4.59% in the HPLC system.

Quantification

To consider the wide differences in the molar absorptivities of the compounds present in the sample, and also specific influences of the chromatographic system, several HPLC calibration factors were determined (Table IV), as mentioned above, using samples with known amounts of santonin and sesquiterpene lactones, which were as far as possible isolated on a preparative scale from plant material or synthesized from helenalin and tiglin acid.

As there are still several compounds with unknown calibration factors or that are being co-eluted with others, the total amount of sesquiterpene lactones in flowerheads of *A. chamissonis* ssp. *foliosa* was calculated by taking one component, *e.g.*, the main compound, as a reference substance (Table V) that would be suitable for simple standardization requirements.

TABLE VI

PARTIAL AMOUNTS OF 11,13-ANHYDRO- AND 11α,13-DIHYDRO- COMPOUNDS IN FLOWER-HEADS OF *A. CHAMISSONIS* SSP. *FOLIOSA* AND TOTAL CONTENT CALCULATED AS SUM OF THESE VALUES

No.	*Calculated as*	*mg/g dry weight*					
		11,13-Anhydro compound		*11α,13-Dihydro compound*		*Total content*	
		GC	*HPLC*	*GC*	*HPLC*	*GC*	*HPLC*
3	6-Tigloyl-H	3.32	7.58				
8	6-Tigloyl-DH			3.85	6.32		
	Sum					7.08	13.90
11	Arnifolin	3.42	4.07				
14	11α,13-Dihydroarnifolin			4.05	5.50		
	Sum					7.47	9.63

On the other hand, standardization by choosing a reference substance could only be successful if there are qualitative and quantitative similarities in the sesquiterpene lactone patterns of plant materials from different geographic origins. Studies of the distribution and concentration of sesquiterpene lactones in flowerheads of several *A. chamissonis* ssp. *foliosa* plants cultured in Düsseldorf and originating from different areas of the U.S.A. offered a variable compound composition. The results will be reported in a later paper.

Therefore, it might be more precise and practicable to use different reference substances according to the different sesquiterpene lactone substitution types, forming groups of compounds with only small differences in their molar absorptivities. Splitting the total amount of sesquiterpene lactones into parts representing derivatives with 11α,13-dihydro and 11,13-anhydro structures (Table VI) and/or on the basis of the different types of substitution on the cyclopentane ring (Table VII) will be more useful for comparing different samples and for obtaining comparable values for standardization purposes.

TABLE VII

PARTIAL AMOUNTS OF HELENALIN, DIHYDROHELENALIN, THEIR ESTERS AND COMPOUNDS WITH 2α-HYDROXYCYCLOPENTAN-4-ONE (I) AND 2α-ACETYL-4α-HYDROXY- OR 2α,4α-DIACETYLCYCLOPENTANE (II) STRUCTURES IN FLOWERHEADS OF *A. CHAMISSONIS* SSP. *FOLIOSA*

Compound(s)	*Calculated as*	*mg/g dry weight*	
		GC	*HPLC*
Helenalin (H)	Helenalin	1.03	1.38
Dihydrohelenalin (DH)	Dihydrohelenalin	0.40	0.36
H-esters	Tigloyl-H	0.46	1.29
DH-esters	Tigloyl-DH	1.39	2.15
Arnifolins (I)	Arnifolin	1.54	1.53
11α,13-Dihydroarnifolins	Dihydroarnifolin	2.31	2.45
Chamissonolides (II)	Chamissonolide	0.48	0.63
Sum		7.61	9.79

Depending on the reference substances that are taken as a basis of the calculation, the sesquiterpene lactone content in the dried Arnica flowerheads determined by HPLC varies in the range 0.63–1.74%. The GC and HPLC values are closer if the total HPLC result represents the sum of several specific portions, each indicated by the most accurate calibration factor. Quantitative determination using our previously described spectrophotometric method[8] yielded a total of 0.55% for the same plant material, restricted to the components mentioned above and calculated with respect to 6-O-acetyl-11α,13-dihydrohelenalin.

In conclusion, the HPLC and GC systems in combination with the sample preparation as described can be used to determine and identify sesquiterpene lactones in various species of Arnica. Results for typical samples can be obtained within 3 h, including sample preparation.

ACKNOWLEDGEMENT

Financial support from the DFG is gratefully acknowledged.

REFERENCES

1 R. I. Evstratova, A. I. Ban'kovskii, V. I. Sheichenko and K. S. Rybalko, *Khim. Prir. Soedin.*, (1971) 270.
2 R. I. Evstratova, V. I. Sheichenko, K. S. Rybalko and A. I. Ban'kovskii, *Khim. Farm. Zh.*, (1969) 39; *Sb. Nauchn. Rab. Vses. Nauchno-Issled. Inst. Lek. Rast.*, (1970) 148; *C.A.*, 76 (1972) 141046a.
3 G. Willuhn, J. Junior, J. Kresken, G. Pretzsch and D. Wendisch, *Planta Med.*, (1985) 398.
4 G. Willuhn, J. Kresken and D. Wendisch, *Planta Med.*, 47 (1983) 157.
5 G. Willuhn and J. Kresken, *Planta Med.*, 45 (1982) 132.
6 J. Kresken and G. Willuhn, in preparation.
7 A. K. Picman, *Biochem. Syst. Ecol.*, 14 (1986) 255.
8 W. Leven and G. Willuhn, *Planta Med.*, (1986) 537.
9 G. R. Jamieson, E. H. Reid, B. P. Turner and A. J. Jamieson, *Phytochemistry*, 15 (1976) 1713.
10 B. Marchand, H. M. Behl and E. Rodriguez, *J. Chromatogr.*, 265 (1983) 97.
11 O. Spring, T. Priester, H. Stransky and A. Hager, *J. Plant Physiol.*, 120 (1985) 321.
12 D. W. Hill, H. L. Kim and B. J. Camp, *J. Agric. Food Chem.*, 27 (1979) 885.
13 C. Wandel and G. Willuhn, *Farm. Tijdschr. Belg.*, 61e (1984) 362.
14 D. Strack, P. Proksch and P. G. Gülz, *Z. Naturforsch.*, Teil C, 35 (1980) G15.

Journal of Chromatography, 410 (1987) 343–353
Elsevier Science Publishers B.V., Amsterdam — Printed in The Netherlands

CHROM. 19 992

COMPARISON OF PACKED COLUMN AND CAPILLARY COLUMN SUPERCRITICAL FLUID CHROMATOGRAPHY AND HIGH-PERFORMANCE LIQUID CHROMATOGRAPHY USING REPRESENTATIVE HERBICIDES AND PESTICIDES AS TYPICAL MODERATE POLARITY AND MOLECULAR WEIGHT RANGE MOLECULES

JULIA R. WHEELER* and MARY ELLEN McNALLY
E. I. du Pont de Nemours & Co., Inc., Agricultural Products Department, Experimental Station, Wilmington, DE 19898 (U.S.A.)
(Received July 29th, 1987)

SUMMARY

The role of supercritical fluid chromatography (SFC) as a viable technique for analyzing agricultural products has been investigated using packed and capillary column methodology. The goal was to question the strengths and weaknesses of each of the techniques as possible approaches to separation strategies for thermally labile compounds as compared to the currently used high-performance liquid chromatography methodology. Representative herbicides have been examined with the techniques to compare such factors as linearity of response, limit of detection and reproducibility. In the literature so far, a direct numerical comparison of these three techniques for the analysis of real samples has not been presented.

Results indicate that faster analyses, lower detection limits and greater injection to injection reproducibility are obtainable with packed column SFC. No appreciable difference in the linearity of response between the three techniques was noted. It has been well documented that the capillary SFC affords greater efficiencies and higher resolution [H. E. Schwartz, *LC · GC, Mag. Liq. Gas Chromatogr.*, 5 (1987) 14]. Capillary SFC can also be interfaced to a variety of detectors not as easily accomplished with packed column SFC. Capillary SFC therefore still has a viable position in the analysis of low and moderate molecular weight and polarity molecules.

INTRODUCTION

The purpose of this investigation was to determine the role of supercritical fluid chromatography (SFC) in the analysis of typical herbicides and pesticides. These thermally labile, moderately polar compounds have traditionally been analyzed by reversed-phase high-performance liquid chromatography (HPLC). Limitations of HPLC include lack of a universal detector, difficult separation of polar metabolites and precursors from less polar parent compounds and formulation mixtures, and removal of large quantities of mobile phase in fraction collection studies. Our purpose was to assess the value of SFC with respect to these problems.

0021-9673/87/$03.50

Literature reports have demonstrated SFC effective in analyzing a wide variety of compounds, including high-molecular-weight polymers, antibiotics, carbamate pesticides, steroids and lipids [1–4]. SFC is a low-temperature analytical technique, a feature compatible with the separation of thermally labile compounds. Due to high solute diffusivity in a less dense supercritical mobile phase compared to a liquid mobile phase as in LC, the analysis time is faster with packed column SFC (PC-SFC). When gas chromatographic (GC) type capillary columns are used in capillary SFC (CSFC), higher efficiencies and more resolution are obtained for additional separation power in complex samples and matrices[5,6].

In this investigation, both PC-SFC and CSFC techniques have been examined. The goal was to survey the strengths and weaknesses of both in developing separation strategies and incorporating SFC into routine use. It had been established that the PC-SFC technique provides for higher sample capacity and shorter analysis times[7]. Fraction collection of larger quantities of materials for further analysis could be facilitated with this technique. The packed column instrument used in these studies utilizes UV detection routinely, thus allowing mobile phase modifiers to be employed. With its binary pumping system, a gradient mobile phase profile can be achieved, a feature not commercially available with any capillary instrument to date.

The known strengths of CSFC include the option to easily interface with a variety of detectors such as the mass[8] and infrared (IR) spectrometers [9,10], the ultraviolet (UV)[11], nitrogen-phosphorus and universal flame ionization detectors[5]. We have also found that analyses conducted with CSFC can provide insight into method development using the packed column instrument. However, method development time with the packed column instrument is generally much quicker.

With a numerical assessment of ruggedness in mind, five herbicides, representative of a variety of agricultural related compounds, were analyzed with HPLC, PC-SFC and CSFC. Limits of detection, reproducibility and linearity of response are compared.

EXPERIMENTAL

Instrumentation

For HPLC experiments several liquid chromatographic instruments were used. They were: a Varian 5500 liquid chromatograph equipped with a Model 200 variable-wavelength UV detector and a Model 8085 autosampler, Hewlett Packard 1090M and 1090A liquid chromatographs equipped with photodiode array detectors and either an HP79994A analytical work station or a HP-85B personal computer.

PC-SFC experiments were conducted with a Hewlett Packard 1082B liquid chromatograph modified to allow a supercritical mobile phase to be used. Modifications, detailed elsewhere[12], included: a heat exchanger cooled with circulating ethylene glycol at each of the diaphragm pump heads, a heated region after the mixing chamber but prior to the injector and column to ensure a supercritical mobile phase at the head of the column, a second heat exchanger after the oven to prevent a temperature differentiation between the mobile phase and the detector, a high pressure UV detector cell and a back pressure regulator to maintain supercritical pressures throughout the system.

The CSFC experiments were conducted with a Lee Scientific supercritical fluid

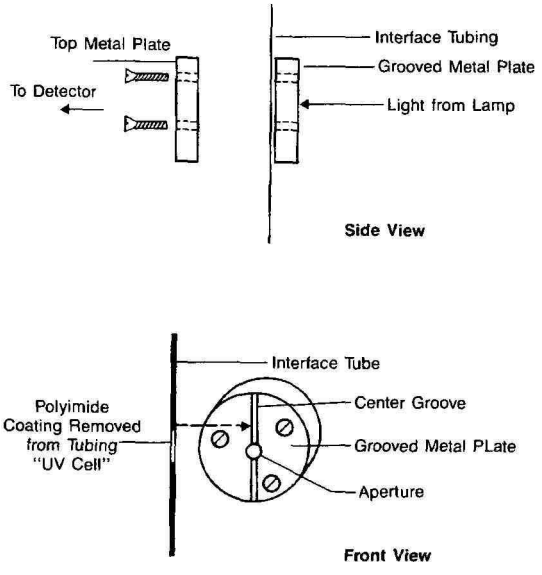

Fig. 1. UV cell placement in Kratos UV detector.

chromatograph, Series 501. The CSFC instrument was equipped with a flame ionization detector and nitrogen-phosphorus detector. A Kratos 770 UV detector was interfaced to the CSFC instrument in-house, allowing the use of a variety of mobile phase modifiers inappropriate with the flame ionization detector. The capillary interface line was connected to the chromatographic column inside the oven and drawn through the flame ionization detector orifice into the Kratos detector situated on top of the CSFC instrument. This position was chosen to reduce the length of capillary tubing outside the oven.

The polyimide coating was removed from a small portion of the capillary interface tubing to provide a UV transparent cell. Minor modifications to the detector facilitated the interfacing process. A metal plate was drilled with a vertical groove and a center hole to restrict movement of the capillary UV cell inside the detector[13]. The interface line was taped onto the front of the metal plate directly in the sample light beam with black electrical tape. Additional masking of the aperture was necessary to prevent stray light from entering the detector (see Fig. 1).

Two horizontal slits were cut in the detector head which allowed it to slide into place on the optical bench rails without disturbing the capillary UV cell (see Fig. 2).

A restrictor was connected to the tube after the detector to maintain pressure throughout the system. Restrictor clogging was a persistent problem. The restrictor tip was placed in a beaker of methylene chloride during the course of the experiment. Clogging was greatly reduced; rapid detection of blockage was then possible.

Compounds investigated

The compounds examined as a representative sampling of moderately polar herbicides were: Oust®, Glean®, Karmex®, Harmony® and Nustar®. Oust, a sulfon-

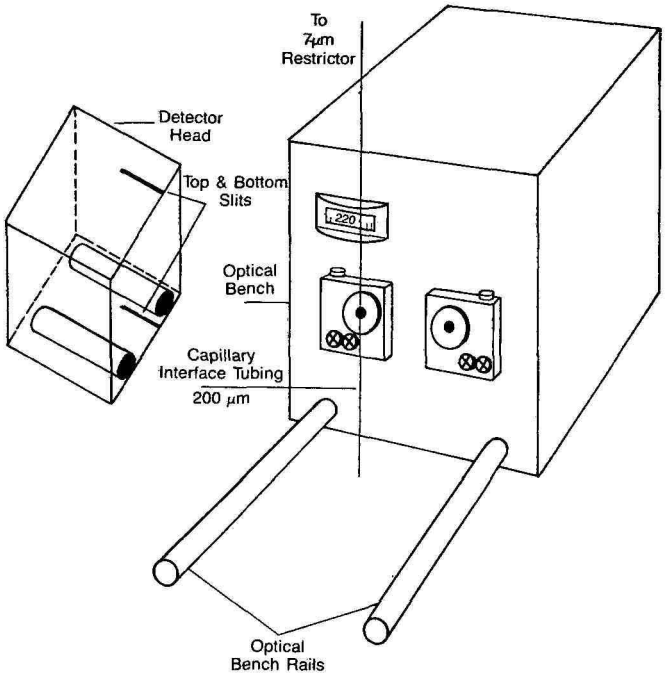

Fig. 2. Modifications to the Kratos 770 UV detector.

GLEAN®

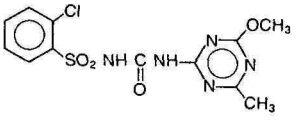

KARMEX®

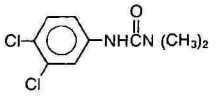

HARMONY®

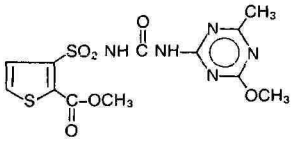

OUST®

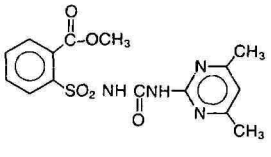

NUSTAR®

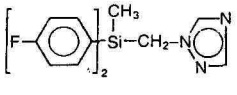

Fig. 3. Structures of the agricultural compounds used.

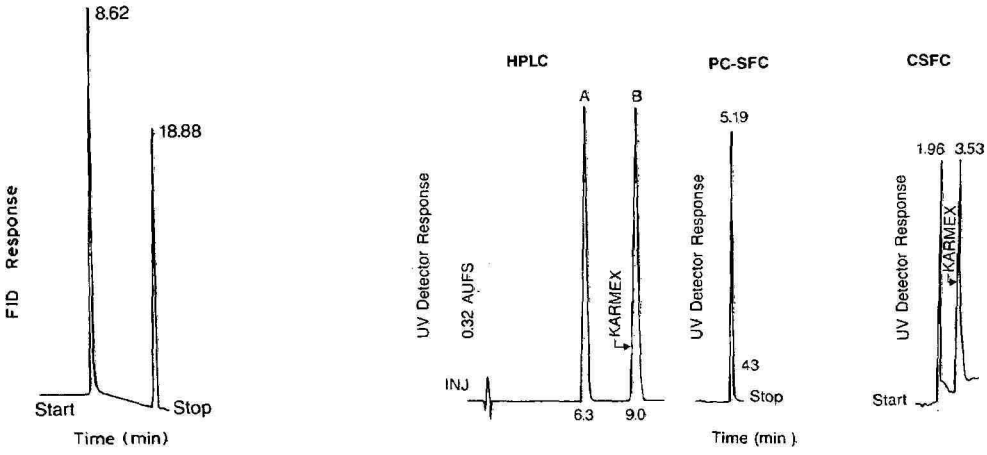

Fig. 4. Typical CSFC chromatogram for Glean herbicide. Column: SB-phenyl 50, 17 m × 100 μm I.D. Mobile phase: carbon dioxide. Injection loop: 200 nl, 1:20 split. Oven temperature: 80°C. Density program: initial, 0.25 g/ml; hold, 12 min; ramp, 0.1 g/ml/min; final, 0.65 g/ml.

Fig. 5. Comparative chromatograms of Karmex herbicide. *HPLC*. Column: Zorbax® ODS, 25 cm × 4.6 mm I.D. Mobile phase: acetonitrile–water (35:65). Detection: UV at 254 nm. Injection volume: 10 μl. Flow-rate: 2.0 ml/min. Oven temperature: 45°C. A = Internal standard; B = Karmex. *PC-SFC*. Column: Zorbax SIL, 25 cm × 4.6 mm I.D. Mobile phase: 5% methanol in carbon dioxide. Detection: UV at 211 nm. Injection volume: 10 μl. Flow-rate: 5.0 ml/min. Oven temperature: 45°C. *CFSC*. Column: SB-methyl, 15 m × 100 μm I.D. Mobile phase: carbon dioxide. Detection: UV at 211 nm. Injection volume: 200 nl, no split. Oven temperature: 60°C. Density of carbon dioxide: 0.35 g/ml.

ylurea, and Karmex, a phenyl methylurea, are general herbicides for use in controlling weeds for a variety of crops including sugar cane, pineapples and citrus fruits. Glean and Harmony are sulfonylurea cereal herbicides, and Nustar is a silicon fungicide. See Fig. 3 for structures.

RESULTS AND DISCUSSION

Predominantly HPLC has been used in assay and impurity method development for these agricultural products. Initial experiments in our laboratory showed SFC to be effective in analyzing representative agricultural products. Quantitative information needed to be generated using both PC-SFC and CSFC techniques to justify ruggedness. The advantages of faster analysis times and increased separation efficiencies would not be realized unless reproducibility and durability could be proven for both the packed and capillary column techniques.

A typical example CSFC chromatogram obtained for these compounds is shown in Fig. 4 for Glean herbicide. In order to shorten the analysis times normally achieved with CSFC, to make them competitive with the retention times in LC and PC-SFC, shorter columns and density programs designed to reduce retention times were used. These columns and the chromatographic conditons used for CSFC, PC-SFC and HPLC can be seen in Figs. 5–9. Included in these figures are sample chromatograms of the five representative compounds for each of the techniques. The quantitative results generated with these conditions are in Tables I–V.

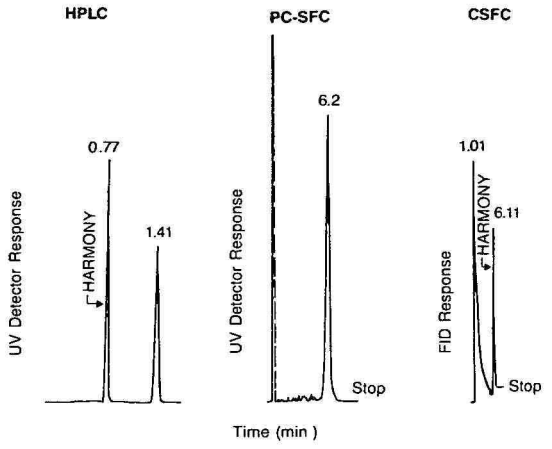

Fig. 6. Comparative chromatograms of Harmony herbicide. *HPLC*. Column: Whatman RAC-II, ODS-3, 10 cm × 4.6 mm I.D. 5 μm particle size. Mobile phase: acetonitrile–water (pH 3.0) (46:54). Detection: UV at 254 nm. Flow-rate: 3.0 ml/min. Injection volume: 10 μl. Oven temperature: 45°C. *PC-SFC*. Column: Zorbax SIL, 25 cm × 4.6 mm I.D. Mobile phase: 8% methanol in carbon dioxide. Detection: UV at 220 nm. Flow-rate 5.0 ml/min. Injection volume: 10 μl. Oven temperature: 45°C. *CSFC*. Column: SB-phenyl 50, 3 m × 100 μm I.D. Mobile phase: carbon dioxide. Detection: FID, 400°C. Injection volume: 200 nl, 1:20 split. Oven temperature: 100°C. Density program of carbon dioxide: initial, 0.45 g/ml; hold, 5 min; ramp, to 0.6 g/ml at 0.1 g/ml/min; hold, 5 min; quit, 0.45 g/ml.

PC-SFC

PC-SFC has demonstrated detection limits, reproducibility and linearity comparable to those obtained with HPLC. The PC-SFC approach offers faster analysis times due to the lower densities of the supercritical mobile phases *versus* liquids in

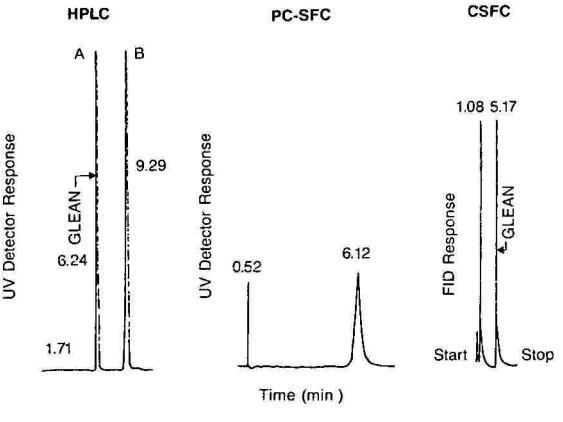

Fig. 7. Comparative chromatograms of Glean herbicide. *HPLC*. Column: Zorbax ODS, 25 cm × 4.6 mm I.D. Mobile phase: acetonitrile–water (pH 3.0) (28:72). Detection: UV at 254 nm. Injection volume: 10 μl. Flow-rate: 2.0 ml/min. Oven temperature: 45°C. A = Glean; B = internal standard. *PC-SFC*. Column: Zorbax SIL, 25 cm × 4.6 mm I.D. Mobile phase: 4% methanol in carbon dioxide. Detection: UV at 220 nm. Injection volume: 10 μl. Flow-rate: 5.0 ml/min. Oven temperature: 45°C. *CSFC*. Column: SB-phenyl 50, 3 m × 100 μm I.D. Mobile phase: carbon dioxide. Detection: FID, 350°C. Injection volume: 200 nl, 1:20 split. Oven temperature: 100°C. Density of carbon dioxide: 0.6 g/ml.

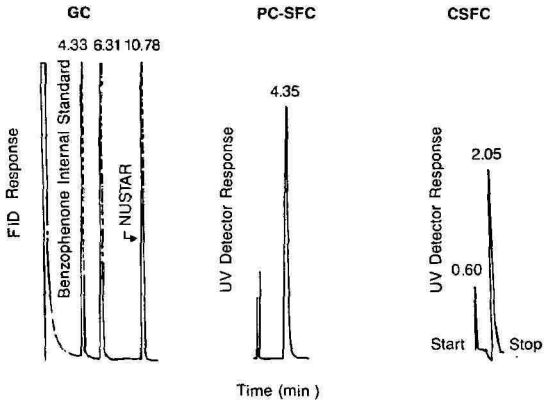

Fig. 8. Comparative chromatograms of Nustar herbicide. *GC*. Column: 1.2 m × 2 mm I.D. glass tube packed with 3% SP-2100 DB on 100/120 mesh Supelcoport. Oven temperature: 140°C for 2 min to 250°C at 12°C/min. Detection: FID. Injection volume: 2 μl. *PC-SFC*. Column: Zorbax SIL, 25 cm × 4.6 mm I.D. Mobile phase: 4% methanol in carbon dioxide. Oven temperature: 45°C. Detection: UV at 210 nm. Injection volume: 10 μl. Flow-rate: 5.0 ml/min. *CSFC*. Column: SB-phenyl 50, 3 m × 100 μm I.D. Mobile phase: carbon dioxide. Oven temperature: 100°C for 1 min to 50°C at 50°C/min. Detection: UV at 210 nm. Injection volume: 200 nl, no split. Density of carbon dioxide: 0.55 g/ml.

LC. One of the reasons lower detection limits are possible with PC-SFC is the larger usable UV window of pure carbon dioxide. Carbon dioxide as a mobile phase is more UV transparent than normal LC solvents at a wider wavelength range.

Addition of mobile phase modifiers such as methanol to the carbon dioxide

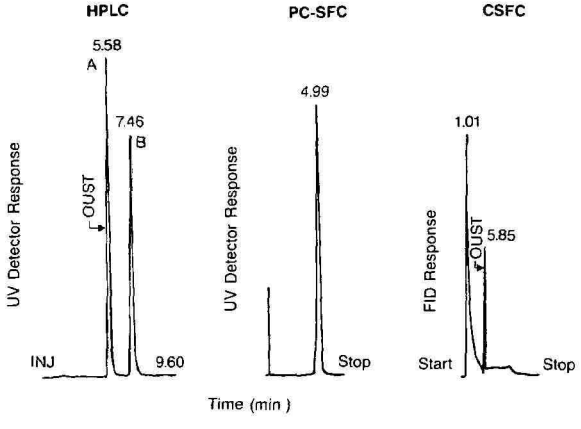

Fig. 9. Comparative chromatograms of Oust herbicide. *HPLC*. Column: Zorbax ODS, 15 cm × 4.6 mm I.D. Mobile phase: acetonitrile–water (pH 2.2) (35:65). Detection: UV at 254 nm. Injection volume: 10 μl. Flow-rate: 1.5 ml/min. Oven temperature: 45°C. *PC-SFC*. Column: Zorbax SIL, 25 cm × 4.6 mm I.D. Mobile phase: 5% methanol in carbon dioxide. Detection: UV at 228 nm. Injection volume: 20 μl. Flow-rate: 5 ml/min. Oven temperature: 45°C. *CSFC*. Column: SB-phenyl 50, 3 m × 100 μm I.D. Mobile phase: carbon dioxide. Detection: FID, 350°C. Injection volume: 200 nl, 1:20 split. Oven temperature: 100°C. Density program of carbon dioxide: initial, 0.45 g/ml; hold, 5 min; ramp, to 0.6 g/ml at 0.1 g/ml/min; hold, 5 min; quit, 0.45 g/ml.

TABLE I

COMPARATIVE RESULTS OBTAINED FROM ANALYSIS OF KARMEX HERBICIDE

R.S.D. = Relative standard deviation; I.S. = internal standard.

	HPLC	*PC-SFC*	*CSFC*
Average R.S.D. (%) (peak area)	0.6	4.3 (no I.S.)	4.5 (no. I.S.)
Linear range examined (mg/ml)	0.14–0.24	0.318–3.18	2.15–5.35
Correlation coefficient	0.9999	0.9999	0.9999
Detection limit (mg/ml)	0.010	0.008	0.269 (UV) 0.049 (FID)

TABLE II

COMPARATIVE RESULTS OBTAINED FROM ANALYSIS OF HARMONY HERBICIDE

	HPLC	*PC-SFC*	*CSFC*
Average R.S.D. (%) (peak area)	0.4	4.1 (no I.S.)	5.3 (no I.S.)
Linear range examined (mg/ml)	0.18–0.3	0.058–0.724	11.96–16.04
Correlation coefficient	0.9999	0.9999	0.9998
Detection limit (mg/ml)	0.01	0.011	0.028 (FID) 2.98 (UV)

TABLE III

COMPARATIVE RESULTS OBTAINED FROM ANALYSIS OF GLEAN HERBICIDE

	HPLC	*PC-SFC*	*CSFC*
Average R.S.D. (%) (peak area)	1.2	2.5 (no I.S.)	2.9 (no I.S.)
Linear range examined (mg/ml)	0.03–0.05	0.0023–1.117	9.115–11.35
Correlation coefficient	0.9999	0.9999	1.0000
Limit of detection (mg/ml)	0.001	0.002	0.084 (FID) 1.87 (UV)

TABLE IV

COMPARATIVE RESULTS OBTAINED FROM ANALYSIS OF NUSTAR HERBICIDE

	HPLC	*PC-SFC*	*CSFC*
Average R.S.D. (%) (peak area)	0.5	1.9 (no I.S.)	2.8 (no I.S.)
Linear range examined (mg/ml)	2.5–5.0	0.0099–0.99	2.08–4.16
Correlation coefficient	0.9999	0.9999	0.9968
Detection limit (mg/ml)	0.010	0.008	0.630 (UV)

TABLE V

COMPARATIVE RESULTS OBTAINED FROM ANALYSIS OF OUST HERBICIDE

	HPLC	*PC-SFC*	*CSFC*
Average R.S.D. (%) (peak area)	0.5	0.8 (no I.S.)	5.4 (no I.S.)
Linear range examined (mg/ml)	0.288–0.48	0.0645–1.29	5.4–7.1
Correlation coefficient	0.9999	0.9999	0.9997
Detection limit (mg/ml)	0.001	0.003	0.017 (FID)

mobile phase allows the polarity of the mobile phase to be adjusted to improve resolution and efficiency. To date, methanol, acetonitrile, freon-13 and methylene chloride have been investigated. The availability of a variety of mobile phase modifiers provides a great deal of flexibility to achieve optimal separation for a variety of compounds. Very adequate separations of the agricultural products examined have been obtained from each other and their precursors with methanol modified carbon dioxide and a silica stationary phase.

There is a wide choice of stationary phases available with packed columns; virtually all commercially available LC columns can be adapted for use with SFC. The temperature of the separation is more limited than with CSFC. This is because of LC column temperature limitations; we expect new column technology to address this limitation as use of packed columns becomes more widespread. Higher column temperature limits will enable greater percentages of mobile phase modifiers to be used while still maintaining supercritical conditions; applications to larger molecular weight species will then be possible.

Packed columns have higher loading capacities than do capillary open tubular columns; therefore, smaller concentrations of materials can be detected with the packed columns. Analysis times are shorter than those obtained with CSFC and separation of the species of interest from a large solvent peak produced with a flame ionization detector is not necessary. Additionally, the ease of operation in PC-SFC is greater than with CSFC; there is no need for injection splitters often required with the capillary system. Little or no clogging is evidenced with the back pressure regulator used for the packed column system as opposed to the pressure restrictors used with the capillary system.

Injection to injection reproducibility was better with packed *versus* capillary instruments. Carry-over from previous injections was found with CSFC, attributed in part to the use of an injection splitter. This sample carry-over was less apparent when the packed column system was used; greater precision over repetitive chromatograms resulted.

Our supercritical work was not conducted with an internal standard such as the one used when the HPLC samples were analyzed. Precision results should improve if an internal standard was used.

CSFC

CSFC is known to offer advantages over PC-SFC and LC in the resolution and efficiency of separation. In the types of samples focused on in this discussion, that is low molecular weight, moderate polarity agricultural chemicals, the increased

resolution and efficiency although advantageous in some separation strategies are not of principle concern. In this application, SFC is being explored because of its suitability to thermally labile species. However, it should not be overlooked that this is only one relevant avenue of the technique and the resolution and efficiency aspects are of vital concern in the examination of other difficult samples.

In terms of linearity, CSFC is comparable to PC-SFC over the concentration ranges examined for flame ionization detection (FID). With UV detection, cell design currently controls the linear range; again developments in this direction are imminent. At present, there are no commercially available UV cells or detectors for use with capillary columns.

The Kratos detector we have outfitted for CSFC use needs a more effective means of focusing the sample light beam on the UV cell. Currently, it is not as sensitive as the flame ionization detector. To increase the available signal, cells which can handle the low capillary volumes but also withstand the high pressures of SFC are needed. Due to the cylindrical shape of the cell presently employed, the absorbance *versus* concentration relationship is no longer linear over the range predicted by Beer's Law. Alternative cell designs are being investigated.

The use of density, pressure or temperature programming greatly affected the baseline and thus the detection limits obtained due to changes in the refractive index of the mobile phase. In order to generate acceptable quantitative data with the UV detector, the density, pressure or temperature had to be constant during elution of the peak(s) of interest.

Detection limits in PC-SFC, based on the initial solution concentrations, are up to an order of magnitude lower than in CSFC. This is due to the limited capactities of the capillary columns and the split injection system. In terms of total mass detected, accounting for injection volume and split ratio, the CSFC with FID is more sensitive than the packed column with UV detection.

An additional advantage of CSFC is the number of available detectors. In addition to the normal GC detectors (*i.e.*, flame ionization, flame photometric and nitrogen-phosphorus detectors) not regularly utilized in liquid chromatography, the IR and mass spectrometers can easily be interfaced. UV and mass spectrometric (MS) detectors allow the use of a variety of polar mobile phase modifiers in CSFC.

The current method of analysis for Nustar fungicide is a GC technique. Although the efficiencies obtained using SFC do not approach those of capillary GC, the versatility in types of compounds that can be chromatographed using SFC is demonstrated.

CONCLUSIONS

SFC offers advantages in chromatographic analysis of agricultural herbicides and pesticides over HPLC. Faster analyses times, comparable detection limits, efficient separations coupled with the variety of available detectors offered by the combination of PC-SFC and CSFC allow greater flexibility. The mild conditions required to maintain carbon dioxide in a supercritical state make it exceptionally attractive as a mobile phase in separating thermally labile herbicides and pesticides. Even with the addition of polar modifiers, thermal requirements are less than those needed for GC. These advantages make SFC a viable alternative to HPLC in analysis of agricultural products.

The limit of detection, greater sample capacity, reproducibility and ease of operation lend PC-SFC advantageous over CSFC and equivalent to LC for routine assay or impurity analyses.

PC-SFC is compatible with the use of semi-preparative or preparative scale columns, allowing the benefits of a supercritical mobile phase for large-scale fraction collection. Carbon dioxide evolution leaves cleaner samples with only small amounts of modifiers if they are used at all. Method development using the packed column instrument is much quicker due to the faster analysis in PC-SFC as compared to LC or CSFC.

CSFC with open tubular columns affords a larger number of theoretical plates for high-resolution separations of complex samples. The variety of detection methods in CSFC is particularly advantageous over LC for identification of unknown materials.

REFERENCES

1 T. L. Chester, D. P. Innis and G. D. Owens, *Anal. Chem.*, 57 (1985) 2243.
2 B. W. Wright and R. D. Smith, *J. High Resolut. Chromatogr. Chromatogr. Commun.*, 8 (1985) 8.
3 A. T. Balchunas, M. J. Capacci, M. J. Sepaniak and M. P. Maskarinec, *J. Chromatogr. Sci.*, 23 (1985) 381.
4 D. W. Later, B. E. Richter and M. R. Anderson, *LC - GC, Mag. Liq. Gas Chromatogr.*, 4 (1986) 992.
5 J. C. Fjeldsted and M. L. Lee, *Anal. Chem.*, 56 (1984) A618–A628.
6 R. D. Smith, H. T. Kalinoski, H. R. Udseth and B. W. Wright, *Anal. Chem.*, 56 (1984) 2476.
7 H. E. Schwartz, *LC-GC, Mag. Liq. Gas Chromatogr.*, 5 (1987) 14.
8 B. W. Wright, H. T. Kalinoski, H. R. Udseth and R. D. Smith, *J. High Resolut. Chromatogr. Chromatogr. Commun.*, 9 (1986) 145.
9 M. E. Hughes and J. L. Fasching, *J. Chromatogr. Sci.*, 24 (1985) 535.
10 S. L. Pentoney, Jr., K. H. Shafer and P. R. Griffiths, *J. High Resolut. Chromatogr. Chromatogr. Commun.*, 9 (1986) 169.
11 M. Novotny, *J. High Resolut. Chromatogr. Chromatogr. Commun.*, 9 (1986) 137.
12 D. R. Gere, R. Board and D. McManigill, *Anal. Chem.*, 54 (1982) 736.
13 B. Richter, personal communication.

Journal of Chromatography, 410 (1987) 355–361
Elsevier Science Publishers B.V., Amsterdam — Printed in The Netherlands

CHROM. 19 924

HIGH-PERFORMANCE LIQUID CHROMATOGRAPHIC SEPARATION OF THE ENANTIOMERS OF SUBSTITUTED 2-ARYLOXYPROPIONIC ACID METHYL ESTERS

ROXANE DERNONCOUR and ROBERT AZERAD*
Laboratoire de Chimie et Biochimie Pharmacologiques et Toxicologiques, UA 400 du CNRS, Université René Descartes, 45 Rue des Saints-Pères, 75270-Paris Cedex 06 (France)
(Received July 30th, 1987)

SUMMARY

A series of racemic aryl-substituted 2-aryloxypropionic acids were found to be directly resolved as enantiomeric methyl ester derivatives, using a Pirkle (covalently bound) (*R*)-N-(3,5-dinitrobenzoyl)phenylglycine column. In all instances where a significant separation was obtained, the first eluted enantiomer had the 2*R* configuration, a result consistent with an interaction model involving hydrogen bonding between the carbonyl oxygen of the solute and the amide nitrogen of the chiral stationary phase, associated with the usual aromatic π–π (donor–acceptor) interaction and a third unidentified, probably steric repulsive interaction.

INTRODUCTION

A large number of methods are available for the analytical separation of chiral carboxylic acids enantiomers using preliminary derivatization with optically pure reagents to form diastereoisomeric compounds; both amides[1–10] and esters[11,12] have been extensively used for this purpose. However, this method suffers from several complications, such as possible enantiomeric contamination of the derivatizing agent, unequal rates of reaction of each enantiomer with a chiral molecule and the frequent need for intermediate purification of the diastereoisomeric mixture, involving the risk of partial separation. All of these problems can be avoided by using direct resolution of an enantiomeric pair, using a chiral stationary phase (CSP)-based chromatographic system[13]. In this respect, the covalently bound (*R*)-N-(3,5-dinitrobenzoyl)phenylglycine high performance liquid chromatography column developed by Pirkle and co-workers[14–18] has been successfully used for the direct enantiomeric resolution of a variety of chiral molecules. For example, several anti-inflammatory α-methylarylacetic acids have been resolved as secondary or tertiary amide derivatives[18–20]. The order of elution of such compounds is consistent with interaction models involving, as an essential requirement, the stacking of amide dipoles from the solute and the chiral stationary phase[16,20–22].

In a study of the enzymatic hydrolytic resolution of the methyl esters of aryl-substituted 2-aryloxypropionic acids[23,24], some of which are interesting pharma-

0021-9673/87/$03.50

cological agents[25,26] and others well known herbicides[27] or useful auxiliary chiral resolving reagents[28,29], it became necessary to develop a rapid, direct technique to correlate quantitatively the enantioselectivity of the hydrolysis and the amount of hydrolysed acid or remaining ester. Although methyl ester derivatives were less likely to enter the general interaction model for the usual Pirkle CSP, the direct analysis of the residual ester was thought to be more practicable than amide derivatization of the acid. This paper describes the successful high-performance liquid chromatographic (HPLC) separation and simultaneous determination of most of the enantiomeric pairs of a number of methyl esters of the general type 1–3 and the correlation of the elution order of such esters with their absolute configuration.

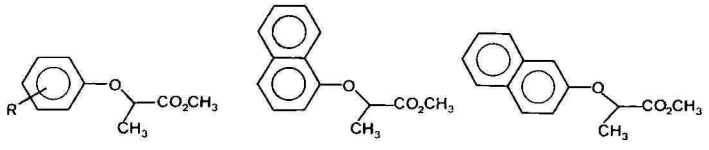

1 2 3

EXPERIMENTAL

Chemicals

Racemic 2-phenoxy-, 2-(2′-chlorophenoxy)-, 2-(3′-chlorophenoxy), 2-(4′-chlorophenoxy)-, 2-(2′,4′-dichlorophenoxy)- and 2-(2′,4′,5′-trichlorophenoxy)propionic acids were commercially available (Aldrich, Milwaukee, WI, U.S.A.) and converted into their methyl esters through the corresponding chlorides, generated by reaction with thionyl chloride. Other substituted phenoxypropionic esters were synthesized by the reaction of the corresponding substituted sodium (or potassium) phenoxide with methyl 2-bromopropionate in dimethylformamide or *tert.*-butanol, followed by distillation or silica gel chromatography. Pure (or enriched) (*R*)- and (*S*)-enantiomers were obtained either through resolution of (*R*)-phenylglycinolamide derivatives (1a,g,h,j) on a silica gel column[1,2,24] or by enantioselective esterase hydrolysis (1b,n–r)[23,24], or by synthesis [(*R*)-1a–m, (*R*)-2 and (*R*)-3] from (*S*)-2-bromopropionic acid, prepared from L-alanine[24,29,30]. Hexane (HPLC grade) was purchased from Rathburn Chemicals (Walkerburn, U.K.). All other chemicals and solvents were of analytical-reagent grade.

Chromatographic conditions

Chromatography was performed with an Altex 110A pump equipped with a Rheodyne 20-μl loop and a Pye Unicam LC–UV detector, set at specified wavelengths (see Table I), depending on the absorption of the esters. Data were processed with a Shimadzu C-R3A integrator–recorder. The column was a Bakerbond DNBPG covalent stainless-steel column (25 cm × 4.6 mm I.D.) with a γ-aminopropyl 5-μm spherical silica packing modified with (*R*)-N-(3,5-dinitrobenzoyl)phenylglycine (Baker, Phillipsburg, NJ, U.S.A.), operated with 2-propanol–hexane mixtures at a flow-rate of 1.0–1.5 ml/min.

RESULTS AND DISCUSSION

The enantiomeric separation of a series of twenty methyl esters of 2-aryloxypropionic acids, unsubstituted or substituted in the *ortho-*, *meta-* or *para*-position of the aromatic ring with methyl, methoxy, nitro or chloro groups, was attempted on the CSP column, with appropriate mixtures of 2-propanol–hexane (0.25–8%) as solvent. Table I lists the capacity and separation factors for the enantiomeric esters, together with the absolute configuration of the first eluted enantiomer, as determined by comparison with corresponding optically pure or enantiomerically enriched esters. The best resolution was obtained for naphthoxypropionic esters 2 and 3 (Fig. 1). Only *o*-carboxymethyl (1b), *o*-methoxy (1h) and nitrophenoxy esters (1e–g) were not significantly separated on this column, even when using solvent mixtures of lower eluting power. In all other instances, provided that the amount of enantiomers injected was maintained sufficiently low, the resolution factor obtained (R = 1.05–1.7) was suitable for the quantitative determination of the enantiomeric excess in the 2–98% range (Fig. 2). The order of elution was unchanged in the whole series, the (R) invariably being eluted before the (S)-enantiomeric ester.

TABLE I

SEPARATION OF SUBSTITUTED 2-ARYLOXYPROPIONIC ACID METHYL ESTERS ON AN (*R*)-DINITROBENZOYLPHENYLGLYCINE COVALENTLY BOUND COLUMN

Compound	*R*	*Detection wavelength (nm)*	*2-Propanol in hexane (%)*	*k'**	*α***	*R****	*Configuration of first-eluted enantiomer*
1a	H	269	0.25	1.87	1.100	1.5	*R*
			2.5	0.65	1.080	–	*R*
1b	*o*-CO_2CH_3	289	2.5	3.32	1.000	0	–
			5.0	2.41	1.000	0	–
			8.0	2.02	1.000	0	–
1c	*m*-CO_2CH_3	292	2.5	2.01	1.079	1.05	*R*
1d	*p*-CO_2CH_3	253	2.5	2.34	1.073	1.1	*R*
1e	*o*-NO_2	259	8.0	2.30	1.025	0.4	*R*
1f	*m*-NO_2	268	8.0	1.42	1.000	0	–
1g	*p*-NO_2	303	8.0	1.87	1.000	0	–
1h	*o*-OCH_3	276	2.5	1.98	1.000	0	–
1i	*m*-OCH_3	274	0.25	4.71	1.126	1.65	*R*
			2.5	1.25	1.126	1.05	*R*
1j	*p*-OCH_3	289	2.5	1.38	1.099	1.2	*R*
1k	*o*-CH_3	272	0.25	1.36	1.187	1.5	*R*
1l	*m*-CH_3	272	0.25	2.04	1.149	1.7	*R*
1m	*p*-CH_3	278	0.25	2.11	1.144	1.7	*R*
1n	*o*-Cl	275	0.25	2.08	1.116	1.5	*R*
1o	*m*-Cl	274	0.25	1.55	1.104	1.2	*R*
1p	*p*-Cl	279	0.25	1.67	1.089	1.1	*R*
1q	2',4'-Di-Cl	284	0.25	1.53	1.092	1.15	*R*
1r	2',4',5'-Tri-Cl	288	0.25	1.20	1.114	1.15	*R*
2	1'-Naphthyl	292	2.5	1.63	1.262	2.8	*R*
3	2'-Naphthyl	273	2.5	1.54	1.256	2.5	*R*

* Capacity factor of first-eluted enantiomer.
** Separation factor.
*** Resolution factor.

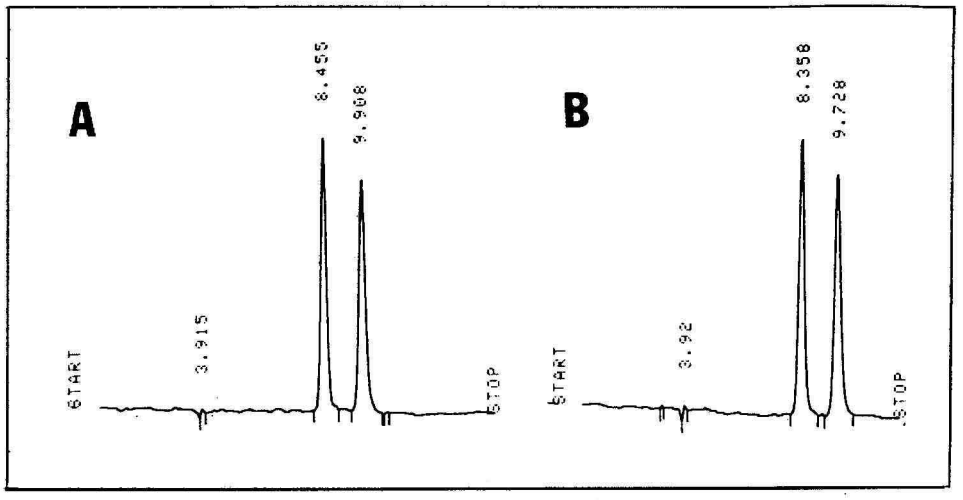

Fig. 1. Resolution of racemic mixtures of (A) 1'-naphthoxypropionic acid methyl ester 2 and (B) 2'-naphthoxypropionic acid methyl ester 3. Solvent, 2-propanol–hexane (2.5:97.5); detection at (A) 292 and (B) 273 nm.

The CSP employed in this study was (*R*)-N-(3,5-dinitrobenzoyl)phenylglycine, covalently bound via an amide linkage to the aminopropyl-silica support. Several sites of this CSP can, in principle, interact with solute molecules in various combinations to give a large number of conceivable interaction modes[14,18,21]. In a series, it is expected that only one interaction mode is operating and, provided that this involves important constraints on the spatial orientation of CSP and solute, the stereochemical difference between enantiomeric solute molecules produces enantiomeric discrimination. However, variations in the structure of the enantiomeric solute molecule may involve modifications in the combinations of interacting sites and/or in the conformation constraints, which is probably at the origin of the reversal in the elution order of enantiomeric compounds that has been observed in several series[31,32].

A three-point interaction model has been proposed for amide compounds by Pirkle *et al.*[18], in which chiral recognition arises essentially from aryl π–π donor–acceptor interactions and antiparallel amide dipoles stacking between the CSP and the solute; in this conformation, the orientation of the alkyl group attached to the asymmetric carbon atom is thought to be determinant for the stability of the CSP–solute complex. This model has been supported by a number of experimental observations, including the resolution and the order of elution of amides of 2-arylpropionic acids (*S* before *R*), whereas the corresponding esters are not separated[20,21], a fact which was attributed to the lower dipole moment of esters compared with amides (and possibly to the lower conformation constraints of esters).

A set of structural features similar to that of aryloxypropionic esters may be found in enantiomeric esters of N-aryl-α-amino acids, which show very large separation factors (α = 2–13) when chromatographed on the same CSP[33]. This high selectivity has been interpreted through a model involving three interaction sites of

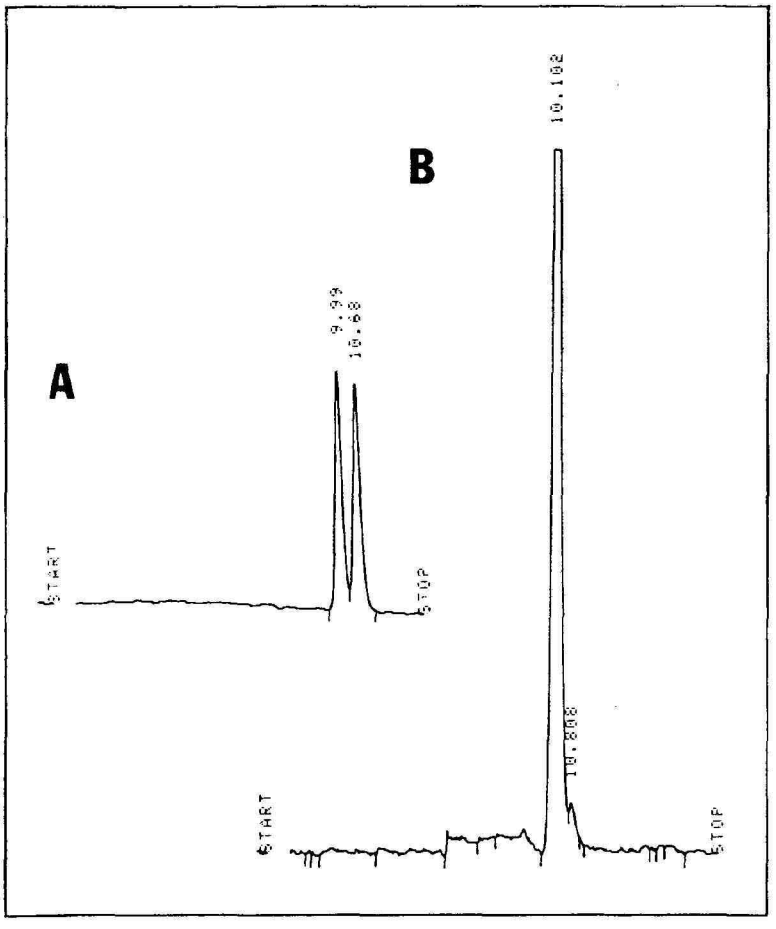

Fig. 2. Resolution of enantiomeric mixtures of 2-phenoxypropionic acid methyl ester 1a. (A) Racemic mixture; (B) 99:1 mixture of the (*R*)- and (*S*)-enantiomers. Solvent, 2-propanol–hexane (0.2:99.8); detection at 269 nm.

the solute in a clockwise or anticlockwise arrangement: π-donor, hydrogen bond acceptor (C=O) and hydrogen bond donor (NH).

Our experiments show that it is possible, with the 2-aryloxypropionate series, to obtain a satisfactory general resolution of methyl esters. However, only two interaction sites can be clearly identified in such molecules (π-donor and carbonyl-hydrogen bond acceptor). This suggests that the ester–amide dipole stacking, previously dismissed for the arylpropionate esters, or more simply hydrogen bonding between the solute carbonyl oxygen and the CSP amide nitrogen, is actually operative, in conjunction with the usual π–π interaction and a third undentified site, to promote, with the α-methyl group negative steric interaction, an adequate enantiomeric discrimination (Fig. 3). It should be noted that in such a representation, owing to the planar symmetry of the dinitrobenzoylamide group, the steric interaction of the α-methyl group is certainly not sufficient to allow any enantiomeric discrimina-

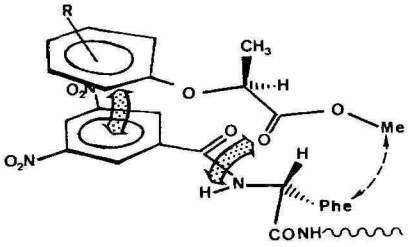

Fig. 3. Hypothetical interaction model for the (*R*)-CSP and an (*S*)-2-aryloxypropionic acid methyl ester. Note that the two depicted interactions, which can be expected to occur identically below the CSP plane for the (*R*)-aryloxypropionate, are not sufficient to account for the discrimination of enantiomers, unless completed, for example, by the steric repulsive interaction occurring between the O-methyl ester and the phenyl groups.

tion, as both enantiomers can interact similarly, above or below the CSP plane. Such a feature has frequently been overlooked in models and emphazises the need for a supplementary interaction site, which has to be dependent on the remaining part of the CSP, and attached to a substituent of the asymmetric carbon atom of phenylglycine different from the NH group[34]; in this respect, a steric repulsive interaction between the O-methyl ester group of the solute and the CSP phenyl group, apparent in molecular models, is a good condidate. In addition, it is possible that other interaction modes, leading to the same enantiomeric preference, have been disregarded, such as the aryl π–π interaction between the aryl groups of phenylglycine (in competition with the dinitrophenyl group) and arylpropionates (or aryloxypropionates). However, such a model is not likely, because of the higher π-acidity of the 3,5-dinitrobenzoyl ring. Moreover, the increase in separation factor (see Table I) noted for naphthyl-substituted derivatives (high basicity π-donors) is a generally observed feature, which has been associated with reinforced π–π interactions with the dinitrophenyl group of the CSP[16,20,32]. The presence of a π-acceptor group in nitrophenoxypropionic esters may similarly explain the lack of selectivity of the CSP for these esters. It is necessary to note, however, that the size of the separation factor does not exactly parallel the π-basicity enhancement of substituted aryloxypropionates (see for example, the carbomethoxy or methoxy derivatives, Table I).

CONCLUSION

Although results of this study demonstrate that many substituted 2-aryloxypropionic acid methyl ester enantiomers can be satisfactorily separated by HPLC on a currently available CSP, it appears that the interpretation of the enantiomeric discrimination is not straightforward. Nevertheless, it is interesting that the weighted average of the complex interactions and conformations involved finally results in a unique order of elution for the enantiomers of this series.

REFERENCES

1 G. Helmchen, G. Nill, D. Flockerzi, W. Shule and M. S. K. Youssef, *Angew. Chem., Int. Ed. Engl.*, 18 (1979) 62.

2 G. Helmchen, G. Nill, D. Flockerzi and M. S. K. Youssef, *Angew. Chem., Int. Ed. Engl.*, 18 (1979) 63.
3 G. J. Van Giessen and D. G. Kaiser, *J. Pharm. Sci.*, 64 (1975) 798.
4 D. G. Kaiser, G. J. Van Giessen, R. J. Reisher and W. J. Wechter, *J. Pharm. Sci.*, 65 (1976) 269.
5 J. Goto, N. Goto and T. Nambara, *J. Chromatogr.*, 239 (1982) 559.
6 R. J. Bopp, J. F. Nash, A. S. Ridolfo and E. R. Shepard, *Drug. Metab. Dispos.*, 7 (1979) 356.
7 H. Nagashima, Y. Tanaka and R. Hayashi, *J. Chromatogr.*, 345 (1985) 373.
8 J. K. Stoltenborg, C. V. Puglisi, F. Rubio and F. M. Vane, *J. Pharm. Sci.*, 70 (1981) 1207.
9 T. Tamegai, T. Tanaka, T. Kaneko, S. Ozaki, M. Ohmae and K. Kawabe, *J. Liq. Chromatogr.*, 2 (1979) 551.
10 J. M. Maître, G. Boss and B. Testa, *J. Chromatogr.*, 299 (1984) 397.
11 I. W. Wainer, *J. Chromatogr.*, 202 (1980) 478.
12 E. J. D. Lee, K. M. Williams, G. G. Graham, R. O. Day and G. D. Champion, *J. Pharm. Sci.*, 73 (1984) 1542.
13 R. Däppen, H. Arm and V. R. Meyer, *J. Chromatogr.*, 373 (1986) 1.
14 W. H. Pirkle, D. W. House and J. M. Finn, *J. Chromatogr.*, 192 (1980) 143.
15 W. H. Pirkle, J. M. Finn, J. L. Shreiner and B. C. Hamper, *J. Am. Chem. Soc.*, 103 (1981) 3964.
16 W. H. Pirkle, C. J. Welch and M. H. Hyun, *J. Org. Chem.*, 48 (1983) 5022.
17 W. H. Pirkle and A. Tsipouras, *J. Chromatogr.*, 291 (1984) 291.
18 W. H. Pirkle, J. M. Finn, B. C. Hamper, J. Shreiner and J. R. Pribish, in E. L. Eliel and S. Okuda (Editors), *Asymmetric Reactions and Processes in Chemistry*, ACS Symposium Series, No. 185, American Chemical Society, Washington, DC, 1982, p. 245.
19 I. W. Wainer and T. D. Doyle, *J. Chromatogr.*, 259 (1983) 465.
20 I. W. Wainer and T. D. Doyle, *J. Chromatogr.*, 284 (1984) 117.
21 I. W. Wainer and T. D. Doyle, *LC, Liq. Chromatogr. HPLC Mag.*, 2 (1984) 88.
22 W. H. Pirkle, *Tetrahedron Lett.*, 24 (1983) 5707.
23 R. Dernoncour and R. Azerad, *Tetrahedron Lett.*, (1987) in press.
24 R. Dernoncour, S. Letellier and R. Azerad, unpublished results.
25 D. T. Witiak, T. C.-L. Ho, R. E. Hackney and W. E. Connor, *J. Med. Chem.*, 11 (1968) 1986.
26 Y. Kawashima, N. Hanioka and H. Kozuka, *J. Pharm. Dyn.*, 7 (1984) 286.
27 C. R. Worthing (Editor), *The Pesticide Manual*, BCPC Publications, London, 6th ed., 1979, p. 329.
28 J. Jacques, A. Collet and S. H. Wilen, *Enantiomers, Racemates and Resolutions*, Wiley, New York, 1981.
29 J. Gabard and A. Collet, *Nouv. J. Chim.*, 10 (1986) 685.
30 S. C. G. Fu, S. M. Birbaum and J. P. Greenstein, *J. Am. Chem. Soc.*, 76 (1954) 6054.
31 M. Kasai, C. Froussios and H. Ziffer, *J. Org. Chem.*, 48 (1983) 459.
32 T. D. Doyle and I. W. Wainer, *J. High Resolut. Chromatogr. Chromatogr. Commun.*, 7 (1984) 38.
33 W. H. Pirkle, T. C. Pochapsky, G. S. Mahler and R. E. Field, *J. Chromatogr.*, 348 (1985) 89.
34 I. W. Wainer and M. C. Alembik, *J. Chromatogr.*, 367 (1986) 59.

Journal of Chromatography, 410 (1987) 363–372
Elsevier Science Publishers B.V., Amsterdam — Printed in The Netherlands

CHROM. 19 958

DETERMINATION OF VANCOMYCIN RELATED SUBSTANCES BY GRADIENT HIGH-PERFORMANCE LIQUID CHROMATOGRAPHY

EUGENE L. INMAN
Lilly Research Laboratories, Eli Lilly and Company, Indianapolis, IN 46285 (U.S.A.)
(Received August 10th, 1987)

SUMMARY

A gradient high-performance liquid chromatographic method for the determination of vancomycin related substances is described. This method was developed to profile vancomycin, co-fermentation products, and degradation products. The resultant chromatograms confirm the multifactored nature of vancomycin, separating a number of peaks from the main component. The development of acceptable chromatographic performance is described, with the final method intended for use as a control assay. Quantitation of total related substances is made by comparing the relative area of the main peak to total peak area in a pair of chromatograms from a stock solution and a twenty-five fold dilution. A rapid-scan UV detector was used to demonstrate the similar spectral characteristics of the vancomycin related substances, confirming the validity of the relative area approach. Statistical method validation data are included, evaluating the use of this method for quantitative applications. Example applications demonstrate the effectiveness of this method.

INTRODUCTION

The determination of vancomycin in various matrices has historically employed the microbiological assay[1], with radioimmunoassay[2], fluorescent polarization immunoassay[3,4] and fluorescence immunoassay[5] methods described in the literature. Chromatographic procedures have been developed for the determination of vancomycin in blood serum[6–8] or a mixture of antibiotics[9,10]. Optimization of chromatographic parameters and extraction procedures has led to increasingly sensitive vancomycin methods[11,12]. While these are effective in clinical applications, a method has not been described for the determination of vancomycin related substances, instrumental in the evaluation of bulk drug and formulated products.

Vancomycin is a mixture of similarly structured compounds, with vancomycin B the compound of greatest abundance[13]. The vancomycin factors vary widely in microbiological activity; therefore, the microbiological assay yields a result representing a concentration weighted summation of the individual factor activities. For a more complete understanding of the chemical nature of vancomycin, a gradient high-

performance liquid chromatographic (HPLC) method was developed with special emphasis placed on the separation of the vancomycin related substances. This paper describes that method, considerations in the development process, and evaluation of the method for use as a control assay.

The methods described to date are isocratic with quantitation based on the area of the vancomycin B peak. These determinations are made *versus* a reference standard whose chemical purity is unknown, or assumed to be 100%. This assumption has proven to be inaccurate. The method described herein does not require a reference standard and was developed for the evaluation of the entire vancomycin mixture. The related substances assay is complementary to a chemical purity method implementing a reference standard. The method has been used for monitoring process changes, stability profiling, and establishing improved accuracy in chemical purity determinations.

EXPERIMENTAL

Apparatus

Development work was performed on a Varian 5500 gradient HPLC system with integrated UV-200 variable-wavelength detector and 8085 Autosampler (Varian, Walnut Creek, CA, U.S.A.). Data collection and reduction was done on a central chromatography computer system with data storage, manipulation, and graphic capabilities[14,15]. The HPLC column was an Altex Ultrasphere-ODS 25 cm × 4.6 mm I.D. column with 5 μm packing (Altex, Berkeley, CA, U.S.A.). A sample loop of 20-μl volume was used for all injections. UV spectra were obtained by a Beckman 165 Scanning UV detector (Beckman, San Ramon, CA, U.S.A.).

Reagents

HPLC-grade acetonitrile, methanol, and tetrahydrofuran were purchased from Mallinckrodt (Paris, KY, U.S.A.). Phosphoric acid (65%), triethylamine, and *o*-toluamide were of analytical reagent grade. The triethylamine quality affects the gradient baseline and should be routinely monitored by running a water blank. Purified water was obtained from a Milli-Q purifying system (Millipore, Bedford, MA, U.S.A.). All vancomycin samples were prepared at Eli Lilly and Company.

Mobile phases

An aqueous buffer was prepared by adding 4 ml triethylamine to 2 l water and adjusting the pH to 3.2 with phosphoric acid. Mobile phase A was prepared by adding 70 ml acetonitrile and 10 ml tetrahydrofuran to 920 ml buffer solution. Mobile phase B was prepared by adding 290 ml acetonitrile and 10 ml tetrahydrofuran to 700 ml buffer solution. Each mobile phase was thoroughly mixed, degassed briefly, and covered to reduce evaporation.

The mobile phase program included an isocratic region of 100% mobile phase A for the initial 12 min, a linear ramp from 100% mobile phase B over 8 min, and 2-min isocratic region at 100% mobile phase B. Equilibration was re-established within 30 min from injection. A flow-rate of 1.5 ml/min was used throughout the analysis.

Sample preparation

Vancomycin HCl is readily soluble in aqueous solutions, but pH adjustment is required for vancomycin base and other salts. All dilutions were made with mobile phase A. Water has proven to be an inappropriate sample solvent under selected experimental conditions[16]. Vancomycin base was solubilized by the addition of a few drops of 1 *M* hydrochloric acid. Stock solutions were prepared at 10 mg/ml by weighing an appropriate quantity of sample. These solutions were diluted to 0.4 mg/ml with mobile phase A for further chromatographic evaluation.

RESULTS AND DISCUSSION

Development considerations

HPLC confirms the multifactored nature of vancomycin. Initially, a gradient was run to assess the range of compound polarities within a vancomycin sample. The chromatogram in Fig. 1 demonstrates the profile obtained using a gradient from 5 to 90% acetonitrile, with the detector set at 254 nm. This indicated that a gradient spanning a narrower range of solvent strength was needed for routine sample evaluation. Method conditions were selected to focus on the region where the most peaks were observed in the broad chromatogram. A linear gradient was used to generate the chromatogram in Fig. 2, spanning a range of *ca.* 7 to 28% acetonitrile, with detection at 254 nm. Methodology based on this gradient profile has been described previously[17]. For use as a control method, however, gradient program changes were developed to reduce variability in chromatographic profiles observed between instruments.

The chromatographic properties of vancomycin are characteristic of those observed for other peptides[18]. That is, retention times are extremely sensitive to mobile phase changes. Gradient elution reduces the observed sensitivity but results in reduced resolution from compounds with similar structures. A gradient program was developed to include an initial isocratic region where the majority of the separation takes place. By premixing the solvents, instrumental differences in mobile phase composition are reduced. In order to prepare mobile phases of reproducible strength, mobile phase A was adjusted with acetonitrile or buffer solution as needed until the main peak fell within an acceptable retention window. This was proven to be quite

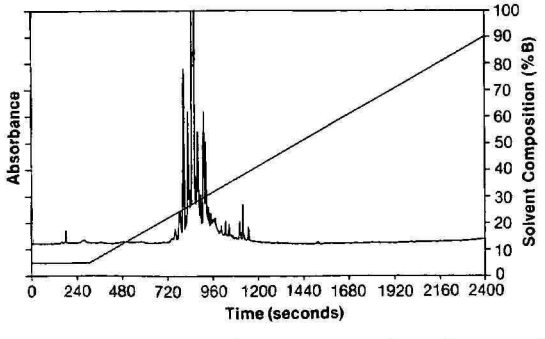

Fig. 1. Chromatogram of vancomycin using a linear gradient from 5 to 90% acetonitrile (mobile phase B) in triethylamine–phosphoric acid (TEAP) buffer.

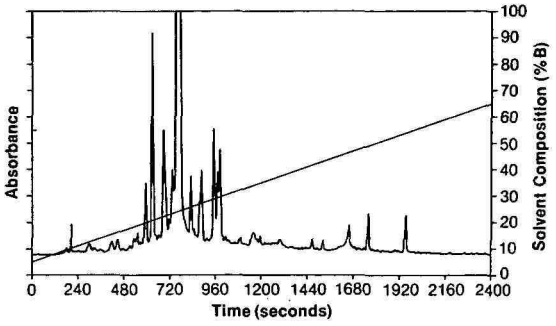

Fig. 2. Chromatogram of vancomycin using a linear gradient from *ca.* 7 to 28% acetonitrile in TEAP buffer. Mobile phase A: 95% TEAP buffer, 5% acetonitrile; mobile phase B: 60% TEAP buffer, 40% acetonitrile.

effective for routine use. The mobile phase was ramped to 100% solution B to elute any remaining peaks from the column. Mobile phase B was not adjusted due to reduced sensitivity to solvent strength during the later portion of the separation. The mobile phase strengths span the range defined in the original development and has been adequate for all samples assayed to date.

The chromatographic parameters in this method represent a compromise between baseline resolution of all peaks and inadequate resolution of peaks whose presence may lead to an understanding of production process change effects or degradation mechanisms. It was anticipated that one might encounter peaks that were unique to the sample of interest. No attempt was made to resolve and identify every peak found, but rather, a sample profiling was sought.

Relative factor sensitivity

Due to the complexity of the vancomycin chromatograms, several assumptions must be applied for the consistent quantitation of related factors. The fundamental assumption is that the molar absorptivities of the related compounds are approximately equal. To confirm this, several spectroscopic and chromatographic experiments were performed.

Two general approaches were used to determine the relative responses for the vancomycin related substances. First, a sample of stressed vancomycin was chromatographically evaluated at several wavelengths. This sample contained most of the peaks observed in available vancomycin materials. Second, another sample was spectroscopically evaluated using a rapid-scan UV detector, providing a UV spectrum for many of the peaks as they were eluted. From these experiments, several conclusions were drawn about the relative absorptivities of vancomycin elated factors.

Fig. 3 includes the chromatograms of the stressed vancomycin sample obtained at four wavelengths: 230, 240, 254, and 280 nm. Wavelength 280 nm was selected in that it corresponds to a maximum in the UV spectrum of vancomycin B. Wavelength 254 nm was selected in that it was expected to provide more universal detection, expecially for those compounds that are structurally different from vancomycin B. Wavelengths 230 and 240 nm were investigated in that they provide increased sensitivity and may be of interest where sensitivity improvements are needed. The chro-

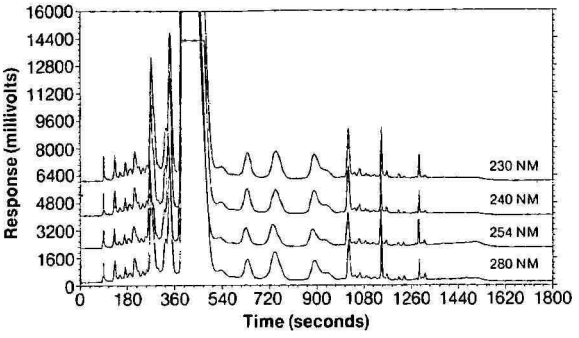

Fig. 3. Stressed vancomycin sample chromatograms at four different wavelengths. Each has been scaled for direct comparison.

matograms in Fig. 3 have been electronically scaled for direct comparison. Note that the chromatograms are nearly identical.

Another degraded sample was used to evaluate the UV spectra of the related factor peaks. UV spectra were obtained with a rapid-scan detector for 21 peaks as they eluted, identified as shown in Fig. 4. The spectra for several representative peaks are included in Fig. 5. The spectra were nearly identical with differences in attenuation only for all peaks in this sample. From these data, one can conclude that the chromophore for the vancomycin related substances remains relatively unchanged.

Calculations based on relative area are acceptable approximations and provide valuable estimates for sample comparisons. Ideally, one would need to have reference standards established for each of the observed related substances for accurate quantitation. For vancomycin, this would be an impossible goal. Due to the limited amounts of isolated factors available, experimental evaluation was limited to the experiments described. The basic assumption of similar molar absorptivities appears to be valid. For routine sample evaluation, a wavelength of 280 nm has been used.

Calculations

For routine quantitation of vancomycin related substances, a high-low sample comparison was used. This approach derives its name from the use of a pair of sample solutions, the high corresponding to a higher sample concentration and the low cor-

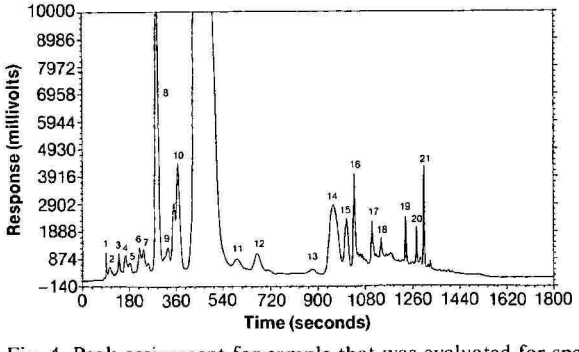

Fig. 4. Peak assignment for sample that was evaluated for spectral characteristics of each eluted peak.

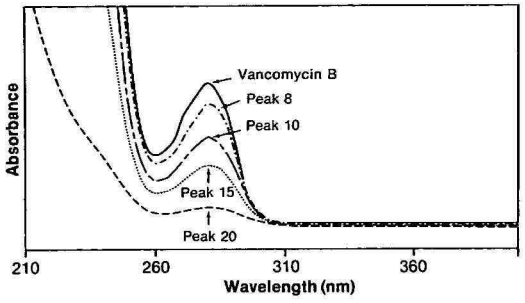

Fig. 5. UV spectra for vancomycin and four representative peaks as they elute from the column.

responding to a lower sample concentration. A pair of chromatograms is obtained as shown in Fig. 6. Results are generated by comparisons made between these chromatograms. The lower concentration sample is selected so that the main peak falls within the linear region of the detector response and the higher concentration sample is selected so that the largest impurity peak has about the same area as the main peak in the lower concentration sample. In this way, the main peak in the chromatogram from the more concentrated solution is offscale or falls outside the linear region of the detector response. The calculations do not include the area of the main peak in this latter chromatogram.

The determination of total related substances was calculated using the following equation:

$$\text{Amount related substances (\%)} = \frac{\text{(area 1)}}{\text{(area 1 + area 2)}} \cdot 100\% \qquad (1)$$

where area 1 is the total area of the peaks other than the peak for the main component in the high concentration sample chromatogram divided by the dilution factor between the high and low solutions, and area 2 is the area of the vancomycin B in the low concentration sample chromatogram. By using the dilution factor, one projects

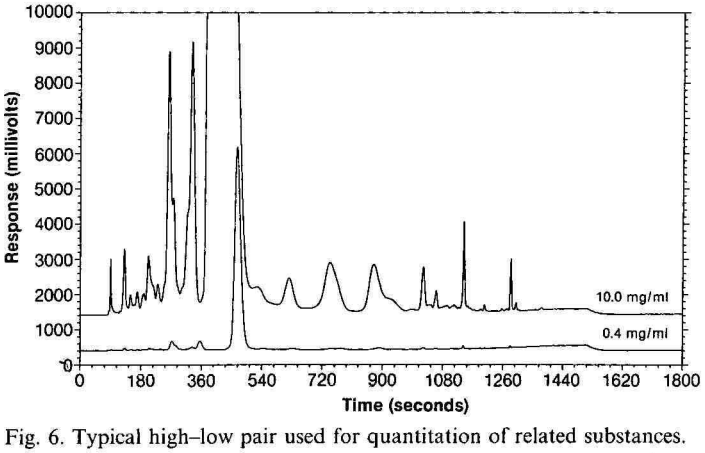

Fig. 6. Typical high–low pair used for quantitation of related substances.

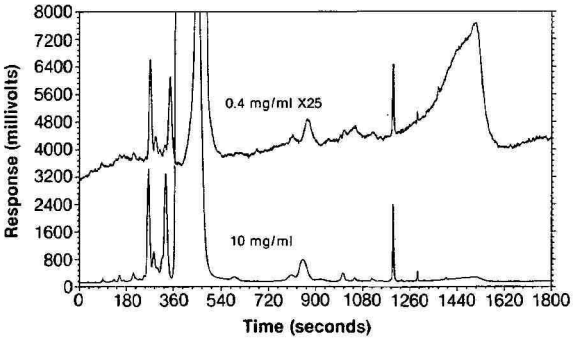

Fig. 7. High concentration chromatogram compared to electronically amplified chromatogram of a diluted solution.

the area of the main peak that goes offscale from the area of the meain peak in the dilute sample chromatogram. One can use the same chromatograms to determine the relative percentage of an individual peak i using the following equation:

$$\text{factor } i\ (\%) = \frac{(\text{area } i)}{(\text{area } 1 + \text{area } 2)} \cdot 100\% \tag{2}$$

where area i is the area of the peak of interest in the high concentration sample chromatogram divided by the dilution factor. The high–low approach provides added sensitivity to the final determination. This is illustrated in Fig. 7 where a comparison is made between the high concentration chromatogram and amplification of the low concentration chromatogram by a factor corresponding to the dilution factor. Note that the chromatograms are nearly identical except in signal-to-noise considerations.

Method validation

Linearity, precision, and stability of sample solutions were evaluated for this method. To evaluate the linearity of the method, seven solution pairs were assayed over the concentration ranges 0.08–0.8 mg/ml and 2–20 mg/ml. For the vancomycin B peak, a relative standard deviation (R.S.D.) of 1.1%, a log–log slope of 1.02, and a coefficient of determination of 0.9997 were obtained from the lower concentration solutions. For the total related factors in the concentrated solutions, an R.S.D. of 1.9%, a log–log slope of 0.98, and a coefficient of determination of 0.9991 were obtained. For the largest individual peak at about a 2% level, an R.S.D. of 1.8%, a log–log slope of 0.98, and a coefficient of determination of 0.9992 were obtained from the higher concentration solutions.

To evaluate method reproducibility, single day and multiple day assays were run. Ten replicates from a single lot of vancomycin were assayed on a single day to give a percentage factor B relative standard deviation of 0.14%. Three lots of vancomycin were assayed on each of five successive days, yielding an average R.S.D. of 0.22% for percentage factor B. This clearly demonstrated that intralaboratory precision is quite acceptable.

Note that the precision of the percentage factor B result is much better than one would expect from the precision of individual injections. For example, the ten

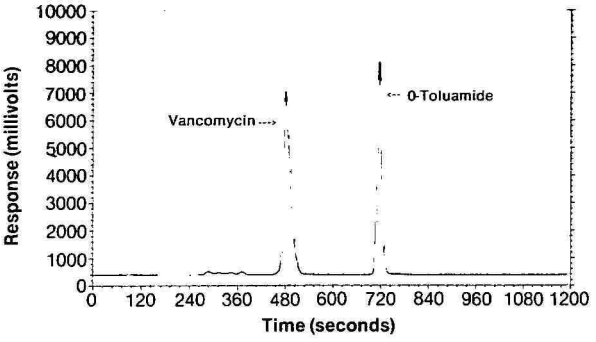

Fig. 8. Typical system suitability chromatogram.

replicates used to calculate the single day precision described above yielded an R.S.D. of 0.14%. However, the R.S.D. of the ten highs and ten lows were 1.19 and 1.24%, respectively. The improved precision is realized because the related factor areas appears in both the numerator and denominator in eqn. 1. Also, areas 1 and 2 are not independent in that the solutions are prepared from a single sample weight. This demonstrates the advantage of the high-low approach.

To determine the stability of stock sample solutions, three lots of vancomycin were prepared, stored at refrigerated and room temperatures, and assayed daily for five days. The average percentage factor B change was found to be -0.2% per day and -0.4% per day, respectively. For each determination, fresh dilutions were made from the aged stock solution. Solutions that are not run within 8 h after preparation should be refrigerated until assayed.

System suitability

A system suitability test was developed for the routine application of this method. This test is run on a separate test solution and chromatographic parameter adjustments are made until the test specifications are met. To run the system suitability test, a solution is prepared containing 0.4 mg/ml vancomycin and 0.4 mg/ml *o*-toluamide in mobile phase A–methanol (95:5). Dissolution of the *o*-toluamide is aided by dissolving initially in methanol. The test is run under isocratic conditions at 100% mobile phase A, without the gradient ramp after 12 min. A typical chromatogram is shown in Fig. 8. The selection of *o*-toluamide was based on its retention characteristics only.

The chromatographic parameters of retention time, tailing, and theoretical plates are used to measure system performance. Resolution has been found to be a poor performance check due to the much greater sensitivity of vancomycin to mobile phase strength than that of *o*-toluamide. Acceptable separation is achieved if the retention time of vancomycin lies between 450 and 540 s and that of *o*-toluamide between 660 and 780 s. The test chromatogram is evaluated for tailing and theoretical plates for the vancomycin peak, and is calculated as described in ref. 19. A tailing maximum limit of 1.8 and a theoretical plate count minimum of 1400 have been set for acceptable system performance. Chromatographic parameters are adjusted until these criteria are met.

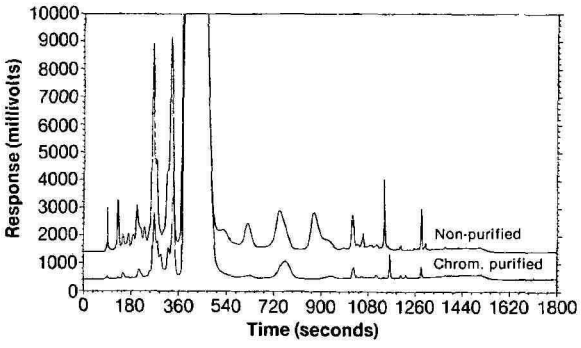

Fig. 9. Chromatographic comparison of purified and non-purified vancomycin. Each solution is 10 mg/ml.

Applications

This method has been effectively used to monitor vancomycin related substances in a variety of applications. For example, the chromatograms in Fig. 9 illustrate the dramatic difference in related substances between two vancomycin products (5% *vs.* 18%). This method has also been used to trace chromatographic profile changes for vancomycin under various stress conditions (Fig. 10). Not only is the overall related substances quantitation indicative of product differences, but differences can be assigned to specific changes observed in the individual chromatograms. Solution stability has also been monitored by this method. In Fig. 11, a solution of vancomycin that has been stored for twelve months is compared to a freshly prepared solution from a typical production lot.

This method has been used to monitor in-process chemical purity as well. The approach used in this method is ideal for this purpose because the result is independent of sample moisture or other residual solvents, often a problem for samples of this nature. The method is also applicable to solution samples and complements a reference standard comparative assay.

CONCLUSIONS

A gradient HPLC method has been described for the determination of vancomycin related substances. This method has demonstrated good accuracy and pre-

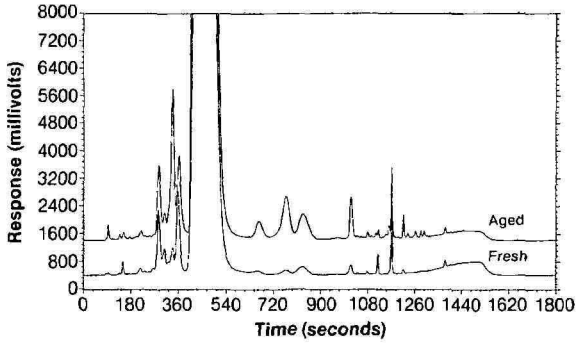

Fig. 10. Vancomycin profile changes observed for vials stored over time at an elevated temperature.

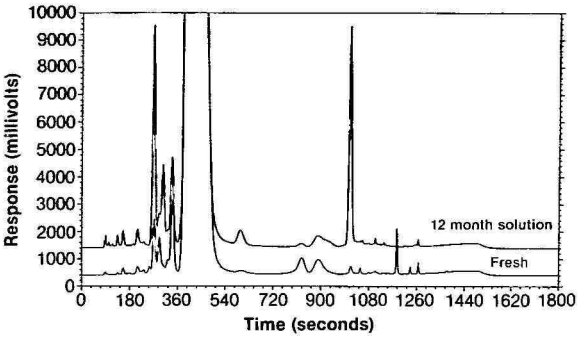

Fig. 11. Vancomycin solution stability compared to a freshly prepared lot.

cision characteristics. A profile of related substances is obtained, although baseline separation of all peaks is not achieved. Wavelength selection is not critical in that most vancomycin related factors have similar UV absorption spectra, with the optimum wavelength determined by sensitivity requirements. The quantitation of vancomycin related substances is not effected by non-UV absorbing species, important for materials that are hygroscopic. Several considerations used during the method development process are detailed, and a statistical evaluation of method performance is described. Finally, this method has been effective in monitoring purity improvements made in this synthesis of the product, both for in-process monitoring and as a control assay on the final product.

REFERENCES

1 C. A. Walker and B. Kopp, *Antimicrob. Agents Chemother.*, 13 (1978) 30.
2 K. B. Crossley, J. C. Rostchafer, M. M. Chern, K. E. Mead and D. E. Zaske, *Antimicrob. Agents Chemother.*, 17 (1980) 654.
3 P. A. Ristuccia, A. M. Ristuccia, J. H. Bidanset and B. A. Cunha, *Ther. Drug Monit.*, 6 (1984) 238.
4 K. S. Schwenzer, C. H. J. Wang and J. P. Anhalt, *Ther. Drug Monit.*, 5 (1983) 341.
5 M. A. Pfaller, D. J. Krogstad, G. G. Granich and P. R. Murray, *J. Clin. Microbiol.*, 20 (1984) 311.
6 F. Jehl, C. Gallion, R. C. Thierry and M. Monteil, *Antimicrob. Agents Chemother.*, 27 (1985) 503.
7 J. B. L. McClain, R. Bongiovanni and S. Brown, *J. Chromatogr.*, 231 (1982) 463.
8 J. R. Uhl and J. P. Anhalt, *Ther. Drug Monit.*, 1 (1979) 75.
9 R. L. Kirchmeier and R. P. Upton, *Anal. Chem.*, 50 (1978) 349.
10 R. Sztaricskai, J. Borda, M. M. Puskas and R. Bognar, *Antibiotics*, 36 (1983) 1691.
11 F. N. Bever, P. R. Finley, C. Fletcher and J. Williams, *Clin. Chem.*, 30 (1984) 1586.
12 R. J. Hoagland, J. E. Sherwin and J. M. Phillips, Jr., *J. Anal. Toxicol.*, 8 (1984) 75.
13 G. K. Best, N. H. Best and N. N. Durham, *Antimicrob. Agents Chemother.*, 4 (1968) 115.
14 J. L. Bollinger, E. W. Bradt and J. Zynger, presented at the *Pittsburgh Conference, Atlantic City, NJ, 1983*, Paper No. 391.
15 J. L. Bollinger and J. Zynger, presented at *Pittsburgh Conference, New Orleans, LA, 1985*, Paper No. 432.
16 E. L. Inman, in preparation.
17 L. T. Grady (Editor), *Pharmacopeial Forum*, Vol. 11, No. 4, United States Pharmacopeial Convention, Inc., Rockville, MD, July–Aug. 1985, p. 535.
18 L. R. Snyder and M. A. Stadalius, in Cs. Horváth (Editor), *High Performance Liquid Chromatography*, Vol. 4, Academic Press, New York, 1986, pp. 195-312.
19 J. P. Foley and J. G. Dorsey, *Anal. Chem.*, 55 (1983) 730.

Journal of Chromatography, 410 (1987) 373–382
Elsevier Science Publishers B.V., Amsterdam — Printed in The Netherlands

CHROM. 20 008

CHROMATOGRAPHIC METHODS FOR THE ANALYSIS OF VANCOMYCIN

ADRIAN H. THOMAS* and PENELOPE NEWLAND
Division of Chemistry, National Institute for Biological Standards and Control, Blanche Lane, South Mimms, Hertfordshire EN6 3QG (U.K.)
(Received August 28th, 1987)

SUMMARY

Four thin-layer chromatographic systems were developed for the separation of vancomycin, related antibiotics and degradation products. Bioautography was suitable for detecting trace amounts of biologically active components. High-performance liquid chromatography was used to examine the composition of vancomycin and other glycopeptide antibiotics and to monitor the stability of vancomycin. Degradation of vancomycin lead to changes in the composition which were not matched by a similar loss of potency.

INTRODUCTION

Vancomycin belongs to a group of glycopeptide antibiotics, all members of which possess closely related chemical structures[1,2]. Vancomycin was discovered in 1956 and is currently being used increasingly for the treatment of infections due to methicillin-resistant *Staphylococcus aureus* and *Clostridium difficile* induced colitis[3]. Specifications in the *British Pharmacopoeia* for vancomycin have remained unchanged since its introduction as a therapeutic agent. In order to improve the specificity of the current pharmacopoeial monograph several thin-layer chromatographic (TLC) systems have been examined to distinguish vancomycin from other related glycopeptide antibiotics. Chromatographic methods are also required to analyse the composition of commercial vancomycin and to monitor its stability. The separations achieved will be shown.

A number of paper and thin-layer chromatographic systems have been described for the identification of vancomycin and demethylvancomycin[4], the detection of vancomycin A[5,6] (aglucovancomycin) and the differentiation of the glycopeptide antibiotics[7,8]. Commercial vancomycin[9,10] and demethylvancomycin[11] have been purified by gradient elution from CM-Sephadex.

High-performance liquid chromatography (HPLC) has been used to monitor the concentration of vancomycin in serum[12–15] and to compare the glycopeptide group of antibiotics[8,16,17]. Vancomycin and demethylvancomycin have been differentiated by HPLC[18].

0021-9673/87/$03.50

Reports on the composition and degradation of vancomycin are sparse. Early work showed that vancomycin consisted of at least three different biologically active components and the major component readily formed the two components of lesser activity[9]. HPLC has been used to follow the transformation of vancomycin to CDP-I[19], a crystalline degradation product formed by the hydrolytic loss of ammonia[20]. A reversed phase HPLC assay developed for the simultaneous determination of vancomycin, anisomycin and trimethoprim in an antibacterial mixture revealed that vancomycin consisted of one major and several minor components[21]. A commercial sample of vancomycin examined by HPLC was found to contain 9% of a crystalline degradation product (CDP-I) and other minor constituents none greater than 5% (some of which were tentatively identified as mono- and didechlorovancomycin and their CDP-type rearrangement products[22]). An HPLC procedure has been proposed for use by the *United States Pharmacopia* to limit the composition of vancomycin to not less than 80% and any related component to not more than 9%[23].

Aqueous solutions of vancomycin are not stable at 25 and 37°C[24–26] and even refrigerated solutions have been reported to have a limited shelf life[26,27]. Recent report of the incompatibility of vancomycin and ceftazidime indicates the need for HPLC to monitor both the quality and possible degradation of vancomycin[28].

EXPERIMENTAL

Materials

The glycopeptide antibiotics examined are listed with their suppliers in Table I. Also studied was the International Standard for Vancomycin[29] and samples which had been included in degradation studies maintained at the following temperatures: 20 and 37°C for 25 years and 56°C for 15 years. Aglucovancomycin and crystalline degradation product I (CDP-I) were prepared by mild acid hydrolysis[20].

TLC

The following pre-coated chromatoplates were used: silica gel 60 and silica gel 60W (E. Merck), Uniplates reversed-phase (Analtech) and carboxymethyl cellulose (J. T. Baker), analytical-grade solvents and reagents (BDH) and *p*-nitrobenzenediazonium tetrafluoroborate (Sigma).

TABLE I

GLYCOPEPTIDE ANTIBIOTICS EXAMINED

Antibiotic	*Source*
A-35512B, actaplanin, vancomycin, demethylvancomycin	Lilly Research Laboratories, Indianapolis, IN, U.S.A.
Demethylvancomycin	National Institute for Control of Pharmaceutical and Biological Products, Beijing, China
Actinoidin A, actinoidin B, carboxyristomycin	Institute of New Antibiotics, Moscow, U.S.S.R.
Avoparcin	American Cyanamid, Pearl River, U.S.A.
Ristocetin A, ristocetin B	Abbott Laboratories, North Chicago, IL, U.S.A.
Teicoplanin	Gruppo Lepetit, Milan, Italy

TABLE II

CHROMATOGRAPHIC SYSTEMS

System	*Stationary phase*	*Mobile phase*	*Development temperature (°C)*
A	Reversed phase	5% ammonium hydrogencarbonate–dioxane (3:7)	4
B	Silica gel 60W	1% ammonium hydrogencarbonate–methanol (9:1)	20
C	Silica gel 60	1% ammonium carbonate–propan-2-ol (9:11)	20
D	Carboxymethyl-cellulose	0.9% diammonium hydrogenorthophosphate, pH 8.3	28

Solutions (3 μl) containing 2 mg ml^{-1} of antibiotic in water were applied to the plates by means of micropipettes and the plates were placed in filter-paper-lined chromatographic chambers which have been saturated for 2 h. Details of the chromatographic systems which were found to be useful are given in Table II.

The plates were developed over a distance of 150 mm, then air-dried and sprayed with freshly prepared aqueous solution of *p*-nitrobenzenediazonium tetrafluoroborate (1 mg ml^{-1}). For biological detection, the air-dried plates were covered with a 4-mm thick layer of antibiotic assay medium A (ref. 30), inoculated with a spore suspension of *Bacillus subtilis* NCTC 8236 and incubated at 35°C for 18 h. Antibacterial activity was revealed as clear zones of inhibition of growth. To enhance the contrast between the zone and the surrounding growth the bioautograph was sprayed with an aqueous solution of *p*-iodonitrotetrazolium (2 mg ml^{-1}) and incubated for 5 min.

HPLC

The apparatus consisted of two reciprocating pumps on a gradient controller (Constametric I, Constametric II G, and a gradient master, Model 1601, Laboratory Data Control) and a variable-wavelength spectrophotometer (Model CE 272, Cecil Instruments) fitted with a 75-μl flow-through cell. Two in-line filters, 2 μm and 0.5 μm porosity, were placed between the injector (Rheodyne, Model 7125) and the polymeric analytical HPLC column PLRP-S 100A, 8 μm, 150 × 4.6 mm (Polymer Labs.). The mobile phase was filtered through a glass microfibre filter and degassed prior to use. It consisted of 0.02 *M* borate buffer pH 8.6 containing acetonitrile (HiPerSolv, BDH), the selected gradient elution profile gave a linear increase in acetonitrile concentration from 8 to 16% (v/v) in 17.5 min, total run took 35 min. The flow-rate was 0.5 ml min^{-1}. The antibiotics were dissolved in distilled water (0.25 mg ml^{-1}), 20-μl volumes were injected. The eluent was monitored at 235 nm sensitivity (0.5 a.u.f.s.). The relative composition of the samples was determined by normalisation of peak areas measured with a computing integrator (Model SP 4270, Spectra-Physics); it was assumed that all the components have the same absorbance at 235 nm.

RESULTS

TLC

Four TLC systems were devised which were capable of distinguishing vancomycin from other glycopeptide antibiotics and vancomycin-related substances including the degradation products aglucovancomycin and CDP-I. The water-resistant wettable silica gel 60 pre-coated TLC plates allowed the use of a completely aqueous eluent which had a faster running time (2 h) than the conventional precoated silica gel plates (6 h). The R_F values obtained with systems A and C were very similar. A low temperature (4°C) was required to obtain the optimum separation with system A. A slightly elevated temperature (28°C) was found to be critical for system D. System B was found to be the most robust. The R_F values of all the substances examined on the four systems are reported in Table III. In each system ristocetin B was shown to consist of two components, minor components were also detected in ristocetin A and avoparcin. Fast Red GG (*p*-nitrobenzenediazonium tetrafluoroborate) is a TLC spray reagent for the detection of phenols and amines which proved to be very suitable for visualizing the glycopeptide antibiotics thus eliminating the need for bioautographic detection. All the systems were suitable for bioautography which still remains a useful method for demonstrating antibacterial activity. Minor contaminants could readily be detected, *e.g.*, traces of vancomycin and aglucovancomycin in a sample of demethylvancomycin, and aglucovancomycin and demethylvancomycin in degraded vancomycin (Fig. 1).

TABLE III

R_F VALUES OF GLYCOPEPTIDE ANTIBIOTICS AND DERIVATIVES OBTAINED ON DIFFERENT TLC SYSTEMS

TLC systems as in Table II. Number in parenthesis is a minor component.

Compound	*TLC system*			
	A	*B*	*C*	*D*
Vancomycin	0.37	0.46	0.36	0.52
Demethylvancomycin	0.53	0.70	0.49	0.63
Aglucovancomycin	0.75	0.85	0.78	0.27
CDP-I	0.48	0.82	0.50	0.76 (0.46)
Ristocetin A	0.34	0.57	0.28	0.31
Ristocetin B	0.33	0.51	0.33	0.17
	0.29	0.50	0.25	0.10
Avoparcin	(0.61) 0.29	0.49	0.24	0.55
Teicoplanin	0.81	0.76	0.75	0.05
Actinoidin A	0.19	0.30	0.20	0.15
Actinoidin B	0.24	0.39	0.24	0.21
Carboxyristomycin	0.57	0.85	0.38	0.75
A-35512B	0.71	0.64	0.46	0.29

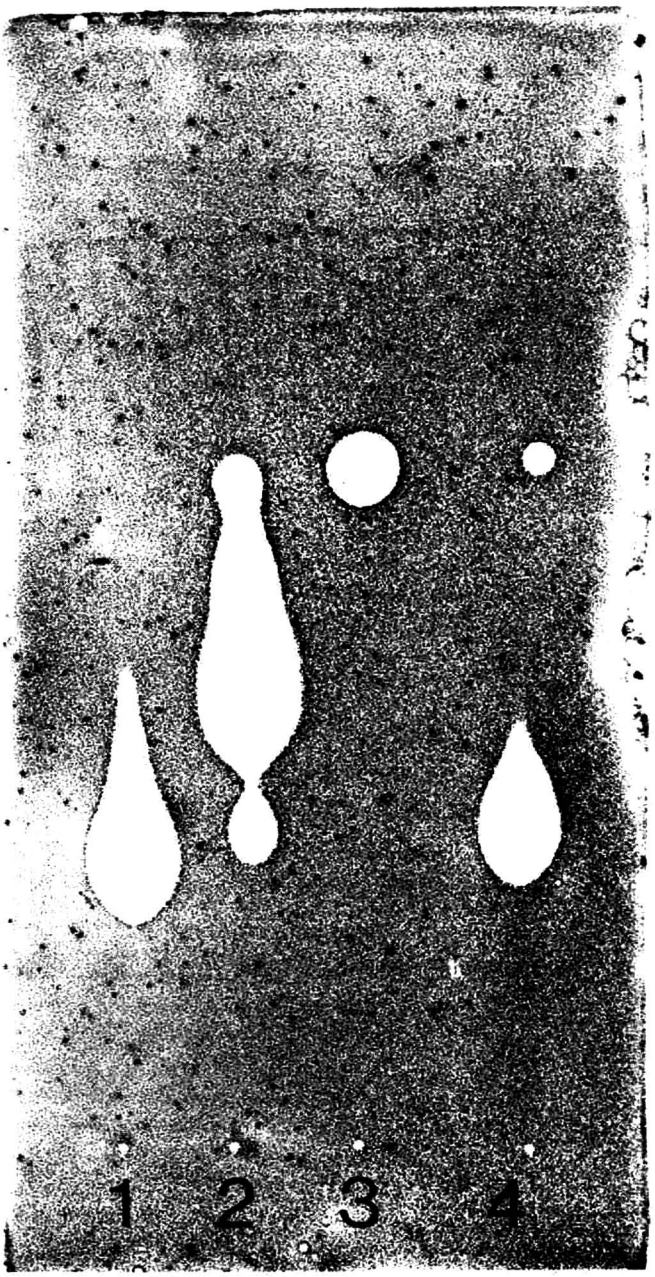

Fig. 1. Thin-layer chromatogram of the components of vancomycin detected with *Bacillus subtilis* NCTC 8236. Uniplate reversed-phase; 5% ammonium hydrogencarbonate–dioxane (3:7). 1 = vancomycin, 12 μg; 2 = demethylvancomycin, 18 μg; 3 = aglucovancomycin, 32 μg; 4 = vancomycin heated at 56°C for 15 years, 24 μg.

TABLE IV

COMPOSITION (%) OF GLYCOPEPTIDE ANTIBIOTICS DETERMINED BY HPLC

Composition (%) of glycopeptide antibiotics based on the measurement of peak areas of the components separated by HPLC. Column, PLRP-S 100A, 150 × 4.6 mm; eluent, 0.02 *M* borate buffer pH 8.6 containing acetonitrile, 8% (v/v) increasing linearly to 16% (v/v) in 17.5 min; flow-rate, 0.5 ml min^{-1}; absorbance at 235 nm. Glycopeptide antibiotics: I = vancomycin, II = demethylvancomycin, III = ristocetin A, IV = ristocetin B, V = A-35512B, VI = actinoidin A, VII = actinoidin B, VIII = carboxyristomycin. Major components > 10% are represented in italics.

Peak No.	*k'*	*I*	*II*	*III*	*IV*	*V*	*VI*	*VII*	*VIII*
1	0.88			1.61	0.34				*63.95*
3	1.19	0.05			0.54				
4	1.32					1.51			0.62
5	1.39		0.21						
6	1.48								1.25
7	1.68			0.15					
8	1.74	0.33		0.62		0.71			*23.45*
9	1.92					0.86			
10	2.07		0.44		0.58				0.93
11	2.19				1.27				
12	2.34	0.82	0.32			0.58			0.91
13	2.42				1.55	1.04			
14	2.56	0.29		1.59	0.92		0.75	0.57	0.11
15	2.80		0.13	*93.04*	*14.68*	*72.19*	1.61	*15.21*	0.40
16	2.93		0.40						5.60
17	3.11				*30.17*	*11.06*	*95.99*	*60.27*	2.27
18	3.33	2.56	*93.65*	0.44		2.95			
19	3.37				5.74			*13.38*	
20	3.54	1.02			5.62				
21	3.72	*90.26*	2.29	2.34	2.21	6.78	0.68	9.51	0.51
22	3.94		0.23		0.83				
24	4.15	3.40	0.51	0.21	*35.57*	2.32			
25	4.58	0.24	0.68				0.64		
26	5.12	1.45					0.34	1.07	

HPLC

The HPLC method developed confirmed the heterogenous nature of the glycopeptide antibiotics especially those which are not used therapeutically, 28 different components were revealed in the antibiotics examined (Table IV). The peaks have been numbered and the major components marked (italics) in the chromatogram to assist in the recognition of those components that occur in more than one antibiotic. Chromatograms of the separation of vancomycin, degraded vancomycin, demethylvancomycin and CDP-I are shown in Figs. 2–5. Most of the antibiotics were well differentiated, the two actinoidins and ristocetin B share a number of major components. The structurally related antibiotics ristocetin A and A-35512 B could not be differentiated by this method though they can be separated on a LiChrosorb RP-8 column[16]. The method described here was optimised for the analysis of vancomycin.

Most of the vancomycin samples examined contained more than 85% vancomycin and 4–6% demethylvancomycin (Table V). On a weight basis demethylvancomycin is 10% more active than vancomycin, so slight differences in the composition

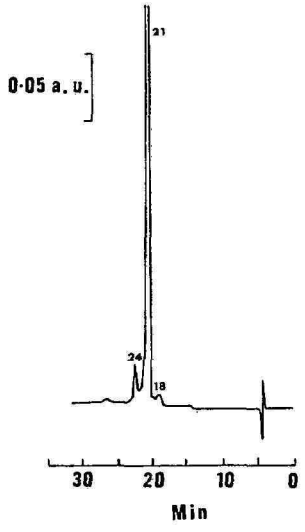

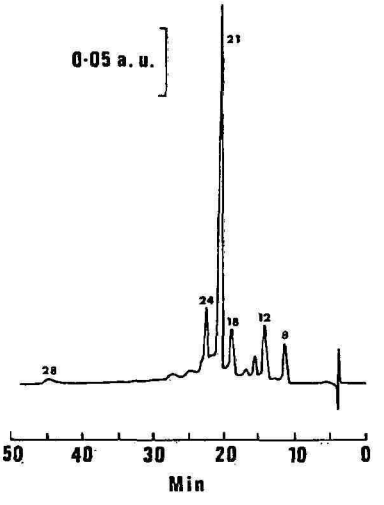

Fig. 2. Chromatogram of vancomycin. Column, PLRP-S 100A, 150 × 4.6 mm. Eluent, 0.02 *M* borate buffer pH 8.6 containing acetonitrile 8% (v/v) increasing linearly to 16% (v/v) in 17.5 min; flow-rate 0.5 ml min^{-1}; absorbance at 235 nm. Peak numbers refer to identification as in Table V.

Fig. 3. Chromatogram of a sample of vancomycin heated at 56°C for 15 years. Conditions as in Fig. 2.

of the samples are not reflected in their estimated potencies (Table V). Accelerated degradation studies on the International Standard for Vancomycin resulted in a loss of vancomycin and an increase in demethylvancomycin and several other minor components but despite these changes antibacterial activity was not completely abolished.

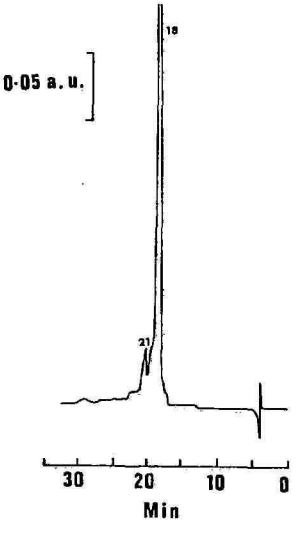

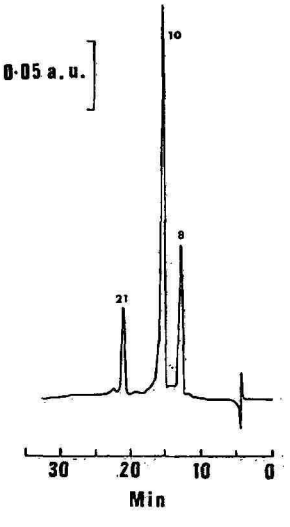

Fig. 4. Chromatogram of demethylvancomycin. Conditions as in Fig. 2.

Fig. 5. Chromatogram of crystalline degradation product I. Conditions as in Fig. 2.

TABLE V

COMPOSITION (%) AND POTENCY OF SAMPLES OF VANCOMYCIN AND DEGRADED VANCOMYCIN DETERMINED BY HPLC AND MICROBIOLOGICAL ASSAY RESPECTIVELY

HPLC conditions as in Table IV. Peak identification: 8 = CDP-I minor form, 12 = CDP-I major form, 18 = demethylvancomycin, 21 = vancomycin, 28 = aglucovancomycin.

Peak No.	*k'*	*Sample*											
		1	*2*	*3*	*4*	*5*	*6*	*7*	*8*	*9*	*20°C*	*37°C*	*56°C*
2	0.94					0.16						0.09	0.20
3	1.19	0.05	0.18	0.44	0.12	0.18	0.56			0.19		0.12	0.38
8	1.74	0.33	0.39	0.45					0.43	0.22	2.30	3.99	6.07
10	2.07						0.28				0.18	0.48	1.24
12	2.34	0.82	2.22	1.67	1.26	1.08	2.78		1.85	1.51	2.22	4.41	9.65
14	2.56	0.29	0.66	0.56	0.34	0.28	0.41	1.53	0.48	0.34	0.37	0.97	3.46
15	2.80		0.79	0.45	0.46	0.15	0.25	0.35	0.22	0.03	0.21	0.54	2.57
17	3.11		1.15		0.60	0.50	0.56		0.31				
18	3.33	2.56	6.23	6.65	5.26	5.94	5.32	4.84	4.52	4.55	5.90	8.86	9.47
20	3.54	1.02	1.09	0.70	0.90	0.95	3.04	0.79	0.74	0.87	1.10	1.27	0.93
21	3.72	90.26	83.05	79.72	85.99	86.96	77.49	88.39	86.55	87.42	81.88	70.15	49.48
23	4.06				1.40				0.32				
24	4.15	3.40	1.52	5.54		0.35	5.77	1.74	1.65	2.22	4.15	5.50	8.45
25	4.85	0.24	0.30	0.91	0.17	2.35	0.78	0.10	0.19	0.21	0.16	0.62	1.67
26	5.12	1.45	2.42	2.90	2.60	0.28	2.75	2.27	2.72	2.44	1.52	2.24	2.11
27	5.39										0.31	0.80	
28	7.70												4.32
Potency (I.U. mg^{-1})		1007	920	956	990	1040	858	944	941	944	855	664	369

In order to identify some of the minor peaks the following derivatives of vancomycin were prepared: aglucovancomycin and CDP-I. When subjected to HPLC the aglucovancomycin exhibited a retention time of 45 min (k' 7.70). CDP-I gave two peaks, k' 1.74 and 2.34 representing 20% and 64% respectively together with 9% residual vancomycin. The two constituents were thought to correspond to the two isomeric forms of CDP-I[19,31]. No succinimide intermediate was detected. Degradation of the International Standard for Vancomycin lead to the formation of both forms of CDP-I plus some other unidentified components (Table V); aglucovancomycin (5%) was detected only in the sample maintained at 56°C for 15 years.

CONCLUSIONS

The TLC systems described using chemical detection represent a marked improvement over the existing tedious paper chromatographic method with bioautographic detection for the identification of vancomycin. The identity of vancomycin may also be confirmed by HPLC. The changes that occur during the degradation of vancomycin can be conveniently monitored by HPLC. Because vancomycin may contain more than one bioactive component there is no direct correlation between vancomycin content and biological potency nonetheless, HPLC should become a specific method of assay for vancomycin.

ACKNOWLEDGEMENT

We wish to thank Mr. Navneet R. Sharma for the bioassay of the vancomycin samples.

REFERENCES

1 P. R. Pfeiffer, *Rev. Infect. Dis.*, 3 (1981) S 205.
2 J. C. J. Barna and D. H. Williams, *Annu. Rev. Microbiol.*, 38 (1984) 339.
3 R. S. Griffith, *Rev. Infect. Dis.*, 3 (1981) S 200.
4 L. D. Boeck, F. P. Mertz, R. K. Wolter and C. E. Higgins, *J. Antibiot.*, 37 (1984) 446.
5 J. R. Fooks, I. J. Mcgilveray and R. D. Strickland, *J. Pharm. Sci.*, 57 (1968) 314.
6 *Code of Federal Regulations, Food and Drugs Title 21*, Part 455.85, U.S. Government Printing Office, Washington, DC, 1986, p. 756.
7 M. R. Bardone, M. Paternoster and C. Coronelli, *J. Antibiot.*, 31 (1978) 170.
8 R. D. Sitrin, G. W. Chan, J. J. Dingerdissen, W. Holl, J. R. E. Hoover, J. R. Valenta, L. Webb and K. M. Snader, *J. Antibiot.*, 38 (1985) 561.
9 G. K. Best, N. H. Best and N. N. Durham, *Antimicrob. Agents Chemother.*, 8 (1968) 115.
10 M. Nieto and H. R. Perkins, *Biochem. J.*, 123 (1971) 773.
11 Z. Yu, L. Yu-fen and Z. Chang-liang, *Chinese J. Antibiot.*, 11 (1986) 414.
12 J. R. Uhl and J. P. Anhalt, *Ther. Drug. Monit.*, 1 (1979) 75.
13 R. J. Hoagland, J. E. Sherwin and J. M. Phillips, *J. Anal. Toxicol.*, 8 (1984) 75.
14 F. Jehl, H. Monteil, C. Gallion and R. C. Thierry, *Pathol. Biol.*, 33 (1985) 511.
15 J. Bauchet, E. Pussard and J. J. Garaud, *J. Chromatogr.*, 414 (1987) 472.
16 F. Sztaricskai, J. Borda, M. M. Puskas and R. Bognar, *J. Antibiot.*, 36 (1983) 1691.
17 A. Borghi, C. Coronelli, L. Faniuolo, G. Allievi, R. Pallanza and G. G. Gallo, *J. Antibiot.*, 37 (1984) 615.
18 L. Yu-fen and Z. Yu, *Chinese J. Antibiot.*, 11 (1986) 24.
19 C. M. Harris, H. Kopecka and T. M. Harris, *J. Am. Chem. Soc.*, 105 (1983) 6915.
20 F. J. Marshall, *J. Med. Chem.*, 8 (1965) 18.

21 R. L. Kirchmeier and R. P. Upton, *Anal. Chem.*, 50 (1978) 349.
22 C. M. Harris, H. Kopecka and T. M. Harris, *J. Antibiot.*, 38 (1985) 51.
23 *Pharmacopeial Forum*, The United States Pharmacopeial Convention, Rockville, MD, 12 (1986) 1058.
24 H. M. Higgins, W. H. Harrison, G. M. Wild, H. R. Bungay and M. H. McCormick, *Antibiotics Annu.*, (1957–1958) 906.
25 J. M. Mann, D. L. Coleman and J. C. Boyden, *J. Hosp. Pharm.*, 28 (1971) 760.
26 R. N. Greenberg, A. M. K. Saeed, D. L. Kennedy and R. McMillian, *Antimicrob. Agents Chemother.*, 3 (1987) 610.
27 L. Mallet, G. P. Sesin, J. Ericson and D. G. Fraser, *N. Engl. J. Med.*, 307 (1982) 445.
28 C. J. Cairns and J. Robertson, *Pharm. J.*, 238 (1987) 577.
29 J. W. Lightbown, P. de Rossi and P. Isaacson, *Bull. WHO*, 47 (1972) 343.
30 *British Pharmacopoeia*, HMSO, London, 1980, p. A123.
31 M. P. Williamson and D. H. Williams, *J. Am. Chem. Soc.*, 103 (1981) 6580.

Journal of Chromatography, 410 (1987) 383–394
Elsevier Science Publishers B.V., Amsterdam — Printed in The Netherlands

CHROM. 19 988

CHARACTERIZATION OF ORGANOTIN SPECIES USING MICROBORE AND CAPILLARY LIQUID CHROMATOGRAPHIC TECHNIQUES WITH AN EPIFLUORESCENCE MICROSCOPE AS A NOVEL IMAGING DETECTOR

W. R. BLAIR, E. J. PARKS*, G. J. OLSON and F. E. BRINCKMAN
Ceramics Chemistry and Bioprocesses Group, National Bureau of Standards, Gaithersburg, MD 20899 (U.S.A.)
and
M. C. VALEIRAS-PRICE and J. M. BELLAMA
Department of Chemistry and Biochemistry, University of Maryland, College Park, MD 20742 (U.S.A.)
(Received August 18th, 1987)

SUMMARY

The novel application of a UV epifluorescence microscope as an imaging detector for microbore and capillary high-performance liquid chromatography (HPLC) is reported. The microscope is focused on an in-line quartz flow cell incorporated down stream of a microbore HPLC column or directly on an optically clear portion of fused-silica capillary columns for analyte detection. The effect of different fluorescent ligand to analyte ratios on detection limits is also reported, as well as the effect of different image volume sizes produced by changes in microscope objective lens magnification power. Determination of relative sensitivities and detection limits for methyl- and butyltin compounds, complexed with fluorescent dyes, reveals that the organotins show decreasing sensitivity as the number of alkyl substituents on the tin atom increases, with minimum detectable amounts of 6–160 pg of analyte–ligand complex.

INTRODUCTION

Certain trace metal elements can be toxic or essential to man, depending on their concentration and molecular form. Some may form toxic ligated species in the environment as a result of biotic or abiotic processes. Examples of such elements include mercury, lead, arsenic, cadmium, and tin. In marine and estuarine environments these metals may all be found either in the water column, in sediments, or in the tissues of the pelagic and benthic communities. The trace and ultratrace detection and speciation methodology required for molecular characterization of the various metals or their ligated products differs for each metal and for each sample matrix. Transformations from metal to organometal species may be mediated environmentally, for example, with methyl iodide[1] or methylcobalamin[2], with resultant mobili-

0021-9673/87/$03.50

zation and transport of toxic species. On the other hand, toxic species such as tributyltin may be degraded in water to relatively non-toxic species of lower alkyl number.

The use of organotin compounds has increased greatly in the last 15–20 years[3]. The largest single use of these compounds is to improve the high-temperature stability of poly(vinyl chloride) plastics, where mono- and di-organotin species are used extensively[4]. Diorganotins are also used as stabilizers for polyurethane foams and as catalysts in the synthesis of silicones[5]. Biocidal applications typically employ the tri-substituted organotins, such as triphenyl- and tricyclohexyltin, found in agricultural chemicals, and tributyltin, incorporated in wood preservatives and in antifouling coatings for ships and marine installations[6–9]. The tetraorganotins have no large industrial outlets, but are used primarily as intermediates in the manufacture of other organotin compounds[10].

Since anthropogenic inputs of tin into the environment have increased over the years, major concerns have developed over the presence of organotin compounds in aquatic systems (in sediments, water, and tissues of aquatic organisms). In sea water, concentrations of tributyltin as low as 0.5 μg/l (0.5 ppb) are lethal to sheepshead minnows[11], lobster larvae, zoeal shore crabs[12], and mysid shrimp[13]. Accurate speciation and quantitation of tributyltin and other substituted tin species in sea water are especially important wherever tributyltin containing marine antifouling coatings are used on boat and ship hulls. The need to speciate organotins at ultratrace concentrations (ng/l) has mandated development of methods having much lower detection limits than previously available.

In the late 1970s, reports describing methods for the speciation of organotins in environmental samples at μg to ng per liter concentrations began to appear. In general, these methods relied upon purge and trap or solvent extraction techniques aided by derivatization with sodium borohydride or Grignard reagents to remove organotins from environmental samples. Separation of the sparged or extracted organotins was typically achieved by boiling point or gas chromatographic (GC) means, with tin detection by electron capture[14], flame emission[15,16], atomic absorption[17], or mass spectrometry[18]. More recently, applications of the above methods, with some modifications, to the analysis of natural waters and sediments have resulted in reports describing the routine speciation of butyltin compounds at ng/l concentrations[19–22].

Methods for organotin speciation employing high-performance liquid chromatography (HPLC), especially for butyltins, are less abundant in the literature than methods using boiling point or GC separation techniques. Jewett *et al.*[23] were the first to speciate di- and tributyltin by HPLC, using a graphite furnace atomic absorption detector, but their method required relatively large quantities of analyte (100 ng or more per species).

The reagents 3-hydroxyflavone (flavonol) and 2′,3,4′,5,7-pentahydroxyflavone (morin) have been shown to form fluorescent complexes with both inorganic and organic tin compounds. Blunden and Smith report that 1:1 mixtures of $(C_4H_9)_2SnCl_2$, $(CH_3)_2SnCl_2$, or $C_6H_5SnCl_3$ with flavonol in toluene produce strongly fluorescent complexes[24]. Arakawa and Wada[25] determined the relative fluorescence intensities of nine organotin–morin complexes to be: 99.4 for $(C_3H_7)_2SnCl_2$, 99.2 for $(C_2H_5)_2SnCl_2$, 51.7 for $(C_4H_9)_2SnCl_2$, 42.5 for $(CH_3)_2SnCl_2$, 12.7 for $(C_6H_5)_3SnCl$, 10.2 for $C_4H_9SnCl_3$, 2.8 for $(C_3H_7)_3SnCl$, 2.2 for $(C_2H_5)_3SnCl$, and

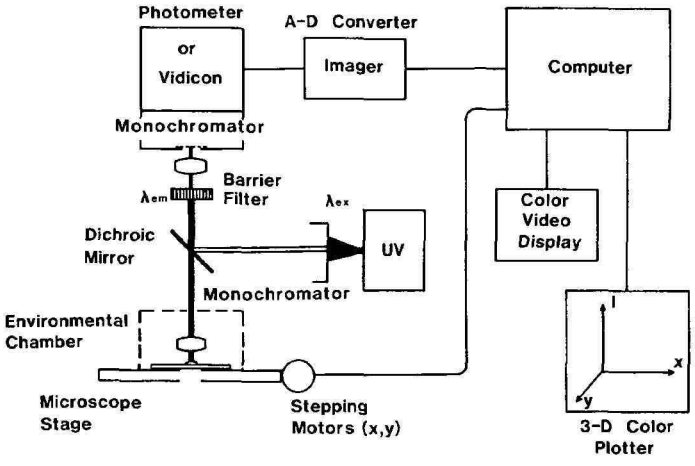

Fig. 1. Schematic diagram of the microscopic UV epifluorescence imaging system. A-D = Analog-to-digital; 3-D = three-dimensional.

1.6 for $(C_4H_9)_3SnCl$. The fluorescence properties of various organotin compounds complexed with morin or flavonol have been used advantageously for their speciation by HPLC with detection by fluorescence spectroscopy[26,27].

The speciation techniques described in this paper utilize fluorescence detection of organotin–fluorophor complexes by epifluorescence microscopy, which provides sensitivity at picogram levels. Used with existing methods for organotin extraction and preconcentration, epifluorescence detection improves the detection limits for ultratrace speciation measurements. Epifluorescence examination of particulates or individual algal or bacterial cells holds promise for becoming a definitive method for locating the sites where chemically or biologically mediated transformations (*e.g.*, methylation, reduction) of metals occur on or in particulates or living cells.

EXPERIMENTAL*

A Zeiss universal microscope (Carl Zeiss, New York, NY, U.S.A.) equipped for epifluorescence operation provided the basis of the UV epifluorescence imaging system shown schematically in Fig. 1. A high-pressure mercury arc lamp produced UV radiation, with wavelengths selected by filtration. Emission wavelength to be monitored was selected by monochrometer and directed to a Zeiss Model SF photometer. The UV radiation from the mercury arc source was reflected to the object plane by a dichromatic mirror, which also passed emission radiation from the excited organotin–fluorophor complex to the photometer for quantification of emission intensity. The photometer output was sent to an analog-to-digital converter for computerized data collection and/or recorded on a strip chart recorder.

* Certain commercial products or equipment are mentioned in order to adequately describe experimental procedures. In no case does such identification imply endorsement by the National Bureau of Standards, nor does it imply that the material is necessarily the best available for the purpose. Contributions from the National Bureau of Standards are not subject to copyright.

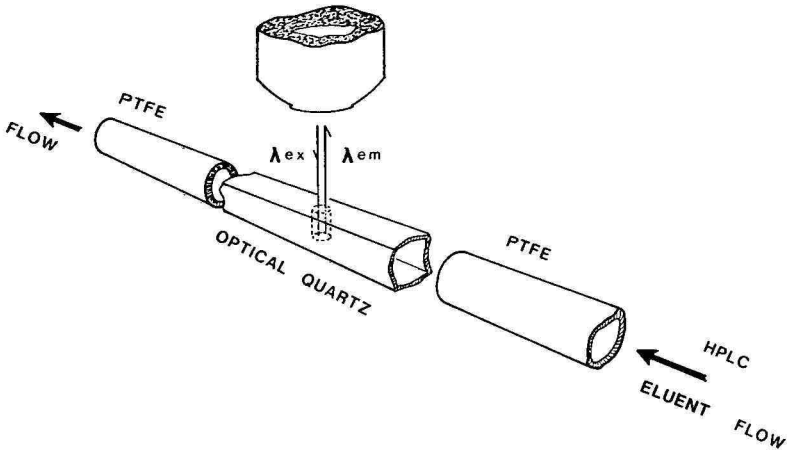

Fig. 2. Diagram of the optical quartz flow cell used when the imaging system was operated as an epifluorescence UV detector for FIA and HPLC. PTFE tubing, shrink fitted to the quartz tube, was terminated with adaptors that allowed connection to typical HPLC fittings. The quartz tube was attached to a glass microscope slide to facilitate positioning on the microscope stage for objective lens focusing.

Organotins (obtained from commercial suppliers and used without further purification) were detected and quantified in both flow injection (FIA) and microbore HPLC modes by using a special flow microcell of square cross section (500 μm) made of fused optical quartz (Wilmad Glass, Buena, NJ, U.S.A.). The quartz microcell (Fig. 2) was attached to a conventional glass microscope slide and positioned under an oil immersion objective lens with a magnification of 63 ×. In the work reported here, a measuring aperture of 2.5 mm diameter was used, which produced an image plane of 31.7 μm or 50.0 μm in diameter respectively, when a 63 × oil immersion or 40 × dry objective lens was employed.

The quartz microcell formed an integral portion of the eluent tubing from a dual piston microbore HPLC pump with ceramic-lined liquid contact surfaces (LKB Instruments, Bromma, Sweden). PTFE eluent tubing was attached to the quartz microcell by heat shrinking the PTFE onto the quartz tubing. An image volume of $3.95 \cdot 10^{-4}$ μl was created when the 63 × oil immersion objective lens was used. Samples were injected into the LC system by a syringe loaded injection valve that incorporated a 1-μl sample loop (Rheodyne, Cotati, CA, U.S.A.). In this mode of operation, the epifluorescence microscope system functioned as a versatile detector for FIA or as a microscopic imaging volume for metal/fluorophor detection at the cellular *in vivo* level. Both flavonol (excitation = 365 nm, emission = 453 nm) and morin (excitation = 420 nm, emission = 500 nm) were used to generate fluorescent organotin complexes. Flavonol and morin compounds were obtained from Eastman (Rochester, NY, U.S.A.).

In instances where analytes possess fluorescent properties, selection of the appropriate excitation and emission wavelengths allows detection. The separation of 9-methylanthracene and perylene, both fluorescent compounds, on a glass-lined C_{18} column is shown in Fig. 3.

This imaging system was also used as an on-line detector for a liquid chro-

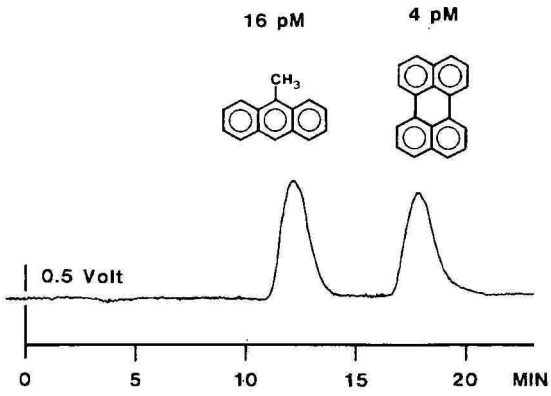

Fig. 3. Chromatogram showing the fluorescence emission peaks recorded during the separation of 9-methylanthracene and perylene on a glass-lined microbore C_{18} column (250 × 1 mm I.D., particle size 3 μm). Mobile phase, acetonitrile–water (70:30); flow-rate, 80 μl/min; pressure, 52 bar; λ_{ex} = 365 nm; λ_{em} = 440 nm.

matograph employing open-tubular capillary gas chromatographic columns with chemically bonded stationary phases. This application permits speciation via chromatographic separation of the various organotin moieties present in an injected sample. A diagram of the capillary column application is shown in Fig. 4. Light from

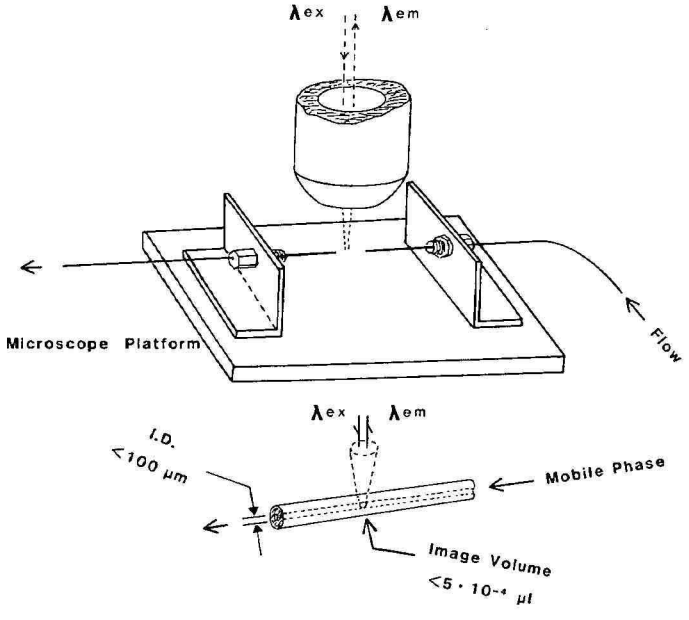

Fig. 4. Drawing of the bracket used to position a fused-silica capillary column on the microscope stage under an objective lens. The bracket was fabricated from a brass plate and two 90° brass angles. The angle pieces had 1/16-in. Swagelok unions soldered to them which, with appropriately sized graphite ferrules, could be tightened to hold the column firmly. The column was installed in the bracket before the inner bonded phase and outer polyamide coatings were removed by heating with a torch. Once heated, the column was not removed from the bracket to prevent breakage at the clear, unprotected portion.

the excitation source was focused on a clear area in the capillary column, created by heating the column to a bright red color with a butane–oxygen brazing torch while flowing oxygen through the column. This treatment removed both the bonded stationary phase from inside the column and the polyimide coating from the outside of the column for a length of 3–5 mm. Due to the fragile nature of the capillary column following removal of the external polyimide coating, the column was clamped into a special fixture prior to heating with the torch. The entire fixture, with column installed, then attached directly to the microscope stage, thus protecting the fragile, clear area of the column from breakage during handling.

As presently implemented, the oil immersion microscope lens cannot be used with the capillary GC columns due to mechanical interference between lens and column holding fixture. A dry objective, providing a magnification of 40× was used with the capillary GC columns. The detection limits for this configuration could be improved by modifying the column-holding fixture to permit use of an oil immersion lens.

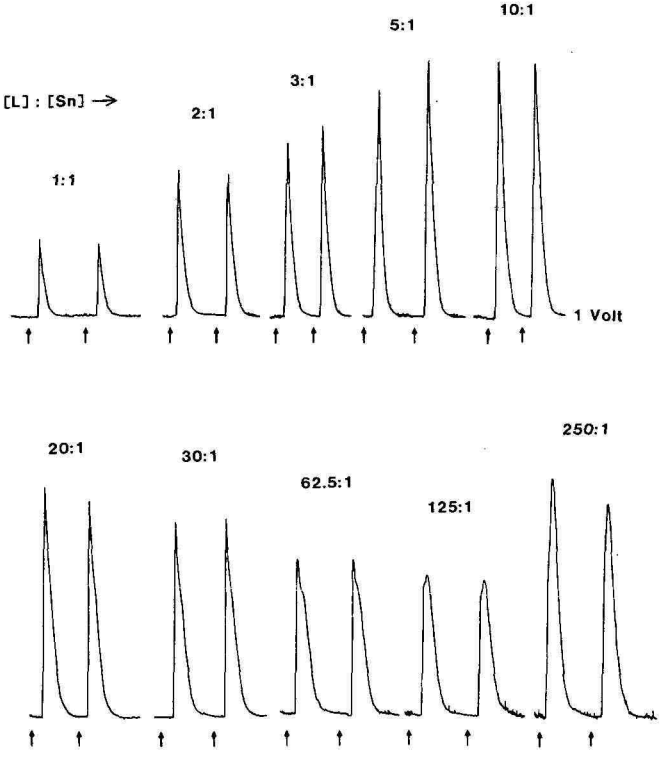

Fig. 5. Illustration showing FIA determination of the optimum ratio of fluorescent ligand (flavonol) to $C_4H_9SnCl_3$ analyte. The $C_4H_9SnCl_3$ concentration was held constant ($2.5 \cdot 10^{-11}$ mol per injection) as the flavonol concentration was increased. Fluorescence intensity, monitored at 453 nm, increased to a maximum at a ratio of 10:1 (ligand to analyte) and then decreased. At the very high ratio of 250:1, uncomplexed flavonol began to contribute to the emission signal and emission intensity shows some increase. Mobile phase, methanol; flow-rate, 160 μl/min; λ_{ex} = 365 nm; λ_{em} = 453 nm.

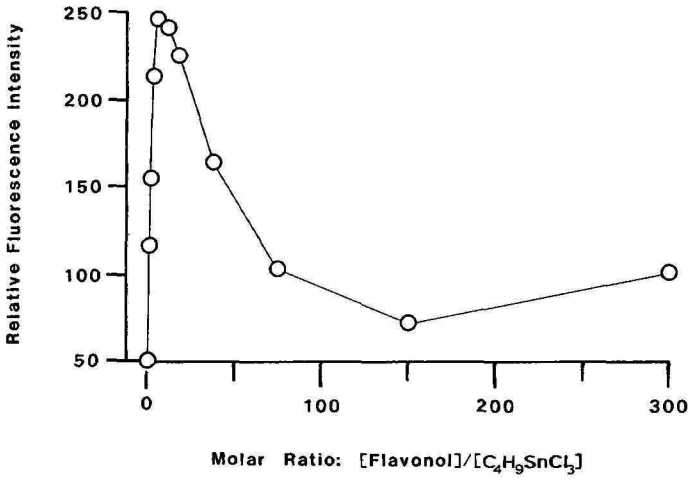

Fig. 6. Graphical presentation of relative emission intensity *versus* the molar ratio of fluorescent ligand to analyte for the flavonol–$C_4H_9SnCl_3$ system. $C_4H_9SnCl_3$, $2.5 \cdot 10^{-11}$ mol per injection; mobile phase, methanol; flow-rate, 160 μl/min; λ_{ex} = 365 nm; λ_{em} = 453 nm.

RESULTS AND DISCUSSION

The specific ratio of fluorescent ligand to analyte had a pronounced effect on the fluorescence intensity of the resulting ligand–analyte complex. Fig. 5 illustrates the determination of the optimum ratio of $C_4H_9SnCl_3$ to flavonol for FIA. The $C_4H_9SnCl_3$ concentration was held constant as the flavonol concentration was increased. Signal intensity at 453 nm increased to a maximum as the optimum ratio of 10:1 (ligand to analyte) was reached and then diminished as the 10:1 ratio was exceeded. At very high ratios of flavonol to butyltin, the uncomplexed flavonol began to contribute significantly to the signal, even though the flavonol emission peak was at 530 nm. The shoulder on the right side of the peak at the 62.5:1 ratio (Fig. 5) represents the flavonol peak, which grew larger at higher flavonol to tin ratios. The

TABLE I

RELATIVE SENSITIVITY OF TIN COMPLEXES AND EPIFLUORESCENCE MICROSCOPE IMAGING DETECTION LIMITS

Sensitivity	$CH_3SnCl_3 > (CH_3)_2SnCl_2 > (CH_3)_3SnCl$ $C_4H_9SnCl_3 > (C_4H_9)_2SnCl_2 > (C_4H_9)_3SnCl$	
Detection limits	$SnCl_4$	5.7 pg
	CH_3SnCl_3	27 pg
	$C_4H_9SnCl_3$	157 pg
Excitation wavelength	365 nm	
Emission wavelength	450–460 nm	
Flow-rate	80–160 μl/min	
Mobile phase	Methanol	

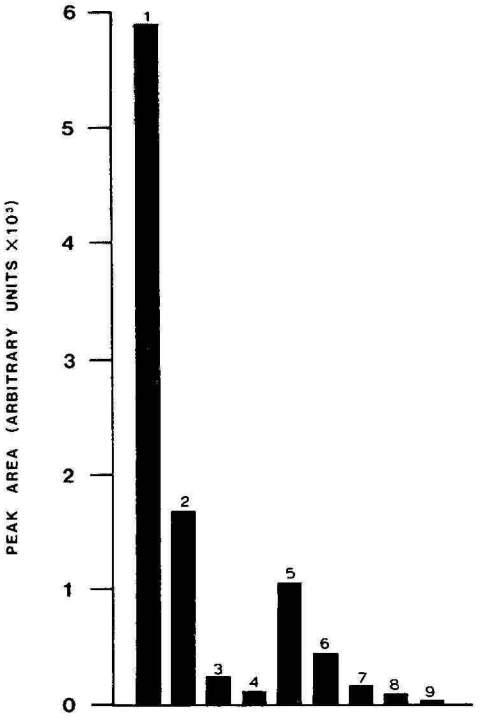

Fig. 7. Graph showing the relative sensitivities of different tin compounds to epifluorescence detection during FIA, with excitation, emission, and flow-rate parameters the same for each analyte. Inorganic Sn(IV) has the greatest sensitivity, with the organotins in the methyl- and butyl-substituted groups showing the highest sensitivity for species that have the fewest number of alkyl substituents. Amount of tin in each sample, 6 ng; flow-rate, 80 μl/min; image volume, $4 \cdot 10^{-4}$ μl; λ_{ex} = 365 nm; λ_{em} = 400 nm. 1 = $SnCl_4$; 2 = CH_3SnCl_3; 3 = $(CH_3)_2SnCl_2$; 4 = $(CH_3)_3SnCl$; 5 = $C_4H_9SnCl_3$; 6 = $(C_4H_9)_2SnCl_2$; 7 = $(C_4H_9)_3SnCl$; 8 = $(C_6H_5)_3SnCl$; 9 = methanol blank.

flavonol was apparently slightly more retained than the complex in the capillary. A graph of the relative fluorescence intensity *versus* the molar ratios of flavonol to $C_4H_9SnCl_3$, as determined above, is shown in Fig. 6.

The relative sensitivities and minimum detectable amounts of some methyl- and butyltin compounds complexed with optimum amounts of flavonol are listed in Table I. The greatest sensitivity was achieved with inorganic Sn(IV), with the organotins showing decreasing sensitivity as the number of alkyl substituents on the tin atom increased. A graph showing the fluorescence intensity versus the degree of alkyl substitution for Sn(IV) and several methyl- and butyltin compounds is presented in Fig. 7.

The effect of a change in the magnification of the microscope objective lens or a change in the inner dimensions of the microcell on the detection limits of fluorescing analytes is demonstrated by the data in Table II and the graph presented in Fig. 8. Although there appears to be a simple relationship between the detection limit and the magnification power of the objective lens or the dimensions of the microcell (as lens magnification power is increased or microcell dimensions reduced, smaller and

TABLE II

DETECTOR EFFICIENCY: IMAGE VOLUME *VS.* MAGNIFICATION

DL^{95} = Detection limit (95% confidence interval); IV = image volume.

Species	*Flow-rate (μl/min)*	*Column*	*I.D. (μm)*	*Image volume (μl · 10^4)*	*DL^{95} (ng)*	*Efficiency (DL/IV)*
Sn^{IV}	60	Fused-silica capillary	100	1.96	41	20.9
Sn^{IV}	80	Quartz flow cell	500	9.82	157	16.0
$C_4H_9Sn^{IV}$	60	Fused-silica capillary	100	1.96	33	16.8
Sn^{IV}	80	Quartz flow cell	500	3.95	5.7	1.44*

* Oil immersion lens, 63× magnification.

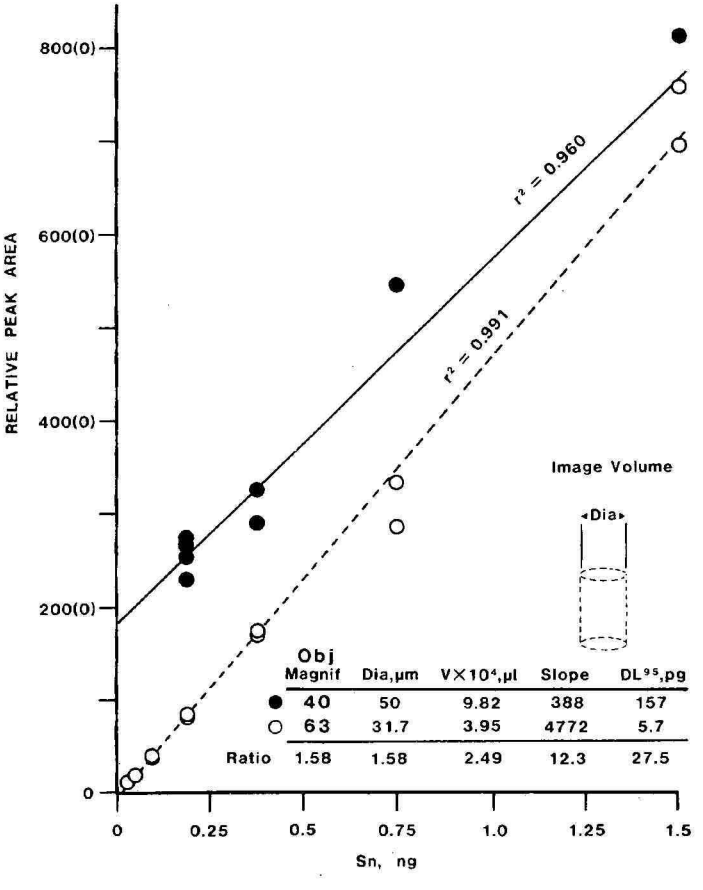

Fig. 8. FIA of $SnCl_4$–flavonol (1:1) in methanol. Example showing the effect of image volume on sensitivity and detection limits of epifluorescence microscope imaging system (DL, 95% confidence interval). The image volume was changed by the use of microscope objective lenses providing final magnifications of 500× and 788×. Flow-rate, 80 μl/min; λ_{ex} = 365 nm; λ_{em} = 460 nm. Obj = Objective; Magnif = magnification; Dia = diameter; V = volume.

smaller quantities of analyte are detected), this represents an over-simplification of the numerous factors influencing fluorescence intensity in microfluorometry. As the subtended angle of an objective lens, expressed as the numerical aperture of the lens, becomes larger, as it does when an oil immersion lens is substituted for a dry objective, the fluorescence intensity increases exponentially with the increase in numerical aperture. However, fluorescence intensity decreases exponentially with an increase in total magnification[28]. The observation that smaller analyte quantities are detectable when an oil immersion lens is substituted for a lower power dry lens indicates that these two factors do not totally cancel each other. The reader is directed to refs. 29–31 for a theoretical discussion of these variables, since it lies beyond the scope of this paper.

In using the epifluorescence microscope as a detector for capillary column HPLC, advantage may be taken of the benefits provided by wall-coated open-tubular (WCOT) columns. For example, efficiencies of 2000–4800 plates per meter (50000–120 000 plates for a 25-m column) are routinely cited as the minimum performance criteria for WCOT columns. In contrast, a typical HPLC column of 200 mm × 4.6 mm I.D., packed with 5-μm particles, provides 12000–16000 plates. Solvent consumption is reduced because the WCOT columns require only 50–200 μl/min solvent flow-rates *versus* the 1–3 ml/min flow-rates required by conventional HPLC columns to maintain optimum linear flow velocities. As the internal diameter of a column decreases, the efficiency and resolution of the column improve. The WCOT columns provide increased mass sensitivity as a result of their small internal diameters. The mass sensitivity of a column is directly proportional to the square of the column radius[32]. Thus, a reduction in radius from 100 μm to 50 μm would reduce by a factor of 4 the quantities of analyte detectable. The latter property or advantage is particularly important when LC is applied as a diagnostic tool for environmental, biomedical, and biochemical samples, where the quantity of these samples can be very limited. Reduction of column radius, however, can improve chromatographic behavior only to a certain point, due to limitations in the rest of the equipment. For example, band broadening results when analyte is dispersed in the mobile phase, in the sample valve, connecting tubing, or detector cell, thus seriously impairing column resolution. The above discussion points to one major advantage offered by the on-line detection system. Since the detector cell consists of a microscopic image volume within the column itself, band broadening due to analyte dilution in the detector cell is essentially eliminated.

CONCLUSIONS

The advantages of using the ultraviolet epifluorescence microscope as a sensitive detector for either FIA or microbore HPLC combine those of microscopic imaging and ultra sensitive fluoresence detection. One further advantage of the epifluorescence detector being developed now is its applicability to the imaging of bacterial cells in either a flow-injection or a stopped-flow mode. The uptake of organotins or other metals or organometals by organisms can be studied by exposing cells to a metal or metal containing compound, then staining the cells with a fluorescent reagent that complexes with the metal of interest. Using the characteristic fluorescence wavelength of the complex, those cells or areas of cells that have accumulated metal

can be identified. With fluorescent cell sorting techniques, the cells accumulating metal species could be separated from those that show no fluorescence. Conversely, the solubilization of a metal from an ore or metal containing substrate by microbiological activity could also be monitored. With larger cells, for example algal cells instead of bacterial cells, actual localization of the metal species of interest on or within the cell may be possible. We feel that this is one of the most promising applications for the microscopic epifluorescence detector.

ACKNOWLEDGEMENTS

We wish to thank Dr. Steve Chesler for his assistance in the design and fabrication of the bracket used to position capillary columns on the microscope stage.

REFERENCES

1 J. S. Thayer, G. J. Olson and F. E. Brinckman, *Environ. Sci. Technol.*, 18 (1984) 726.
2 W. P. Ridley, L. J. Dizikes and J. M. Wood, *Science (Washington, D.C.)*, 197 (1977) 329.
3 S. J. Blunden, L. A. Hobbs, P. J. Smith, in H. J. M. Bowen (Editor), *Environmental Chemistry*, The Royal Society of Chemistry, London, 1984, p. 49.
4 D. Lanigan, E. L. Weinberg, in J. J. Zuckerman (Editor), *ACS Advances in Chemistry Series 157*, American Chemical Society, Washington, DC, 1976.
5 S. Karpel, *Tin Its Uses*, 132 (1982) 14.
6 P. J. Smith and L. Smith, *Chem. Brit.*, 11 (1975) 208.
7 R. Cockcroft, *J. Inst. Wood Sci.*, 6 (1974) 2–8.
8 J. A. Montemarano and E.J. Dyckman, *J. Paint Technol.*, 47 (1975) 59.
9 C. J. Evans and P. J. Smith, *J. Oil Col. Chem. Assoc.*, 58 (1975) 160.
10 W. P. Neumann, *The Organic Chemistry of Tin*, Wiley Interscience, New York, 1970, 282 pp.
11 G. S. Ward, G. C. Cramm, P. R. Parrish, H. Trachman and A. Slesinger, in D. R. Branson and K. L. Dickson (Editors), *Aquatic Toxicology and Hazard Assessment, Fourth Conference, ASTM STP 737*, American Society for Testing and Materials, Philadelphia, PA, 1981, p. 183.
12 R. B. Laughlin and W. J. French, *Bull. Environ. Contam. Toxicol.*, 25 (1980) 802.
13 P. F. Seligman, *Fate and Effects of Organotin Antifouling Leachates in the Marine Environment, Progress Report for Energy Research and Development Office*, David H. Taylor Ship Research and Development Center, Bethesda, MD, 1984.
14 C. J. Sonderquist and D. G. Crosby, *Anal. Chem.*, 50 (1978) 1435.
15 R. S. Braman and M. A. Tompkins, *Anal. Chem.*, 51 (1979) 12.
16 R. J. Maguire and H. Huneault, *J. Chromatogr.*, 209 (1981) 458.
17 V. F. Hodge, S. L. Seidel and E. D. Goldberg, *Anal. Chem.*, 51 (1979) 1256.
18 H. A. Meinema, T. Burger-Wiesma, G. Versluis-de Hann and E. Ch. Gevers, *Environ. Sci. Technol.*, 12 (1978) 288.
19 A. O. Valkirs, P. F. Seligman, P. M. Stang, V. Homer, S. H. Lieberman, G. Vafa and C. A. Dooley, *Mar. Pollut. Bull.*, 17 (1986) 319.
20 C. L. Matthias, J. M. Bellama, G. J. Olson, F. E. Brinckman, *Environ. Sci. Technol.*, 20 (1986) 609.
21 R. J. Maguire, R. J. Tkacz, Y.K. Chau, G. A. Bengert and P. T. S. Wong, *Chemosphere*, 15 (1986) 253.
22 M. A. Unger, W. G. MacIntyre, J. Greaves and R. J. Hugget, *Chemosphere*, 15 (1986) 461.
23 K. L. Jewett and F. E. Brinckman, *J. Chromatogr. Sci.*, 9 (1981) 583.
24 S. J. Blunden and P. J. Smith, *J. Organometal. Chem.*, 226 (1982) 157.
25 Y. Arakawa and O. Wada, *Anal. Chem.*, 55 (1983) 1901.
26 T.-H. Yu and Y. Arakawa, *J. Chromatogr.*, 258 (1983) 189.
27 W. Langseth, *Talanta*, 31 (1984) 975.
28 H. M. Holz, *Worthwhile Facts About Fluorescence Microscopy*, Carl Zeiss, Oberkochen, 1975.
29 J. S. Ploem, *Z. Wiss. Mikrosk.*, 68 (1967) 129.

30 M. Sernetz and A. Thaer, *J. Microsc.*, 91 (1970) 43.
31 E. D. Cehelnik, K. D. Mielenz and R. A. Velapoldi, *J. Res. Natl. Bur. Stand. (U.S.)*, 79 (1975) 1.
32 R. P. W. Scott, in J. C. Giddings, E. Grushka, J. Cazes and P. R. Brown (Editors), *Small Bore Columns in Liquid Chromatography* (*Advances in Chromatography*, Vol. 22), Marcel Dekker, New York, 1983, pp. 247–294.

Journal of Chromatography, 410 (1987) 395–411
Elsevier Science Publishers B.V., Amsterdam — Printed in The Netherlands

CHROM. 19 936

DETERMINATION OF PRESERVATIVES IN COSMETIC PRODUCTS

I. THIN-LAYER CHROMATOGRAPHIC PROCEDURE FOR THE IDENTIFICATION OF PRESERVATIVES IN COSMETIC PRODUCTS

N. DE KRUIJF*, M. A. H. RIJK, L. A. PRANOTO-SOETARDHI and A. SCHOUTEN
TNO-CIVO Food Analysis Institute, Department of Toxicological Analysis, P.O. Box 360, 3700 AJ Zeist (The Netherlands)
(First received June 9th, 1987; revised manuscript received August 5th, 1987)

SUMMARY

A thin-layer chromatographic procedure is presented for the separation and identification of preservatives that are listed in the current EEC Council Directive on cosmetic products or have been permitted in the past.

The method consists of an extraction of acidified cosmetics with methanol, separation of the extracts by thin-layer chromatography on aluminium oxide and silica gel-coated plates using one developing solvent, and visualization of the preservatives on the plates using short-wavelength UV light and six detection reagents.

The retention behaviour and the detectability of 88 preservatives were investigated, of which 74 were characterized by this method. The preservatives in fourteen commercial cosmetic products were tentatively identified by the procedure described.

In general this method will permit the routine detection of preservatives in cosmetics in an approximate concentration of 0.1% (w/w).

INTRODUCTION

Preservation of cosmetic products is necessary in order to prevent alteration and degradation of the formulation through microbial contamination, and to protect the consumer. The use of a single preservative is sometimes insufficient to preserve the complex formulations in use. Therefore, combinations of several preservatives, which exhibit an enhanced antimicrobial effectiveness, are often used.

Many preservatives and mixtures of preservatives are commonly used in cosmetic products[1–5]. In 1982 the original European Economic Community (EEC) Council Directive on cosmetic products[6] was amended to add an annex (Annex VI) listing some 70 substances authorized for use as preservatives in the manufacture of cosmetic products[7]. In 1983 a Commission Directive was issued permitting the use of two additional preservatives in cosmetic products[8]. Recently Annex VI has been amended again[9], and now the EEC Council Directive on cosmetic products contains some 60 preservatives or groups of related preservatives that are either definitively or pro-

0021-9673/87/$03.50

visionally permitted for use at specified maximum concentrations. To verify compliance with this Directive, methods for the identification and the quantitation of these preservatives in cosmetic products are indispensable, and a study was undertaken to develop a screening procedure to identify the preservatives listed.

The screening method devised comprises the use of both thin-layer chromatography (TLC) and high-performance liquid chromatography (HPLC), and is suitable for the identification of many of the preservatives mentioned in the EEC Council Directive in cosmetic products, even if mixtures of preservatives are present in the sample. This paper describes a TLC procedure that enables the preliminary identification of many of the investigated preservatives. Confirmatory information on the identity of the preservatives is obtained by comparison of the results of this TLC procedure with those of an HPLC procedure, which will be described in a subsequent paper.

A number of TLC methods for the separation and identification of preservatives used in cosmetics have been described. The majority of these separations deal with only a limited number of preservatives[10–16], while others, which include a large number of preservatives[17–19], are not quite suitable for the identification of multicomponent preservative systems in cosmetic products, or require the use of various developing solvents in combination with a variety of detection systems and, as a result, are rather time-consuming.

This paper describes a relatively rapid screening procedure for the separation and tentative identification of preservatives using TLC. The preservatives covered by the procedure are those listed in the current EEC Council Directive on cosmetic products, or those permitted in the past but recently deleted from Annex VI of this Council Directive[9]. This TLC procedure could act as a preliminary screening, and any preservatives detected could then be confirmed and the amounts present determined using appropriate analytical methods.

The method consists of a simple but effective sample preparation procedure, separation by TLC on aluminium oxide and silica gel-coated plates using one developing solvent, and visualization of the preservatives on the plates by short-wavelength UV light and six detection reagents.

EXPERIMENTAL

Apparatus

Apparatus used included a short-wavelength UV light (Camag, Muttenz, Switzerland), a TLC developing tank lined with filter paper, spray apparatus and a Philips TUV 15 W UV light (Philips, Eindhoven, The Netherlands) without filter and mounted in a dark cabinet. Precoated silica gel 60 F254 TLC plates (20 × 20 cm, layer thickness 0.25 mm) with concentrating zone were obtained from E. Merck (Darmstadt, F.R.G.). Thin-layer plates (20 × 20 cm) precoated with aluminium oxide 1B-F were obtained from J.T. Baker Chemicals (Deventer, The Netherlands).

Reagents

All chemicals and solvents employed were of reagent-grade quality and were used without further purification. The developing solvent used was ethyl acetate–diisopropyl ether–96% ethanol–25% (w/v) ammonia (55:30:10:2). All preservatives were commercial grade and are listed in Table I.

TABLE I

PRESERVATIVE REFERENCE MATERIALS

*EEC No.**		*EEC name***	*Synonym*	*Maximum authorized concentration (%)***
I	*II*			
1.1	1.1	Benzoic acid		0.5
1.1	1.1	Benzoic acid, methylester	Methylbenzoate	0.5 (acid)
1.1	1.1	Benzoic acid, ethylester	Ethylbenzoate	0.5 (acid)
1.1	1.1	Benzoic acid, *n*-propylester	Propylbenzoate	0.5 (acid)
1.1	1.1	Benzoic acid, *n*-butylester	Butylbenzoate	0.5 (acid)
1.1	1.1	Benzoic acid, benzylester	Benzylbenzoate	0.5 (acid)
1.2	1.2	Propionic acid		2.0
1.3	1.3	Salicylic acid		0.5
1.4	1.4	Sorbic acid		0.6
1.5	1.5	Formaldehyde		0.2***
1.6	1.6	2,2′-Dihydroxy-3,3′,5,5′,6,6′-hexachlorodiphenylmethane	Hexachlorophene	0.1
1.7	1.7	*o*-Phenylphenol		0.2
1.7	1.7	*o*-Phenylphenol, sodium salt		0.2 (phenol)
1.8	1.8	Pyridine-1-oxide-2-thiol, zinc salt	Zinc pyrithione	0.5
1.9	1.9	Potassium metabisulphite		0.2 (SO_2)
1.10	1.10	Sodium iodate		0.1
1.11	1.11	1,1,1-Trichloro-2-methylpropanol-2	Chlorbutanol	0.5
1.12	1.12	*p*-Hydroxybenzoic acid		0.4
1.12	1.12	*p*-Hydroxybenzoic acid, methylester	Methylparaben	0.4 (acid)
1.12	1.12	*p*-Hydroxybenzoic acid, ethylester	Ethylparaben	0.4 (acid)
1.12	1.12	*p*-Hydroxybenzoic acid, *n*-propylester	Propylparaben	0.4 (acid)
1.12	1.12	*p*-Hydroxybenzoic acid, *n*-butylester	Butylparaben	0.4 (acid)
1.13	2.4	Dehydroacetic acid		0.6
1.13	2.4	Dehydroacetic acid, sodium salt		0.6 (acid)
1.14	2.5	Formic acid		0.5
1.15	2.8	1,6-Di(4-amidino-2-bromophenoxy)-*n*-hexane di(2-hydroxyethylsulphonate)	Dibromohexamidine, isethionate	0.1
1.18	2.13	Undecylenic acid		0.2
1.19	2.15	5-Amino-1,3-di(2-ethylhexyl)-hexahydro-5-methylpyrimidine	Hexetidine	0.1§

(*Continued on p. 398*)

TABLE I (*continued*)

*EEC No.**		*EEC name***	*Synonym*	*Maximum authorized concentration (%)***
I	*II*			
1.20	2.18	5-Bromo-5-nitro-1,3-dioxane	Bronidox	0.1§
1.21	2.19	2-Bromo-2-nitropropane-1,3-diol	Bronopol	0.1
1.22	2.24	2,4-Dichlorobenzyl alcohol		0.15
1.23	2.25	3,4,4′-Trichlorocarbanilide	Triclocarban	0.2
1.24	2.26	*p*-Chloro-*m*-cresol	PCMC	0.2
1.25	2.28	2,4,4′-Trichloro-2′-hydroxydiphenyl ether	Triclosan	0.3
1.26	2.32	*p*-Chloro-*m*-xylenol	PCMX	0.5
1.27	2.36	Imidazolidinyl urea	Germall 115	0.6
1.28	2.42	Polyhexamethylenediguanide hydrochloride		0.3
1.29	2.43	Phenoxyethanol		1.0
1.30	2.44	Hexamethylenetetramine	Methenamine	0.15
1.31	2.48	1-(3-Chloroallyl)-3,5,7-triaza-1-azonia adamantane chloride	Dowicil 200	0.2
1.32	2.49	1-Imidazolyl-1-(4-chlorophenoxy)-3,3-dimethylbutan-2-one	Climbazol	0.5
1.33	2.50	Dimethylol-dimethylhydantoin	DMDMH	0.6
1.34	2.51	Benzyl alcohol		1.0
1.35	2.57	1-Hydroxy-4-methyl-6-(2,4,4-trimethylpentyl)-2-pyridone, monoethanolamine salt	Octopirox	0.5§§
1.36	2.59	1,2-Dibromo-2,4-dicyanobutane		0.1
1.37	2.20	3,3′-Dibromo-5,5′-dichloro-2,2′-dihydroxydiphenylmethane	Bromophen	0.1
1.38	2.37	4-Isopropyl-3-methylphenol		0.1
1.39	2.45	5-Chloro-2-methyl-4-isothiazoline-3-one + 2-methyl-4-isothiazoline-3-one, with magnesium chloride and magnesium nitrate	Kathon CG	0.003
2.1	2.2	Boric acid		3.0***
2.2	2.3	Glycerol-*p*-chlorophenylether	Chlorphenesin	0.5
2.3	2.9	1,3-Di(4-amidino-2-bromophenoxy)-*n*-propane, di(2-hydroxyethylsulphonate)	Dibromopropamidine, isethionate	0.1
2.4	2.55	Alkyl (C_{12}–C_{22})trimethylammonium bromide		0.1
2.5	2.58	3-Heptyl-2-(3-heptyl-4-methyl-4-thiazolin-2-ylidenemethyl)-4-methylthiazolinium iodide	Pionin	0.002
2.6	2.60	4,4-Dimethyl-1,3-oxazolidine		0.1
2.7	2.18	5-Bromo-5-nitro-1,3-dioxane	Bronidox	0.1§§
2.8	2.13	Undecylenic acid, monoethanolamide		0.2 (acid)

2.8	2.13	Undecylenic acid, polydiethanolamide		0.2	(acid)
2.8	2.13	Undecylenic acid, monoethanolamide sulphosuccinate, disodium salt		0.2	(acid)
2.9	2.17	2-Benzyl-4-chlorophenol	Chlorophene	0.2	
2.10	2.38	N-Methylolchloracetamide		0.3	
2.11	2.47	Bis(N-oxopyridyl-2-thio)aluminium camphosulphonate	Pyrithione aluminium camsilate	0.2	
2.12	2.30	N-(Trichloromethylthio)-4-cyclohexene-1,2-dicarboximide	Captan	0.06	
2.13	2.41	Bis(pyridine-1-oxide)-2,2′-disulphide	Pyrithione disulphide	0.2	
2.14	2.56	Phenoxypropanol		1.0	
2.15	2.53	Diisobutyl-phenoxy-ethoxy-ethyl-dimethylbenzylammonium chloride	Benzethonium chloride	0.1	
2.16	2.54	Alkyl (C_8–C_{18})dimethylbenzylammonium chloride	Benzalkonium chloride	0.25	
2.18	2.15	5-Amino-1,3-di(2-ethylhexyl)-hexahydro-5-methylpyrimidine	Hexetidine	0.1§§	
2.19	2.6	*p*-Hydroxybenzoic acid, benzylester	Benzylparaben	0.1	(acid)
2.20	2.7	1,6-Di(4-amidinophenoxy)-*n*-hexane, di(2-hydroxyethylsulphonate)	Hexamidine, isethionate	0.1	
2.21	2.16	Benzylformal		0.2	
2.22	2.22	Chloracetamide		0.3	
2.23	2.52	Dodecylguanidine acetate		0.1§§	
2.24	2.31	1,6-Di(N-p-chlorophenyl-N′-diguanido)-*n*-hexane, digluconate	Chlorhexidine, digluconate	0.3	
2.24	2.31	1,6-Di(N-p-chlorophenyl-N′-diguanido)-*n*-hexane, dihydrochloride	Chlorhexidine · 2HCl	0.3	
2.25	2.35	Tri(*β*-hydroxyethyl)hexahydrotriazine	Triazinetriethanol	0.2	
–	2.1	6-Acetoxy-2,4-dimethyl-1,3-dioxane	Dimethoxane	0.2	
–	2.12	Sorbic acid, isopropylester		0.6	(acid)
–	2.14	*d*-Usnic acid		0.2	
–	2.14	*l*-Usnic acid		0.2	
–	2.21	Tetrabromo-*o*-cresol		0.3	
–	2.23	3,4-Dichlorobenzylalcohol		0.15	
–	2.27	4,4′-Dichloro-3-trifluoromethylcarbanilide	Halocarban	0.3	
–	2.29	5,5′-Dichloro-2,2′-dihydroxydiphenylmethane	Dichlorophene	0.2	
–	2.33	Dichloro-*m*-xylenol	DCMX	0.1	
–	2.34	8-Hydroxyquinoline		0.3	
–	2.39	Monomethylol-dimethylhydantoin	MDMH	0.2§§§	
–	2.40	Pyridine-1-oxide-2-thiol, sodium salt	Sodium pyrithione	0.5	
–	2.46	2-Hydroxypyridine-N-oxide	Hydroxypyridinon	0.5	

* According to EEC Commission Directive 86/199/EEC of 26 March 1986 (I); according to EEC Council Directive 82/368/EEC of 17 May 1982 and EEC Commission Directive 83/496/EEC of 22 September 1983 (II).

** According to EEC Commission Directive 86/199/EEC of 26 March 1986; for preservatives not mentioned in this directive: according to EEC Council Directive 82/368/EEC of 17 May 1982 and EEC Commission Directive 83/496/EEC of 22 September 1983.

*** Except for products for oral hygiene.

§ For products rinsed off after use.

§§ For products not rinsed off after use.

§§§ Expressed as free formaldehyde or theoretically available formaldehyde.

Reference solutions, each containing 1 mg/ml of a mixture of methanol and 4 *M* formic acid (19:1) were prepared for all preservatives excepting *l*-usnic acid, *d*-usnic acid, zinc pyrithione, germall·115, potassium metabisulphite and sodium iodate, where solutions (1 mg/ml) were used in chloroform (*l*-usnic acid, *d*-usnic acid and zinc pyrithione), in a mixture of 70% aqueous methanol and 4 *M* formic acid (19:1) (germall 115) or in a mixture of 90% aqueous methanol and 4 *M* formic acid (19:1) (potassium metabisulphite and sodium iodate).

The following detection reagents were used: bromocresol green spray reagent (R1), Gibbs' spray reagent (R2), Dragendorff's reagent (R3), Millon's reagent (R4), Purpald spray reagent (R5) and ammoniacal silver nitrate spray reagent (R6).

Samples

A selection of fourteen cosmetic products, representing many different cosmetic sample types, was purchased from local outlets.

Preparation of samples

A test portion of *ca.* 1 g of sample was weighed into a 50-ml glass tube with screw cap. After addition of 0.5 ml of 4 *M* formic acid and 9.5 ml of methanol the tube was closed and vigorously shaken for 1 min. If required, the mixture was gently heated in a water-bath maintained at 60°C, to melt any lipid phase and to facilitate the extraction of preservatives into the methanol phase.

The extract was stored overnight. If necessary the mixture was filtered using a disposable filter holder. A 2-ml aliquot of the clear sample solution was pipetted into a 5-ml sample vial.

Thin-layer chromatography

Aliquots of 10 μl of each of the preservative reference solutions and aliquots of 25 μl of each of the sample solutions were applied at a starting line in the concentrating zone of a series of five TLC plates precoated with silica gel. To facilitate application of the solutions, the TLC plates were placed on a hot plate covered with an aluminium plate of 20 × 20 cm and a thickness of *ca.* 6 mm to obtain a uniform heat distribution. The surface temperature of the hot plate was regulated at *ca.* 60°C. In the same manner, 10 μl of each of the reference solutions and 25 μl of each of the sample solutions were applied to a TLC plate precoated with aluminium oxide. In addition, 10 μl of a 0.1% (w/v) solution of benzylparaben (reference substance) in a mixture of methanol and 4 *M* formic acid (19:1) were applied to each TLC plate.

A developing tank was lined with filter paper, and 100 ml of the developing solvent were placed in it. The tank was allowed to equilibrate for 20 min at room temperature (20–22°C) before use. Each TLC plate was placed in the tank and allowed to develop at room temperature to a distance of *ca.* 15 cm from the baseline. Then the plates were removed from the tank and thoroughly dried by means of a stream of hot air.

Visualization of preservatives

The developed dried plates were first examined with short-wavelength UV light. The spots thus obtained were outlined with a pencil for future location. Subsequently the preservatives were visualized in the chromatograms by the following six detection reagents.

Reagent 1: bromocresol green spray reagent. A 0.06% (w/v) solution of bromocresol green (3,3',5,5'-tetrabromo-*m*-cresolsulphonphthalein) in ethanol was prepared daily. The dried TLC plate was sprayed with the reagent until a uniform blue background was obtained. Thus acids appeared as yellow spots and basic compounds, such as quaternary ammonium compounds, as dark blue spots.

Reagent 2: Gibbs' spray reagent. A 0.4% (w/v) solution of 2,6-dichloroquinonechloroimide in methanol was prepared daily (spray reagent A). In addition a 10% (w/v) aqueous solution of sodium carbonate was prepared (spray reagent B). The TLC plate was successively sprayed with spray reagent A and spray reagent B. Thus phenolic compounds, with the exception of the parabens, appeared as blue spots on a grey background.

Reagent 3: Dragendorff's reagent. To a solution containing 1.7 g of bismuth nitrate hydrate in 20 ml of acetic acid were added 80 ml of water, 65.0 g of potassium iodide dissolved in 200 ml of water, and 200 ml of acetic acid. The solution was made up to 1 l with water (solution A). In addition a solution containing 20.0 g of barium chloride dihydrate in 100 ml of water was prepared (solution B). A spray reagent was prepared immediately before use by mixing two portions of solution A with one portion of solution B. The TLC plate was sprayed with the mixture obtained. Thus quaternary ammonium compounds appeared as orange spots on a light yellow background.

Reagent 4: Millon's reagent. A ready-made solution of mercury(II) nitrate (Merck Reagent No. 9026) was obtained from E. Merck. Because of the toxicity of the reagent the following procedure was applied. A woollen paint roller (length *ca.* 10 cm, O.D. *ca.* 3.5 cm, thickness of wool–layer 2–3 mm) was dipped into the reagent and was rolled over the TLC plate until the plate was evenly wetted. Thus *p*-hydroxybenzoic acid and its esters, as well as salicylic acid, appeared as red spots on a white background. Some other compounds containing hydroxyl groups appeared as yellow spots.

Reagent 5: Purpald spray reagent. A 1% (w/v) solution of 4-amino-3-hydrazino-5-mercapto-1,2,4-triazole (AHMT) in 1 *M* sodium hydroxide was prepared. The TLC plate was sprayed with the reagent. In this manner aldehydes and aldehyde-releasing compounds appeared as violet spots on a white-yellow background. Some compounds containing hydroxyl groups were revealed by yellow or orange spots.

Reagent 6: ammoniacal silver nitrate spray reagent. To a solution containing 1.7 g of silver nitrate in 10 ml of water, 5 ml of a 25% (w/v) ammonium hydroxide solution were added. The solution was made up to 200 ml with acetone. The dried TLC plate was irradiated for 30 min with a Philips TUV 15 W UV light at a distance of *ca.* 20 cm. The plate was subsequently sprayed with detector reagent and again irradiated with UV light for 30 min. Thus halogenated compounds appeared as black spots on a light grey background. Application of this reagent on TLC plates coated with aluminium oxide resulted in an almost colourless background. In this manner an optimum detection limit for the investigated preservatives was obtained.

The hR_F values for the located spots were calculated and the colours recorded. It was checked whether the development characteristics of the reference substance benzylparaben were affected by variations in the chromatographic conditions and, if so, allowance was made for this when calculating the hR_F values. To identify tentatively the preservatives in cosmetic products the hR_F value, the behaviour under

TABLE II

R_F VALUES, UV ABSORPTION AND REACTION TO DETECTION REAGENTS OF PRESERVATIVES ON SILICA GEL AND ALUMINIUM OXIDE-COATED TLC PLATES

Developing solvent: ethyl acetate–diisopropyl ether–96% ethanol–25% (w/v) ammonia (55:30:10:2); detection reagents: R1 = bromocresol green spray reagent; R2 = Gibbs' reagent; R3 = Dragendorff's reagent; R4 = Millon's reagent; R5 = Purpald spray reagent; R6 = ammoniacal silver nitrate spray reagent.

*EEC No.**		*Preservative*	*Silica gel plates*							*Aluminium oxide plates*		
I	*II*		$R_F \cdot 100$	*UV*	*R1*	*R2*	*R3*	*R4*	*R5*	$R_F \cdot 100$	*UV*	*R6*
1.1	1.1	Benzoic acid	1	+	Yellow	–	–	–	–	0	+	–
1.1	1.1	Methylbenzoate	–	–	–	–	–	–	–	–	–	–
1.1	1.1	Ethylbenzoate	–	–	–	–	–	–	–	–	–	–
1.1	1.1	Propylbenzoate	–	–	–	–	–	–	–	–	–	–
1.1	1.1	Butylbenzoate	–	–	–	–	–	–	–	–	–	–
1.1	1.1	Benzylbenzoate	66	+	–	–	–	–	–	65	+	–
1.2	1.2	Propionic acid	–	–	–	–	–	–	–	–	–	–
1.3	1.3	Salicylic acid	2	+	Yellow	Blue	–	Orange	–	0	+	Yellow
1.4	1.4	Sorbic acid	0	+	Yellow	–	–	–	Violet	0	+	Yellow
1.5	1.5	Formaldehyde	–	–	–	–	–	–	–	–	–	–
1.6	1.6	Hexachlorophene**	17	+	Yellow	Blue	–	W.*** Yellow	–	6	+	Black
			3	+	–	Blue	–	–	–	0	+	Black
1.7	1.7	*o*-Phenylphenol	65	+	–	Blue	–	Orange	–	61	+	–
1.7	1.7	*o*-Phenylphenol, sodium salt	65	+	–	Blue	–	Orange	–	61	+	–
1.8	1.8	Zinc pyrithione	5–15	+	–	Yellow	–	–	–	0–11	+	Pink
1.9	1.9	Potassium metabisulphite	–	–	–	–	–	–	–	–	–	–
1.10	1.10	Sodium iodate	–	–	–	–	–	–	–	–	–	–
1.11	1.11	Chlorbutanol	–	–	–	–	–	–	–	60	–	Black
1.12	1.12	*p*-Hydroxybenzoic acid	1	+	Yellow	Blue	–	Red	–	0	+	–
1.12	1.12	Methylparaben	53	+	–	–	–	Red	–	25	+	–
1.12	1.12	Ethylparaben	54	+	–	–	–	Red	–	29	+	–
1.12	1.12	Propylparaben	55	+	–	–	–	Red	–	31	+	–
1.12	1.12	Butylparaben	56	+	–	–	–	Red	–	31	+	–
1.13	2.4	Dehydroacetic acid	3	+	–	–	–	–	–	0	+	–
1.13	2.4	Dehydroacetic acid, sodium salt	3	+	–	–	–	–	–	0	+	–
1.14	2.5	Formic acid	–	–	–	–	–	–	–	–	–	–
1.15	2.8	Dibromohexamidine, isethionate	–	–	–	–	–	–	–	0	+	Brown

1.18	2.13	Undecylenic acid	0	–	Yellow	–	–	–	White	–	–	–
1.19	2.15	Hexetidine	47	–	Blue	Brown	Orange	–	White	69	–	W.brown
1.20	2.18	Bronidox	62	–	–	–	–	–	W.yellow	62	–	Black
1.21	2.19	Bronopol	43	+	–	Orange	–	–	Violet	4	–	Black
1.22	2.24	2,4-Dichlorobenzylalcohol	–	–	–	–	–	–	–	60	–	Black
1.23	2.25	Triclocarban	61	+	–	–	–	W.yellow	–	57	+	Black
1.24	2.26	*p*-Chloro-*m*-cresol	60	–	–	Blue	–	Red	–	53	–	Black
1.25	2.28	Triclosan	65	+	–	Blue	–	–	Orange	44	+	Black
1.26	2.32	*p*-Chloro-*m*-xylenol	63	+	–	Blue	–	Violet	Orange	53	+	Black
1.27	2.36	Germall 115	0	–	–	–	–	–	Violet	–	–	–
1.28	2.42	Polyhexamethylenediguanide hydrochloride	–	–	–	–	–	–	–	0	–	Black
1.29	2.43	Phenoxyethanol	54	–	–	–	–	Yellow	–	53	+	–
1.30	2.44	Methenamide	–	–	–	–	–	–	–	7	–	White
1.31	2.48	Dowicil 200	3	–	–	Violet	Orange	–	Violet	28	–	Black
										0	–	Black
1.32	2.49	Climbazol	53	+	Violet	W. blue	Orange	–	–	57	+	Black
1.33	2.50	Dimethylol-dimethylhydantoin	25	–	–	Brown	–	–	Violet	–	–	–
1.34	2.51	Benzylalcohol	–	–	–	–	–	–	–	–	–	–
1.35	2.57	Octopirox	2	–	Blue	Blue	–	Pink	–	0	+	–
			7	+	–	–	–	–	–			
1.36	2.59	1,2-Dibromo-2,4-dicyanobutane	–	–	–	–	–	–	–	65	+	Brown
1.37	2.20	Bromophen	27	+	–	Blue	–	Yellow	Orange	8	+	Black
1.38	2.37	4-Isopropyl-3-methylphenol	64	–	–	–	–	W.orange	–	60	+	Brown
1.39	2.45	Kathon CG	–	–	–	–	–	–	–	49	+	Black
2.1	2.2	Boric acid	–	–	–	–	–	–	–	–	–	–
2.2	2.3	Chlorphenesin	30	+	–	White	–	Orange	–	14	+	Black
2.3	2.9	Dibromopropamidine, isethionate	–	–	–	–	–	–	–	0	+	Brown
2.4	2.55	Alkyl(C_{12}-C_{22})trimethylammonium bromide	0	–	Blue	–	Orange	–	–	0	–	Black
2.5	2.58	Pionin	0	+	–	–	Orange	–	–	2	+	Grey
2.6	2.60	4,4-Dimethyl-1,3-oxazolidine	–	–	–	–	–	–	–	–	–	–
2.7	2.18	Bronidox	62	–	–	–	–	–	W.yellow	62	–	Black
2.8	2.13	Undecylenic acid, monoethanolamide	28	–	–	–	–	–	White	–	–	–
2.8	2.13	Undecylenic acid, polydiethanolamide	20	–	–	–	–	–	White	–	–	–
			5	–	–	–	–	–	White			

(*Continued on p. 404*)

TABLE II (*continued*)

*EEC No.**		*Preservative*	*Silica gel plates*							*Aluminium oxide plates*		
I	*II*		$R_F \cdot 100$	*UV*	*R1*	*R2*	*R3*	*R4*	*R5*	$R_F \cdot 100$	*UV*	*R6*
2.8	2.13	Undecylenic acid, monoethanolamide sulphosuccinate, disodium salt	28	–	–	–	–	–	White	–	–	–
2.9	2.17	Chlorophene	65	+	–	Blue	–	Yellow	Orange	61	+	Black
2.10	2.38	N-Methylolchloracetamide	20	–	–	W.brown	–	–	Violet	13	–	Black
2.11	2.47	Pyrithione aluminium camsilate	66	+	–	–	Orange	–	–	0	+	White
			24	+	–	W.yellow	Orange	–	–	3	+	White
			8	+	–	–	–	–	–	30	+	White
			3	+	–	Yellow	–	–	–	59	+	White
			5	+	–	–	–	–	–			
2.12	2.30	Captan	10–65	–	–	Brown	–	–	–	0–53	–	Black
			68	–	–	Brown	–	–	–	65	–	Black
2.13	2.41	Pyrithione disulphide	3	+	–	Yellow	–	–	–	1–11	+	Yellow
			24	+	–	–	–	–	–			
			6	+	–	–	–	–	–			
2.14	2.56	Phenoxypropanol	60	–	–	–	–	Yellow	–	57	+	W.brown
2.15	2.53	Benzethonium chloride	0	+	Blue	–	Orange	Red	–	0	+	Black
2.16	2.54	Benzalkonium chloride	0	+	Blue	–	Orange	–	Violet	0	+	Black
2.18	2.15	Hexetidine	47	–	Blue	Brown	Orange	–	White	69	–	W.brown
2.19	2.6	Benzylparaben	55	+	–	–	–	Red	–	30	+	–
2.20	2.7	Hexamidine, isethionate	–	–	–	–	–	–	–	0	+	Brown
2.21	2.16	Benzylformal	–	–	–	–	–	–	–	–	–	–

2.22	2.22	Chloracetamide	–	–	–	–	–	–	–	31	–	Black
2.23	2.52	Dodecylguanidine acetate	0	–	Blue	–	Orange	–	–	2	+	–
2.24	2.31	Chlorhexidine, digluconate	0	+	–	–	Orange	–	–	0	+	Black
2.24	2.31	Chlorhexidine.2HCl	0	+	–	–	Orange	–	–	0	+	Black
2.25	2.35	Triazinetriethanol	1	–	–	Brown	–	–	Violet	–	–	–
–	2.1	Dimethoxane	–	–	–	–	–	–	–	–	–	–
–	2.12	Sorbic acid, isopropylester	–	–	–	–	–	–	–	67	+	–
–	2.14	*d*-Usnic acid	12	+	–	Grey	–	Yellow	–	0	+	Brown
–	2.14	*l*-Usnic acid	12	+	–	Grey	–	Yellow	–	0	+	Brown
–	2.21	Tetrabromo-*o*-cresol	18	+	–	W.blue	–	–	Orange	2	+	Black
–	2.23	3,4-Dichlorobenzylalcohol	–	–	–	–	–	–	–	60	–	Black
–	2.27	Halocarban	60	+	–	–	–	W.yellow	–	58	+	Black
–	2.29	Dichlorophene	46	+	White	Blue	–	Yellow	Orange	9	+	Black
			11	+	–	Blue	–	Yellow	Orange			
–	2.33	Dichloro-*m*-xylenol	61	+	–	–	–	–	–	28	+	Black
–	2.34	8-Hydroxyquinoline	2–25	+	–	W.blue	–	Orange	Pink	0–10	+	Black
–	2.39	Monomethylol-dimethylhydantoin	41	–	–	Grey	–	–	–	13	–	White
–	2.40	Sodium pyrithione	3	+	–	Yellow	–	–	–	2	+	–
			6	+	–	–	–	–	–	13	+	White
			9	+	–	–	–	–	–			
			24	+	–	Yellow	–	–	–			
–	2.46	Hydroxypyridinon	0	+	–	Violet	–	Yellow	–	0	+	–

* According to EEC Commission Directive 86/199/EEC of 26 March 1986 (I); according to EEC Council Directive 82/368/EEC of 17 May 1982 and EEC Commission Directive 83/496/EEC of 22 September 1983 (II).

** In cases where more than one spot is observed in a chromatogram obtained for a preservative reference material, the results are presented in order of decreasing intensity.

*** W = Weak spot.

UV radiation and the colour of each of the spots in a chromatogram obtained for a cosmetic sample were then compared with the results obtained for reference substances under similar conditions.

RESULTS AND DISCUSSION

All preservatives mentioned in the current EEC Council Directive on cosmetic products, except thiomersal, phenylmercury and germall II, of which no reference material was available, were examined by the described procedure. In addition, a number of preservatives permitted previously but now deleted from the Directive were included in the investigation. In these experiments, *ca.* 10 μg of each of the preservatives were applied to the TLC plates. The results obtained (Table II) are dependent on the amount of the preservatives spotted on the plates. If, for example, 10 μg of 4-isopropyl-3-methylphenol is applied to a TLC plate, no visible spot will be obtained after development of the plate and spraying with detection reagent 2; on the other hand, a clear orange spot is observed when 50 μg are used.

Using the TLC screening procedure most of the investigated preservatives are detectable by one or more of the applied visualization procedures. Those that are not have been included in Table II to demonstrate that the presence of such compounds does not interfere with the determination of those that are detected.

In general this method will permit the routine detection of preservatives present in cosmetics in an approximate concentration of 0.1% (w/w), while preservatives that produce strongly or distinctively coloured spots (*e.g.* parabens) can be readily detected at even lower levels. For preservatives that produce weakly or indistinctly coloured spots only higher concentrations are detectable by this TLC procedure. A higher sensitivity can be achieved by applying more of the sample solution onto the TLC plate, although detection will then often be hampered by the increasing influence of interferences present in the cosmetic products. The development of an additional, more rigorous sample clean-up procedure would be necessary to facilitate the detection of some of these preservatives on the TLC plates.

For the identification of preservatives in unknown cosmetic formulations, the following procedure proved to be most effective. The sample solutions are submitted to the complete TLC screening procedure. The hR_F values of the spots in the chromatograms obtained are calculated. Unknown preservatives are then tentatively identified by comparison of the calculated hR_F value and the colour of the spot observed with results obtained for reference substances under similar conditions (Table II). To confirm the identity of preservatives possibly detected in cosmetic products, the TLC procedure is partly repeated, using plates on which sample solutions are spotted together with standards of the preservatives tentatively identified in these samples, in combination with appropriate detection systems.

This procedure was applied to a wide variety of cosmetic products containing unknown preservatives. The results obtained and the preliminary conclusions based on these results are presented in Table III.

Whenever possible, it is of course highly desirable that the presence of preservatives in cosmetic samples as indicated by the TLC procedure be confirmed by an additional independent differentiation method. For this purpose an HPLC procedure has been developed that will be described in a subsequent paper. A final

TABLE III

QUALITATIVE TLC DETERMINATION OF PRESERVATIVES IN COMMERCIAL COSMETIC PRODUCTS

Developing solvent: ethyl acetate–diisopropyl ether–96% ethanol–25% (w/v) ammonia (55:30:10:2); detection reagents: R1 = bromocresol green spray reagent; R2 = Gibbs' reagent; R3 = Dragendorff's reagent; R4 = Millon's reagent; R5 = Purpald spray reagent; R6 = ammoniacal silver nitrate spray reagent.

Cosmetic product	*Results obtained using silica gel-coated TLC plates*							*Results obtained using alumina-coated TLC plates*			*Preliminary conclusions*
	$R_F \cdot 100$	*UV*	*R1*	*R2*	*R3*	*R4*	*R5*	$R_F \cdot 100$	*UV*	*R6*	
Body lotion	1	–	–	–	Orange	–	–				Cationic compound
	53	+	–	–	–	Red	–	26	+	–	Parabens
	73	+	–	–	–	–	–				Unknown compound
	77	–	Blue	–	Yellow	–	Violet				Basic cosmetic constituent
Baby oil	0	–	Yellow	–	–	–	–	–	–	–	Unknown acidic compound
	79	–	Blue	–	–	–	–	–	–	–	Basic cosmetic constituent
Night cream	2	+	Yellow	–	Orange	Red	–	–	–	–	*p*-Hydroxybenzoic acid*, cationic compound*, or unknown compound
	52	+	–	–	–	Red	–	27	+	–	Parabens
	75	–	–	–	–	–	Violet	–	–	–	Basic cosmetic constituent
Tinted day cream	1	+	Yellow	–	–	Red	–	–	–	–	*o*- Or *p*-hydroxybenzoic acid
	3	–	Blue	–	–	–	–	–	–	–	Cationic compound*
	38	+	–	–	–	–	–	–	–	–	Unknown compound
	53	+	–	–	–	Red	–	26	+	–	Parabens
	56	+	–	–	–	Red	–	26	+	–	Parabens
	73	+	Blue	–	Orange	Orange	–	65	+	–	4-Isopropyl-3-methylphenol
Hand cream	0	–	Yellow	–	Orange	–	–	–	–	–	Unknown compound
	4	–	Blue	–	Orange	–	–	–	–	–	Unknown compound
	7	–	Blue	–	Orange	–	–	–	–	–	Unknown compound

(*Continued on p. 408*)

TABLE III (*continued*)

Cosmetic product	*Results obtained using silica gel-coated TLC plates*							*Results obtained using alumina-coated TLC plates*			*Preliminary conclusions*
	$R_F \cdot 100$	*UV*	*R1*	*R2*	*R3*	*R4*	*R5*	$R_F \cdot 100$	*UV*	*R6*	
	10	–	Blue	–	Orange	–	–	–	–	–	Unknown compound
	18	–	Blue	–	Orange	–	–	–	–	–	Unknown compound
	38	–	–	–	–	–	Violet	–	–	–	Unknown compound
	48	+	–	–	–	Red	–	27	+	–	Parabens
	75	–	Blue	–	–	–	Violet	–	–	–	Basic cosmetic constituent
Toothpaste	2	+	Yellow	–	–	–	–	5	–	Black	Unknown halogenated compound
Foot powder	0	–	–	–	Orange	Red	–	0	–	Brown	Benzethonium chloride*
	75	–	Blue	–	–	–	Violet	–	–	–	Basic cosmetic constituent
Face powder	0	+	Yellow	–	–	–	–	–	–	–	Benzoic acid*
	53	+	–	–	–	Red	–	29	+	–	Parabens
	57	+	–	–	–	Red	–				Parabens
	74	+	–	–	–	–	–	67	+	–	Benzylbenzoate*
	77	–	+	–	–	–	Violet	–	–	–	Basic cosmetic constituent
Deodorant	0	–	–	–	Orange	–	–	0	–	Brown	Unknown compound
	69	–	Blue	–	–	–	Violet	–	–	–	Basic cosmetic constituent
	72	+	–	–	–	–	–	–	–	–	Unknown compound
	75	–	Blue	–	Orange	–	Violet	–	–	–	Basic cosmetic constituent

Eau de toilette	73	+	–	–	–	–	–	67	+	–	Benzylbenzoate
	77	–	–	–	–	–	Yellow	–	–	–	Unknown compound
Toilet soap	0–7	+	Yellow	–	Orange	–	W.violet**	2–6	+	White	Basic cosmetic constituent
	21	–	–	Blue	–	–	W.violet	0	–	Black	Hexachlorophene or bromophene*
	41–59	+	–	–	–	–	W.violet	–	–	–	Basic cosmetic constituent
Eye make-up	0	–	–	–	W.orange	–	–	–	–	–	Unknown compound
	52	+	–	–	–	Red	–	29	+	–	Parabens
	56	+	–	–	–	Red	–				Parabens
	63	+	–	–	–	–	–	63	+	White	Benzylbenzoate*
	76	–	Blue	–	W.orange	–	Violet	–	–	–	Basic cosmetic constituent
Lipstick	2	+	Yellow	Red	Red	Red	Pink	1	+	–	Basic cosmetic constituent
	31	+	Blue	Grey	–	–	Pink				Unknown compound
	49	+	–	–	–	Red	Pink	31	+	–	Parabens
	57–77	+	Blue	–	Orange	Yellow	Pink	62	+	–	Basic cosmetic constituent
Shampoo	1	+	Yellow	Blue	Orange	Red	–	0	+	Black	*p*-Hydroxybenzoic acid*, cationic* and halogenated compound
	6	–	Blue	–	Orange	–	–	–	–	–	Unknown compound
	9	–	Blue	–	Orange	–	–	–	–	–	Unknown compound
	11	+	–	–	–	Red	–	6	+	Brown	Unknown hydroxyl group containing compound
	17	–	–	Brown	Orange	–	Violet				Undecylenic acid polydiethanolamide
	21	–	Blue	Brown	–	–	Violet				Undecylenic acid polydiethanolamide
	49	+	–	–	–	Red	–	29	+	–	Parabens
	67	+	–	Blue	–	–	–	61	+	–	*o*-Phenylphenol

* Conclusion not clear, but the presence of this compound cannot be excluded.
** W = Weak spot.

identification of the preservatives present in cosmetic samples is achieved by an independent comparison of the results obtained for a cosmetic product by means of the TLC procedure and the HPLC procedure with the results obtained for reference substances.

As the investigated TLC procedure requires the use of only one developing solvent, the hR_F values of the spots in all chromatograms obtained using silica gel-coated plates in combination with various specific detection reagents can be directly compared. This is a significant advantage over procedures that involve various developing solvents[17]. In this manner the interpretation of the chromatograms obtained is considerably facilitated, and differentiation between preservatives and other cosmetic constituents can readily be made. In addition, this TLC procedure involves visualization of the preservatives by means of various detection reagents that are specific for functional groups. This enables the detection of most preservatives according to their chemical class, *i.e.* acids, phenolics, cationics, parabens, halogenated compounds, aldehydes and aldehyde-releasing compounds.

Although this TLC screening procedure can contribute a great deal to the identification of many of the investigated preservatives, it appeared to be inadequate to obtain a satisfactory separation of all 74 detectable preservatives. For a number of the detectable preservatives, for which hR_F values were obtained ranging from 0 to 10 using silica gel-coated plates, only poor separation was achieved. In addition, the visualization of these preservatives was sometimes obscured by interferences. When combinations of these preservatives are present in a cosmetic product, only the chemical class of the preservatives can be established on the basis of the characteristic colour reactions obtained by means of the specific detection reagents. If, for example, no substantial interferences are present at the starting points on the silica gel-coated plates, acid preservatives and quaternary ammonium salts are clearly recognizable, although these compounds cannot be determined individually. Halogenated compounds can also be detected at the origin, but their visualization is often obscured by interferences.

For some halogenated preservatives with hR_F values varying from 50 to 60 inadequate separation was obtained on alumina-coated plates. To obtain a satisfactory separation of these preservatives, which is necessary to enable the identification of all these specific compounds, the application of additional developing solvents should be considered.

ACKNOWLEDGEMENTS

Thanks are due to the Commission of the European Communities (Directorate General for the Environment, consumer Protection and Nuclear Safety) for permission to publish this work, and to Mr. J. L. Collin for continued interest and support.

REFERENCES

1 E. L. Richardson, *Cosmet. Toiletries*, 96 (1981) 91.
2 K. H. Wallhäusser, in J. J. Kabara (Editor), *Cosmetic and Drug Preservation*, Marcel Dekker, New York, 1984, p. 605.
3 B. Croshaw, *J. Soc. Cosmet. Chem.*, 28 (1977) 3.
4 R. A. Cowen and B. Steiger, *Cosmet. Toiletries*, 92 (1977) 15.

5 W. E. Rosen and P. A. Berke, *J. Soc. Cosmet. Chem.*, 24 (1973) 663.
6 *Council Directive 76/768/EEC, Off. J. Eur. Commun.*, L 262 (1976) 169.
7 *Council Directive 82/368/EEC, Off. J. Eur. Commun.*, L 167 (1982) 1.
8 *Commission Directive 83/496/EEC, Off. J. Eur. Commun.*, L 275 (1983) 20.
9 *Commission Directive 86/199/EEC, Off. J. Eur. Commun.*, L 149 (1986) 38.
10 M. B. Graber, I. I. Domsky and M. E. Ginn, *J. Am. Oil Chem. Soc.*, 46 (1969) 529.
11 H. König and M. Schüller, *Fresenius' Z. Anal. Chem.*, 294 (1979) 36.
12 H. Gottschalck and T. Oelschläger, *J. Soc. Cosmet. Chem.*, 28 (1977) 497.
13 J. W. Copius-Peereboom and H. W. Beekes, *J. Chromatogr.*, 14 (1964) 417.
14 D. S. Ryder, *J. Soc. Cosmet. Chem.*, 25 (1974) 535.
15 R. Matissek and A. Dross, *Dtsch. Lebensm. Rundsch.*, 79 (1983) 269.
16 C. H. Wilson, *J. Soc. Cosmet. Chem.*, 26 (1975) 75.
17 H.-J. Schmahl and E. Hieke, *Fresenius' Z. Anal. Chem.*, 304 (1980) 398.
18 D. H. Liem, *Cosmet. Toiletries*, 92 (1977) 59.
19 G. Richard, P. Gataud, J. C. Arnaud and P. Boré, in P. Boré (Editor), *Cosmetic Analysis*, Marcel Dekker, New York, 1985, Ch. 7, p. 157.

Journal of Chromatography, 410 (1987) 413–418
Elsevier Science Publishers B.V., Amsterdam — Printed in The Netherlands

CHROM. 19 927

HIGH-PERFORMANCE LIQUID CHROMATOGRAPHIC DETERMINATION OF SIX *p*-HYDROXYBENZOIC ACID ESTERS IN COSMETICS USING SEP-PAK FLORISIL CARTRIDGES FOR SAMPLE PRE-TREATMENT

YUMIE MAEDA*, MASATOSHI YAMAMOTO, KAZUHIRO OWADA, SHIRO SATO and TOSHIO MASUI

Shizuoka Prefectural Institute of Public Health and Environmental Science, 4-27-2, Kita-ando, Shizuoka 420 (Japan)

and

HIROYUKI NAKAZAWA and MASAHIKO FUJITA

Institute of Public Health, 4-6-1, Shirokane-dai, Minato-ku, Tokyo 108 (Japan)

(First received July 14th, 1987; revised manuscript received August 4th, 1987)

SUMMARY

A rapid and simple method is described for the simultaneous determination of methyl, ethyl, isopropyl, *n*-propyl, isobutyl and *n*-butyl *p*-hydroxybenzoic acid esters (parabens) in cosmetics by high-performance liquid chromatography (HPLC). The method involves a single extraction of parabens with diethyl ether and clean-up on a Sep-Pak Florisil cartridge. Fat-soluble excipients in the diethyl ether extracts are removed through the cartridges with hexane–chloroform (75:25). Parabens are then eluted from the cartridges with hexane–ethyl acetate (70:30) and determined by HPLC on a reversed-phase column with water–methanol (50:50) as the mobile phase using *sec.*-butylpraben as an internal standard. The method was applied to samples with complicated matrices such as cream, milk lotion, lotion and cleansing foam, and the recoveries were 99.0–102.3% with coefficients of variation of 0.3–1.2%.

INTRODUCTION

p-Hydroxybenzoc acid esters (parabens) have been widely used as antimicrobial agents in cosmetics because of their broad antimicrobial spectrum with relative low toxicity, good stability and non-volatility[1]. In addition to methyl-, ethyl-, *n*-propyl- and *n*-butylparabens, isopropyl- and isobutylparabens have been included in the Japan Cosmetic Ingredients Dictionary (JCID) since 1985, which authorizes the use of six parabens singly or in combination in cosmetics.

Methods for determining parabens in samples with complicated matrices such as foods, pharmaceuticals and cosmetics consist of two steps, extraction and quantification.

Diethyl ether extractions were commonly used for the isolation of parabens from samples[2]. To remove substances that might interfere in the determination, the use of disposable Extrelut clean-up columns has been suggested[3]. Daenens and La-

0021-9673/87/$03.50

ruelle[4] reported a silica gel column chromatographic clean-up with light petroleum to remove interferents in foods and Mikami *et al.*[5] proposed a clean-up procedure for cosmetics involving double-layer column chromatography and liquid–liquid extraction. However, these clean-up procedures are complicated and time consuming for routine analysis.

Many methods for the determination of extracted parabens have been reported, including thin-layer chromatography (TLC)[2], gas chromatography (GC)[4,6] and high-performance liquid chromatography (HPLC)[3,5,7–9]. Although TLC is suitable for qualitative detection, it is inadequate for quantitation, and GC methods require derivatization prior to injection and involve tedious procedures. In HPLC applications, separations of these compounds using gradient elution[3,7] or ion depression[9] have been reported. Dong and DiCesare[8] suggested a very rapid quantitative method for determining methyl- and *n*-propylparabens in cosmetic products using normal-phase HPLC. However, these methods are unsatisfactory for determining six parabens accurately in cosmetics.

The purpose of this study was to investigate efficient extraction and simple clean-up procedures for removing fat-soluble excipients from cosmetics and to establish a method for the simultaneous and accurate determination of six parabens in cosmetics.

EXPERIMENTAL

Apparatus and operating conditions

A Model LC-6A liquid chromatograph (Shimadzu, Kyoto, Japan) equipped with a Shimadzu SIL-6A auto-sampler and a Shimadzu CTO-6A column oven was used. A Zorbax ODS column (250 mm × 4.6 mm I.D., 5 μm) (DuPont, Wilmington, DE, U.S.A.) was used at 50°C. The mobile phase was water–methanol (50:50) at a flow-rate 1.0 ml/min and the eluate was monitored with a Shimadzu SPD-6A UV detector, operating at 254 nm with attenuation at 0.04 a.u.f.s. Peak areas were determined with a Shimadzu Chromatopac C-R2A integrator.

A Model SCR 20BA centrifuge (Hitachi, Tokyo, Japan), a Model UT-6 ultrasonic bath (Kokusan Electronic, Tokyo, Japan) and a Model N-2 rotary evaporator (Tokyo Rikakikai, Tokyo, Japan) were used.

A Sep-Pak Florisil cartridge was obtained from Waters Assoc. (Milford, MA, U.S.A.).

Reagents

Methyl-, ethyl-, isopropyl-, *n*-propyl-, isobutyl- and *n*-butylparabens were purchased from Tokyo Kasei (Tokyo, Japan). *sec.*-Butylparaben (Tokyo Kasei) was used as an internal standard.

Methanol was of special HPLC grade (Wako, Osaka, Japan). As the mobile phase for HPLC, 500 ml of water and 500 ml of methanol were combined in a 1-l volumetric flask, mixed thoroughly and degassed in a ultrasonic bath before use. Tetrahydrofuran, diethyl ether, hexane, chloroform and ethyl acetate were of analytical-reagent grade. Solvents for rinsing and elution of the cartridges were hexane–chloroform (75:25) and hexane–ethyl acetate (70:30), respectively.

Calibration graphs

Amounts of 100 mg of each of the six parabens were dissolved together in 100 ml of methanol. The stock standard solution obtained was diluted with methanol to obtain final concentrations of 1–50 μg/ml. An internal standard (20 μg/ml) was incorporated in these solutions. Aliquots (10 μl) of these working solutions were injected into the chromatograph and the peak-area ratio was plotted against concentration by an internal standard method.

Sample preparation

To an accurately weighed portion (*ca.* 1.0 g) of cosmetic sample in a 20-ml beaker, 5 ml of tetrahydrofuran were added and dispersed in a ultrasonic bath for 1 min. This solution was transferred into a 200-ml separating funnel and 2 ml of internal standard solution (1 mg/ml methanol), 50 ml of saturated sodium chloride solution and 5 ml of 10% H_2SO_4 were added, followed by extraction with 50 ml of diethyl ether. The diethyl ether layer was dried with anhydrous sodium sulphate and evaporated to dryness at 40°C under reduced pressure. The residue was dissolved in 10 ml of methanol and centrifuged at 5000 rpm (3000 *g*) for 5 min. A 2-ml volume of the supernate was evaporated to dryness and the residue dissolved in 10 ml of hexane–chloroform (75:25). Aliquots of 1 ml of hexane–chloroform solution were passed through a Sep-Pak Florisil cartridge and rinsed with 15 ml of hexane–chloroform (75:25). Parabens were eluted from the cartridge with 10 ml of hexane–ethyl acetate (70:30). The eluate was evaporated to dryness and the residue was dissolved in 2 ml of methanol and placed in a ultrasonic bath for 1 min. A 10-μl portion of the methanol solution was subjected to HPLC. The parabens contents of the samples were determined from the calibration graphs.

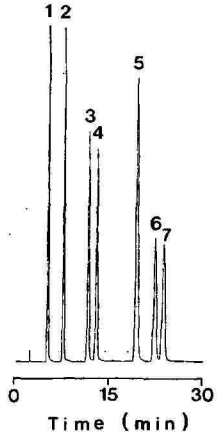

Fig. 1. HPLC trace of a standard mixture of parabens. 1 = Methyl- (0.1 μg), 2 = ethyl- (0.1 μg), 3 = isopropyl- (0.1 μg), 4 = *n*-propyl- (0.1 μg), 5 = *sec.*-butyl- (internal standard, 0.2 μg), 6 = isobutyl- (0.1 μg), 7 = *n*-butylparaben (0.1 μg), respectively. Column, Zorbax ODS (5 μm) (250 mm × 4.6 mm I.D.); mobile phase, water–methanol (50:50); flow-rate, 1.0 ml/min; column temperature, 50°C; detection, UV at 254 nm (0.04 a.u.f.s.); injection volume, 10 μl.

RESULTS AND DISCUSSION

Duplicate extraction with diethyl ether has commonly been applied for the isolation of parabens from cosmetics[2]. This study was aimed at simplifying the pre-treatment and a single diethyl ether extractions was attempted. Good resolution of the six parabens and the internal standard on the chromatogram was achieved, as shown in Fig. 1.

The calibration graphs for the six parabens were linear over the range 1–50 μg/ml with a regression coefficient of 0.999. The detection limits for each paraben were 10 ng, sufficient to determine the levels normally used in cosmetic chemistry.

To increase the accuracy we used *sec.*-butylparaben as an internal standard. However, some of the cosmetics analysed showed low recoveries of *n*-butylparaben reference compared with the declared amounts, as shown in Table I. The reason why a single extraction was insufficient with some cosmetic samples may be that they contained various kinds of emulsifying agents. In such instances, solubilization of the sample in 5 ml of tetrahydrofuran prior to diethyl ether extraction was effective, and suffcient recoveries of *n*-butylparaben were then obtained, in addition to methyl- and *n*-propylparabens.

Cosmetics contain various lipids, emulsifiers, surfactants, detergents and volatile oils that are extracted by diethyl ether, and these excipients interfere in the determination of parabens. Therefore, a suitable clean-up prior to HPLC measurement was necessary. Florisil, which has been used as a standard adsorbent in the determination of pesticide residues[10] and sterols[11], was thought to be suitable for the clean-up of cosmetics.

In our study, a disposable Sep-Pak Florisil cartridge was applied to remove interfering substances and other co-extractives. Preliminary experiments showed that the six parabens were quantitatively eluted from the cartridges with 10 ml of hexane–ethyl acetate (70:30).

Recovery studies were performed on variou samples of cream, milk lotions, lotions and cleansing foams to which no parabens had been previously added. The results obtained are shown in Table II. Excellent recoveries and good precision were

TABLE I

COMPARISON OF PRE-TREATMENT WITH AND WITHOUT TETRAHYDROFURAN ON EXTRACTION OF PARABENS FROM COMMERCIAL COSMETICS

Sample	*Pre-treatment**	*Paraben***		
		Methyl-	*Ethyl-*	*n-Butyl-*
Cream	A	99.0 (0.5)	—***	98.1 (0.8)
	B	95.8 (0.9)	—	80.5 (1.7)
Milk lotion	A	98.2 (0.7)	99.8 (0.5)	98.3 (1.7)
	B	98.2 (2.2)	98.9 (2.2)	75.9 (1.9)

* A, With tetrahydrofuran; B, without tetrahydrofuran.

** Percent of declared concentration [average of three replicates determinations with coefficient of variation (%) in parentheses].

*** Not declared.

TABLE II

RECOVERIES OBTAINED BY THE PROPOSED METHOD OF PARABENS ADDED TO COSMETICS

Sample	*Recovery (%)**					
	Methyl-	*Ethyl-*	*Isopropyl-*	*n-Propyl-*	*Isobutyl-*	*n-Butyl-*
Cream	99.5 (0.7)	100.3 (0.7)	99.4 (0.6)	99.4 (0.6)	99.9 (1.5)	100.2 (0.6)
Milk lotion	102.3 (1.1)	101.3 (0.7)	100.8 (0.6)	101.0 (0.6)	100.1 (1.1)	100.8 (0.8)
Lotion	99.0 (1.1)	99.9 (0.6)	100.1 (0.5)	100.0 (0.6)	101.1 (0.9)	99.8 (0.9)
Cleansing foam	99.3 (1.2)	101.6 (0.3)	100.9 (0.6)	101.0 (0.7)	100.2 (0.3)	99.9 (0.6)

* 1.0 mg of each paraben added to 1.0 g of cosmetics. Results are averages of five determinations with coefficients of variation (%) in parentheses.

observed. The recoveries of all the parabens indicate that the proposed extraction procedure is highly specific with essentially no interference from other components of the cosmetic sample.

For the clean-up procedure (removal of fats and various excipients, rinsing the cartridge and elution of parabens), less than 5 min is sufficient when using the disposable cartridge. It offers considerably savings in time (10–20%) and materials (30–50%) compared with previous methods[2–5], especially when dealing with samples that tend to form emulsions.

Fig. 2A shows a typical chromatogram of parabens extracted from a commercial cosmetic. The eluates from the clean-up column are generally so clean and free from interfering compounds that matrix peaks can hardly be observed in the chromatogram. Methyl-, ethyl-, *n*-propyl- and *n*-butylparabens are commonly used singly or in combination in cosmetics. However, as shown in Fig. 2B, isopropyl- or isobutylparaben is used in some cosmetic samples, especially imported types. In Ja-

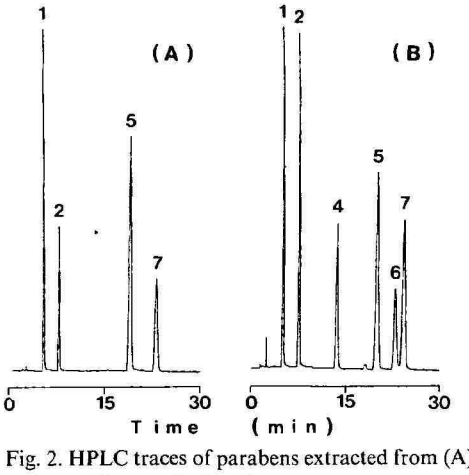

Fig. 2. HPLC traces of parabens extracted from (A) commercial milk lotion and (B) cleansing foam. Peaks and conditions as in Fig. 1.

pan, the use of the six parabens has been permitted since 1985, leading to the necessity for their determination.

In summary, the proposed method allows simple, rapid and efficient extraction and clean-up and the accurate simultaneous determination of six parabens, and should be suitable for the routine analysis of parabens in various cosmetics.

REFERENCES

1 F. F. Cantwell, *Anal. Chem.*, 48 (1976) 1854.
2 *Standard Methods of Analysis for Hygiene Chemists —with Commentary,* Pharmaceutical Society of Japan, Kanehara, Tokyo, 1983, p. 1335.
3 U. Leuenberger, R. Gauch and E. Baumgartner, *J. Chromatogr.*, 173 (1979) 343.
4 P. Daenens and L. Laruelle, *J. Assoc. Off. Anal. Chem.*, 56 (1973) 1515.
5 E. Mikami, N. Noda, S. Yamada, J. Hayakawa and K. Uno, *Eisei Kagaku,* 32 (1986) 34.
6 E. Weisenberg, B. Gershon and J. Schoenberg, *J. Assoc. Off. Anal. Chem.*, 60 (1977) 56.
7 L. Gagliardi, A. Amato, A. Basili, G. Cavazzutti, E. Gattervecchia and D. Torelli, *J. Chromatogr.*, 315 (1984) 465.
8 M. W. Dong and J. L. DiCesare, *J. Chromatogr. Sci.*, 20 (1982) 49.
9 H. Nakaguma, K. Tajima and T. Konishi, *Eisei Kagaku,* 31 (1985) 32.
10 L. A. Hu, G. A. S. Ansari, M. T. Moslen and E. S. Reynolds, *J. Chromatogr.*, 241 (1982) 419.
11 N. Fujimoto, M. Katai and H. Meguri, *Bunseki Kagaku,* 35 (1986) 482.

Journal of Chromatography, 410 (1987) 419–426
Elsevier Science Publishers B.V., Amsterdam — Printed in The Netherlands

CHROM. 19 950

SEPARATION AND DETERMINATION OF STABLE METALLO–CYANIDE COMPLEXES IN METALLURGICAL PLANT SOLUTIONS AND EFFLUENTS BY REVERSED-PHASE ION-PAIR CHROMATOGRAPHY

B. GRIGOROVA*, S. A. WRIGHT and M. JOSEPHSON
Anglo American Research Laboratories, P.O. Box 106, Crown Mines 2025 (South Africa)
(First received June 29th, 1987; revised manuscript received August 10th, 1987)

SUMMARY

The advance of liquid chromatography made feasible the identification of the different metallo–cyanide complexes. A technique for their simultaneous separation and determination, involving reversed-phase ion-pair partition chromatography with UV detection, is proposed. The mobile phase contains 2.5 m*M* tetrabutylammonium hydrogen sulphate as the pairing reagent and methanol as the organic solvent. A C_{18} Novapak cartridge with 4 μm packing is used as the stationary phase. The procedure is simple and rapid: separation and measurement are accomplished in 30 min. The method is accurate: the relative mean error is less than 1% for all complexes except $Cu(CN)_2^-$ (2.72%). The precision is good, with relative standard deviations from 1.14% to 2.83% for the individual complexes.

INTRODUCTION

Since the pioneering work of Small *et al.*[1], liquid chromatography has expanded considerably. During the past decade, a variety of separation mechanisms and detection techniques have been developed. The application of reversed-phase high-performance liquid chromatography (HPLC) with UV detection, in particular, has increased rapidly. The technique provides a high degree of flexibility, and thus has found a wide variety of analytical applications. Because the separations are based on well-understood mechanisms, optimization for any particular analysis is straightforward[2].

In recent years the gold hydrometallurgical industry has come to recognize the need for a reliable analytical procedure for identification and measurement of the individual metallo–cyanide complexes. Knowledge of the types of these species is essential for optimum control of the process. The demand for the determination of metallo–cyanide complexes in aqueous environments[12,13], and for the control of the cyanide destruction column, is also increasing rapidly. The latter plays a significant role in the prevention of pollution[7,10], and presents a further need for a rapid and accurate analytical method for identification of cyanide species.

0021-9673/87/$03.50

Recent advances in reversed-phase HPLC[4–6,8] have enabled the identification and determination of the stable metallo–cyanide complexes[9].

The aim of the work reported here was to provide a rapid, selective and sensitive analytical procedure for the stimultaneous determination of stable metallo–cyanide complexes. Procedural simplicity and accurate measurement were prime objectives.

EXPERIMENTAL

Principle

The principle of ion-pair chromatography was applied in the separation procedure, *i.e.* the partitioning of ion-pairs between a polar mobile phase and a hydrophobic stationary phase. The elution and subsequent separation of the metallo–cyanide complexes followed in order of decreasing ion-pair polarity, the more polar pair being eluted earlier. The cyanide complexes of Cu^+, Ag^+, Fe^{2+}, Co^{3+}, Ni^{2+}, Fe^{3+} and Au^+ were identified spectrophotometrically. The direct UV detection technique was utilized, using the UV-absorbing capacity of the metallo-cyanide complexes, combined with the UV-transparent properties of the mobile phase.

Acetonitrile is commonly preferred to methanol as organic solvent, on the grounds of stability, transparency in the UV region of the spectrum, and higher separation efficiency. However, we chose to use methanol because of its very competitive price, while the separation efficiency was maintained. The pairing reagent, low-UV tetrabutylammonium hydrogen sulphate, was from Waters' paired-ion chromatography (PIC) range, specifically formulated to eliminate background interference in the low-UV range. The length of the carbon chain of the PIC reagent influences sample retention time: a longer carbon chain results in greater retention.

The solution of ionic cyanide complexes was introduced into the mobile phase, consisting of 2.5 m*M* tetrabutylammonium hydrogen sulphate and methanol. The ion-pairs formed were partitioned onto the non-polar reversed-phase column. Retention of the complexes was governed by the degree of relative non-polarity of the ion-pair, a deciding factor in their affinity for the stationary phase.

Reagents

All reagents used were of analytical grade or manufactured specifically as chromatographic reagents. Standard calibration solutions of 1000 mg/l for all metallocyanide complexes were prepared by dissolution of their potassium salts in water. The pH value of all standard solutions was adjusted to pH > 10 to prevent degradation of the complexes. It was found that, at this value, all solutions are stable for more than 3 months. Dilute working solutions of 1 mg/l to 20 mg/l, were prepared fresh every day. All solutions were filtered through a 0.45-μm filter membrane and degassed prior to use.

The mobile phase, prepared from low-UV reagents, was 2.5 m*M* tetrabutylammonium hydrogensulphate–methanol (70:30, v/v).

Apparatus

A Waters liquid chromatograph was used. The equipment consisted of a Model 590 delivery system, a Rheodyne fixed-loop injector (20 μl), a RCM-100 radial com-

pression system fitted with a C_{18} Novapak cartridge column, packed with 4-μm particles, a variable-wavelength UV detector Model 481, and a Model 740 data processor. The reagent-grade water was supplied by a Milli-Q water purification system. An ultrasonic bath was used for sample and reagent degassing. A vacuum system was used for filtration of samples and standards.

Chromatographic procedure

A flow-rate of 1 cm^3/min for the mobile phase and a recorder chart speed of 0.5 cm/min were selected. The detection wavelength chosen was 210 nm. The sample was injected after a stable baseline was obtained; *ca.* 20 min were required. After separation, the different metallo–cyanide complexes were identified from their retention times (t_R). The concentrations of the complexes were calculated from the peak areas by the data processor.

RESULTS AND DISCUSSION

The separation and determination of the seven stable metallo–cyanide complexes most commonly encountered in solutions from the gold metallurgical industry and related effluents were investigated: $Cu(CN)_2^-$, $Ag(CN)_2^-$, $Fe(CN)_6^{4-}$, $Co(CN)_6^{3-}$, $Ni(CN)_4^{2-}$, $Fe(CN)_6^{3-}$ and $Au(CN)_2^-$. Fig. 1 shows the chromatogram of the separation of all seven complexes in a synthetic solution. The chromatographic conditions were those described above. Well-defined peaks and very good resolution were observed. The separation and determination were completed in 30 min.

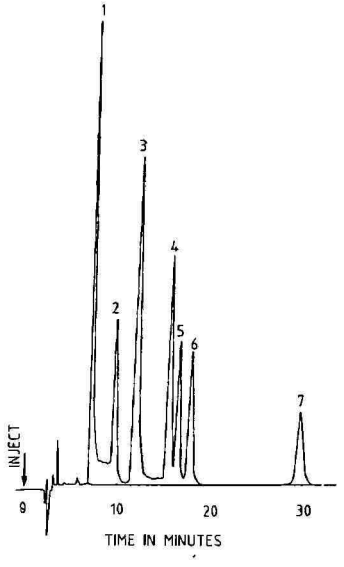

Fig. 1. Chromatogram of a synthetic solution containing seven stable metallo–cyanide complexes. The concentration of all components was 10 mg/l. Peaks: 1 = $Cu(CN)_2^-$; 2 = $Ag(CN)_2^-$; 3 = $Fe(CN)_6^{4-}$; 4 = $Co(CN)_6^{3-}$; 5 = $Ni(CN)_4^{2-}$; 6 = $Fe(CN)_6^{3-}$; 7 = $Au(CN)_2^-$. Chromatographic conditions are given in the text.

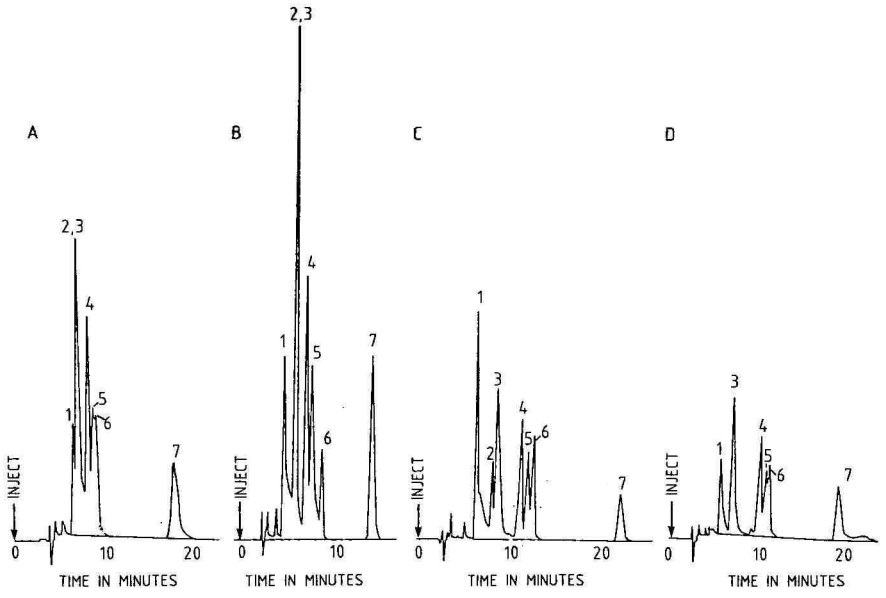

Fig. 2. Comparison of the separation of metallo–cyanide complexes with different molarities of the ion-pairing reagent: PIC A–methanol (65:35) was used. (A) 1.5 m*M*; (B) 2.0 m*M*; (C) 2.5 m*M*; (D) 2.7 m*M*. Peaks: 1 = $Cu(CN)_2^-$; 2 = $Ag(CN)_2^-$; 3 = $Fe(CN)_6^{4-}$; 4 = $Co(CN)_6^{3-}$; 5 = $Ni(CN)_4^{2-}$; 6 = $Fe(CN)_6^{3-}$; 7 = $Au(CN)_2^-$. The concentrations of the complexes were various. $Ag(CN)_2^-$ is not present in chromatogram D.

The investigative work commenced with the determination of the elution time and the sensitivity of each individual metallo–cyanide complex. The mobile phase used was 2.5 m*M* PIC A–methanol (65:35). After establishing that the retention times differed sufficiently for simultaneous separation and determination of the complexes, the work continued with the determination of the optimum molarity of the pairing reagent, tetrabutylammonium hydrogensulphate. The four concentrations of the PIC A reagent tested were 1.5 m*M*, 2.0 m*M*, 2.5 *M* and 2.7 m*M*, with the ratio PIC A–methanol maintained at 65:35. Poor resolution of the complexes was observed with 1.5 m*M*, PIC A, and when the concentration was increased, the separation improved. Better overall separation, but coelution of the argento- and ferrocyanide complexes, was recorded at 2.0 m*M*. At 2.7 m*M*, tailing of the aurocyanide complex and very poor resolution of the nickelo- and ferricyanide complexes were recorded. The best separation was achieved with 2.5 m*M* PIC A. Nevertheless, the resolution of the cupro-, argento- and ferrocyanide complexes was not satisfactory. The results of the test are shown in Fig. 2.

The possibility of improving the resolution of the complexes was investigated. Three solutions of mobile phase with methanol contents of 30%, 32% and 35% were tested (Fig. 3). The separation of the complexes was completed in less than 22 min when the methanol concentration was 35%, but poor resolution for the argento- and ferrocyanide complexes was obtained. The low displacement potential of the cuprocyanide complex also resulted in extensive peak tailing; the effect was reduced sensitivity. The time of elution for 32% methanol was 26 min, and 28 min for 30%

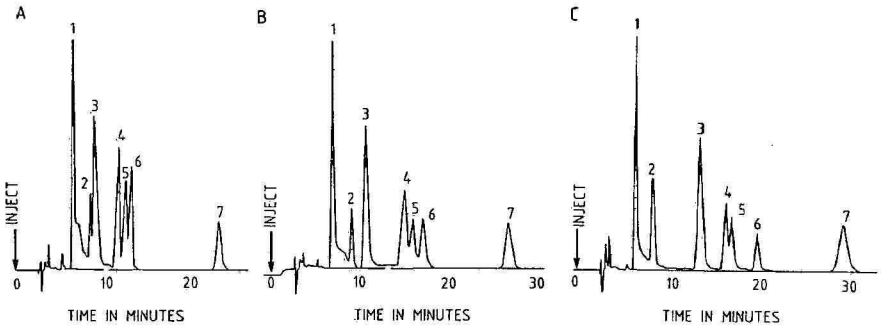

Fig. 3. Comparison of the separation of metallo–cyanide complexes with different concentrations of the mobile phase, PIC A–methanol: (A) 65:35; (B) 68:32; (C) 70:30. Peaks: 1 = $Cu(CN)_2^-$; 2 = $Ag(CN)_2^-$; 3 = $Fe(CN)_6^{4-}$; 4 = $Co(CN)_6^{3-}$; 5 = $Ni(CN)_4^{2-}$; 6 = $Fe(CN)_6^{3-}$; 7 = $Au(CN)_2^-$. Chromatographic conditions are given in the text.

methanol. The tailing of the cuprocyanide peak was reduced most effectively at the lower concentration of the organic solvent, and the overall resolution was better. The 30% methanol concentration was therefore selected.

The sensitivity of the metallo–cyanide complexes at different wavelengths was also studied. Several wavelengths, covering the UV range, were tested (Table I). It was observed that the most sensitive wavelength for the argento-, nickelo-, cobalti- and ferricyanide complexes was 200 nm, while the highest sensitivity for aurocyanide was at 205 nm, for the cuprocyanide at 210 nm, and for the ferrocyanide at 220 nm. The general tendency was towards reduction in sensitivity of the metallo–cyanide complexes above the 210 nm wavelength, with the exception of the ferrocyanide. As a compromise, the 210 nm wavelength was chosen. Fig. 4 shows a comparison of the sensitivities of the stable metallo–cyanide complexes at wavelengths of 205 nm, 210 nm and 214 nm.

The accuracy of the method was shown to be very good: the relative mean error was 1% for all complexes, other than $Cu(CN)_2^-$. Additional work, with an ionic modifier to eliminate peak tailing of the cuprocyanide complex and to improve the accuracy of its determination, is in progress. The precision of the technique was also

TABLE I

SENSITIVITY OF THE METALLO–CYANIDE COMPLEXES AT DIFFERENT WAVELENGTHS

The concentration of all complexes was 5 mg/l.

Complex	*Area counts* × 10^4					
	200 nm	*205 nm*	*210 nm*	*214 nm*	*220 nm*	*225 nm*
$[Cu(CN)_2]^-$	15.09	27.61	39.09	38.00	25.49	23.06
$[Ag(CN)_2]^-$	76.95	74.80	55.32	42.45	25.65	22.04
$[Fe(CN)_6]^{4-}$	38.86	48.92	58.06	62.51	69.70	64.81
$[Ni(CN)_4]^{2-}$	61.98	56.21	41.50	26.46	8.43	3.68
$[Co(CN)_6]^{3-}$	79.24	74.77	63.32	46.10	22.49	10.65
$[Fe(CN)_6]^{3-}$	35.98	34.40	33.52	28.04	19.97	13.86
$[Au(CN)_2]^-$	27.18	29.54	26.49	22.11	9.05	6.50

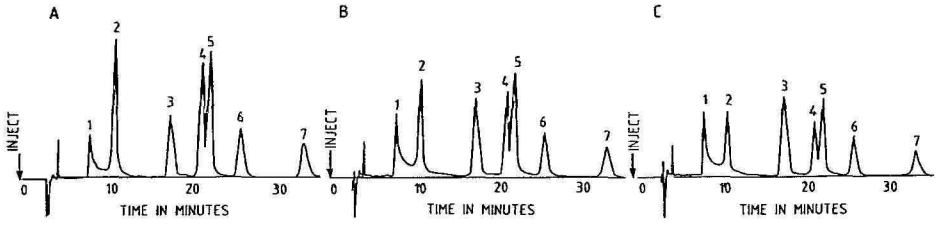

Fig. 4. Comparison of the sensitivity of the metallo–cyanide complexes at different wavelengths: (A) 205 nm; (B) 210 nm; (C) 214 nm. The concentration of all complexes was 5 mg/l. Peaks: 1 = $Cu(CN)_2^-$; 2 = $Ag(CN)_2^-$; 3 = $Fe(CN)_6^{4-}$; 4 = $Co(CN)_6^{3-}$; 5 = $Ni(CN)_4^{2-}$; 6 = $Fe(CN)_6^{3-}$; 7 = $Au(CN)_2^-$.

good: the relative standard deviation for the individual complexes was between 1.14% and 2.83%, when a 20-μl sample of 10 mg/l concentration was injected. The statistical data obtained from synthetic solutions are recorded in Table II.

The determination of low concentrations of the cobalticyanide complex in solutions from the gold metallurgical plant is of special interest, because of its deleterious effect on the activated carbon and the resin employed in the process; thus the detection of the cobalti-complex at low levels is of great importance. The detection limit of the procedure, using the 20-μl fixed-loop, was found to be 0.5 mg/l. When a lower level of detection is required, the sample volume should be increased to 100 μl, thus permitting metallo–cyanides at a concentration of 0.1 mg/l to be determined. The efficiency of the method was demonstrated on metallurgical plant solution containing different metallo–cyanide complexes, as well as samples from an environmental protection plant, *i.e.* a cyanide destruction column. Typical chromatograms are shown in Figs. 5 and 6.

The ion-pair technique was evaluated against the existing analytical method: the acid reflux procedure. The latter provides data on the total cyanide concentration only. Samples without the cobalticyanide complex were chosen for the evaluation because of the inadequacy of the acid reflux technique to produce reliable data on

TABLE II

THE PRECISION AND ACCURACY OF THE HPLC TECHNIQUE

The concentration of all complexes was 10 mg/l, with the exception of $[Ni(CN)_4]^{2-}$, which was 9.52 mg/l. The mean, relative standard deviation and relative mean error were obtained from fifteen replicates.

Complex	*Mean value (mg/l)*	*Relative standard deviation (%)*	*Relative mean error (%)*
$[Cu(CN)_2]^-$	9.73	1.84	2.72
$[Ag(CN)_2]^-$	10.08	1.59	0.85
$[Fe(CN)_6]^{4-}$	9.93	2.13	0.75
$[Co(CN)_6]^{3-}$	10.03	1.80	0.33
$[Ni(CN)_4]^{2-}$	9.53	2.05	0.11
$[Fe(CN)_6[^{3-}$	10.08	2.83	0.80
$[Au(CN)_2]^-$	10.06	1.14	0.58

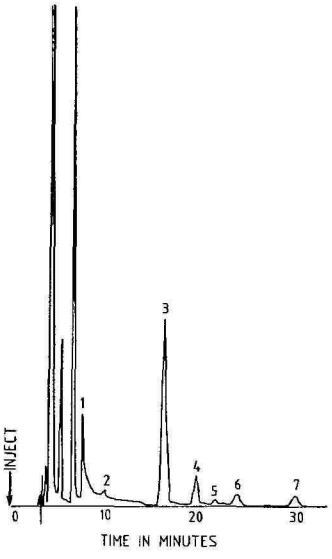

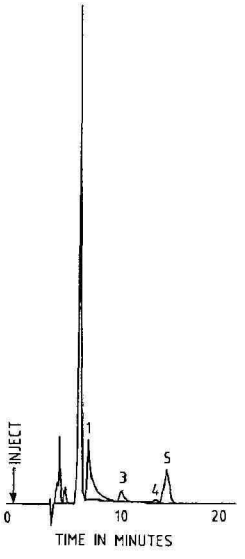

Fig. 5. Chromatograms of a solution from a gold metallurgical plant. The concentrations of the metallo–cyanide complexes were: 1 = 6.8 mg/l $Cu(CN)_2^-$; 2 = 2.8 mg/l $Ag(CN)_2^-$; 3 = 10.8 mg/l $Fe(CN)_6^{4-}$; 4 = 5.3 mg/l $Co(CN)_6^{3-}$; 5 = 0.6 mg/l $Ni(CN)_4^{2-}$; 6 = 2.5 mg/l $Fe(CN)_6^{3-}$; 7 = 2.7 mg/l $Au(CN)_2^-$.

Fig. 6. Chromatogram of a sample from a cyanide destruction column. Peaks: 1 = 3.1 mg/l $Cu(CN)_2^-$; 3 = 0.7 mg/l $Fe(CN)_6^{4-}$; 4 = 0.4 mg/l $Co(CN)_6^{3-}$; 5 = 6.4 mg/l $Ni(CN)_4^{2-}$.

TABLE III

EVALUATION OF THE HPLC TECHNIQUE AGAINST THE CLASSICAL REFLUX METHOD

A and B were metallurgical plant solutions. C, D, E and F were solutions from a cyanide destruction plant.

Sample identification	*Total CN^- concentration (mg/l)*	
	Acid reflux	*HPLC*
A*	130***	128
B*	220***	221
C**	170	174
D**	155	155
E**	120	124
F**	143	143

* The metallo–cyanide complexes present were $[Cu(CN)_2]^-$, $[Ag(CN)_2]^-$, $[Ni(CN)_4]^{2-}$ and $[Au(CN)_2]^-$.

** The metallo–cyanide complexes present were $[Cu(CN)_2]^-$, $[Fe(CN)_6]^{4-}$ and $[Ni(CN)_4]^{2-}$.

*** Modified classical reflux procedure ensures complete dissociation of stable $[Au(CN)_2]^-$ complex (see ref. 3).

$Co(CN)_6^{3-}$: only 52% of the complex is recovered by the classical procedure[11]. A modified acid reflux method[3], to ensure the complete dissociation of the aurocyanide complex, was used on the occasions when $Au(CN)_2^-$ was present. The data from the chromatograms, converted into total CN^- content, agreed well with the results obtained from the classical acid reflux technique. Results of the comparison are shown in Table III.

CONCLUSIONS

The reversed-phase ion-pair HPLC technique allows separation and determination of stable metallo–cyanide complexes, while eliminating the problems of precise pH, temperature control, reproducibility and short column-life that are associated with ion-exchange. The simplicity and accuracy of the procedure make it indispensible for rapid determination of stable metallo–cyanide complexes. The proposed method is applicable to solutions from metallurgical processes, cyanide destruction columns and effluents, thus revolutionizing many of the classical analytical techniques, especially in the fields of extractive metallurgy and environmental protection.

ACKNOWLEDGEMENTS

This paper is published with the approval of the Anglo American Corporation of South Africa Limited (AAC) and the work was partly funded by the Gold and Uranium Division of the AAC.

REFERENCES

1 H. Small, T.S. Stevens and W. C. Bauman, *Anal. Chem.*, 47 (1971) 1801–1809.
2 T. Jupille, *Int. Lab.*, December (1985) 82–89.
3 B. Grigorova, *AARL Ref. No. CA32, Internal Report,* Anglo American Research Laboratories, Crown Mines, October 1982.
4 J. S. Fritz, *Anal Chem.*, 59 (1987) 335–344.
5 K. Harrison, W. C. Beckham, Jr., T. Yates and C. D. Carr, *Int. Lab.*, April (1986) 90–94.
6 H. G. Barth, W. E. Barber, C. H. Lochmüller, R. E. Majors and F. E. Regnier, *Anal. Chem.*, 58 (1986) 211–239.
7 W. F Koch, *J. Res. Natl. Bur. Stand. (U.S.)*, 88 (1983) 157–161.
8 A. M. Bond, I. D. Heritage and G. G. Wallace, *Anal. Chem.*, 54 (1982) 582–585.
9 C. Pohlandt, *S. Afr. J. Chem.*, 38 (1985) 110–114.
10 P. Jandik, *J. Anal. Purif.*, (1986) 80–83.
11 F. J. Ludzack, W. Moore and C. C. Ruchhoft, *Anal. Chem.*, 26 (1954) 1784–1792.
12 E. J. Serfass, R. B. Freeman, B. F. Dooge and W. Zabban, *Plating*, 39 (1952) 267–273.
13 L. S. Bark and H. G. Higson, *Analyst (London)*, 88 (1963) 751–760.

Journal of Chromatography, 410 (1987) 427–436
Elsevier Science Publishers B.V., Amsterdam — Printed in The Netherlands

CHROM. 19 933

HIGH-PERFORMANCE LIQUID CHROMATOGRAPHIC METHOD FOR DETERMINING TRICHOTHECENE MYCOTOXINS BY POST-COLUMN FLUORESCENCE DERIVATIZATION

AKIRA SANO*, SATOSHI MATSUTANI, MASAO SUZUKI and SHOJI TAKITANI
Faculty of Pharmaceutical Sciences, Science University of Tokyo, 12, Ichigaya-funagawara-machi, Shinjuku-ku, Tokyo 162 (Japan)
(Received July 27th, 1987)

SUMMARY

The method described here is based on a separation of deoxynivalenol, nivalenol and fusarenon-X on a C_{18} column using aqueous acetonitrile, and successive post-column fluorescence derivatization involving an alkaline decomposition to form formaldehyde and modified Hantzsch reaction with methyl acetoacetate and ammonium acetate (λ_{ex} = 370 nm and λ_{em} = 460 nm). By this method, 5–10 ng of the standard trichothecenes could be determined. By employing a clean-up procedure with a florisil column and a Sep-Pak CN cartridge, 61.4–96.9% recoveries were obtained for deoxynivalenol and nivalenol added to corn, wheat and barley at concentration levels of 0.05–1 ppm.

INTRODUCTION

Trichothecene mycotoxins (Table I) are toxic fungal metabolites produced by various species such as *Fusarium* and *Trichothecium*, and over 60 trichothecenes have been identified. Among them, however, only two type B trichothecenes, deoxynivalenol (DON) and nivalenol (NIV), are often found in cereals and feeds, and have been implicated in major problems of food safety[1–4]. A sensitive and selective method for simultaneous determination of DON and NIV is needed, and chromatographic procedures are suitable. Thin-layer chromatography (TLC)[5–7] and gas chromatography (GC) with flame ionization detection (FID)[8], electron-capture detection (ECD)[3,8,9] and mass spectrometry (MS)[2,3] have been widely used. On the other hand, the applicability of high-performance liquid chromatography (HPLC) with a UV detector[4,10], based on the absorptivity of the α,β-enone system of type B trichothecenes, is often limited by lack of specificity because of the need to use low wavelengths (*ca.* 225 nm). A pre-column derivatization method using *p*-nitrobenzoyl chloride has been reported to form a chromophore with an absorption maximum of *ca.* 254 nm[11]. The method has the disadvantages that the reagent gives an interfering peak and its derivatization step is time-consuming. We considered that HPLC with post-column fluorescence detection is probably one of the more suitable methods because it per-

0021-9673/87/$03.50

TABLE I

STRUCTURES OF TRICHOTHECENE MYCOTOXINS

Type A

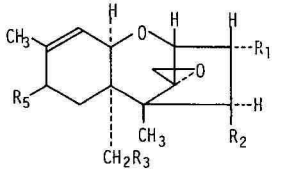

Type B

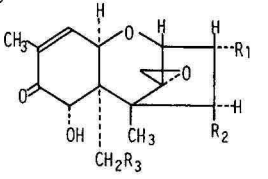

Mycotoxin (abbreviation)	R_1	R_2	R_3	R_5	*Mycotoxin (abbreviation)*	R_1	R_2	R_3
T-2 toxin (T-2)	OH	$OCOCH_3$	$OCOCH_3$	$OCOCH_2CH(CH_3)_2$	Deoxynivalenol (DON)	OH	H	OH
Diacetoxyscirpenol (DAS)	OH	$OCOCH_3$	$OCOCH_3$	H	Nivalenol (NIV)	OH	OH	OH
					Fusarenon-X (F-X)	OH	$OCOCH_3$	OH

mits efficient separation, selective detection and direct injection of the sample solution after clean-up without further treatment.

Previously we reported a method for determination of trichothecenes based on the chromogenic or fluorogenic reaction of formaldehyde produced from trichothecenes by an acid decomposition reaction[12]. However, application of similar reactions to an HPLC post-column derivatization system was found to be difficult because of the necessity to use viscous concentrated sulphuric acid. We have now found that type B trichothecenes, such as DON and NIV, give formaldehyde when heated with aqueous alkali. A modified Hantzsch reaction[13] for the derivatization of formaldehyde with methyl acetoacetate and ammonium acetate seemed to be appropriate because of its simplicity, selectivity and sensitivity. This paper reports the optimized post-column derivatization of type B trichothecenes and its application to cereal samples.

EXPERIMENTAL

Chemicals and materials

Trichothecenes were obtained from Wako Pure Chemicals (Osaka, Japan). Florisil (60–100 mesh, Wako) and Sep-Pak CN cartridge (Waters Assoc., MA, U.S.A.) were used for clean-up of cereal samples. Water used was purified on a Milli RO-Milli Q system (Millipore, MA, U.S.A.). TLC of reaction products was carried out with silica gel 60 TLC plates (E. Merck, Darmstadt, F.R.G.) with ethyl acetate as the developing solvent. All chemicals used were of analytical-reagent grade.

Chromatographic system

Fig. 1 is a schematic diagram of the HPLC system for analysis of the trichothecenes. A C_{18} column [250 mm × 4 mm I.D., Hibar LiChrosorb RP-18 (10 μm), E. Merck] was eluted with acetonitrile–water (15:85). The column temperature was ambient. A guard column (LiChroCART RP-18, E. Merck) was placed before the analytical column. The mobile phase was pumped at a flow-rate of 1.0 ml/min by a Shimadzu high-performance liquid chromatograph LC-6A (Shimadzu, Kyoto, Japan). Sample was injected with a 25-μl Hamilton syringe through a Rheodyne 7125 loop injector (Rheodyne, CA, U.S.A.). The eluate from the column was conducted to the fluorescence reactor system. All coils in the reaction system were made of PTFE. An aqueous sodium hydroxide solution (0.15 *M*) was first added to the eluate

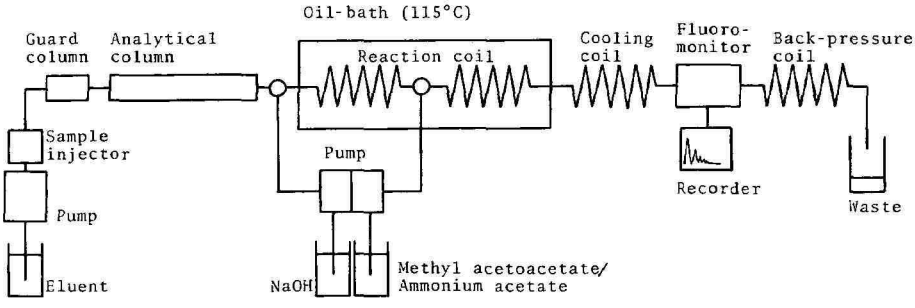

Fig. 1. Flow diagram for the HPLC post-column derivatization of trichothecene mycotoxins.

stream at the tee connector by one arm of a double-plunger type mini-micro pump (type KHD-W-52; Kyowa Seimitsu, Tokyo, Japan) at a flow-rate of 0.5 ml/min, and then the mixture was passed through a first reaction coil (8 m × 0.5 mm I.D.) immersed in a 115°C oil-bath (Thermo Regulater LTZ-112; Tabai Espec, Osaka, Japan). After the first reaction, a mixture of methyl acetoacetate (30 m*M*) and ammonium acetate (2 *M*) (prepared daily) was added at a flow-rate of 0.5 ml/min from another side of the double-plunger pump, and the mixture was passed through a second reaction coil (6 m × 0.5 mm I.D.) immersed in a 115°C oil-bath. After the fluorescence reaction, the mixture was passed through a cooling coil (1 m × 0.5 mm I.D.) immersed in a water-bath. The fluorescence intensity was monitored at 460 nm emission and 370 nm excitation by a Hitachi F-1000 fluorescence spectrophotometer (Hitachi, Tokyo, Japan) equipped with a flow-cell (12 μl) and a xenon lamp, and recorded with a recorder (type RC-125 M; JASCO, Tokyo, Japan). The outlet of the flow cell was connected to a 10 m back-pressure coil (0.5 mm I.D.).

When simultaneous measurement with both UV and fluorescence detection is needed, a UV detector (spectrophotometric detector SPD-2A, Shimadzu) was connected between the outlet of the analytical column and the inlet of the reactor system and operated at 225 nm.

Extraction and clean-up procedure

The procedure used in the present study was essentially the same as the method of Tanaka *et al.*[3], except that a Sep-Pak CN cartridge, rather than a Sep-Pak silica cartridge, was used for the final treatment of materials. The schematic procedure is shown in Fig. 2.

Quantitation of trichothecenes

An aliquot (10 μl) of the standard solution or sample solution prepared from

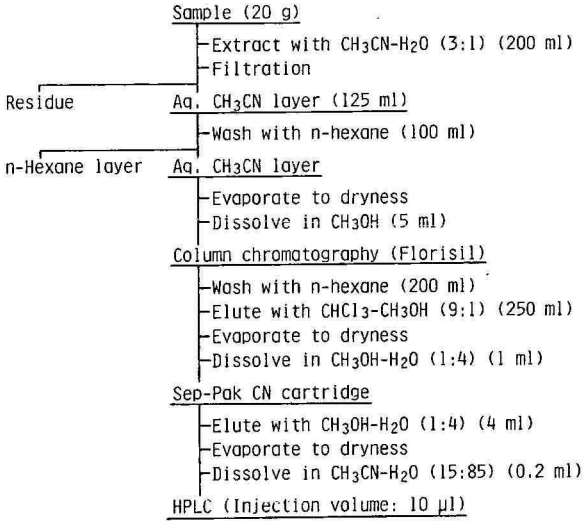

Fig. 2. Extraction and clean-up of trichothecene mycotoxins in cereals.

cereals was injected into the chromatograph. The amount of trichothecenes was calculated from the working curve of the peak height.

RESULTS AND DISCUSSION

Preliminary experiments by manual procedure

In preliminary experiment, it was found that trichothecenes classified as type B, such as DON, NIV and fusarenon-X (F-X), liberated formaldehyde when treated with alkali. Since formaldehyde is more reactive to various fluorogenic reagents than the parent molecules, it has been chosen for the fluorescence reaction. For this purpose, a modified Hantzsch reaction reported by Kawai and Tsutsui[13] was used, because it proceeds under mild condition and also because of its high sensitivity and selectivity for formaldehyde.

The following manual procedure was used for preliminary experiments and to confirm the liberation of formaldehyde from trichothecenes: to 200 μl of sample solution were added 200 μl of 0.1 *M* aqueous sodium hydroxide solution and the mixture was heated at 80°C for 20 min. The solution was cooled, and 200 μl each of 4 *M* aqueous ammonium acetate and 40 m*M* aqueous methyl acetoacetate were added. The mixture was heated at 80°C for 5 min then allowed to cool. The fluorescence intensity and the fluorescence excitation and emission spectra were measured with a Hitachi F-3000 fluorescence spectrophotometer using 1 × 1 cm quartz cell.

By this method, only type B trichothecenes showed a greenish blue fluorescence. Type A trichothecenes, such as T-2 toxin and diacetoxyscirpenol, did not fluoresce. Although DON is known to give an intramolecular rearrangement product when treated with aqueous sodium hydroxide[14], a reaction in which formaldehyde is released under alkaline conditions has not been reported previously.

Water-miscible organic solvents, such as alcohols and acetonitrile, water and these mixtures could be used as a reaction medium. This suggested the use of the present reaction in a post-column derivatization system, after separation on a reversed-phase column.

Fluorescence excitation and emission spectra of DON, NIV and F-X were the same as those of the product resulting from formaldehyde (excitation maximum, 379 nm; emission maximum, 460 nm). TLC of the reaction mixtures obtained from DON, NIV and F-X showed single fluorescent spots (R_F 0.76), which were exactly the same as that of authentic dimethyl 1,4-dihydrolutidine-3,5-dicarboxylate[13]. This confirms that the fluorescence of the reaction product can be attributed to the reaction between the reagents and the formaldehyde released from trichothecenes.

Separation

Simultaneous separation of DON and NIV can be achieved by using reversed-phase HPLC with a mobile phase of aqueous methanol[4,10]. Aqueous acetonitrile was also used for HPLC determination of DON[15]. On the other hand, the fluorescence derivatization of trichothecenes also proceeded in aqueous solvents, as described above. Acetonitrile was a more suitable component for the reaction medium than methanol because of formaldehyde contamination in the latter. The most favourable concentration of acetonitrile for the separation of DON, NIV and F-X was found to be 15% for LiChrosorb RP-18 used as a stationary phase. As shown in Table II, these trichothecenes could be separated within 10 min.

TABLE II

ANALYTICAL DATA FOR TRICHOTHECENE MYCOTOXINS

Mycotoxin	*Retention time (min) (mean ± S.D.*)*	*Determination range (ng/10 μl)*	*R.S.D.** (%) of peak height*
Nivalenol	4.7 ± 0.04	5–5000	3.1 (30), 0.64 (300)
Deoxynivalenol	6.0 ± 0.04	5–5000	4.2 (30), 0.88 (300)
Fusarenon-X	8.4 ± 0.09	10–5000	5.4 (30), 1.1 (300)

* Standard deviation, $n = 10$.

** Relative standard deviation, $n = 10$; the numbers in parentheses are the relevant concentrations in ng/10 μl.

Optimization of the fluorescence reaction in post-column reactor system

Optimization of the post-column reaction was examined by using a standard mixture of DON, NIV and F-X [200 ng of each in 10 μl of acetonitrile–water (15:85)]. Representative data from DON are shown in Figs. 3 and 4, and NIV and F-X gave similar results. Conditions for the formaldehyde formation reaction were examined first. Fig. 3 shows the effect of the sodium hydroxide concentration. The peak height reached an almost constant value over the concentration range 0.1–0.15 *M* sodium hydroxide. Thus 0.15 *M* solution was used. The reaction proceeded slowly at below

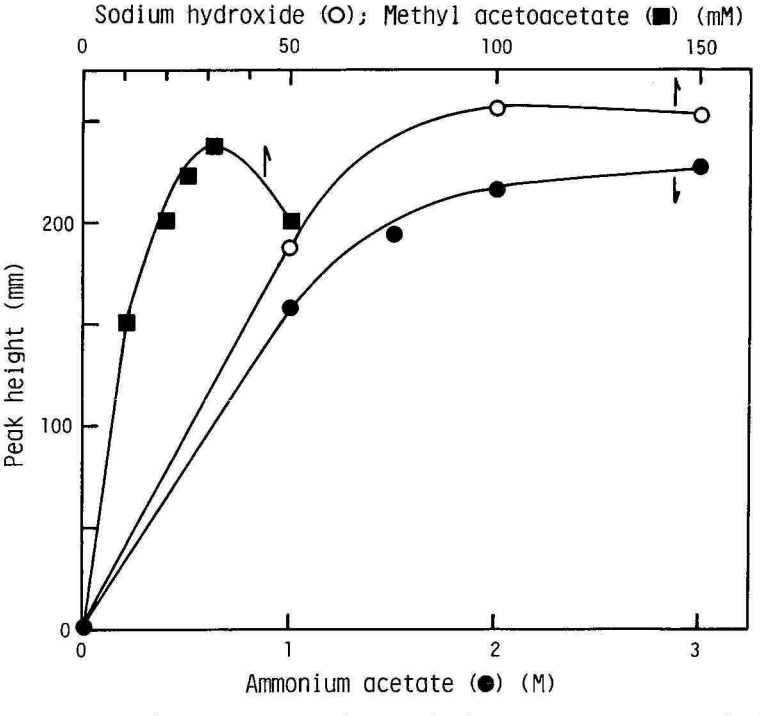

Fig. 3. Effect of reagent concentrations on the fluorescence development of DON (200 ng/injection). (○) Sodium hydroxide; (●) ammonium acetate; (■) methyl acetoacetate. For the HPLC conditions, see text.

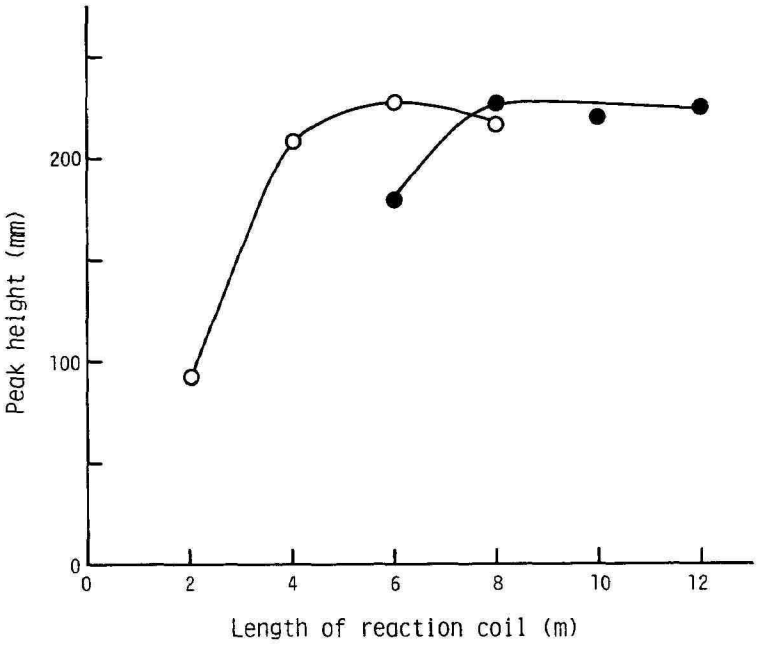

Fig. 4. Effect of the length of reaction coil on the fluorescence development of DON (200 ng/injection). (●) Alkaline decomposition reaction; (○) modified Hantzsch reaction. For the HPLC conditions, see text.

105°C, but the reaction accelerated at higher temperature and almost constant peak heights were obtained in temperature range 110–120°C. Thus 115°C was selected. The effect of the length of PTFE tubing on the formaldehyde formation was studied. As shown in Fig. 4, an almost constant peak height was obtained at 8–12 m, so 8 m of tubing were used.

Fig. 3 also shows the effect of reagent concentrations on the Hantzsch reaction of formaldehyde released. The use of an aqueous solution containing 2 *M* ammonium acetate and 30 m*M* methyl acetoacetate gave the best results. Although the modified Hantzsch reaction would be expected to proceed under mild conditions, the reaction was also done at 115°C for simplification of the system. The use of tubing lengths of 6–8 m gave an almost constant peak height (Fig. 4), so 6 m of tubing were used.

Calibration curves

Linear calibration curves were obtained for DON, NIV and F-X over the concentration ranges given in Table II. Relative standard deviations of peak height were 0.6–5.4%. Detection limit were 5 ng for DON and NIV and 10 ng for F-X, at a signal-to-noise ratio of 2.

Reaction yield

The total yield of the reaction was estimated by comparison of the peak heights obtained for a standard formaldehyde solution and for the trichothecenes. In this experiment, the apparatus used was the post-column reactor system from which

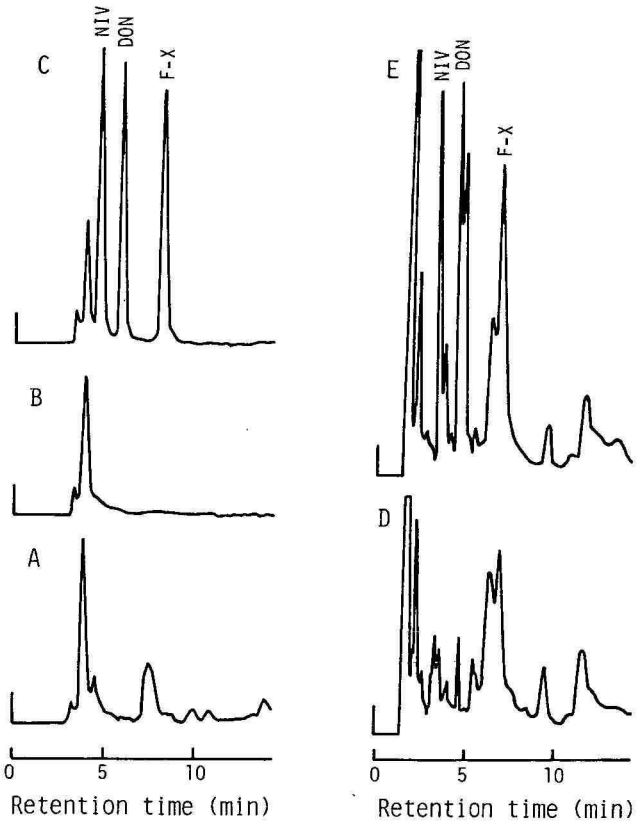

Fig. 5. Chromatograms with fluorescence (A-C) and UV (D-E) detection of extract of corn after clean-up with florisil (A), and florisil and Sep-Pak CN cartridge (B–E). (A, B and D) Blank corn; (C and E) corn spiked with DON, NIV and F-X (corresponding to 1 ppm). For the HPLC conditions and the clean-up procedure, see text.

guard column and analytical column had been removed. The temperature of the first 8-m coil was ambient for the reaction of formaldehyde. The reaction yields obtained for DON, NIV and F-X were found to be ca. 60%.

Clean-up of DON, NIV and F-X in corn samples

The recovery of trichothecenes, especially NIV, in cereal samples is significantly influenced by the clean-up procedure employed. Tanaka *et al.*[3] reported that recovery of NIV could be improved by using acetonitrile–water (3:1) rather than aqueous methanol as the extraction solvent. Therefore, we tested their clean-up procedure for corn samples prior to the HPLC analysis. As shown in Fig. 5A, it was found that the method is effective for DON but not for NIV and F-X, owing to the presence of interfering peaks. The use of a Sep-Pak silica cartridge, which was used by Tanaka *et al.*[3], showed no significant elimination of the interfering peaks. Other cartridges were therefore tested and Sep-Pak CN was found to be highly effective (Fig. 5B and C). NIV, DON and F-X could be recovered quantitatively by eluting

TABLE III

RECOVERIES OF TRICHOTHECENES SPIKED TO VARIOUS CEREALS

Cereal	*Spiked (μg/g)*	*Recovery (%) (mean ± S.D.*)*	
		Nivalenol	*Deoxynivalenol*
Corn	0.05	61.4 ± 6.3	80.4 ± 8.5
Corn	1.0	68.6 ± 3.5	79.5 ± 0.9
Wheat	1.0	88.5 ± 5.5	96.6 ± 5.0
Barley	1.0	90.6 ± 5.4	96.9 ± 4.8

* Standard deviation, $n=4$.

with 4 ml of methanol–water (1:4) from the cartridge. Chromatograms obtained by UV detection at 225 nm are also showed in Fig. 5 (D and E). These results clearly show the usefulness of the fluorometric method. It is much more selective than the method with UV detection. Similar results were also obtained for wheat and barley samples.

Recovery test for DON and NIV in cereal samples

Recovery tests were performed using corn, wheat and barley spiked with known amounts of DON and NIV. The results are shown in Table III. More than 60% recoveries were obtained with standard deviations of 0.9–8.8%. The detection limit was found to be 20 ppb* for NIV and DON in corn at a signal-to-noise ratio of 2. About 20–50 ppb of NIV and DON may be detectable in wheat and barley, though exact detection limits have not been estimated for both cases.

Among the available methods, GC has been most frequently used. However, GC–FID[8] is neither sensitive and selective. GC–ECD[3,8,9] and GC–MS[2,3] are most sensitive and selective, and these methods permit the detection of trichothecenes in cereals at 2–20 ppb levels. However, even if these techniques are used, it should be emphasized that there are problems, such as deactivation of the column packings, contamination of the detector[16], and interference in the quantitation[2] caused by coexistent substances. Contamination levels of DON and NIV in agricultural samples have been reported to be more than 20–30 ppb in the most cases in which DON and/or NIV were found[1–4]. Torelance levels for DON established by the Canadian Government and the Food and Drug Administration (U.S.A.) are below 0.3–2 ppm[17]. Thus the HPLC–fluorometric method described here seems to be useful for screening cereal samples for DON and NIV because of its simplicity, selectivity and sensitivity.

REFERENCES

1 T. Yoshizawa, in H. Kurata and Y. Ueno (Editors), *Toxigenic Fungi—Their Toxins and Health Hazard*, Kodansha, Tokyo and Elsevier, Amsterdam, 1984, pp. 292–300.
2 W. Blaas, M. Kellert, S. Steinmeyer, R. Tiebach and R. Weber, *Z. Lebensm. Unters. Forsch.*, 179 (1984) 104.

* The American billion (10^9) is meant.

3 T. Tanaka, A. Hasegawa, Y. Matsuki, K. Ishii and Y. Ueno, *Food Addit. Contam.*, 2 (1985) 125.
4 D. R. Lauren and R. Greenhalgh, *J. Assoc. Off. Anal. Chem.*, 70 (1987) 479.
5 S. Takitani, Y. Asabe, T. Kato, M. Suzuki and Y. Ueno, *J. Chromatogr.*, 172 (1979) 335.
6 A. Sano, Y. Asabe, S. Takitani and Y. Ueno, *J. Chromatogr.*, 235 (1982) 257.
7 M. W. Trucksess, S. Nesheim and R. M. Eppley, *J. Assoc. Off. Anal. Chem.*, 67 (1984) 40.
8 H. Kamimura, M. Nishijima, K. Yasuda, K. Saito, A. Ibe, T. Nagayama, H. Ushiyama and Y. Naoi, *J. Assoc. Off. Anal. Chem.*, 64 (1981) 1067.
9 P. M. Scott, S. R. Kanhere and E. J. Tarter, *J. Assoc. Off. Anal. Chem.*, 69 (1986) 889.
10 A. Visconti and A. Bottalico, *Chromatographia*, 17 (1983) 97.
11 R. Maycock and D. Utley, *J. Chromatogr.*, 347 (1985) 429.
12 T. Kato, Y. Asabe, M. Suzuki and S. Takitani, *Anal. Chim. Acta*, 106 (1979) 59.
13 S. Kawai and C. Tsutsui, *Bunseki Kagaku*, 33 (1984) E73.
14 J. C. Young, *J. Agric. Food Chem.*, 34 (1986) 919.
15 H. L. Chang, J W. DeVries, P. L. Larson and H. H. Patel, *J. Assoc. Off. Anal. Chem.*, 67 (1984) 52.
16 Y. Onji, M. Uno, H. Nagami, Y. Dohi and T. Moriyama, *Shokuhin Eiseigaku Zasshi*, 28 (1987) 50.
17 L. P. Hart and W. E. Braselton, Jr., *J. Agric. Food Chem.*, 31 (1983) 657.

Journal of Chromatography, 410 (1987) 437–446
Elsevier Science Publishers B.V., Amsterdam — Printed in The Netherlands

CHROM. 19 963

DETERMINATION OF NITRODIPHENYLAMINES BY LIQUID CHROMATOGRAPHY AND DUAL-ELECTRODE AMPEROMETRIC DETECTION

ARNE BERGENS
Department of Analytical Chemistry, University of Uppsala, P.O. Box 531, S-751 21 Uppsala (Sweden)
(Received June 12th, 1987)

SUMMARY

A method for the determination of nitrodiphenylamines in nitrocellulose-based propellants has been developed. The method is based on series dual amperometric detection in high-performance liquid chromatography. The electrochemical behaviour of 2-nitrodiphenylamine, 4-nitrodiphenylamine, 4-nitroso-2-nitrodiphenylamine and 2,4'-dinitrodiphenylamine was briefly studied in order to optimize the detection conditions. The linear concentration range of the method is 0.03–50 μM, which is quite sufficient for the levels of important nitro derivatives present in ageing propellants. Detection limits of 20 nM were achieved for the four test compounds, and the relative standard deviation was typically 1.0–2.0%. The method is demonstrated by the determination of 2-nitrodiphenylamine and 4-nitrodiphenylamine in propellant samples of different ages.

INTRODUCTION

Diphenylamine (DPA) is a stabilizing agent for nitrocellulose and hence continues to be one of the most important stabilizing additives in nitrocellulose-based propellants. DPA significantly prolongs the safe storage time of a propellant product by eliminating reactive HNO_3 and different NO_x species liberated in the degradation of nitrocellulose. Thus, protection of nitrocellulose against the detrimental exposure to HNO_3 and NO_x is achieved.

Reaction of DPA with HNO_3 and NO_x produces a number of nitro and nitroso derivatives[1]. Hence, the ageing progress of a particular propellant batch can be followed by monitoring the gradual build-up of various nitro derivatives. For this purpose, a number of selected qualitative and quantitative methods have been employed, including thin-layer chromatography[1] and straight phase liquid chromatography[2,3]. The present work was undertaken with the purpose of evaluating the use of electrochemical detection (ED) in reversed-phase high-performance liquid chromatography (HPLC) as an analytical tool for the determination of nitro derivatives formed during stabilizer degradation in stored propellants.

For electroactive compounds, HPLC–ED offers several advantages over UV detection in terms of selectivity and sensitivity. ED also provides a more uniform response for the same types of compound compared with UV detection, which de-

0021-9673/87/$03.50

pends on the molar absorptivities of the eluting compounds at a fixed wavelength (excluding diode-array detectors).

Aromatic nitro groups can be reduced electrochemically at both glassy carbon electrodes and mercury electrodes. Applications using direct reductive HPLC–ED[4] for the analysis of explosives thus far has not played any important role. One reason for this is the extreme cathodic potentials required to reduce nitro compounds, *e.g.* nitrodiphenylamines. Direct reductive HPLC–ED presents inconvenient operational problems because of the necessity of avoiding interference from oxygen present in the mobile phase and samples. The reduction products in aqueous acidic media are hydroxylamines, which in turn can be oxidized at moderate potentials, suitable for analytical determinations. Therefore, with the use of a dual-electrode amperometric detector mounted in a series configuration, the difficulties can be at least partly overcome by using the first electrode as a generator electrode of easily oxidized species. In order to optimize the detection conditions, a special voltammetric characterization of four selected nitro derivatives was performed.

The compounds investigated were 4-nitrodiphenylamine (4-NO_2-DPA), 2-nitrodiphenylamine (2-NO_2-DPA), 4-nitroso-2-nitrodiphenylamine (4-NO-2-NO_2-DPA) and 2,4′-dinitrodiphenylamine (2,4′-diNO_2-DPA).

EXPERIMENTAL

Apparatus

For voltammetric characterization, an EG&G Princeton Applied Research, PAR 174A polarographic analyser was used. The glassy carbon electrode (GCE) used in the experiments was purchased from Metrohm, and the electrode fitted a rotating electrode assembly (Metrohm, 2.628.0020). The GCE was enclosed in a PTFE housing with an exposed area of 7.07 mm^2 (Metrohm, 6.1204.040). A platinum wire was used as auxiliary electrode, and the reference electrode, to which all reported voltammetric potentials are referred, was a silver–silver chloride (Metrohm, 6.0724.140). The electrochemical cell was a 20-ml glass vessel with a water-jacket (Metrohm, 6.1418.220), which was kept at constant temperature (25 ± 0.5°C) by a conventional thermostat.

The HPLC system consisted of a syringe-pump, (Instrumentation Specialities Corp., ISCO Model 314) and a six-port Valco injection valve with either a 20-μl or a 50-μl sample loop. Separations were made on a 10 cm × 4.6 mm I.D. RP-18, Spheri-5 column with a 1.5 cm × 4.6 mm I.D. precolumn, (Brownlee Labs.). The amperometric detection system was controlled by two LC-4B potentiostats (Bioanalytical Systems, U.S.A.). The dual-electrode thin-layer cell was purchased from Bioanalytical Systems, and it consisted of two blocks: one Kel-F block containing the two GCEs each 3.2 mm in diameter and 0.6 mm apart, and one made of stainless steel that served as the auxiliary electrode. The two blocks were pressed together around a 50-μm thick gasket (Bioanalytical Systems, TG-5M), which defined, the thin-layer channel. The reference electrode was a silver–silver chloride (Bioanalytical Systems) and was positionned in the usual manner downstream in the eluent. The thin-layer cell was placed in a stainless-steel box to shield it from electrostatic disturbance. All chromatograms were recorded on a Kipp & Zonen strip-chart recorder or a Shimadzu CR-3 A integrator.

Reagents

The mobile phase components, acetonitrile, *m*-chloroacetic acid and 2-propanol, were all purchased from Merck and were of pro analysi grade. They were used without further purification.

4-NO_2-DPA and 2-NO_2-DPA were purchased from Aldrich and used as received. 4-NO-2-NO_2-DPA and 2,4'-diNO_2-DPA were supplied by Nobel Chemicals (Sweden) and used as received after verification of purity with UV detection and ED. All standard solutions were prepared weekly and refrigerated between measurements.

Procedures

Voltammetry. Voltammetric characterization experiments were performed with the mobile phase as medium. Portions of 10 ml were used, and appropriate amounts of standard solutions were added (100–1000 μl). Nitrogen saturated with the mobile phase was used for deaeration of the supporting electrolyte. Before each experiment the GCE was pretreated as previously described[5]. A sweep-rate of 50 mV/s was used in all voltammetric experiments using static or rotating electrodes.

Chromatography. The mobile phase composition was 0.1 *M* *m*-chloroacetic acid buffer (pH 2.7)–2-propanol–acetonitrile (59:26.5:14.5, v/v/v). The mobile phase components were filtered individually through a 0.45-μm filter (type HVLP, Millipore) before mixing. After mixing, degassing and removal of oxygen were performed by purging with argon for 20 min before the pump was filled. Injection loop volumes were 20 μl for standards and 50 μl for propellant samples. All chromatographic experiments were performed at ambient temperature, and a flow-rate of 1.1 ml/min was used throughout in all experiments.

For samples requiring a high sensitivity setting, deoxygenation prior to injection was necessary. Deoxygenation was achieved using a 5-ml conventional disposable syringe with a luer needle to fit in the injection valve. A 2-mm hole was drilled through the wall of the syringe at its 5-ml mark. This hole acted together with the syringe piston as a gas vent. The injection valve was mounted so that its injection port was positioned upright. In the injection valve's load position, argon was allowed to pass through the sample loop and further up through the syringe. After 5–10 min, the argon stream was disconnected from the waste line and the sample loop was immediately filled with a deoxygenated sample solution.

Extraction of samples. Propellant samples (1 g) were carefully weighed and extracted with 50 ml of methylene chloride in a Soxhlet extraction unit (Soxtec System 1040 Extraction unit, Tecator). The methylene chloride was then evaporated at ambient temperature, followed by dissolution of the residue in methanol (Merck, p.a. grade). Before injection into the chromatographic system, the samples were diluted with the mobile phase and filtered through a 0.45 μm filter to remove particulate matter. Sufficient dilution factors for analysis were in the interval 10–50, and a factor of 25 was suitable for most samples.

RESULTS AND DISCUSSION

Voltammetry

Detailed information about the electrochemical reduction of aromatic nitro compounds is available in the literature. The reduction of the aromatic nitro group

is an irreversible four-electron process, which in acidic media gives hydroxylamine as the main product[6–8]. Hydroxylamine can in its turn be oxidized through a two-electron process at moderate potentials where the residual current does not affect the sensitivity and selectivity. Dual amperometric detection is very suitable for compounds undergoing these kinds of reaction. Thus, the reaction scheme for detection is a two-step process:

Reduction:

$$\text{Ar-NH-Ar-NO}_2 + 4\,\text{H}^+ + 4\,\text{e}^- \rightarrow \text{Ar-NH-Ar-NHOH} + \text{H}_2\text{O} \qquad \text{(I)}$$

Oxidation:

$$\text{Ar-NH-Ar-NHOH} \rightleftharpoons \text{Ar-NH-Ar-NO} + 2\,\text{e}^- + 2\,\text{H}^+ \qquad \text{(II)}$$

However, the reaction pattern becomes more complicated when the number of nitro groups increases. Even their relative positions in the aromatic ring may have an influence on the reaction mechanism. Furthermore, the solvent composition and the pH of the solution are factors of great importance.

Cyclic voltammograms of 4-NO_2-DPA, 2-NO_2-DPA, 4-NO-2-NO_2-DPA and 2,4′-diNO_2-DPA showed that all compounds can undergo reduction at a GCE in the chromatographic medium (Fig. 1). 4-NO_2-DPA and 2-NO_2-DPA show well-defined irreversible reduction waves, and oxidation waves appear in the reverse scans, indicating the presence of electroactive reaction products (Fig. 1a and b).

Cyclic voltammograms of 4-NO-2-NO_2-DPA and 2,4′-diNO_2-DPA reveal two

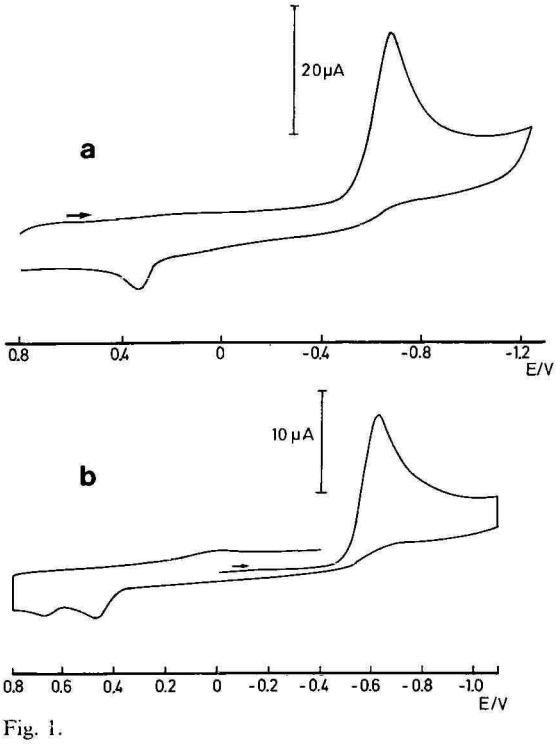

Fig. 1.

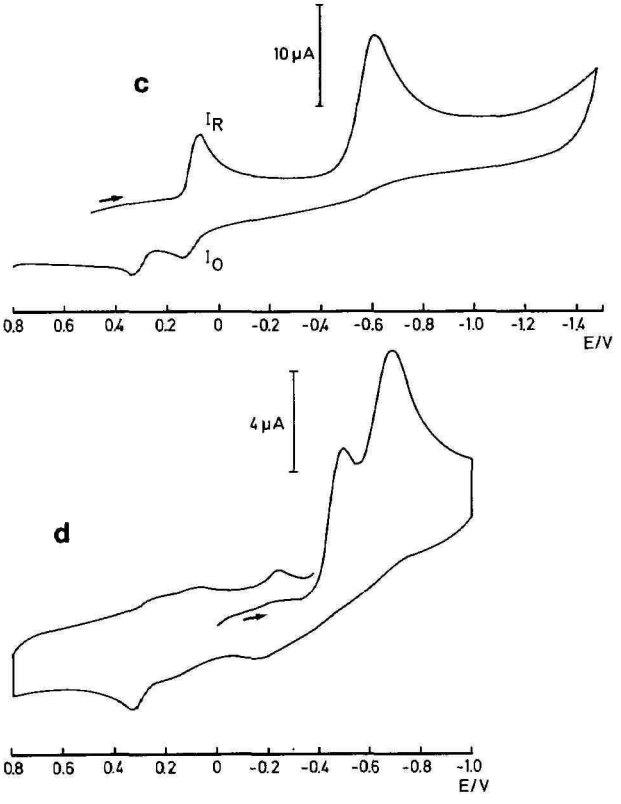

Fig. 1. Cyclic voltammograms of (a) 4-NO_2-DPA 0.15 m*M*, (b) 2-NO_2-DPA 0.28 m*M*, (c) 4-NO-2-NO_2-DPA 0.19 m*M*, (d) 2,4′-diNO_2-DPA 0.13 m*M*. Conditions: 0.05 *M* *m*-chloroacetic acid buffer (pH = 2.7)–2-propanol–acetonitrile (59:26.5:14.5); scan-rate 50 mV/s.

reduction waves, corresponding to separate reducible functionalities in the molecule (Fig. 1c and d). The first wave of 4-NO-2-NO_2-DPA appeared reversible if the scan was reversed at −0.2 V. This result is consistent with the reaction mechanism accepted for the reduction of aromatic nitroso compounds[9,10], which implies the reverse order of reaction (II) above. In the reverse scan of Fig. 1c, two different anodic waves could be observed, the most negative (indicated by I_O) related to the first reversible wave. The other wave can clearly be connected to the oxidation of hydroxylamine formed in the reduction of the nitro group. This wave did not appear when the scan was reversed at −0.2 V. For 2,4′-diNO_2-DPA, the two primary reduction waves appeared closer in the voltammogram (Fig. 1d) and showed irreversible characteristics according to reaction (I).

The normal procedure for optimizing the detection in HPLC–ED is stepwise change of the applied potential and measurement of the current from standards, injected into the flowing mobile phase. The reduction of the nitrodiphenylamines under hydrodynamic conditions was studied using a GCE rotating at 1500 rpm. Fig. 2 shows normalized hydrodynamic voltammograms obtained with the rotating electrode. The background current has been subtracted and the response normalized for

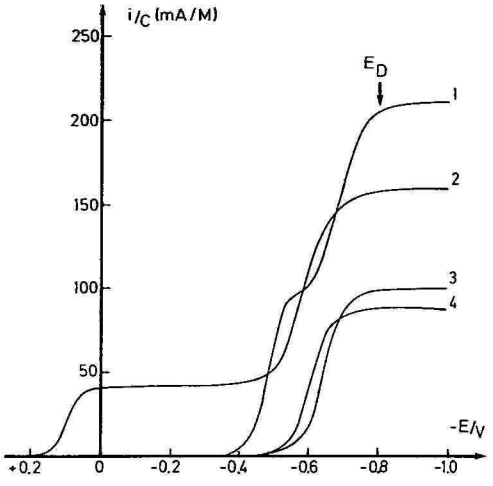

Fig. 2. Normalized hydrodynamic voltammograms obtained with the glassy carbon electrode rotating at 1500 rpm. Curves: 1 = 2,4'-diNO_2-DPA 0.13 mM; 2 = 4-NO-2-NO_2-DPA 0.12 mM; 3 = 4-NO_2-DPA 0.29 mM; 4 = 2-NO_2-DPA 0.28 mM.

the respective compounds. The diffusion-limited current for each compound then appears proportional to the number of electrons involved in the reduction processes, assuming similar values of diffusion coefficients for all four compounds. Results from these experiments are consistent with the predicted reaction schemes (I and II). The rotating-electrode voltammograms support this theory, because the ratio of the normalized diffusion current of wave 1 for 4-NO-2-NO_2-DPA is one-third of the diffusion current of wave 2, which corresponds to 2 and 6 electrons, respectively. Furthermore, the diffusion current of 4-NO_2-DPA amounts to *ca.* two thirds of wave 2 in 4-NO-2-NO_2-DPA. The necessary potentials required for mass transport controlled currents, E_D, are -0.8 V for all compounds (Fig. 2).

However, E_D values obtained from the rotating-electrode experiments must be further verified with the amperometric detector, since the kinetic properties of the electron transfer may vary significantly between GCEs of different origin[11] and pretreatment. Hydrodynamic parameters also differ according to the conditions in the thin-layer channel of the amperometric detector. The tests were performed by the usual procedure for obtaining hydrodynamic voltammograms, with $+0.5$ V applied at the detector electrode (W2). The E_D values were displaced by *ca.* 150 mV cathodically in the amperometric detector. Two or three different potential settings were sufficient to establish the optimum value of E_D for the generator electrode (W1). Therefore, a potential of -1.0 V was used throughout in this work. Fig. 2 is also indicative of the possible selectivity with ED for this type of sample. At -0.1 V, selective detection of 4-NO-2-NO_2-DPA and related nitroso compounds is possible, since other nitro compounds present in the sample matrix will not be reduced. Since background interference causes fewer problems at -0.1 V, currents measured at this potential can be used directly for analytical determinations.

With W1 fixed at -0.1 V, the response at different potentials for the detector electrode (W2) was monitored, and the resulting hydrodynamic voltammograms of

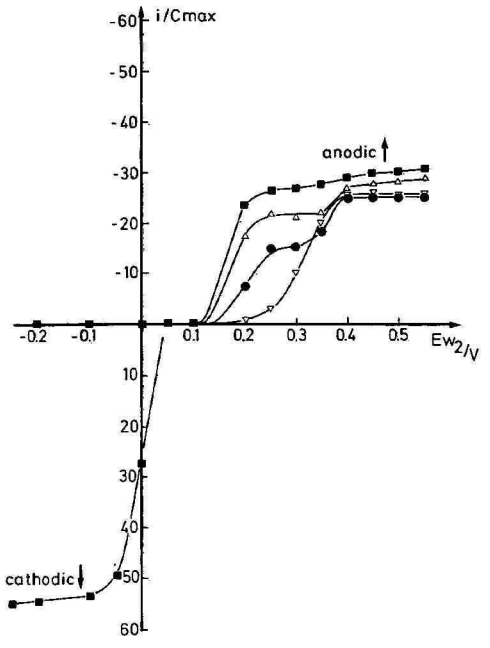

Fig. 3. Normalized hydrodynamic voltammograms obtained with the dual-electrode thin-layer cell. Generator electrode W1 at −1.0 V. (■) 4-NO-2-NO_2-DPA; (△) 2,4'-diNO_2-DPA; (●) 4-NO_2-DPA; (▽) 2-NO_2-DPA. (■) At zero current in the negative potential range symbolises the responses from 2,4'-diNO_2-DPA, 4-NO_2-DPA and 2-NO_2-DPA.

the reaction products of W1 are shown in Fig. 3. The currents were normalized to the maximum concentration in the eluted peaks, which can be calculated using the equation:

$$\frac{C_I}{C_{MAX}} = \frac{\sqrt{2\pi} \cdot V_R}{\sqrt{N} \cdot V_I} \tag{1}$$

where C_{MAX} is the maximum concentration in the band eluting from the column, C_I is the concentration of injected sample, V_I is the injected volume, V_R is the retention volume, and N is the number of theoretical plates. By dividing peak currents by C_{MAX}, a correction for the dilution of each compound is made. A limitation of eqn. 1 is that it is only valied for symmetrical peaks and V_I must be small compared with V_R[12].

A potential of at least +0.4 V is needed to establish diffusion control of currents for all four compounds (Fig. 3). The potentials chosen from the hydrodynamic voltammetry experiments illustrated in Figs. 2 and 3 were W1 = −1.0 V and W2 = +0.45 V, and the results are summarized in Table I.

Calibration graphs for the dual glassy carbon detector were linear in the range 1.6–1000 pmoles injected, which gives a linear concentration range of 0.03–50 μM. The minimum detectable amount was 1 pmol for 4-NO_2-DPA and 2 pmol for 2-NO_2-DPA, calculated as three times the noise level.

TABLE I

HALF-WAVE AND E_D POTENTIALS FOR THE FOUR NITRODIPHENYLAMINES OBTAINED USING HYDRODYNAMIC VOLTAMMETRY

Compound	*Reduction waves** $E_{1/2}$ *(mV)*	*Oxidation waves*** E_D *(mV)*
4-NO_2-DPA	−645	400
2-NO_2-DPA	−608	400
4-NO-2-NO_2-DPA	99, −508	250
2,4'-diNO_2-DPA	−480, −690	250

* From rotating electrode experiments.
** From experiments with the thin-layer cell.

Chromatography

The separation of a standard mixture of the four compounds studied is shown in Fig. 4. The standard mixture was spiked with 0.94 m*M* DPA, which was an estimation of the DPA concentration present in the sample matrix. The nitro derivatives can be selectively detected in presence of a high concentration of DPA (Fig. 4). Oxidation of DPA occurs at +0.6 V and higher potentials of W2. Fig. 4 also shows that DPA gives only a minor disturbance in the baseline after 8 min. Since the signal from the first electrode was not used because of high residual currents, no extensive procedure was employed to deoxygenate the mobile phase, such as continous refluxing under an inert atmosphere[13–15]; however, purging the mobile phase with argon for at least 15 min before filling the pump was found to be important for obtaining maximum sensitivity and reproducibility. Dissolved oxygen in the injected samples was found to cause a systematic peak after 2.1 min, which rendered quantifications of early eluting compounds at low concentrations more difficult, *e.g.* 4-NO-2-NO_2-DPA, owing to the severe tailing of the oxygen peak. This effect, probably arising from oxidation of peroxide at W2[15,16], could be minimized by purging samples with argon immediately before injection (Fig. 4). The purging was performed according

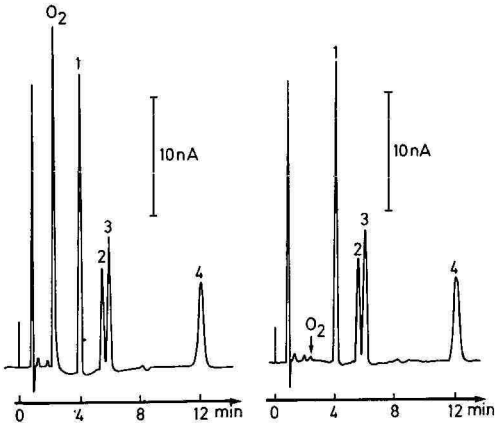

Fig. 4. Chromatograms of a standard mixture spiked with 0.94 mM of DPA before (left) and after (right) purging for 10 min with argon. Peaks: 1 = 4-NO-2-NO_2-DPA 5.27 μM; 2 = 2,4'-diNO_2-DPA 2.85 μM; 3 = 4-NO_2-DPA 6.45 μM; 4 = 2-NO_2-DPA 7.01 μM.

to Lloyd[17], except for a few modifications. The procedure is described in more detail in the Experimental section.

The detector response was observed to decline after 3–5 days of operation owing to deactivation of the generator electrode. After 1 week in operation there was a clear difference in the surface finish of the two GCEs, with a bluish film apparent on W1. The adsorbed film probably resulted from reduction of inorganic impurities in the mobile phase, which could be dissolved from the stainless-steel tubings. Simple polishing of the electrodes with 0.3-μm and 0.075-μm alumina was sufficient to restore the electrode surfaces. The optimum working time of the detector could also be prolonged by keeping the potentials at 0 V overnight.

Application to propellant samples

The method was applied to propellants stored for 1–26 years under normal warehouse conditions. During this storage and consequent degradation of samples, the dominant nitro derivatives appearing were 4-NO_2-DPA and 2-NO_2-DPA. Higher nitrated derivatives would only be expected to appear at higher concentrations in very old propellants or in samples that have been subjected to heat. This investigation was therefore aimed at the determination of 4-NO_2-DPA and 2-NO_2-DPA.

Fig. 5 shows separations of 4-NO_2-DPA and 2-NO_2-DPA from three nitrocellulose-based propellants stored for 16, 20 and 26 years. Besides these two main degradation products, some small traces of higher nitrated products were found. Intact DPA in the samples gives a greater obstruction on the baseline at 8 min than in a standard chromatogram, owing to the larger injection volume. Quantification by calibration curves was abandoned owing to the deactivation of the generator electrode discussed above. Instead, an external standard procedure was chosen, which consisted of alternate injections of standards and samples. Comparison of peak

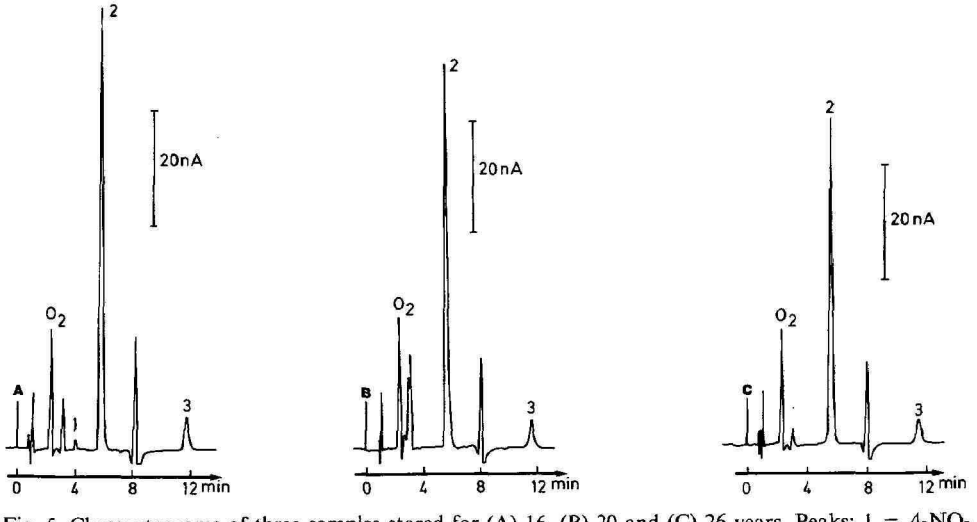

Fig. 5. Chromatograms of three samples stored for (A) 16, (B) 20 and (C) 26 years. Peaks: 1 = 4-NO-2-NO_2-DPA; 2 = 4-NO_2-DPA; 3 = 2-NO_2-DPA.

heights for a 4-NO_2-DPA standard and fresh daily prepared standards gave a relative standard deviation of 1.2% ($n = 9$) with no trend in the results, which indicates that the external standard method should be possible to use.

The sample solutions were found to decrease in 4-NO_2-DPA content corresponding to *ca.* 50% in 24 h on storing overnight. Addition of sodium nitrite to 4-NO_2DPA standards was found to give the same effect, and it is believed that nitrogen oxides are dissolved during the extraction procedure. Subsequent dilution with the acidic mobile phase will then cause further nitrosation of the nitro derivatives as they are exposed to reactive HONO[18]. Injection of sample solutions as soon as possible after dilution (5 min) was found to be sufficient for reproducible results to be obtained. The total time for the analysis of one propellant extract, including dilution, filtering and chromatographic separation, was *ca.* 30 min.

CONCLUSIONS

The investigation demonstrates that reversed-phase HPLC–ED can be used effectively for quality control of propellants. The method possesses a wide linear concentration range and low detection limits, which leaves the operator quite free to choose routines in sample preparations. A more uniform detector response also favours ED over conventional UV-detection. The experimental procedure does not add any further manual procedures to those of previous methods, and its combination of sensitivity, selectivity and low-cost apparatus requirements is advantageous. A limitation of the method that must be borne in mind, however, is the deactivation of the generator electrode.

REFERENCES

1 F. Volk, *Propellants Explos.*, 1 (1976) 90.
2 J. O. Doali and A. A. Juhasz, *Anal Chem.*, 48 (1976) 1859.
3 N. J. Curtis and P. E. Rogasch, *17th International Annual ICT Conference, 1986,* Fraunhofer-Institut für Treib und Explosivstoffe. ICT, D-7507, Pfinztal-Berghausen, F.R.G., p. 43-1.
4 J. B. F. Lloyd, *J. Chromatogr.*, 257 (1983) 227.
5 A. Bergens, K. Lundström and J. Asplund, *Talanta*, 32 (1985) 893.
6 C. K. Mann and K. K. Barnes, *Electrochemical Reactions in Non-Aqueous Systems,* Marcel Dekker, New York, 1970, p. 348.
7 D. A. Roston and P. T. Kissinger, *Anal. Chem.*, 54 (1982) 429.
8 R. O. Allendoerfer and P. H. Rieger, *J. Am. Chem. Soc.*, 88 (1966) 3711.
9 W. Kemula and R. Sioda, *J. Electroanal. Chem.*, 6 (1963) 183.
10 A. J. Bard, in A. J. Bard (Editor) *Encyclopedia of Electrochemistry of the Elements,* Marcel Dekker, New York, vol. XIII, pp. 131–159.
11 L. Bjelica, R. Parsons and R. M. Reeves, *Croat. Chem. Acta*, 53 (1980) 211.
12 L. R. Snyder and J. J. Kirkland, *Introduction to Modern Liquid Chromatography,* Wiley, New York, 2nd ed., 1979, p. 561.
13 D. M. Radzik, J. S. Brodbelt and P. T. Kissinger, *Anal. Chem.*, 56 (1984) 2927.
14 W. A. MacCrehan and R. A. Durst, *Anal. Chem.*, 53 (1981) 1700.
15 K. Bratin and P. T. Kissinger, *Talanta*, 29 (1982) 365.
16 R. J. Taylor and A. A. Humffray, *J. Electroanal. Chem.*, 64 (1975) 85.
17 J. B. F. Lloyd, *J. Chromatogr.*, 256 (1983) 323.
18 T. W. G. Solomons, *Organic Chemistry.* Wiley, New York, 1978, p. 832.

Journal of Chromatography, 410 (1987) 447–452
Elsevier Science Publishers B.V., Amsterdam — Printed in The Netherlands

CHROM. 19 985

Note

Analysis and identification of some aminoether alcohols and their ethers

HENRYK SZEWCZYK and EUZEBIUSZ DZIWINSKI
Institute of Heavy Organic Synthesis, Kędzierzyn-Koźle (Poland)
and
JAN SZYMANOWSKI*
Technical University of Poznań, Pl. Skłodowskiej-Curie 2, 60-965 Poznań (Poland)
(Received August 6th, 1987)

In previous studies[1–3] gas chromatography and mass spectrometry were used to determine the composition of N,N'-di(polyoxyethylene)alkylamines and of N-oligooxyethylene mono- and dialkylamines. Arithmetic retention indices were determined for homologues with various length of oxyethylene chains and alkyl groups, and they were used to identify these compounds. The mass spectra were also registered and discussed.

This paper deals with aminoether alcohols and their ethers of the following formulae:

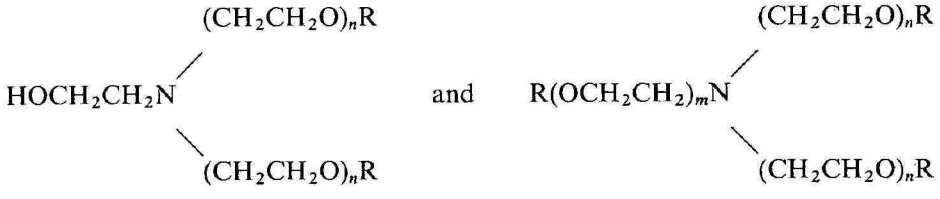

where R = C_4H_9, C_6H_{13} or C_8H_{17}, n = 1,2 and 3, and m = 2 and 3. The synthesis of these compounds and their polarities, as determined by reversed-phase gas chromatography, were discussed previously[4]. Their interfacial activity at the water–toluene interface was also determined and discussed[5].

The aims of this work were to determine the arithmetic retention indices and mass spectra of the investigated compounds and to discuss and correlate these parameters with the structures of the compounds.

EXPERIMENTAL

A gas–liquid chromatograph (Perkin-Elmer Model 900) with a flame ionization detector was used. The separation was carried out in stainless-steel columns (0.9 m × 2.7 mm I.D.). Chromosorb G AW DMCS (60–100 mesh) was used as the support and silicone resin OV-17 (phenylmethylsiloxane) (3%) as the liquid phase. Argon

0021-9673/87/$03.50

was used as the carrier gas, and its flow-rate was 15 cm^3/min. The temperatures of the injector and the detector were 320°C. The column temperature was raised from 150 to 320°C at 4°C/min.

Trimethylsilyl derivatives were prepared in a glass micro reaction vessel (capacity 3 cm^3) fitted with a PTFE-faced rubber septum and cap (Supelco, Bellefonte, PA, U.S.A.). A sample of *ca.* 0.05 g of the aminoether alcohol was weighed and 0.5 cm^3 of N,O-bis (trimethylsilyl)-acetamide (POCh, Gliwice, Poland) was added. The sealed reaction vessel was maintained at 70°C for 40 min and shaken from time to time. After this time silylation was complete and the product was analysed. A mass spectrometer (LKB, type 2091, Bromma, Sweden) was used. The samples were introduced by the direct inlet. An ionization energy of 70 eV, an ion-source temperature of 250°C, a voltage of ion acceleration of 3.5 kV and a sweep time of 7 s were employed. The products were analysed directly or in the form of their trimethylsilyl derivatives.

RESULTS AND DISCUSSION

Analytical data for investigated aminoether alcohols and their ethers are given in Table I. Aminoether alcohols (compounds 1–5) were analysed in the form of their trimethylsilyl derivatives. Only small peaks of impurities were observed on the chromatograms. Their contents, as estimated from the surface area of the peaks and assuming correction coefficients equal to 1, are in the range 0.05–3.5%. Sample chromatograms for mixtures of compounds 1–5 and 6–9 are given in Figs. 1 and 2, respectively.

The values of experimentally determined arithmetic retention indices are given in Table I. They demonstrate that an oxyethylene group and a methylene group correspond to *ca.* 300 and 100 units, respectively, on the arithmetic retention scale. Thus, it seems that increments of the arithmetic retention index determined pre-

TABLE I

ANALYTICAL DATA FOR AMINOETHER ALCOHOLS AND THEIR ETHERS

Compound No.	*Formula*	*n*	*m*	*R*	*Impurities content (%)*	I_A	I_A^{calc}
1	$HOCH_2CH_2N(CH_2CH_2O)_nR$	1	–	C_4H_9	1.7	1900	1949
2		2	–	C_4H_9	2.7	2511	2547
3		2	–	C_6H_{13}	0.6	2874	2947
4		2	–	C_8H_{13}	0.6	3235	3347
5		3	–	C_4H_9	3.0	3103	3145
6	$R(OCH_2CH_2)_mN(CH_2CH_2O)_nR$	1	2	C_4H_9	0.05	2400	2422
7		2	3	C_4H_9	0.8	3263	3293
8		2	3	C_6H_{13}	1.6	3824	3893
9		2	3	C_8H_{17}	3.5	4385	4493

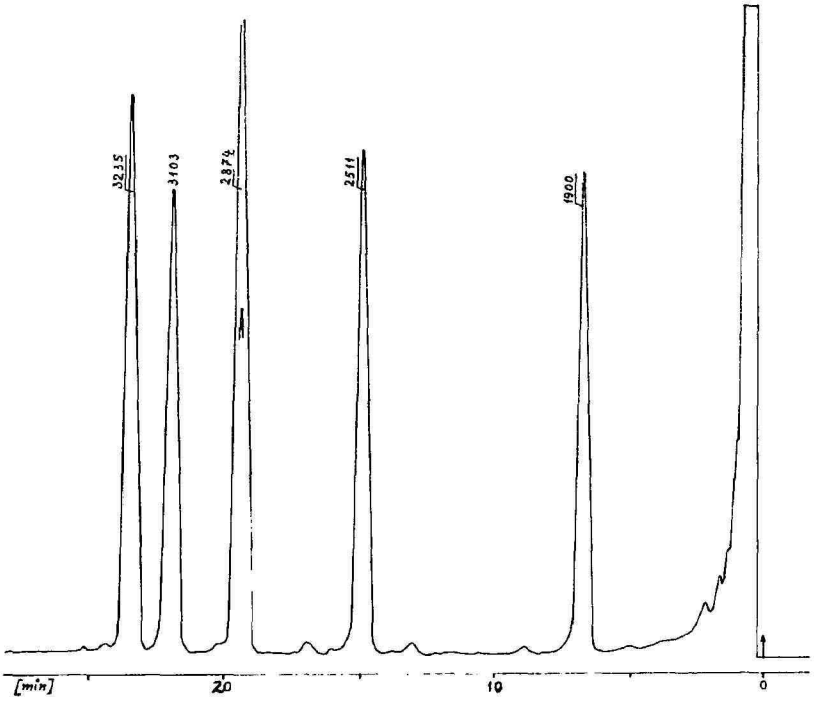

Fig. 1. Chromatogram of a mixture of compounds 1–5.

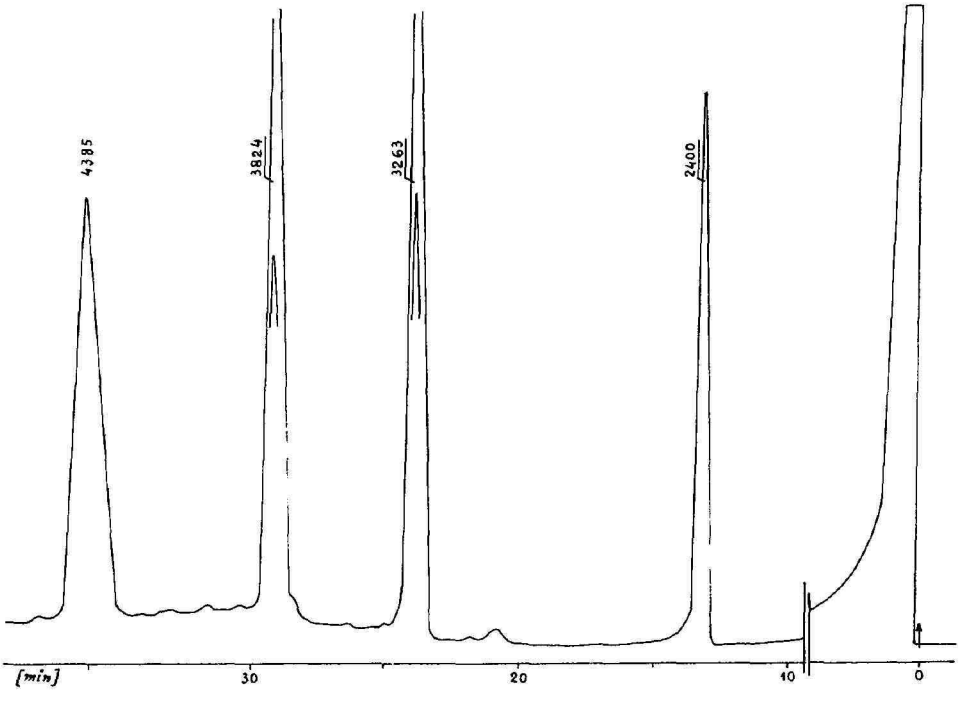

Fig. 2. Chromatogram of a mixture of compounds 6–9.

viously for characteristic fragments present in different oxyethylated alkylamines[3] can also be used for the group of compounds under consideration. Thus, $\Delta I_A(CH_2) = \Delta I_A(CH_3) = 100$, $\Delta I_A(N) = 26$, $\Delta I_A(O) = 99$, $\Delta I_A(OSi(CH_3)_3) = 325$ and $\Delta I_A(OCH_2CH_2) = 299$, and the arithmetic retention index can be estimated as $I_A = \sum_{i=1}^{k} n_i \cdot \Delta I_{A,i}$, where n_i denotes the number of a characteristic group i present in the compound considered, $\Delta I_{A,i}$ stands for the increment of I_A for the group i, and k is the number of the characteristic groups.

The values calculated in this way are given in Table I as I_A^{calc}. Good agreement between experimental and calculated values is observed. The average relative error is *ca.* 1.9%. The following linear relations are observed:

$I_R = 1000 + 300.75\, n_t^{EO}$ for compounds 1, 2 and 5;

$I_R = 1787 + 90.5\, n_t^{C}$ for compounds 2, 3 and 4;

$I_R = 2141 + 93.5\, n_A^{C}$ for compounds 7, 8 and 9;

where n_t^{EO} and n_t^{C} denote the total number of oxyethylene groups and carbon atoms in oligooxyethylene chains and alkyl groups, respectively.

The increments calculated as the gradients of above relations are then equal to $\Delta I_A(CH_2CH_2O) = 301$, $\Delta I_A(CH_2) = 92$ and $\Delta I_A(O) = 117$. Thus, these values differ only somewhat from the previous ones. This means that the increments depend on the structures of the compounds considered, but this effect is relatively weak for the groups of compounds studied.

The arithmetic retention indices of the compounds under consideration can also be estimated from their connectivity indices[6]. Linear relations were obtained for compounds 1–5 and 6–9, respectively (Fig. 3). Their gradients are almost the same and equal to 189.2 and 188.7, respectively. Thus, 1 unit of the connectivity index equal to 189 can be used to estimate the unknown values of the arithmetic retention index for other homologues of the series.

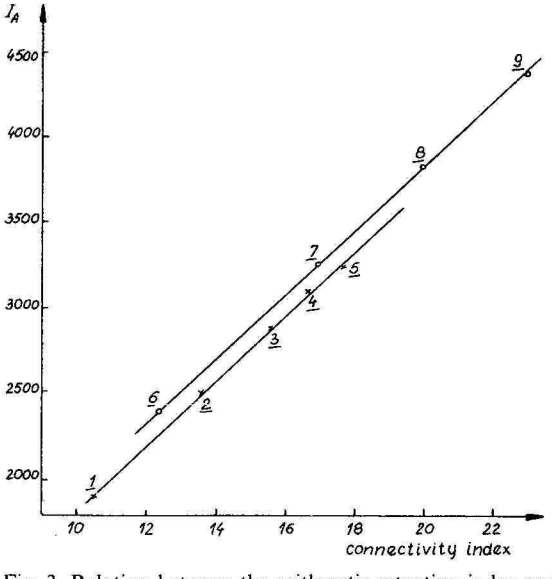

Fig. 3. Relation between the arithmetic retention index and the connectivity index.

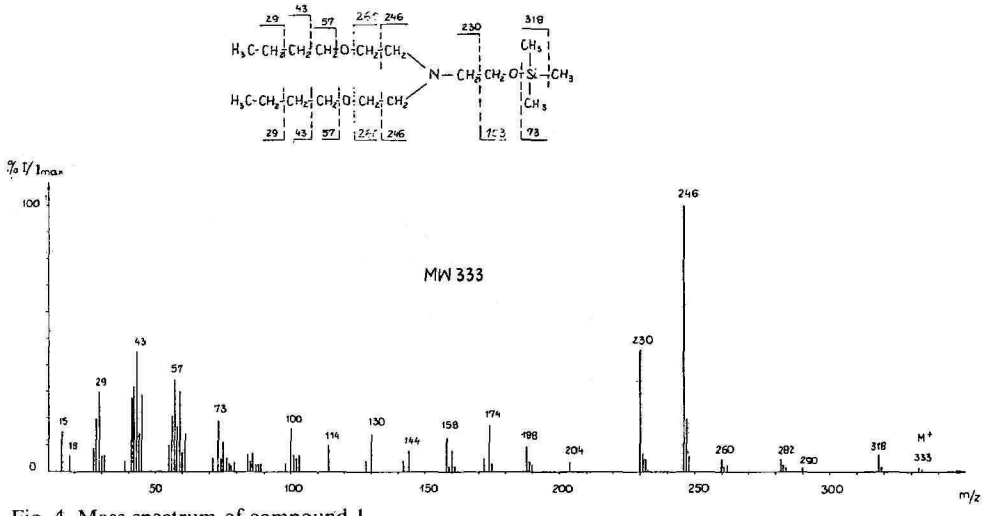

Fig. 4. Mass spectrum of compound 1.

For all the compounds investigated the mass spectra were taken, and two sample spectra, together with fragmentations, are presented in Figs. 4 and 5. In all these spectra parent ions of low intensity are present at m/z 333, 421, 477, 533 and 509 for trimethylsilyl derivatives of compounds 1–5, respectively, and at m/z 361, 493, 577 and 661 for compounds 6–9, respectively. The main fragment ions are

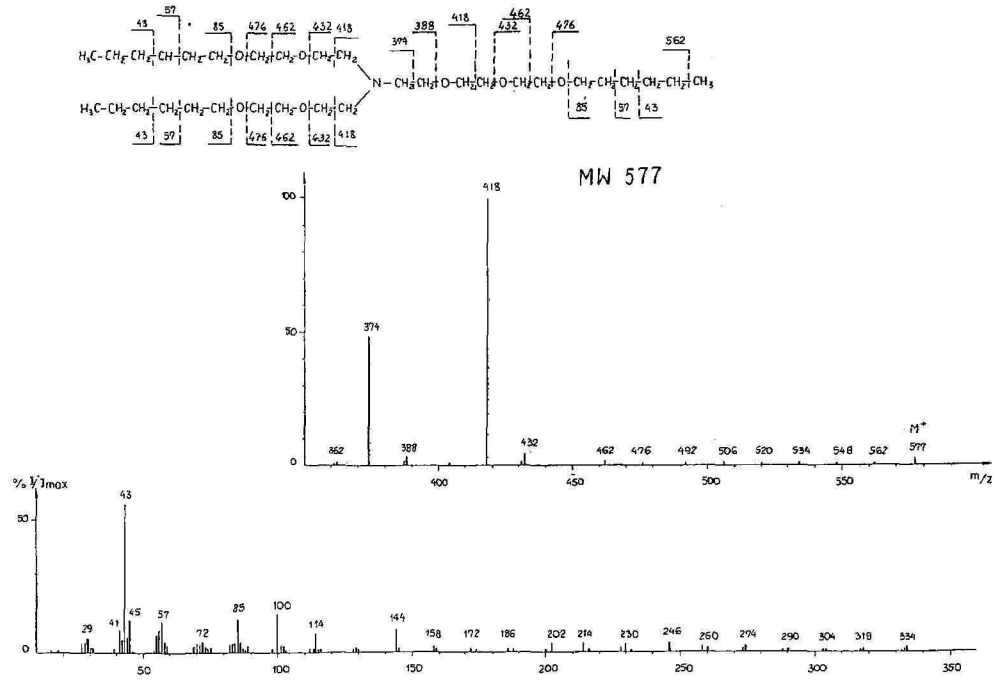

Fig. 5. Mass spectrum of compound 8.

formed as a result of fission of the C–C bond in the oxyethylene units linked to the nitrogen atom. In each case the intensities of these main ions are in the ratio of *ca.* 100:50, *e.g.* at *m/z* 246 and 418 and 374 in Figs. 4 and 5, respectively. This is a result of a similar tendency for splitting of the C–C bond in each oxyethylene unit linked to the nitrogen atom and the presence of two equal alkyl chains. Partial splitting of the C–O bond also occurs in these oxyethylene groups, and appropriate ions of low intensities are observed, *e.g.* at *m/z* 260 and at *m/z* 388 and 432 in Figs. 4 and 5, respectively. Similar partial splitting of the C–C and C–O bonds in the next oxyethylene groups also occurs, and appropriate ions of very low intensities are observed. The next characteristic ions are formed by splitting of alkyl radicals from terminal hydrocarbon chains. Tons at *m/z* 73, $[Si(CH_3)_3]^+$, are also observed.

The mass spectra obtained fully confirm the structure and purity of the investigated compounds.

CONCLUSIONS

The increments determined for characteristic fragments of aminoether alcohols and their ethers can be used to estimate the values of the arithmetic retention index within an error of less than 2%. The values of these increments depend on the structures of the compounds considered, but this effect is relatively small.

The arithmetic retention indices of the compounds considered can also be estimated from their connectivity indices, assuming that 1 unit of the connectivity index is equivalent to 189 units of the arithmetic retention index under the chromatographic conditions used.

The mass spectra fully confirm the structure and purity of the investigated compounds. The main fragment ions are formed by Gission of the C–C bond in the oxyethylene units linked to the nitrogen atom.

ACKNOWLEDGEMENTS

We thank Prof. J. Beger and Dr. K. Ebert for the synthesis of aminoether alcohols and their ethers.

REFERENCES

1 J. Szymanowski, H. Szewczyk and W. Jerzykiewicz, *Tenside Deterg.*, 18 (1981) 130.
2 H. Szewczyk, J. Szymanowski and W. Jerzykiewicz, *Tenside Deterg.*, 19 (1982) 287.
3 J. Szymanowski, A. Voelkel and H. Szewczyk, *J. Chromatogr.*, 360 (1986) 43.
4 A. Voelkel, J. Szymanowski, J. Beger and K. Ebert, *J. Chromatogr.*, 391 (1987) 373.
5 J. Szymanowski and K. Prochaska, *J. Colloid Interface Sci.*, submitted for publication.
6 M. Randic, *J. Chromatogr.*, 161 (1978) 1.

Journal of Chromatography, 410 (1987) 453–457
Elsevier Science Publishers B.V., Amsterdam — Printed in The Netherlands

CHROM. 20 032

Note

Oxidation–elimination of a DNA base from its nucleoside to facilitate determination of alkyl chemical damage to DNA by gas chromatography with electrophore detection

OHANNES MINNETIAN, MANASI SAHA and ROGER W. GIESE*

Department of Medicinal Chemistry in the College of Pharmacy and Allied Health Professions, and Barnett Institute of Chemical Analysis and Materials Science, Northeastern University, 360 Huntington Avenue, Boston, MA 02115 (U.S.A.)

(Received August 10th, 1987)

Exposure of humans to chemicals can create risks of carcinogenesis and mutagenesis. Since these latter events tend to correlate with chemical damage to human DNA, *i.e.*, with "DNA adducts", there is interest in measuring this type of damage. High sensitivity may be needed because a trace amount of a DNA adduct might be significant.

Here we present a powerful analytical strategy, with particular emphasis on the development of one step, for utilizing gas chromatography (GC) or high-performance liquid chromatography (HPLC) with electrophore detection to determine a small amount of an alkyl damaged base derived from human DNA. The step which is emphasized is an oxidation–elimination reaction, adopted from earlier work by others[1–3], that mildly and efficiently releases the base from a nucleoside.

EXPERIMENTAL

The nucleosides, nucleotides and free bases were Sigma grade (Sigma, St. Louis, MO, U.S.A.). They were dried in a desiccator under high vacuum for three days at room temperature. Dimethylsulfoxide (DMSO), acetic anhydride and pivalic anhydride were ACS grade (Baker Chemical, Philipsburg, NJ, U.S.A.). DMSO was dried over magnesium sulfate, distilled and stored over 4A molecular sieves.

Thymidine (0.49 mg) was subjected to a cleavage reaction in a 2-ml reaction vial (American Scientific Products, McGaw Park, IL, U.S.A.). DMSO (100 μl) and acetic anhydride (40 μl) were added, and the reaction was heated for 3 h at 40°C. After the removal of the solvent on a Speed Vac Concentrator the solid was dissolved in 100 μl of 1 *N* ammonium hydroxide and heated at 80°C for 1 h. The mixture was diluted to 25 ml with methanol–water (1:1, v/v) in a volumetric flask and 20 μl were analyzed by HPLC to determine the yield of thymine on a C_{18}-silica column with UV detection at 260 nm. The mobile phase was a gradient of acetonitrile in 0.1 *N* potassium phosphate buffer, pH 5, 2:98 to 20:80 (v/v), in 20 min at 1 ml/min. The other nucleosides were similarly cleaved and analyzed unless noted otherwise.

In order to prepare O^6-methyl-N^9(N^7?)-pentafluorobenzylguanine, a suspen-

0021-9673/87/$03.50

sion of O^6-methylguanine (0.09 g, 0.588 mmol) in 10 ml of acetonitrile was treated with 0.15 g (5.40 mmol) of potassium carbonate and 0.2 ml of pentafluorobenzyl bromide (1.07 mmol). The mixture was stirred for 7 h at room temperature, filtered and evaporated yielding an oily residue. Preparative thin-layer chromatography on silica with hexane–ethyl acetate (3:1) gave 0.12 g (67% yield) of product. ^1H NMR (60 MHz; C^2HCl_3): δ 8.71 (s, 1H), 5.35 (s, 2H); 4.08 (s, 3H), 3.96 (s, 2H). IR ($CHCl_3$): 2920; 1600; 1500 cm^{-1}. MS (*m/z*): 346 (M + 1; PICI), 164 (M − 181; NICI).

RESULTS AND DISCUSSION

N-Alkylation of a DNA base with pentafluorobenzyl bromide[4] can facilitate its analysis by GC or HPLC with electrophore detection (either electron-capture detection, ECD, or electron-capture mass spectrometry, ECMS) for several reasons: (1) a good yield of product can be obtained under mild conditions; (2) the N-alkyl linkage is hydrolytically and thermally stable; (3) the product tends to give a structurally characteristic anion in high yield when subjected to ECMS; and (4) electrophore detection limits for such products reach 10^{-17} mol[4–6]. This reaction is therefore of interest in efforts to determine chemical damage to DNA, *i.e.*, DNA adducts, in studies of carcinogensis and mutagenesis.

The DNA adduct O^6-methylguanine, for example, can arise when DNA is

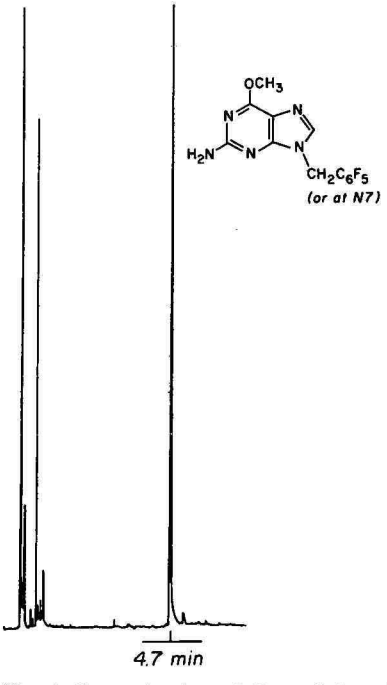

Fig. 1. Determination of 50 pg (injected in 1 μl of toluene) of O^6-methyl-N^9(N^7?)-pentafluorobenzylguanine by GC–ECD. Column: HP-5 fused silica crosslinked 5% phenylmethyl-silicone, 25 m × 0.32 mm I.D., 0.25-μm film thickness (Hewlett-Packard, Palo Alto, CA, U.S.A.). Conditions: on-column injection; column 70 to 280°C at 40°C/min; detector 340°C. Instrument: Varian 3700 gas chromatograph.

exposed to a methylating agent[7]. Derivatization of this base with pentafluorobenzyl bromide yields a product which is highly sensitive to GC with electrophore detection (Fig. 1). Equivalent sensitivity is seen for this product by GC–ECMS based on monitoring the dominant O^6-methylguanine anion at *m/z* 164 (ref. 6). Other bases behave similarly[8], *e.g.* N1-pentafluorobenzyl-N^4-pivalyl-5-methylcytosine, 5-pentafluorobenzyloxymethyl-N1,N3-bis(pentafluorobenzyl)uracil, N1-pentafluorobenzyl-O^4-ethylthymine and N^6-methyl-N9-pentafluorobenzyladenine.

In order to make N-pentafluorobenzylation followed by electrophore detection broadly applicable to detecting many DNA adducts, a general method for mild release of a base from a DNA nucleoside is needed. For this purpose we have utilized the DMSO–acetic anhydride reaction of Albright and Goldman[1]. This or a related DMSO–carbodiimide reaction, when followed by exposure to alkaline conditions, has been shown to effect base release from a DNA nucleoside or nucleotide bearing a free 3′-hydroxyl group[2,3]. The cleavage of the N-glycosidic bond is explained by oxidation of the 3′-hydroxyl group to a ketone followed by base-catalyzed elimination of the nucleobase.

In our version of this reaction, the nucleoside or nucleotide is first oxidized by DMSO–acetic anhydride for 3 h at 40°C. After evaporation, the residue is heated for

TABLE I

RELEASE OF NUCLEOBASE BY OXIDATION–ELIMINATION

The amount of reactant was 0.40 to 2.3 mg unless indicated otherwise. The yield was determined by HPLC based on calibration with authentic product.

Reactant	*Product*	*Yield (%)*
2′-Deoxynucleosides		
Deoxyadenosine	Adenine	57 ± 1*
N^6-Methyldeoxyadenosine	N^6-Methyladenine	69, 63 ± 4*
		59 ± 4**
Deoxycytidine	Cytosine	97 ± 3*
Deoxyguanosine	Guanine	85
O^6-Methyldeoxyguanosine	O^6-Methylguanine	92***
Thymidine	Thymine	97
5′-Deoxythymidine	Thymine	66
O^4-Ethylthymidine	O^4-Ethylthymine	96
Deoxyuridine	Uracil	87 ± 3*, 84§
Ribonucleosides		
Adenosine	Adenine	71
Cytidine	Cytosine	80
Guanosine	Guanine	98
Uridine	Uracil	80
5-Methyluridine	Thymine	73

* Mean ± S.D. for 1.0-mg amounts in triplicate.

** Mean ± S.D. for 50-μg amounts in triplicate. This yield was relative to adenine added as an internal standard at the end of the oxidation reaction, the absolute recovery of which was 94 ± 1%.

*** This yield was obtained after an oxidation time of 1 h. The yield of O^6-methylguanine dropped to 67% after 3 h of oxidation due to decomposition of the product to form an unknown compound that was eluted slightly later by HPLC.

§ Pivalic anhydride was substituted for acetic anhydride.

1 h at 80°C in the presence of 1 *M* ammonium hydroxide to release the nucleobase by an elimination reaction.

As shown in Table I, for several DNA nucleosides including some alkyl DNA adducts, and for ribonucleosides as well, the corresponding nucleobase is obtained by this reaction in a 57 to 97% yield. The reaction is particularly significant for the release of O^4-ethylthymine from the corresponding nucleoside since conventional acid hydrolysis, frequently used to hydrolyze the N-glycosidic bond of a nucleoside or nucleotide, yields thymine when applied to this nucleoside. As anticipated, neither 3′-deoxythymidine nor thymidine 3′-monophosphate, each of which lack a free 3′-hydroxyl group, releases any base when subjected to the reaction sequence (data not shown).

The yields of the nucleobases are not quantitative, due to the formation of unknown side products which sometimes are evident as extraneous peaks in the HPLC chromatogram used to assess the yield. At least for deoxythymidine and deoxyadenosine, the side products do not arise from decomposition of the nucleobase released during the reaction. This was established by quantitatively recovering uracil and adenine after each of these bases was subjected to the oxidation–elimination reaction sequence.

As shown by applying the reaction to both 1.0-mg and 50-μg amounts of deoxyadenosine in triplicate, the yield and precision (63 ± 4 and 59 ± 4%, respectively) are independent of the quantity of nucleoside. This nucleoside was chosen as a worst case to test further these aspects because of its tendency to form a higher amount of side products. The presence of pyridine in the oxidation reaction, as used by others[3], significantly increases the formation of side products (data not shown; this was tested with O^6-methyldeoxyguanosine and N^6-methyldeoxyadenosine).

This oxidation–elimination reaction in conjunction with pentafluorobenzylation opens up a new, general analytical strategy based on electrophore post-labeling to determine a trace amount of chemical damage to human DNA. In this proposed sequence, the DNA is first hydrolyzed enzymatically to nucleosides, a well-established technique. Oxidation–elimination then releases the bases, including the damaged bases, exposing an NH site (or a tautomeric NH site) on each base for mild derivatization by pentafluorobenzyl bromide. The final product, sometimes after further derivatization, then can be detected with high sensitivity by GC or HPLC with electrophore detection.

Three important advantages of this proposed analytical sequence are: (1) it will be applicable to many alkyl DNA adducts (see above for some examples); (2) each of the analytical steps is mild and efficient; and (3) the final product tends to be hydrolytically and thermally stable, while yielding a sensitive, structurally characteristic anion by ECMS.

ACKNOWLEDGEMENTS

This work was sponsored by Grant CA43012 from the National Cancer Institute and Grant CR812740 from the Reproductive Effects Assessment Group of the United States Environmental Protection Agency (EPA). Contribution No. 324 from the Barnett Institute.

REFERENCES

1 J. D. Albright and L. Goldman, *J. Am. Chem. Soc.*, 87 (1965) 4214.
2 K. E. Pfitzner and J. G. Moffat, *J. Am. Chem. Soc.*, 87 (1965) 5661.
3 T. Gabriel, W. Y. Chen and A. L. Nussbaum, *J. Am. Chem. Soc.*, 90 (1968) 6833.
4 J. Adams, M. David and R. W. Giese, *Anal. Chem.*, 58 (1986) 345–348.
5 R. W. Giese and P. Vouros, *Fourth Health Effects Institute Annual Conference, Feb. 8–12, 1987, Charleston, NC*, p. 76.
6 M. Saha and R. W. Giese, in preparation.
7 B. Singer and D. Grunberger, *Molecular Biology of Mutagens and Carcinogens*, Plenum, New York, 1983.
8 O. Minnetian, M. Saha and R. W. Giese, unpublished results.

Journal of Chromatography, 410 (1987) 458–462
Elsevier Science Publishers B.V., Amsterdam — Printed in The Netherlands

CHROM. 19 977

Note

Enantioselective capillary gas chromatography of 1,2-isopropylidene glycerol and O-alkylated glycerol derivatives

NORBERT SCHMIDT and GÜNTHER GERCKEN
Institut für Biochemie und Lebensmittelchemie, Abteilung für Biochemie, Universität Hamburg, D-2000 Hamburg 13 (F.R.G.)
and
WILFRIED A. KÖNIG*
Institut für Organische Chemie, Universität Hamburg, D-2000 Hamburg 13 (F.R.G.)
(Received August 17th, 1987)

In view of the importance of optically pure lipids, synthetic methods for the preparation of glycerol derivatives with a high degree of configurational purity have been published[1–5]. In the course of these syntheses 1,2-isopropylidene glycerol plays a central role as an intermediate for the preparation not only of lipids but also of a great variety of natural compounds[6]. Both enantiomers of isopropylidene glycerol can be obtained by degradation of natural precursors[7–10]. Enantiomeric purity is usually examined by determination of the optical rotation, which may give erroneous results, particularly in the presence of chiral or non-chiral impurities[11]. ^{1}H NMR spectroscopic analysis with chiral shift reagents also could not sufficiently resolve this problem [12,13]. Hirth and Walther[14] have used capillary gas chromatography (GC) of (*R*)-α-methoxy-α-trifluoromethylphenyllactic acid (MTPA, Mosher's acid) esters for the determination of the configurational purity of 1,2-isopropylidene glycerol. However, the use of diastereomeric derivatives has some intrinsic disadvantages. Derivatization may proceed with different reaction rates for the enantiomers and thus may cause erroneous results. Moreover, 100% optical purity of the derivatizing reagent would be a prerequisite for precise measurements.

Enantiomeric separation of acylated and alkylated glycerols by high-performance liquid chromatography (HPLC) was recently described[8,15,21], providing direct methods for the control of enantiomeric purity.

This paper describes methods for direct enantiomeric separation of 1,2-isopropylidene glycerol and of O-alkylated glycerol derivatives by capillary GC on a chiral stationary phase.

EXPERIMENTAL

Chemicals

Phosgene (20% solution in toluene) and isopropyl isocyanate were from Fluka (Buchs, Switzerland). All other solvents and reagents were obtained, if possible in analytical grade, from E. Merck (Darmstadt, F.R.G.).

0021-9673/87/$03.50

Formation of derivatives

1,2-Isopropylidene-*sn*-glycerol (I) was prepared starting from D-mannitol[7], and derivatized to the corresponding isopropyl urethane (II)[16]. 3-O-Butyl-*sn*-glycerol (III) was synthesized by alkylating 1,2-isopropylidene-*sn*-glycerol with butyl bromide as described by Eibl and Wolley[3] for the benzyl derivative, and purified by thin-layer chromatography on silica gel 60 with diethyl ether as solvent. Conversion into the enantiomeric 1-O-butyl-*sn*-glycerol (IV) was carried out using the procedure of Pompipom and Bugianesi[17]. 3-O- (V) and 1-O-butyl-*sn*-glycero-2,3-carbonate (VI) were formed by reaction with phosgene[18]. All racemic compounds were prepared starting from 1,2-isopropylidene-*rac*-glycerol. The synthetic reactions utilized are illustrated schematically in Fig. 1. The derivatives were characterized by combined GC and mass spectrometry.

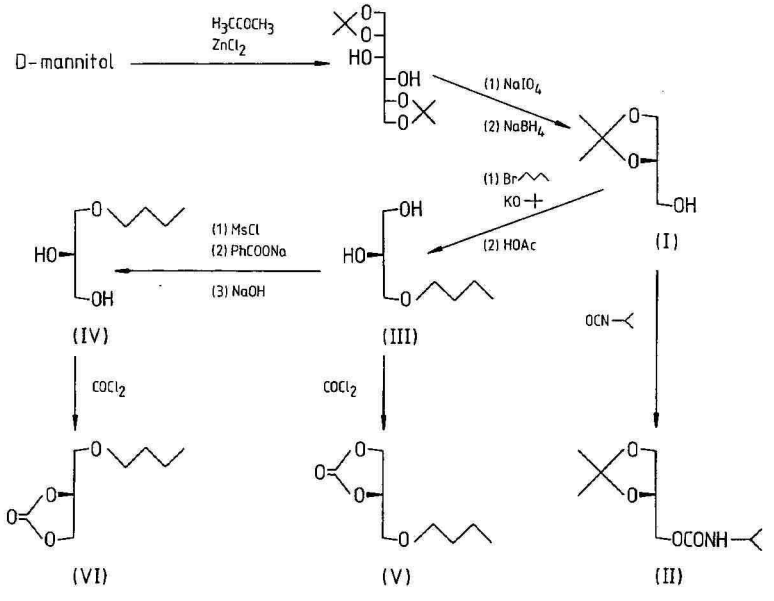

Fig. 1. Synthetic pathway for the preparation of optically active glycerol derivatives. Ms = Methanesulphonyl; Ph = phenyl; Ac = acetyl.

Gas chromatography

The preparation of the chiral stationary phases XE-60-L-valine-(*R*)-α-phenylethylamide and XE-60-L-valine-(*S*)-α-phenylethylamide has been described previously[19]. Fused-silica capillary columns (50 m) with these stationary phases were obtained from Chrompack (Middelburg, The Netherlands). GC measurements were performed with Carlo Erba Model 2101 instruments using split injection and flame ionization detection.

RESULTS AND DISCUSSION

Enantiomeric resolution of chiral alcohols can be achieved in a general way by forming urethanes with isocyanates as derivatizing reagents[16]. This procedure was successfully applied to all kinds of secondary alcohol with XE-60-L-valine-(*S*)-α-phenylethylamide as a chiral stationary phase[20]. However, this method usually fails if the hydroxy group is not directly attached to the chiral centre. In 1,2-isopropylidene glycerol the chiral centre at C-2 is separated from the hydroxy group by a methylene group. Nevertheless, after formation of the isopropyl urethane derivative, the enantiomers are separated under optimal conditions on a 50-m capillary column with XE-60-L-valine-(*S*)-α-phenylethylamide, as demonstrated in Fig. 2. Since the chiral centre is rather far away from the reaction centre, racemization during the derivatization is highly unlikely, thus allowing precise determination of enantiomeric composition.

1,2-Isopropylidene-*sn*-glycerol is also used as a precursor for the preparation of 1(3)-O-alkylated glycerol derivatives. It is therefore of interest to determine the retention of optical purity during this reaction sequence (Fig. 1). In a previous con-

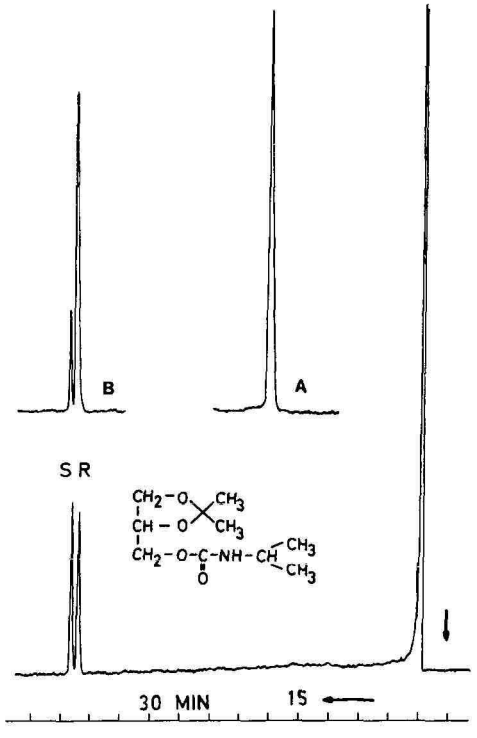

Fig. 2. Enantiomeric separation of isopropylidene glycerol after formation of isopropyl urethane derivative. Insert A: pure (*R*)-enantiomer; insert B: co-injection of racemate and pure (*R*)-enantiomer. (assignment of configuration with respect to underivatized isopropylidene glycerol). Column, 50-m fused-silica capillary with chiral phase XE-60-L-valine- (*S*)-α-phenylethylamide; temperature, 130°C; carrier gas, hydrogen at 1 bar.

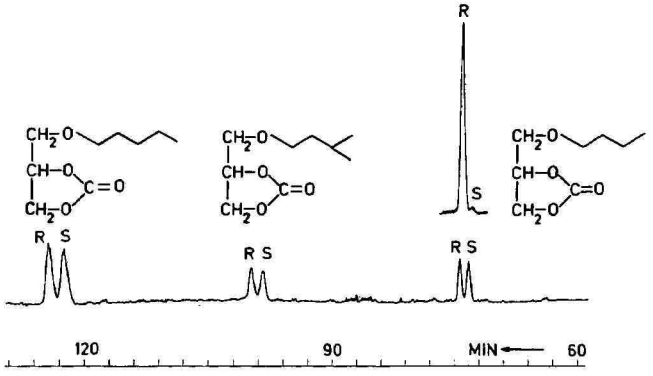

Fig. 3. Enantiomeric separation of 1(3)-O-alkylether derivatives of glycerol after formation of cyclic carbonates. Insert: chromatogram of an almost pure sample of 1-O-*n*-butyl-*sn*-glycero-2,3-carbonate (*R*-enantiomer). Column, 50-m fused-silica capillary with chiral phase XE-60-L-valine-(*R*)-α-phenylethylamide; temperature 120°C; carrier gas, hydrogen at 1 bar.

tribution we have shown that the enantiomers of 1,2-diols can be resolved on capillary columns with XE-60-L-valine-(*R*)-α-phenyl ethylamide after formation of cyclic carbonates with phosgene as reagent[18]. We have prepared the cyclic carbonates of 1(3)-O-alkylated glycerols with methyl, ethyl, isopropyl, isobutyl, *n*-butyl, 3-methylbutyl and *n*-pentyl residues. Baseline separation for the enantiomers is only achieved for the *n*-butyl, 3-methyl-butyl and *n*-pentyl derivatives, as demonstrated in Fig. 3. Only traces of enantiomeric impurities were observed when 'pure enantiomers' were investigated. This proves that alkylation with alkyl bromide and a basic catalyst proceeds without racemization. In accordance with previous observations the (*R*)-enantiomers are eluted after the (*S*)-enantiomers. The procedure described may therefore also be applied to the direct analytical control of enantiomeric purity in the course of ether lipid synthesis, starting from any precursor.

ACKNOWLEDGEMENT

The authors thank Kerstin Dierks for preparative assistance.

REFERENCES

1 R. G. Jensen and R. E. Pitas, *Adv. Lipid Res.*, 14 (1976) 213.
2 F. Paltauf, in H. K. Mangold and F. Paltauf (Editors), *Ether Lipids*, Academic Press, London, 1983, pp. 49–83.
3 H. Eibl, in C. G. Knight (Editor), *From Physical Structure to Therapeutic Applications*, Biomedical Press, Elsevier North-Holland, Amsterdam, 1981, pp. 19–56.
4 H. Eibl, *Angew. Chem.*, 96 (1984) 247.
5 H. Eibl and Wolley, *Chem. Phys. Lipids*, 41 (1986) 53.
6 *Fluka News '85*, Fluka AG, Buchs, p. 36.
7 H. Eibl, *Chem. Phys. Lipids*, 28 (1981) 1.
8 D. R. Kodali, *J. Lipid Res.*, 28 (1987) 464.
9 M. E. Jung and T. J. Shaw, *J. Am. Chem. Soc.*, 102 (1980) 6304.

10 C. M. Lok, J. P. Ward and D. A. van Dorp, *Chem. Phys. Lipids*, 16 (1976) 115.
11 V. Schuring, *Kontakte (Merck)*, No. 1 (1985) 54.
12 J. Bus, C. M. Lok and A. Groenewegen, *Chem. Phys. Lipids*, 16 (1976) 123.
13 J. Bus and C. M. Lok, *Chem. Phys. Lipids*, 21 (1978) 253.
14 G. Hirth and W. Walter, *Helv. Chim. Acta*, 68 (1985) 1863.
15 Y. Itabashi and T. Takagi, *Lipids*, 21 (1986) 413.
16 I. Benecke and W. A. König, *Angew. Chem.*, 94 (1982) 709; *Angew. Chem. Int. Ed. Engl.*, 21 (1982) 709.
17 M. M. Pompipom and R. L. Bugianesi, *Chem. Phys. Lipids*, 35 (1984) 29.
18 W. A. König, E. Steinbach and K. Ernst, *J. Chromatogr.*, 301 (1984) 129.
19 W. A. König, S. Sievers and I. Beneck, in R. E. Kaiser (Editor), *Proceedings Fourth International Symposium on Capillary Chromatography, Hindelang 1981*, Institute for Chromatography and A. Hüthig Verlag, Heidelberg, 1981, p. 703.
20 W. A. König, W. Francke and I. Benecke, *J. Chromatogr.*, 239 (1982) 227.
21 T. Takagi and Y. Itabashi, *J. Chromatogr.*, 366 (1986) 451.

Journal of Chromatography, 410 (1987) 463–465
Elsevier Science Publishers B.V., Amsterdam — Printed in The Netherlands

CHROM. 19 945

Note

Isolation of haem-bearing peptides of haem proteins by the use of adsorption chromatography

ALBERTO CHERSI*, MARIA LUISA TRINCA and ELEONORA MURATTI
Regina Elena Institute for Cancer Research, Viale Regina Elena 291, 00161 Rome (Italy)
(Received July 27th, 1987)

Notwithstanding the availability of fully automatic protein sequencers, the isolation and purification of fragments from complex enzymatic mixtures is still generally required and the recovery of some products may be troublesome. In some cases, direct protein sequencing can be advantageously applied to peptides of particular interest available in reasonable amounts, *e.g.*, when a specific technique enables the isolation of peptides displaying uncommon chemical or physical properties.

In this investigation, we attempted to isolate the haem-bearing peptide(s) from the peptic digest of Pseudomonas cytochrome oxidase using adsorption chromatography on talc. This compound, previously used for the isolation of highly hydrophobic dinitrophenylsulphenyl chloride (DNPS)-treated tryptophan peptides[1–3], might be suitable for the purification of haem-containing fragments, since the porphyrin ring, bound to the polypeptide chain through the cysteines, might confer sufficient hydrophobic properties upon the whole fragment to allow its adsorption on talc columns.

To assess the validity of this approach, a control experiment was first performed on a peptic digest of horse heart cytochrome *c*. A 7-mg amount of protein was digested by pepsin at an enzyme-to-substrate ratio of 2:100, in 0.05 *M* formic acid, at room temperature for 4 h. The digest was lyophilized, dissolved in 2 ml of 0.01 *M* ammonium bicarbonate, then applied to a 4 cm × 1 cm column of talc equilibrated with the same buffer.

The talc for adsorption chromatography was prepared by discarding the fines after suspension of the compound in hot water, and a short period of sedimentation[2]. Chromatography was performed according to the procedure described for the isolation of DNPS-treated tryptophan peptides[2]: the column was washed first with 0.05 *M* ammonium bicarbonate, then with 15% ethanol in bicarbonate and finally with 10% pyridine. The protein peak eluted by the last solvent comprised 94% of the total absorbance at 410 nm loaded onto the column. This fraction, taken to dryness by lyophilization, was then applied to a 100 cm × 0.9 cm column of Sephadex G-25 superfine in 0.05 *M* ammonium bicarbonate containing 5% ethanol. The eluted fractions were monitored at 235 and 410 nm. Apart from slight traces of contaminating materials (7%), the haem peptide emerged as a single symmetric peak. The amino acid composition of this peptide corresponded to that of the undecapeptide 11–21[4].

The same procedure was then employed for the isolation of haem-bearing pep-

0021-9673/87/$03.50

tide(s) of Pseudomonas cytochrome oxidase: 14 mg of this enzyme were kindly provided by Dr. A. Colosimo, University of Rome. The protein had been prepared using immunoaffinity chromatography[5], and was *ca.* 90% pure. A 10-mg amount of this enzyme was digested by pepsin at an enzyme-to-substrate ratio of 2:100, in 0.05 *M* formic acid, at 37°C. The purification procedure for the haem fragment(s) was that described for cytochrome *c*. On G-25 superfine, three peaks were obtained (P1, P2 and P3). The last fraction, colourless, was due to traces of residual pyridine.

The amino acid analysis of an aliquot of P1 and P2 (0.03 mg) is reported in Table I. The samples were first hydrolyzed by 6 *M* hydrochloric acid, at 108°C under vacuum, for 24 h. From peptide P2, carboxypeptidase A (60 min at 37°C, in sodium bicarbonate pH 8.2) liberated 0.9 residues of Leu and 0.6 residues of Val. Leucine aminopeptidase (120 min, in 0.1 *M* Tris buffer pH 8.6 containing 0.001 *M* magnesium chloride) gave 0.8 residues of Gln and traces of Arg. By comparison with the sequence reported for the haem-containing CNBr peptide[6], this fragment may comprise positions 12–21 (Table I). No amino acids were released by digestion of P1 with carboxy peptidases A and B. Leucine aminopeptidase released Asn (0.8 residues), Glu (0.4), Ala (0.4) and traces of Lys. The amino terminal sequence was assumed to be:

TABLE I

AMINO ACID COMPOSITIONS AND PARTIAL SEQUENCES OF THE TWO HAEM-BEARING FRAGMENTS ISOLATED FROM PSEUDOMONAS AERUGINOSA CYTOCHROME OXIDASE

The last sequence corresponds to that reported[6] for the CNBr fragment between positions 3 and 31.

	P1	*P2*
Asp	2.1	
Thr	1.0	
Ser	1.3	
Glu	2.8	1.0
Pro	0.9	
Gly	4.0	2.2
Ala	2.0	1.0
Val	0.8	0.8
1/2 Cys	1.3	1.4
Ile	0.7	
Leu	2.2	0.8
Tyr	0.8	
Phe	1.0	
Lys	2.1	
His	0.9	0.9
Arg	2.2	1.1
Total residues	27	10
Yield (%)	44	41

Sequence:

```
                10                  20                  30
P1  N E A K(Q I Y F Q R C A G C H G V L R K G D T G S P L)
      → → → →
P2                  Q R(C A G C H G)V L
                    → →             ← ←
-F N E A K Q I Y F Q R C A G C H G V L R K G A T G K P L T-
```

Asn-Glu-Ala-Lys-. This fragment may correspond to positions 4–30 of the protein[6]. The resistance of this peptide to carboxypeptidases is consistent with the Pro-Leu sequence at positions 29–30.

When cytochrome oxidase was digested at 37°C for 16 h, formation of the small fragment P2 (yield: 81%) was prevalent while the recovery of P1 was negligible (6%). Apart from the sequence data, this result confirms that both peaks P1 and P2 are derived from the same peptide fragment.

The procedure described appears to be easily applicable to the isolation of the haem-containing peptides from haem proteins, and may be of some practical use, since it does not require sophisticated instruments. Moreover, it should be pointed out that such peptides cannot easily be obtained by chemical synthesis, because of the porphyrin ring linked to Cys 14 and Cys 17 of the enzyme.

ACKNOWLEDGEMENTS

The authors thank Dr. Alfredo Colosimo, University of Rome, for providing the enzyme, and for valuable suggestions.

REFERENCES

1 E. Scoffone, A. Fontana and R. Rocchi, *Biochemistry*, 7 (1968) 971.
2 A. Chersi and R. Zito, *Anal. Biochem.*, 73 (1976) 471.
3 A. Chersi and R. Mage, *Mol. Immunol.*, 17 (1980) 135.
4 E. Margoliash and E. L. Smith, *Nature (London)*, 192 (1962) 1121.
5 M. C. Silvestrini, G. Citro, A. Colosimo, A. Chersi, R. Zito and M. Brunori, *Anal. Biochem.*, 128 (1983) 318.
6 N. Kalkkinen and N. Ellfolk, *Symp. Pap. IUPAC Int. Symp. Chem. Nat. Prod. 11th*, 178 (1978) 79.

Journal of Chromatography, 410 (1987) 466–469
Elsevier Science Publishers B.V., Amsterdam — Printed in The Netherlands

CHROM. 19 957

Note

Improved method for the detection of peroxidase isoenzymes after electrophoretic separation with chlorophyllin, cysteamine and light as a hydrogen peroxide generating system

R. EBERMANN* and H. PICHORNER
Universität für Bodenkultur, Institut für Chemie, Arbeitsgruppe für Lebensmittel-, Umwelt- und Naturstoffchemie, Gregor Mendelstrasse 33, A-1180 Vienna (Austria)
(First received August 3rd, 1987; revised manuscript received August 13th, 1987)

The haem protein peroxidase (E.C. 1.11.1.7) occurs in plants as well as in animals. Many metabolic processes are catalysed by peroxidases, such as lignification, indolyl-3-acetic acid oxidation, cell differentiation, the dimerization of tyrosine in collagen and extensin, and the oxidation of iodide in the thyroid gland [1–5]. Peroxidase is also known to be a stress-indicating enzyme in plants[6]. Its activity is found to be increased in different kinds of stress situation, such as pathogen infection or major changes in environmental conditions[7]. Besides catalase, peroxidase is the most important enzyme in the detoxification of hydrogen peroxide, and it occurs in a multitude of detectable isoenzymes whose physiological role is still under discussion[8,9].

The detection of electrophoretically separated peroxidase isoenzymes by activity-staining is performed by adding the substrate hydrogen peroxide to the incubation solution containing a suitable hydrogen-donating compound, such as benzidine, *o*-dianisidine, ethyl ferulate, or eugenol. A light-induced hydrogen peroxide generation system with rose bengal and glutathione has been described[10]. In this paper we present a more rapid peroxidase detection procedure, consisting of the light sensitizer chlorophyllin as oxygen activator and cysteamine as the reducing agent.

EXPERIMENTAL

Chemicals

Chlorophyllin (sodium–copper salt), rose bengal, *o*-dianisidine, cysteamine and catalase were purchased from Sigma (München, F.R.G.). All other chemicals were of analytical-reagent grade (Merck, Darmstadt, F.R.G.).

Plant material

Wood splinters from chestnut (*Aesculus hippocastanum*) and yew-tree (*Taxus baccata*) were carefully milled and extracted overnight at 4°C (1.0 g in 4 ml of buffer) according to ref. 2.

Polyacrylamide gel electrophoresis (PAGE)

Electrophoresis was performed as reported previously[11]. A volume of 50 μl of

0021-9673/87/$03.50

TABLE I

COMPOSITION OF THE INCUBATION MIXTURE

Component	*Fig. 1*	*Fig. 2*	
		Lane 1	*Lane 2*
Chlorophyllin (m*M*)	1.0	1.0	–
Rose bengal (m*M*)	–	–	0.05
o-Dianisidine (m*M*)	0.1	0.1	0.1
Cysteamine (m*M*)	0.1	0.1	0.1

the crude plant extract was used for one electrophoretic run. PAGE was carried out in a water-cooled block gel apparatus. A separation gel with 15% acrylamide, cross-linked 1:75 with bismethyleneacrylamide (pH 8.6) was used. The electrophoresis buffer was a Tris–glycine system (pH 8.9). For a run of 4 h, a constant voltage of 300 V and a starting current of 100–120 mA were used. After electrophoresis the gels were washed in running water for 1 h and incubated in a solution containing the components listed in Table I. These substances were dissolved in 100 ml of oxygen-saturated phosphate buffer (0.06 *M*, pH 7.0), and the gels were incubated for 2 h at room temperature. During the incubation period, solutions were irradiated with light from a 100 W bulb.

RESULTS

The results of the chlorophyllin–cysteamine light staining technique for peroxidase isoenzymes in shown in Fig. 1. The reaction of peroxidase is inhibited by

Fig. 1. Electrophoretically separated peroxidase isoenzymes stained with *o*-dianisidine in a chlorophyllin–cysteamine light system: chestnut (lane 1), yew-tree (lane 2).

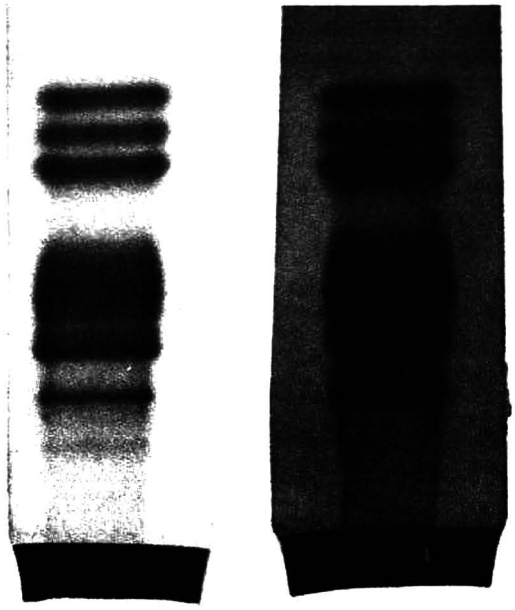

Fig. 2. Electrophoretically separated peroxidase isoenzymes stained with *o*-dianisidine in a chlorophyllin cysteamine–light system (lane 1) and in a rose bengal–cysteamine–light system (lane 2).

catalase (1 U/ml), which provides evidences for the production of hydrogen peroxidase during this reaction (data not shown).

Fig. 2 compares the two staining procedures, chlorophyllin–cysteamine and rose bengal–cysteamine. Both of the dyes are light-activated but rose bengal (lane 2) has the disadvantage of yielding a strong background stain, which chlorophyllin (lane 1) does not give at all. With cysteamine the isoenzyme pattern is completely developed within 2 h, which means a considerable acceleration of hydrogen peroxide production compared with the rose bengal–glutathione system[10].

The proposed mechanism for the formation of hydrogen peroxide includes the following steps: light activation of chlorophyllin, energy transfer from chlorphyllin to oxygen and formation of singlet oxygen, subsequent reduction of singlet oxygen to hydrogen peroxide by cysteamine.

Thus peroxidase detection systems, such as chlorophyllin–cysteamine or rose bengal–cysteamine, avoid an unphysiological excess of hydrogen peroxide in the incubation solution. The hydrogen peroxide produced in the system described is reduced almost simultaneously by *o*-dianisidine or similar phenolic compounds. This is important, since it is known that an excess of hydrogen peroxide might possibly interfere with the common route of peroxidase action (compound I, compound II, free peroxidase) by reducing the ferriperoxidase to enzymically inactive oxyperoxidase (compound III)[12].

REFERENCES

1 J. M. Harkin and J. R. Obst, *Science (Washington, D.C.)*, 180 (1973) 296.
2 R. Ebermann and K. Stich, *Phytochemistry*, 21 (1982) 2401.
3 O. P. Srivastava and R. B. van Huystee, *Can. J. Bot.*, 55 (1977) 2630.
4 D. T. A. Lamport, L. Katona and S. Roerig, *Biochem. J.*, 133 (1973) 125.
5 J. J. Grambow and B. Langenbeck-Schwich, *Planta*, 157 (1983) 131.
6 F. J. Castillo, C. Penel and H. Greppin, *Plant Physiol.*, 74 (1984) 846.
7 B. Halliwell and J. M. C. Gutteridge, *Free Radicals in Biology and Medicine*, Oxford Science Publications, Clarendon Press, Oxford, 1985.
8 L. E. Kay and D. V. Basile, *Plant Physiol.*, 84 (1987) 99.
9 T. Gaspar, T. A. Thorpe and M. Tran Thanh Van, *Acta Horticult.*, 78 (1977) 61.
10 R. Ebermann and W. Gehringer, *J. Chromatogr.*, 348 (1985) 313.
11 R. Ebermann and H. Bodenseher, *Experientia*, 24 (1968) 523.
12 R. Nakajima and I. Yamazaki, *J. Biol. Chem.*, 262 (1987) 2576.

Journal of Chromatography, 410 (1987) 470–473
Elsevier Science Publishers B.V., Amsterdam — Printed in The Netherlands

CHROM. 19 952

Note

Rapid purification of the isoforms of rat liver Cd,Zn-metallothionein by high-performance liquid chromatography

JAROSLAV TURÁNEK*
Institute of Landscape Ecology of the Czechoslovak Academy, Na sádkách 7, 370 05 České Budějovice (Czechoslovakia)
and
JAN KOVÁŘ and HANA ZÁBRŠOVÁ
Department of Biochemistry, Purkynye University, Kotlářská 2, 611 37 Brno (Czechoslovakia)
(Received July 20th, 1987)

Metallothionein was first isolated as a cadmium-containing protein from equine renal cortex by Margoshes and Vallee in 1957[1]. The biological function of metallothionein has not yet been fully clarified, but it is assumed to play some rôle in a wide range of potential homeostatic mechanisms either in catalysis, storage and immune phenomena or in detoxification processes[2].

Isolation procedure commonly used have included fractionation by salts and/or organic solvents, heat treatment, gel filtration and ion-exchange chromatography (IEC). However, gel permeation (GPC) and ion-exchange chromatography are now mostly used[2,3]. For identification of the metallothionein isomers, some authors used high-performance liquid chromatography (HPLC) in combination with atomic absorption spectrophotometry[4–6]. The conventional chromatographic separation of Cd,Zn-metallothionein has several disadvantages, *e.g.*, the sample size and time required.

The aim of the present paper is to describe a quick semipreparative purification using only one HPLC step on a column packed with Spheron-micro DEAE 300.

EXPERIMENTAL

Materials

Rats, weighing 250 g, were fed commercial rat chow *at libidum*. Six subcutaneous injections of cadmium chloride (each 3 mg of cadmium per kg body weight) were administered within 2 weeks. Between each two injections there was one day pause. After the last injection the animals were killed by decapitation under ether narcosis and their livers were stored at −60°C.

Metallothionein preparation

Five rat livers (75 g) were homogenized in two volumes of 10 m*M* Tris–HCl pH 8.5 with 5 m*M* 2-mercaptoethanol (to prevent oxidation) and centrifuged at 20 000 *g* for 30 min. The clear liver extract homogenate was heated at 60°C for 10

min and the precipitate removed by centrifugation at 5000 *g* for 10 min. Metallothionein was precipitated from the supernatant with cold acetone added dropwise to within 50–70%. The precipitate was centrifuged for 10 min at 5000 *g*, resuspended in a small volume (about 2 ml) of 10 m*M* Tris–HCl pH 8.5 and centrifuged at 14 000 *g* for 5 min). The supernatant was rapidly desalted on a glass–PTFE column (100 mm × 12 mm) packed with Sephadex G-25 superfine (Pharmacia, Sweden) equilibrated with 10 m*M* Tris–HCl pH 8.5. All the above steps were monitored by high-performance gel permeation chromatography (HPGPC) on a Superose 12 column (Pharmacia). The column was attached to two pumps (P-500) and a gradient programmer (GP-500) from Pharmacia. 0.15 *M* Sodium chloride in 0.01 *M* Tris–HCl pH 8.5 was used as the mobile phase (flow-rate 1 ml/min). The samples were properly diluted, to enable direct comparison of chromatographic results from different purification steps. The valve V-7 equipped with a 50-μl loop was used to inject the samples. The separations were evaluated by an UV-1 monitor (λ = 254 nm) and a FRAC-100 collector (Pharmacia).

A desalted sample (4 ml) containing metallothionein was applied by a 10-ml superloop (Pharmacia) to an home-made glass–PTFE HPLC preparative column (100 mm × 12 mm) packed with Spheron-micro DEAE (12 μm; Lachema, Czechoslovakia). The column was attached to the above-mentioned chromatographic system. As starting and terminating buffers, 10 m*M* Tris–HCl pH 8.5 and the same buffer with 1 *M* NaCl were used (flow-rate 4 ml/min, back pressure 1.6 MPa).

Chromatographic steps were performed at room temperature. All buffers and samples were filtered through a 0.45-μm filter (Sartorius).

Metallothionein analysis

Metal analysis was carried out by differential pulse polarography (DPP) on a polarograph PRG-4 (Tacussel, France). Cadmium and Zinc were assayed in 0.02 *M* hydrochloric acid by the method of standard additions. Absorption spectra were recorded on a cary 118 spectrometer (Varian, Palo Alto, CA, U.S.A.).

RESULTS AND DISCUSSION

Heating a 30% homogenate to 60°C for 10 min was the first step in the purification protocol. Most of the ballast proteins were precipitated and only thermostable metallothionein, haemoglobin and low-molecular-weight contaminants remained in the supernatant (Fig. 1A). Precipitation with acetone gave a preparation which contained essentially only metallothionein and low-molecular-weight material (Fig. 1B). Rapid desalting on a column of Sephadex G-25 completely removed the low-molecular-weight impurities and acetone resulting from the former step. The purity of the metallothionein preparation with respect to molecular weight is comparable to that obtained by classical GPC on Sephadex G-75 (Fig. 1C). For this reason the time-consuming GPC step was omitted and the desalted sample was directly introduced onto the column of Spheron-micro DEAE. This HPLC purification step is very efficient for the resolution of isometallothioneins from each other (Fig. 2A) so that re-chromatography was not necessary. However, to confirm the homogeneity of the final product, the material was rechromatographed on a MONO Q column (50 mm × 5 mm, Pharmacia) and on Spheron-micro DEAE 300 packed into

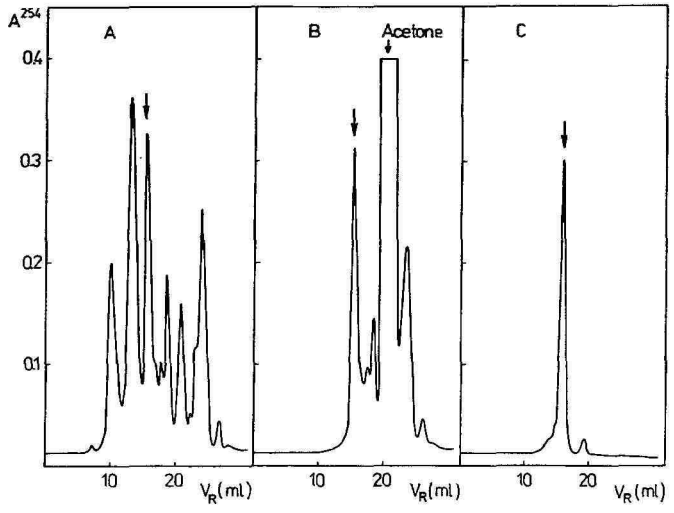

Fig. 1. Chromatography of metallothionein on a Superose 12 column. Buffer: 10 m*M* Tris–HCl pH 8.5 + 0.15 *M* sodium chloride. Flow-rate: 0.75 ml/min. Arrows correspond to metallothionein fraction. About 10 μg of metallothionein in 50-μl sample were applied on the column. (A) Separation of heat-treated homogenate from rat livers. (B) Separation of the acetone-precipitated fraction (50–70%) of the heat-treated homogenate from rat livers. (C) Separation of a desalted preparation resulting from the acetone precipitation.

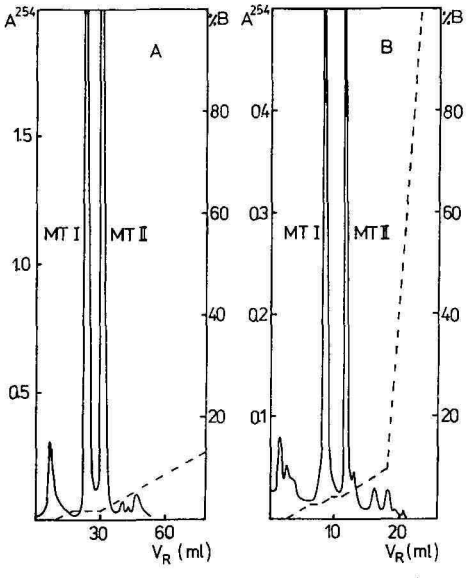

Fig. 2. Chromatographic separation of two isomers of metallothionein (A) Preparative column of Spher-on-micro DEAE 300. Buffers: A = 10 m*M* Tris–HCl pH 8.5; B = 10 m*M* Tris–HCl pH 8.5 + 1.0 *M* sodium chloride. Flow-rate: 4 ml/min. Sample size: 2 ml (about 20 mg of metallothionein). (B) Analytical column of MONO Q. Buffers: as in (A). Flow-rate: 1 ml/min. Sample size: 10 μg of metallothionein in 50 μl of sample.

an analytical home-made glass–PTFE column (70 mm × 5 mm). The results obtained on these two columns are comparable. The separation of isometallothioneins on the MONO Q column is shown in Fig. 2B.

The spectral properties of the isometallothioneins prepared were identical with those described for Cd,Zn-metalllothionein. The purified proteins have a 250 nm/280 nm absorption ratio within the range 17–19 due to the Cd-cysteine coordination complex and aromaric amino acids are absent[2,7,8]. The typical shoulder at 250 nm disappeared after acidification of the sample to pH 1. The molecular weight of metallothionein calculated from the results obtained by GPC on the column of Superose 12 is about 11 000.

Metal analysis by DPP confirmed the presence of cadmium and zinc in the ratio 1.3–2.6. This indicates a variable content of 4–5 cadmium atoms and 2–3 zinc atoms per molecule of metallothionein[2]. No other metals were detectable by DPP in the potential range from 0.0 to −1.3 V.

Under the conditions described above, approximately 9–12 mg of each isoform of Cd,Zn-metallothionein can be recovered in purified form from five rat livers (based on the metal content and spectrophotometric data).

The rapid chromatographic procedure described is suitable for the preparation of homogeneous isoforms of rat liver Cd,Zn-metallothionein in an extremely short time, routinely in 3 h.

EDITOR'S NOTE

Two recent papers in this journal (Chrom. 19 593 and Chrom. 19 632) describe very similar separations. Both these papers had not yet appeared when this manuscript was received by the editor.

REFERENCES

1 M. Margoshes and B. L. Vallee, *J. Am. Chem. Soc.*, 79 (1957) 4813.
2 M. Nordberg and J. H. R. Kägi, *Metallothionein*, Birkhäuser, Basle, 1978.
3 D. R. Winge, R. Premakumar and K. V. Rajagopalan, *Arch. Biochem. Biophys.*, 170 (1975) 242.
4 K. Nomiyama and H. Noyiyama, *J. Chromatogr.*, 228 (1982) 285.
5 K. T. Suzuki, H. Sunaga, Y. Aoki and M. Yamamura, *J. Chromatogr.*, 281 (1983) 159.
6 K. T. Suzuki, *Anal. Biochem.*, 102 (1980) 31.
7 K. B. Nielson and D. R. Winge, *J. Biol. Chem.*, 258 (1983) 13063.
8 J. H. R. Kägi and B. L. Vallee, *J. Biol. Chem.*, 236 (1961) 2435.

Journal of Chromatography, 410 (1987) 474–479
Elsevier Science Publishers B.V., Amsterdam — Printed in The Netherlands

CHROM. 20 047

Note

Coextraction of 5-(hydroxymethyl)-2-furaldehyde with phenolic acids in acid-hydrolyzed plant extracts

JOHN LYDON* and STEPHEN O. DUKE

U.S. Department of Agriculture/Agricultural Research Service, Southern Weed Science Laboratory, Stoneville, MS 38776 (U.S.A.)

and

PAUL A. HEDIN

U.S. Department of Agriculture/Agricultural Research Service, Crop Science Research Laboratory, Mississippi State, P.O. Box 5367, Starkville, MS 39762-5367 (U.S.A.)

(Received September 7th, 1987)

Acid hydrolysis is often used in the extraction of phenolic acids from plant tissues[1,2]. Isolation and identification of phenolic acids is often accomplished using high-performance liquid chromatography (HPLC)[3]. Employing such techniques with a reversed-phase C_{18} column, Murphy and Stutte[4] and Hardin and Stutte[5] reported the presence of gallic acid (based on retention time) in acid-hydrolyzed soybean leaf extracts. While these researchers did not quantify gallic acid, they presented chromatograms indicating that it was the major component in the extracts. Other researchers using similar methods failed to detect gallic acid in acid-hydrolyzed soybean leaf extracts[6,7]. However, they reported the presence of a major, unknown compound that eluted between the retention times of gallic acid and protocatechuic acid. In our studies of plant phenolics, we detected a compound with similar elution characteristics to the previously mentioned unknown in acid-hydrolyzed leaf extracts from a number of plant species. We report here on the identity of this unknown, which probably was previously detected but either unidentified or misidentified by others.

EXPERIMENTAL*

Greenhouse-grown soybean (*Glycine max* L. vc. Davis), pigweed (*Amaranthus retroflexus* L.), ryegrass (*Lolium perenne* L.), and velvet leaf (*Abutilon theophrasti* Medic.) plants were started from seed in 1.2-l pots filled with Jiffy-Mix (Ball Jiffy) potting media and watered with tap water once every four days until seedling establishment. Once established, plants were watered once every other day, with every other watering consisting of a dilute solution of Peters 20-20-20 general purpose

* Mention of a trademark, proprietary product or vendor does not constitute a guarantee or warranty of the product by the U.S. Department of Agriculture and docs not imply its approval to the exclusion of other products or vendors that may also be suitable.

0021-9673/87/$03.50

fertilizer (0.25 g l^{-1}). Yellow nutsedge (*Cyperus esculentus* L.) plants were cultivated similarly except they were started from rhizomes. After 30 days, 5 g fresh weight of leaf tissue were harvested (in the case of soybean only fully expanded fifth trifoliate leaves were used) and extracted using a modified method of Murphy and Stutte[4]. Leaf tissue was ground in a small volume of 2% acetic acid using a mortar and pestle. The slurry was transferred to a boiling flask, brought to 30 ml with 2% acetic acid, and refluxed for 1 h at 100°C. The extract was cooled over ice, brought to room temperature, and suction filtered through Whatman No. 1 filter paper. The filtrate was made 1 *N* hydrochloric acid with addition of 2.9 ml concentrated hydrochloric acid per 32 ml of extract, refluxed 1 h at 100°C, the pH adjusted to 2.5 with concentrated sodium hydroxide, and washed two times with 40 ml HPLC-grade ethyl acetate. The ethyl acetate fractions were combined, evaporated to dryness at 35°C on a rotary evaporator, redissolved in 2 ml HPLC-grade methanol, filtered through a 0.2-μm PTFE syringe filter and analyzed by HPLC. Soybean seed (cv. Centennial) and pith tissue of sugarcane (*Saccharum officinarum* L. var. CP 65-357) were extracted similarly except 1 g dry weight of seed or pith tissue was used.

Except for the column which was a Custom LC 250 × 4.6 mm I.D. Spherisorb 5-μm ODS-I reversed-phase column, the system was composed of Waters Associates HPLC components, which included: two pumps (Model 510), a controller (Model 720), an autosampler (Model 710B), a variable-wavelength detector (Model 490), and a data module (Model 740). The following solvent system and elution profile was used: solvent A, dilute phosphoric acid (pH 2.7); solvent B, HPLC-grade methanol. Elution profile: 0–20 min, 5% B in A at 1.5 ml min^{-1}; 20–30 min, 5–20% B in A at 1.5 ml min^{-1} (linear gradient); 30–50 min, 20% B in A at 1.5 ml min^{-1}. Solvents were filtered through a Gelman Sciences Nylaflo 0.2-μm membrane before use. A sample volume of 5 μl was injected, and detection was performed at 215, 254 or 280 nm. Selection of the wavelength used for detection was automatic and dependent upon the wavelength at which the eluting compound absorbed maximally. After each sample run, the column was washed with 100% B for 10 min at 1.5 ml min^{-1} and then allowed to equilibrate in 5% B in A before reinjection. Retention times and stopped-flow UV-spectral analysis of eluted compounds were compared to that of pure standards of hydroxybenzoic acids (gallic acid, protocatechuic acid, gentisic acid, 4-hydroxybenzoic acid, vanillic acid and syringic acid) and 5-(hydroxymethyl)-2-furaldehyde (HMF).

Stopped-flow UV-spectral analysis was conducted by stopping the solvent flow and trapping the eluting peak in the detector cell. The peak of interest was then scanned from 190 to 350 nm at 1 nm increments and at a speed of 1 nm s^{-1}. Scans were corrected for solvent absorption. Sufficient sample was injected to obtain a response of 0.0990 to 0.110 absorption units at the wavelength of maximal absorption for each peak scanned.

For mass spectral analysis, the same fraction from a series of injections containing the peak of interest (retention time, t_R = 11.84 min) was collected as it eluted from the HPLC column and pooled. The volume was reduced to *ca.* 6 ml under vacuum at 40°C, and loaded on a C_{18} Sep-Pak (previously activated with 3 ml methanol followed by 3 ml deionized water). The Sep-Pak was washed with 6 ml deionized water followed by 6 ml methanol. The methanol eluent was reduced to dryness under vacuum and the residue stored under nitrogen at −10°C until analyzed. Mass spectra

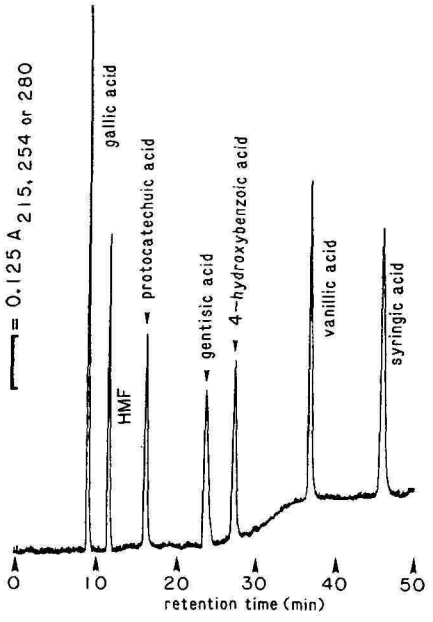

Fig. 1. HPLC elution profile of standards on Spherisorb 5-μm ODS-I. See Experimental section for description of elution system. HMF = 5-(Hydroxymethyl)-2-furaldehyde.

were obtained with a Hewlett-Packard 5985B unit operated in the electron impact mode via insertion of a solid probe.

RESULTS AND DISCUSSION

The elution profile of the standards is presented in Fig. 1. The system used in this study provided better separation of gallate and protocatechuate (Δt_R = 7.3 min, Table I) than that reported in similar studies (Δt_R) ranging from 1 to < 4.5 min[4–7]. All of the hydroxybenzoic acids except 4-hydroxybenzoic acid were monitored at 215

TABLE I

ABSORPTION RATIOS AND RETENTION TIMES (t_R) OF STANDARDS

Compound	*Absorption ratio*		t_R *(min)*
	215/254 nm	*215/280 nm*	
Gallic acid	4.63	2.02	9.19
HMF	0.69	0.13	11.79
Protocatechuic acid	1.82	3.54	16.37
Gentisic acid	5.13	100.00	23.86
4-Hydroxybenzoic acid	0.78	2.19	27.38
Vanillic acid	2.46	4.23	36.86
Syringic acid	8.67	2.49	45.98

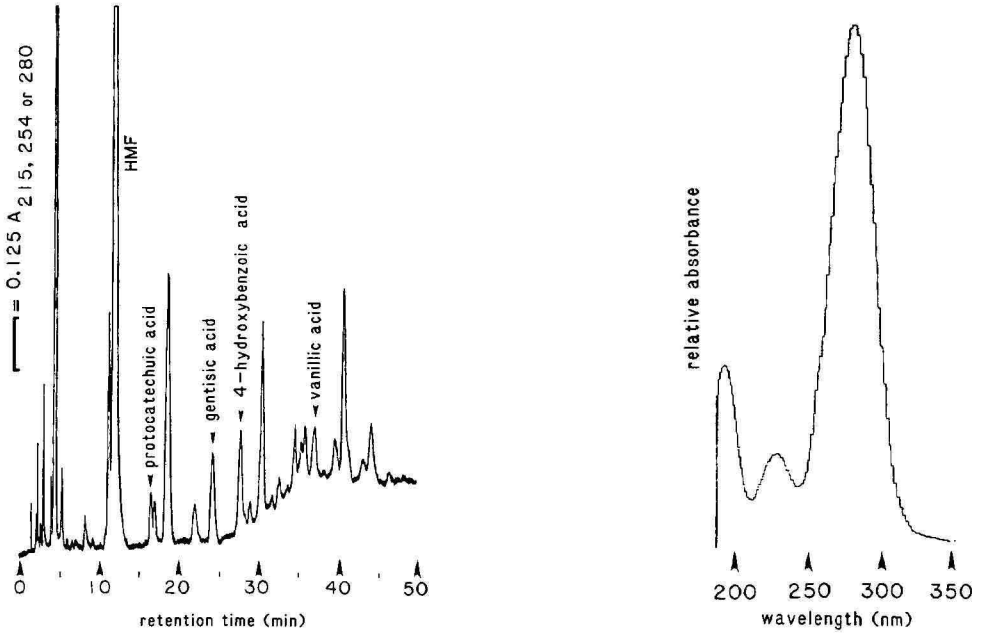

Fig. 2. HPLC chromatogram from acid-hydrolyzed soybean leaf extract. Chromatographic conditions are the same as for the separation of the standards (see Experimental section).

Fig. 3. Spectral absorption of HMF peak (t_R = 11.84 min, Fig. 2) obtained from stopped-flow UV-spectral analysis.

nm, whereas hydroxybenzoic acid was monitored at 254 nm. 5-(Hydroxymethyl)-2-furaldehyde was monitored at 280 nm. The wavelength ratios (Table I) demonstrate that 215 nm is a more efficient wavelength than 254 or 280 nm for detecting hydroxybenzoic acids. Separation of the hydroxybenzoic acids was achieved using a simpler solvent system than that employed by others[4–7], and without the addition of ammonium acetate which would interfer with detection at 215 nm. The pH of the aqueous solvent is crucial because gentisic acid and 4-hydroxybenzoic acid co-elute at pH 2.5.

Gallic acid was not detected in acid-hydrolyzed soybean leaf extracts (Fig. 2).

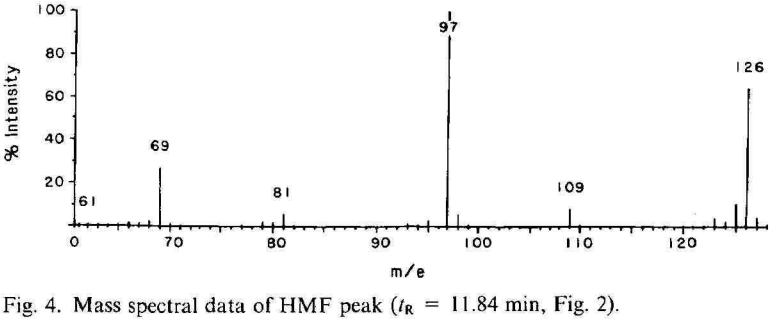

Fig. 4. Mass spectral data of HMF peak (t_R = 11.84 min, Fig. 2).

TABLE II

HMF CONCENTRATION IN ACID-HYDROLYZED EXTRACTS FROM TISSUES OF VARIOUS PLANT SPECIES

Values represent the average of 3 replicates ± 1 S.D. FW = Fresh weight; DW = dry weight.

Species	*Tissue*	*Concentration*	*Units*
Soybean	Leaf	70 ± 19	nmol g^{-1} FW
Soybean	Seed	200 ± 10	nmol g^{-1} DW
Pigweed	Leaf	61 ± 5	nmol g^{-1} FW
Nutsedge	Leaf	236 ± 14	nmol g^{-1} FW
Velvetleaf	Leaf	84 ± 10	nmol g^{-1} FW
Ryegrass	Leaf	131 ± 3	nmol g^{-1} FW
Sugarcane	Pith	181 ± 9	nmol g^{-1} DW

However, other hydroxybenzoic acids such as protocatechuic acid, gentisic acid, 4-hydroxybenzoic acid and vanillic acid were detected in the extracts (Fig. 2). The presence of these hydroxybenzoic acids in acid-hydrolyzed soybean leaf extracts was reported by others[4,5,7].

Stopped-flow UV-spectral analysis of the major component in the extract (Fig. 2; t_R = 11.84 min) produced an absorption spectrum with an absorption maximum at 283 nm, quite unlike that of hydroxybenzoic acids (Fig. 3). Electron impact mass spectral analysis produced a fragmentation pattern (Fig. 4) with *m/e* 126 (M^+), 125, 109, 97, 81 and 69. The mass spectra, absorption spectrum and t_R of pure HMF (not shown) matched that of the major component in the extract. Thus we propose that the compound was HMF. HMF was present in varying quantities in acid-hydrolyzed extracts from tissues of all plant species sampled (Table II). The presence of HMF in these extracts is not surprising considering that HMF is a breakdown product of acid-hydrolyzed sugars[8].

Using HPLC and detection at 280 nm, Buta[6] reported that an acid-hydrolyzed soybean leaf extract contained a major, unidentified compound which eluted between gallic acid and protocatechuic acid. Given the relative retention time of HMF with respect to gallic acid and protocatechuic acid, the frequency of appearance of HMF in acid-hydrolyzed leaf extracts of various plant species, and the relative abundance of it in acid-hydrolyzed soybean leaf extracts, it would appear that the unknown compound in Buta's study was HMF. For similar reasons, as well as the failure of several independent studies to detect gallic acid in acid-hydrolyzed soybean leaf extracts, and because the soybean cultivar used in this study was the same used by Murphy and Stutte[4], we believe that the compound Murphy and Stutte and Hardin and Stutte[5] identified as gallic acid was likely HMF.

CONCLUSION

The HPLC system used in this study provided excellent separation of the hydroxybenzoic acids typically found in plant extracts. The use of low-UV-absorbing solutes and solvents in the solvent system permitted detection at 215 nm which is more efficient for the detection of most hydroxybenzoic acids than conventionally used wavelengths (*i.e.*, 254 or 280 nm). The analysis of extracts from tissues of several

plant species indicated that HMF, an artifact of acid hydrolysis, is typically co-extracted with phenolic acids. Although a number of hydroxybenzoic acids were detected in acid-hydrolyzed soubean leaf extracts, gallic acid was not one of them. Our results indicate that a major constituent in acid-hydrolyzed soybean leaf extracts previously indentified as gallic acid was HMF.

REFERENCES

1 P. Ribereau-Gayon, *Plant Phenolics*, Harner Publ., New York, 1972.
2 J. B. Harborne, *Phytochemical Methods, a Guide to Modern Techniques of Plant Analysis*, Chapman and Hall, London, 1984.
3 D. A. Roston and P. T. Kissinger, *J. Liq. Chromatogr.*, 5 (Suppl. 1) (1982) 75.
4 J. B. Murphy and C. A. Stutte, *Anal. Biochem.*, 86 (1978) 220.
5 J. M. Hardin and C. A. Stutte, *Anal. Biochem.*, 102 (1980) 171.
6 J. G. Buta, *J. Chromatogr.*, 295 (1984) 506.
7 P. M. Porter, W. L. Banwart and J. J. Hassett, *Environ. Exp. Bot.*, 26 (1986) 65.
8 K. Kim and M. K. Hamdy, *Biotechnol. Bioeng.*, 27 (1985) 316.

Journal of Chromatography, 410 (1987) 480–483
Elsevier Science Publishers B.V., Amsterdam — Printed in The Netherlands

CHROM. 20 040

Note

Determination of glycerol in pig plasma by capillary gas chromatography

M. FENTON* and F. X. AHERNE
Department of Animal Science, University of Alberta, Edmonton, Alberta T6G 2P5 (Canada)
(Received September 1st, 1987)

The concentration of glycerol in plasma reflects lipolysis in adipose tissue and can provide an approximate index of fat mobilization. Therefore, a simple and accurate measurement of glycerol in plasma is a very useful tool in understanding diet induced changes in fat metabolism.

Various enzymatic methods for glycerol determination have been published[1–4]. Most of these procedures can be complicated by the presence in plasma of interfering compounds[1] which cannot be completely eliminated during sample preparation. Though there are many procedures for determination of glyceride glycerol by gas chromatography (GC) there are very few methods that are specific for glycerol. The published methods for the GC determination of glycerol[5,6] used packed columns which require long analysis time and lack the resolution and sensitivity necessary for determining plasma glycerol levels. Therefore, a GC method using a capillary column was developed and tested for the quantitative analysis of glycerol in pig plasma.

MATERIALS AND METHODS

Sylon TP (trimethylsilylimidazole–pyridine, 1:4) was obtained from Supelco (Oakville, Canada). Glycerol 99.5% was from Aldrich (Milwaukee, WI, U.S.A.) and 1-dodecanol 98% was purchased from Fisher Scientific (Edmonton, Alberto, Canada). Blood plasma was collected hourly for 24 h on day 2 and 28 of lactation from multiparous sows given high or low levels of feed.

Plasma samples (0.5 ml) were deproteinized in micro centrifuge tubes by adding 1 ml of 95% ethanol. After mixing, tubes were centrifuged for 5 min in an Eppendorf centrifuge, and duplicate 0.5-ml samples were transferred into 1.8-ml mini-vials with screw caps and PTFE-lined septa and evaporated to dryness at room temperature under vacuum.

A 20-μl volume of the internal standard, 1-dodecanol (3 mg/ml in pyridine), and 100 μl of Sylon TP were added to each vial. Trimethylsilyl (TMS) derivatives were formed by heating at 70°C for 20 min and 1 μl was injected into the gas chromatograph. Glycerol standards in a concentration range of 4–17 μg/ml were subjected to the same procedure as the samples. The relative response factor was calculated as the ratio of internal standard peak area to glycerol peak area multiplied by the ratio of the amount of glycerol to that of 1-dodecanol in the standard.

0021-9673/87/$03.50

A Varian Model 3700 gas chromatograph equipped with a flame ionization detector and a splitter injector was used. A 30 m × 0.25 mm I.D., fused-silica SE-30 capillary column, film thickness 0.25 μm (J & W Scientific, Rancho Cordova, CA, U.S.A.), was used under the following conditions: oven temperature was programmed to rise from 110°C to 300°C at a rate of 20°/min after an initial hold for 4 min; injector and detector temperatures were both at 300°C. A split injection mode (1:15) was used with nitrogen carrier gas flow of 1.0 ml/min through the column, and 30 ml/min as the make-up gas to the detector. Air and hydrogen gas flows to the detector were 300 and 30 ml/min, respectively. Quantitation was achieved by measuring peak area using a Hewlett-Packard Series 3353 laboratory automation system (Avondale, PA, U.S.A.).

RESULTS AND DISCUSSION

A chromatogram of the TMS derivatives of glycerol and internal standard mixture is shown in Fig. 1A. The application of our method to normal pig plasma is demonstrated in Fig. 1B. Glycerol and the internal standard were eluted in 6.0 and 8.8 min, respectively, and excellent separation was achieved between the solvent peak, glycerol, internal standard and the later eluting compounds. By using a capillary column the analysis time can be reduced from 60 min[6] to 15 min for plasma samples and superior resolution resulted compared to a packed column[5].

The silylating reagent N-(*tert*-butyldimethylsilyl)-N-methyl-trifluoroacetamide (MTBSTFA) was tried but the reagent peak interfered with the elution of glycerol. Since any unevaporated water in the sample will first react with the derivatizing reagent it is important to have excess reagent as reported by others[7].

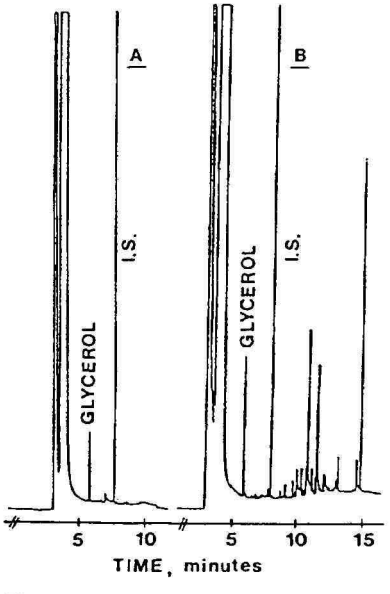

Fig. 1. GC separation of TMS derivatives of glycerol and 1-dodecanol as internal standard (I.S.) in (A) a standard, (B) pig plasma. For conditions of analysis see text.

TABLE I

RECOVERY OF GLYCEROL ADDED TO PLASMA

All analysis were performed on duplicate samples.

Glycerol concentration (μg/ml)				*Recovery (%)*
In sample	*Added*	*Total known*	*Total determined*	
1.85	2.66	4.51	4.55	100.9
2.83	2.66	5.49	5.81	105.8
1.00	1.60	2.60	2.63	101.2
1.00	3.20	4.20	4.22	100.5
1.00	4.80	5.80	5.78	99.6
Mean				101.60
S.D.				2.42
Coefficient of variation (%)				2.38

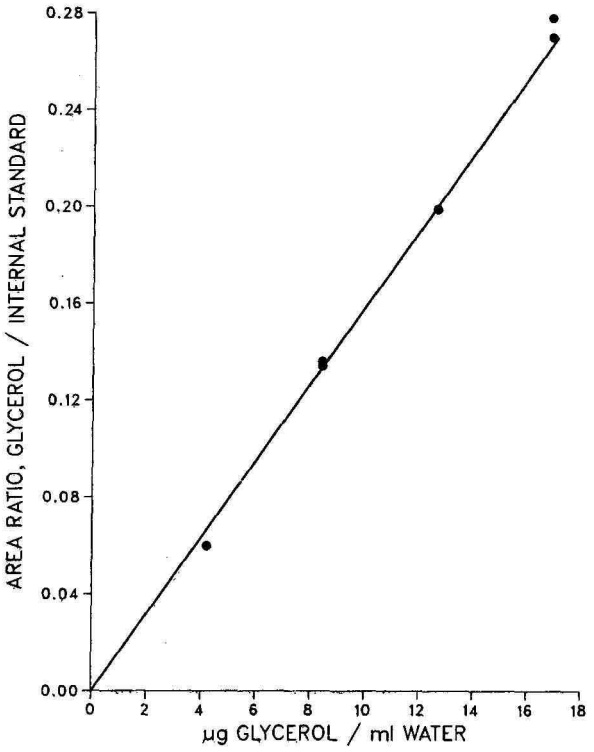

Fig. 2. Glycerol standard curve. Concentration of glycerol is plotted against the area ratio of glycerol to that of internal standard. Two separate measurements for each concentration of glycerol are shown.

There was considerable evaporation of glycerol when dried at higher temperatures (*e.g.* 70–100°C) for a long time. Therefore, it was necessary to perform the evaporation at room temperature in a desiccator with a vacuum pump, which resulted in negligible loss of glycerol. 1-Dodecanol was added to the sample and standards dissolved in pyridine thus eliminating any need for evaporation after addition. Derivatives were found to be stable for 2–3 days if capped tightly to prevent moisture from entering.

Table I shows the results obtained when a recovery study was carried out. Known amounts of glycerol standard were added to different samples of pig plasma and the recoveries were found to be between 99.6 and 105.8.

Linearity of response was demonstrated (Fig. 2) between the ratio of peak areas of glycerol to internal standard and the amount of glycerol in the range 0–17 μg glycerol.

The reproducibility of the method was tested by analyzing twenty pig plasma samples in duplicate. The mean glycerol concentration of twenty measurements was 5.58 μg/ml with a range of 4.14–8.57 μg/ml plasma, the higher levels being encountered with sows fed restricted levels of feed. The coefficient of variation of 1.98% showed excellent precision for this analysis.

The sensitivity of the method is in the same order as was obtained using a fluorometric method[3] and superior to enzymatic glycerol food analysis Kit-UV method (Boeringer-Mannheim) and GC methods using packed columns. The procedure can easily be automated to enable more samples to be analyzed in a day by using an autosampler.

The relatively simple procedure for sample preparation using ethanol as deproteinizing reagent eliminates the need for adding strong acid followed by base to neutralize the sample[1].

Analyzing TMS derivatives of glycerol on a capillary column provides superior resolution, sensitivity, reproducibility and speed of analysis.

ACKNOWLEDGEMENTS

We wish to thank Dr. Elizabeth Lythgoe for supplying the pig blood plasma samples and Terry Fenton for his advice and support.

REFERENCES

1 J. H. Hagen and P. B. Hagen, *Can. J. Biochem. Physiol.*, 40 (1962) 1129.
2 C. S. Frings and H. L. Purdue, *Anal. Chim. Acta*, 34 (1966) 225.
3 L. H. Boobis and R. J. Maughan, *Clin. Chim. Acta*, 132 (1983) 173.
4 O. Wieland, in H. U. Bergmeyer (Editor), *Methods of Enzymatic Analysis*, Vol. 6, Verlag Chemie, Weinheim, 3rd ed., 1984, p. 504.
5 J. Blum and W. R,. Koehler, *Lipids*, 5 (1970) 601.
6 R. M. Matarese and C. Zamponi, *J. Chromatogr.*, 273 (1983) 398.
7 D. Valdez, *J. Chromatogr. Sci.*, 23 (1985) 128.

Journal of Chromatography, 410 (1987) 484–487
Elsevier Science Publishers B.V., Amsterdam — Printed in The Netherlands

CHROM. 19 960

Note

Capillary gas chromatography of neutral sugars as their aldononitrile acetates from the hydrolyzate of corn bran residues

HAN-PING LI
Environmental Protection Research Institute of the Ministry of Light Industry, Beijing (China)
(First received April 22nd, 1987; revised manuscript received June 29th, 1987)

Since high-performance liquid chromatography (HPLC) allows direct injection of samples with no or little pretreatment and sugars are not subject to high temperature, HPLC in aqueous solutions has become a superior technique to gas chromatography (GC) for separating the sugars L-arabinose, D-xylose, D-mannose, D-glucose and D-galactose in biomass and related products, *e.g.*, woods, pulps and papers[1–3]. However, the instrument costs are higher than in GC and HPLC is not as commonly used as GC, especially in the developing countries. Moreover, there is a lack of universal detectors as sensitive as those employed for GC, which has limited the applications of HPLC to sugar analysis. Although pre- and post-column derivatizations can improve the detection of sugars, they negate some of the advantages of HPLC mentioned.

Capillary GC has been widely used for the analysis of sugars because of its high resolution and good sensitivity. As regards the simplicity of the chromatogram and stability of the derivatives for GC separation, alditol acetates and aldonitrile acetates are good choices. Good separation of sugars as their alditol acetates has been obtained on many capillary columns[4–8]. However, the retention times of the alditol acetates are relatively long, furthermore their preparation from monosaccharides is more complicated and time-consuming than that of aldononitrile acetates. The retention times of sugars as their aldononitrile acetates on a glass capillary column (60 m × 0.3 mm) coated with the non-polar stationary phase SE-30 are also relatively long[9–11]. The separation of sugars as their aldononitrile acetates on a fused-silica capillary column (50 m × 0.2 mm) coated with the apolar stationary phase OV-1 has given excellent results in terms of both the resolution and retention times[12]. However, fused-silica capillary columns are not available for routine analysis in many laboratories because of the expense.

In this paper the separation of the wood sugars as their aldonotrile acetates on glass capillary columns coated with polar stationary phases is presented. Two types of glass capillary columns were investigated in the experiments. The five sugars could be nearly baseline separated on the two columns within 12 min. Application of this method to the hydrolyzate of corn bran residues is described.

EXPERIMENTAL

Capillary GC separation was carried out by a Pye Unicam Series 204 chro-

0021-9673/87/$03.50

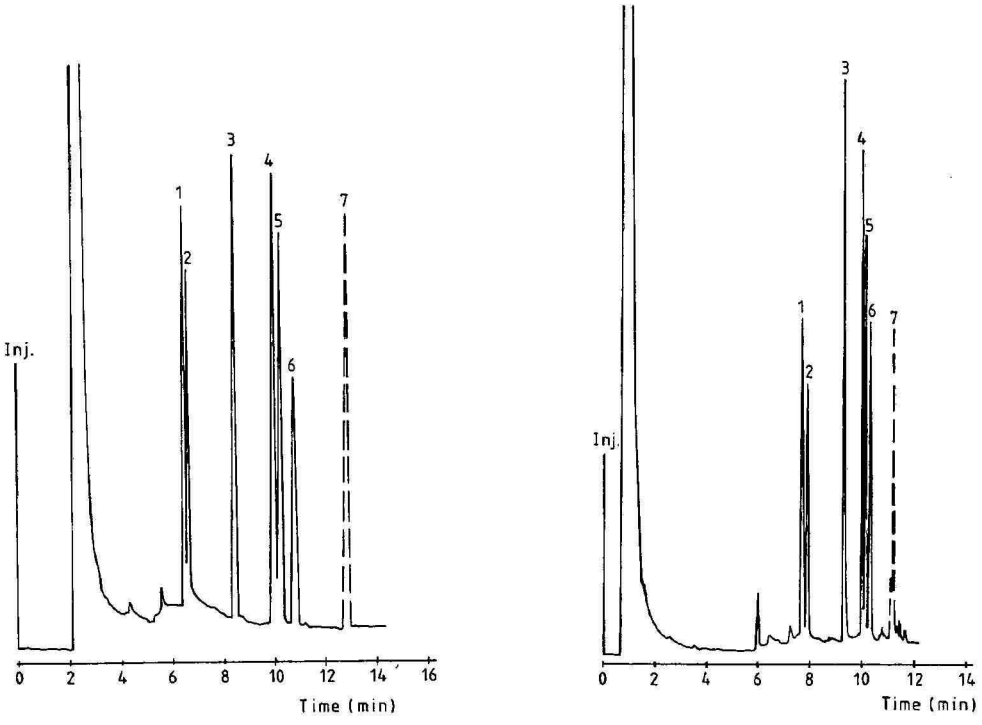

Fig. 1. Gas chromatogram of a standard mixture of the five aldononitrile acetates, arabitol acetate and inositol acetate on the OV-17 capillary column (25 m × 0.5 mm I.D.). Column temperature: 200°C for 4 min, then at 12°C/min to 235°C. Peaks: 1 = L-arabinose; 2 = D-xylose; 3 = arabitol; 4 = D-mannose; 5 = D-glucose; 6 = D-galactose; 7 = inositol (dotted line).

Fig. 2. Gas chromatogram of a standard mixture of the five aldononitrile acetates, arabitol acetate and inositol acetate on the OV-73 column (27 m × 0.3 mm I.D.). Column temperature: 120°C for 3 min, then at 12°C/min to 210°C. Peaks as in Fig. 1.

matograph equipped with flame ionization detection and a PM 8252 dual-pen recorder. Capillary columns: 25 m × 0.5 mm I.D. OV-17, glass, temperature 200°C for 4 min, then at 12°C/min to 235°C; 27 m × 0.3 mm I.D. OV-73, glass, temperature 120°C for 3 min, then at 12°C/min to 210°C. Other GC conditions: injection port, 235°C; detector, 300°C; carrier gas, nitrogen at 2 ml/min; make-up gas, nitrogen at 30 ml/min; splitting ratio, 20:1; sample injection volume, 0.5 μl.

Instead of inositol or inositol acetate, arabitol was used as the internal standard in this work. All reagents and materials used were commercially available from various sources. Standard mixtures of the aldononitrile acetate derivatives of the five sugars were prepared according to the method described[13].

For quantitative analysis, 100 mg of corn bran residues were weighed accurately, 2 ml of 72% sulphuric acid solution were added and the mixture was kept at 30°C for 30 min. Then, the sample was diluted in distilled water to 2% sulphuric acid. A 2-ml aliquot of arabitol standard solution (5.00 mg/ml) was added. Secondary hydrolysis occurred at 105°C for 2 h. After cooling to room temperature, the hydrolyzate was neutralized by saturated barium hydroxide solution to about pH 5. The

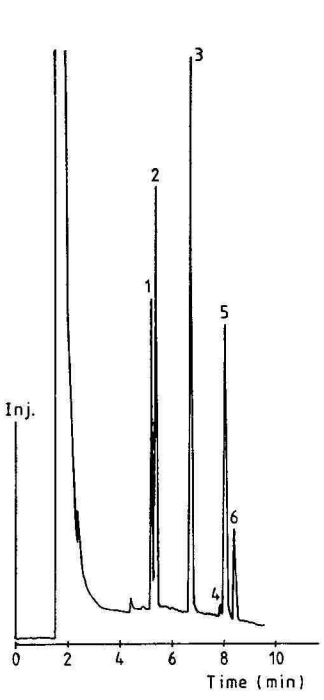

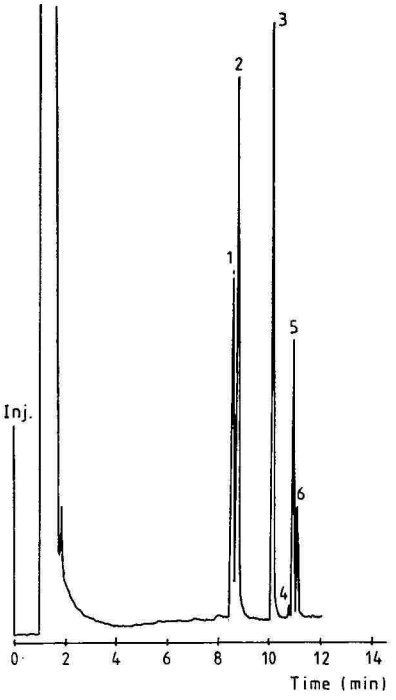

Fig. 3. Gas chromatogram of arabitol acetate and the aldononitrile acetates of the monosaccharides from the hydrolyzate of corn bran residues on the OV-17 column. Details as in Fig. 1.

Fig. 4. Gas chromatogram of arabitol acetate and the aldononitrile acetates of the monosaccharides from the hydrolyzate of corn bran residues on the OV-73 column. Details as in Fig. 2.

filtered solution was evaporated to dryness with a rotatory evaporator. The dry residue was then derivatized to the aldononitrile acetates using the same method as for the standard mixture.

Identification was according to the retention times of the aldononitrile acetates of the individual sugars.

RESULTS AND DISCUSSION

The capillary GC separations of the wood sugars as their aldononitrile acetates on the OV-17 and the OV-73 columns are shown in Figs. 1 and 2, respectively. Near-baseline separation of the five aldoses and the internal standard arabitol was obtained on both columns in about 12 min. In this work, the resolution efficiency of the five sugars and arabitol on the OV-73 column was higher than that on the OV-17 column. This might be due to two main reasons. First, the internal diameter of the OV-17 column is larger than that of the OV-73 column. Secondly, the polarity of the former is higher than that of the latter.

Inositol was usually used as the internal standard. It is time-consuming to obtain a quantitative yield of inositol acetate from inositol. Further more, the solu-

TABLE I

SUGAR COMPOSITIONS OF THE CORN BRAN RESIDUES

Component	*% in total sugars*	*% in the corn bran residues**	*Relative standard deviation (%)*
L-Arabinose	25.9	13.3	6.2
D-Xylose	41.5	21.3	4.2
D-Mannose	1.2	0.6	5.7
D-Glucose	21.2	10.9	11
D-Galactose	10.1	5.2	5.1
Total	99.9	51.3	

* The corn bran residues were dried at 105°C for 3 h.

bility of inositol acetate in water is too low to be used as the internal standard. Arabitol was therefore used for this purpose.

Figs. 3 and 4 show GC separations of the neutral sugars from the hydrolyzate of corn bran residues on the OV-17 and the OV-73 column, respectively. The analytical sugar compositions listed in Table I were obtained on the OV-73 column. It is seen that carbohydrates are the major components in the corn bran residues and are mainly in the form of hemicellulose (arabinoxylan).

The results of this work are comparable to those of Bradbury *et al.*[14]. However, the present ratio of D-glucose to total sugars is higher than that in their paper. The corn bran residues which are a by-product of starch manufacture using corn as the raw material may contain a certain amount of residual starch. Moreover, the D-glucose in the hydrolyzate of the corn bran residues may originate from the cellulose which releases D-glucose in the two-step hydrolysis.

ACKNOWLEDGEMENTS

I thank Professor Ge Chun-Lin, Chief engineer You Xin and Lin Yong-Shou for their interest, Dr. Xie Tian-Min for supplying the capillary columns, reviewing this manuscript, and for his helpful discussions in many fields.

REFERENCES

1 F. E. Wentz, A. D. Marcy and J. Gray, *J. Chromatogr. Sci.*, 20 (1982) 349.
2 M. G. Paice, L. Jurasek and M. Desrochers, *Tappi*, 65 (1982).
3 R. C. Pettersen, V. H. Schwandt and M. J. Effland, *J. Chromatogr. Sci.*, 22 (1984) 478.
4 G. Holzer, J. Oró, S. J. Smith and V. M. Doctor, *J. Chromatogr.*, 194 (1980) 410.
5 C. Green, V. M. Doctor, G. Holzer and J. Oró, *J. Chromatogr.*, 207 (1981) 268.
6 J. Klok, E. H. Nieberg-Van Velzen, J. W. De Leeuw and P. A. Schenck, *J. Chromatogr.*, 207 (1981) 273.
7 R. Oshima, A. Yoshikawa and J. Kumanotani, *J. Chromatogr.*, 213 (1981) 142.
8 R. Oshima, J. Kumanotani and C. Watanabe, *J. Chromatogr.*, 250 (1982) 90.
9 J. Szafranek, C. D. Pfaffenberger and E. C. Horning, *Anal. Lett.*, 6 (1973) 63.
10 C. D. Pfaffenberger, J. Szafranek, M. G. Horning and E. C. Horning, *Anal. Biochem.*, 63 (1975) 501.
11 C. D. Pfaffenberger, J. Szafranek and E. C. Horning, *J. Chromatogr.*, 126 (1976) 535.
12 O. Guerrant and C. W. Moss, *Anal. Chem.*, 56 (1984) 633.
13 R. Varma, R. S. Varma and A. H. Wardi, *J. Chromatogr.*, 77 (1973) 222.
14 A. G. W. Bradbury, D. J. Halliday and D. G. Medcalf, *J. Chromatogr.*, 213 (1981) 146.

Journal of Chromatography, 410 (1987) 488–493
Elsevier Science Publishers B.V., Amsterdam — Printed in The Netherlands

CHROM. 19 995

Note

Determination of *Catharanthus* alkaloids by reversed-phase high-performance liquid chromatography

TOIVO NAARANLAHTI*, MERVI NORDSTRÖM and AARRE HUHTIKANGAS
Department of Pharmaceutical Chemistry, University of Kuopio, POB 6, SF-70211 Kuopio (Finland)
and
MAURI LOUNASMAA
Laboratory for Organic and Bioorganic Chemistry, Technical University of Helsinki, SF-02150 Espoo (Finland)
(First received April 24th 1987, revised manuscript received August 11th, 1987)

High-performance liquid chromatography (HPLC) on a reversed-phase column is commonly used for alkaloid analysis. Indole alkaloids of *Catharanthus roseus* (L.) G. Don can be eluted on reversed-phase columns[1,2] using gradient systems for plant extracts[3] and isocratic systems for cell extracts[4–6] with either UV[1–5] or fluorometric[6] detection.

UV detection is widely used in the analysis of alkaloids from intact plants and cell cultures. However, there are difficulties in peak identification and in evaluation of the purity of separated peaks. As an attempt to overcome these problems, fractionation of plant extracts before HPLC analysis[3,4] is tedious and time-consuming, and the measurement of plate numbers[3] is limited to simple mixtures of components. A simple and rapid method is described here for alkaloid recognition and peak purity evaluation with dual-wavelength absorbance ratio plots and scanned UV spectra. The present investigation deals with the utilization of these techniques in developing a reversed-phase HPLC method for indole alkaloids.

The HPLC gradient method presented in this paper was developed for the quantitative determination of catharanthine and vindoline from leaves of *C. roseus* to select high-producing plants for cell culture studies. In addition to vindoline and catharanthine, the related indole alkaloid serpentine and the bis-indole alkaloids vinblastine and vincristine can also be quantified by this method.

EXPERIMENTAL

Apparatus

A Beckman 342 gradient liquid chromatograph, equipped with two Beckman 114 M solvent-delivery modules, a Beckman 420 controller, a Beckman 165 variable-wavelength detector and an Altex 210 A loop injector (20-μl loop volume) were used. The chromatograms were recorded with a Goerz Se 120 two-channel recorder and integrated with a Shimazu C-RIA Chromatopac integrator.

0021-9673/87/$03.50

Chemicals

Catharanthine hydrochloride and vindoline were generously provided by Prof. W. G. W. Kurz (Plant Biotechnology Institute, National Research Council, Saskatoon, Canada). Serpentine tartrate was purchased from ICN, K&K Labs. (New York, NY, U.S.A.), and ajmalicine hydrochloride, vinblastine sulphate and vincristine sulphate from Sigma (St. Louis, MO, U.S.A.).

HPLC conditions

A Brownlee cartridge column (220 × 4.6 mm I.D.) packed with Spheri-5 RP (18.5 μm) and a guard column (15 × 3.2 mm I.D.) packed with Aquapore ODS (7 μm) were used. Two gradient systems were established: system I for leaf samples and system II for root samples.

System I was methanol–acetonitrile–0.025 *M* ammonium acetate–triethylamine at an initial ratio of 13:32:55:0.2 changing to 19:46:35:0.2. The pH of the buffer was 6.8.

System II was also methanol–acetonitrile–0.025 *M* ammonium acetate–triethylamine, but at an initial ratio of 18:27:55:0.2 changing to 26:39:35:0.2. The pH of the buffer was 7.5.

The gradient profiles are presented in Figs. 1 and 2, respectively. The initial flow-rate was 1.0 ml/min, and after 17 min it was increased to 1.5 ml/min. The UV detection wavelengths were 280 and 254 nm. The ratio threshold was set to 2%.

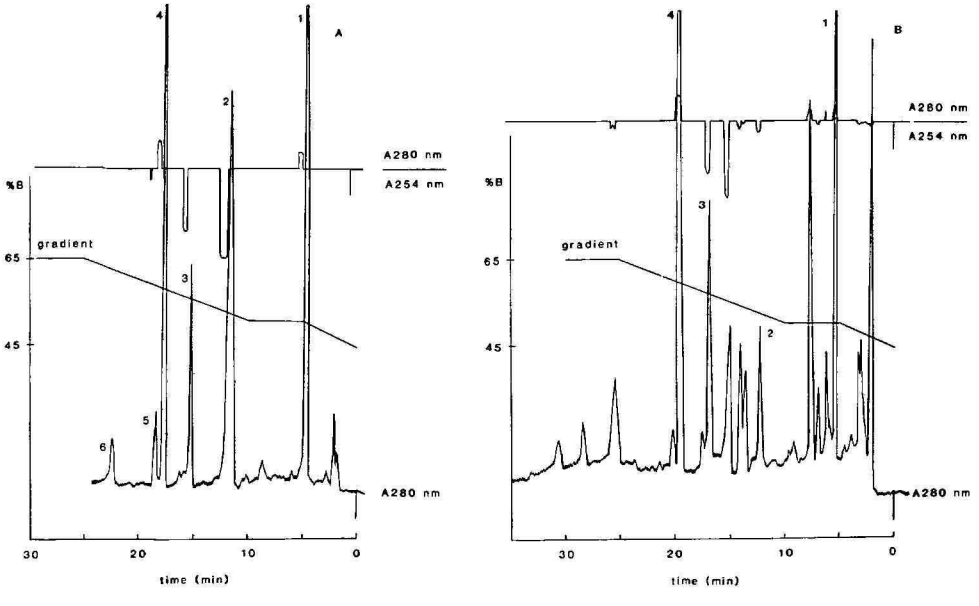

Fig. 1. Chromatograms of a standard mixture (A) and a leaf sample of *C. roseus* (B). Peaks: 1 = methoxytryptamine; 2 = serpentine; 3 = vindoline; 4 = catharanthine; 5 = vincristine; 6 = vinblastine. Gradient system I; pH 6.8; chromatographic details as in text.

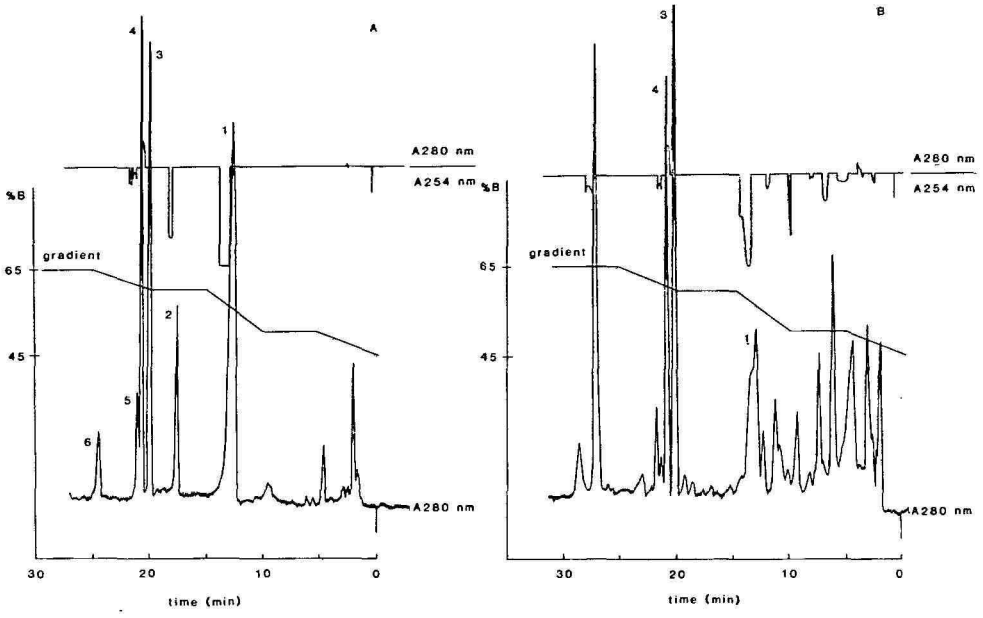

Fig. 2. Chromatograms of a standard mixture (A) and a root sample of *C. roseus* (B). Peaks: 1 = serpentine; 2 = vindoline; 3 = catharanthine; 4 = ajmalicine; 5 = vincristine; 6 = vinblastine. Gradient system II; pH 7.5; chromatographic details as in text.

Sample preparation

Dried leaf and root samples (25 mg of leaves and 10 mg of roots) were extracted and purified according Morris *et al.*[7], except that ethanol was used as an extracting solvent instead of methanol.

To the leaf samples 5-methoxytryptamine (18 μg/ml) was added as an internal standard. For calibration curves standard solutions of catharanthine (30–110 μg/ml) and vindoline (52–156 μg/ml) were prepared and processed in the same way as the plant extracts.

RESULTS AND DISCUSSION

Crude extracts were purified with the solid phase extraction columns applying ion-pair liquid chromatography. Results from the recovery test of the plant extraction process of catharanthine and vindoline are presented in Table I.

The recovery of the purification procedure from standard solutions (catharanthine, vindoline, ajmalicine, serpentine, vinblastine and vincristine) was *ca.* 100%.

HPLC analysis

In spite of the wide range of their solubilities, molecular weights and polarities, a good chromatographic separation of the alkaloids of interest was achieved (Fig. 1). A short analysis time (30 min) with an excellent peak symmetry was obtained by gradient elution. Although reversed-phase chromatography has been widely used in HPLC applications for alkaloid analysis, problems still exist. These compounds can

TABLE I

RECOVERY OF CATHARANTHINE AND VINDOLINE ADDED TO GROUND LEAF MATERIAL OF *C. ROSEUS*

	Amount added (μg)	*Amount found (μg)*	*Recovery (%)*
Vindoline	25	25.72	102.9
	60	61.62	102.7
Catharanthine	20	20.04	100.2
	60	56.76	96.6

give rise to a poor column efficiency and asymmetrical tailing peaks, attributable to a dual-retention mechanism[1,8,9].

Lipophilic amines can be used to convert a dual-retention mechanism into a solvophobic mechanism. In the present study triethylamine was added to the mobile phase: this compound effectively reacts with the residual silanol groups[10]. The NH_4^+ ion from ammonium acetate buffer salt has also a masking effect on these silanol groups[11].

The analytical parameters of the HPLC assay of catharanthine and vindoline are listed in Table II.

Ajmalicine, present only in root samples of *C. roseus*, was coeluted with catharanthine under the HPLC conditions selected for leaf samples. Ajmalicine and catharanthine could be separated by increasing the pH of the mobile phase to 7.5 (Fig. 2).

Evaluation of the peak purity

Real-time absorbance ratio plots and rapidly scanned UV spectra provided by a multiple-wavelength UV-visible detector or a photodiode array UV detector offer a means to recognize unknown components in the chromatogram and to evaluate the peak homogeneity[12–14]

In the present study these techniques were used to establish an HPLC method for plant samples. Together with the retention time data, the peaks were identified by comparing their ratiogram plots with those of standards. For example there is in

TABLE II

QUALITY PARAMETERS OF THE HPLC ASSAY FOR CATHARANTHINE AND VINDOLINE

	Catharanthine	*Vindoline*
Slope	0.0232	0.0045
Intercept	0.1225	0.0533
Correlation	0.986	0.971
Coefficient of variation (%); $n = 10$	3.13 (45 μg/ml) 1.63 (70 μg/ml)	3.04 (78 μg/ml) 3.52 (116 μg/ml)
Limit of detection	10 (μg/ml)	10 (μg/ml)

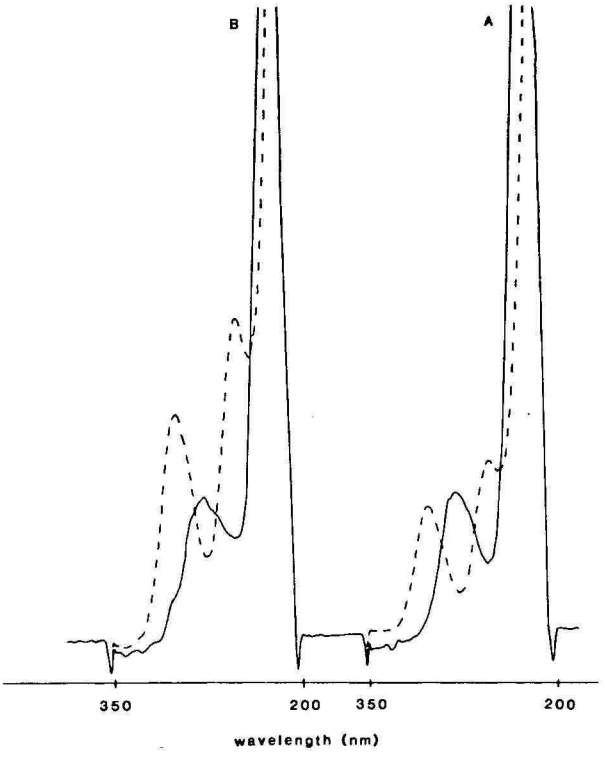

Fig. 3. The UV spectra of catharanthine (solid line) and vindoline (dashed line) scanned from standards (A) and from a leaf sample of *C. roseus* (B).

the leaf sample a solute eluting at the same retention time as vincristine (Fig. 1B) but according to the ratiogram it can be concluded not be vincristine.

A prominent deviation of the flat top of the plot was an indication of two or more overlapping components (see the peak eluting at same retention time as serpentine in Fig. 2B).

The peak homogeneity was also tested by examing the UV spectra at different points of the resolving peak. The UV spectra (Fig. 3) scanned from the peaks of eluting standards of catharanthine and vindoline (Fig. 1A) were in agreement with the spectra from the peaks eluting at the corresponding retention times in the leaf sample (Fig. 1B).

ACKNOWLEDGEMENTS

This work was financially supported by the Technology Development Centre (Helsinki, Finland), by Huhtamäki Oy Pharmaceuticals (Turku, Finland) and by the North-Savo Cultural Foundation (Kuopio, Finland). The skilful technical assistance of Ms. Sari Ukkonen is gratefully acknowledged.

REFERENCES

1 R. Verpoorte and A. Baerheim Svendsen, *Chromatography of Alkaloids, Part B: gas–liquid chromatography and high-performance liquid chromatography*, Elsevier, Amsterdam, 1984, pp. 331–356.
2 S. Görög, B. Herényi and K. Jovánovics, *J. Chromatogr.*, 139 (1977) 203.
3 M. Verzele, L. De Taeye, J. Van Dyck, G. De Decker and C. De Pauw, *J. Chromatogr.*, 214 (1981) 95.
4 J.-P. Renaudin, *J. Chromatogr.*, 291 (1984) 165.
5 W. Kohl, B. Witte and G. Höfle, *Planta Med.*, 47 (1983) 177.
6 J.-P. Renaudin, *Physiol. Veg.*, 23 (1985) 381.
7 P. Morris, A. H. Scragg, N. J. Smart and A. Stafford in R. A. Dixon (Editor), *Plant Cell Culture; a Practical Approach*, IRL Press, Oxford, 1985, pp. 127–167.
8 J. D. Phillipson, N. Supavita and L. A. Anderson, *J. Chromatogr.*, 244 (1982) 91.
9 K. E. Bij, C. S. Horvath, W. R. Melander and A. Nahum, *J. Chromatogr.*, 203 (1981) 65.
10 J. S. Kiel, S. L. Morgan and R. K. Abramson, *J. Chromatogr.*, 320 (1985) 313.
11 C. K. Lim and T. J. Peters, *J. Chromatogr.*, 316 (1984) 397.
12 A. F. Fell, H. P. Scott, R. Gill and A. C. Moffat, *J. Chromatogr.*, 273 (1983) 3.
13 A. C. J. H. Drouen, H. A. H. Billiet and L. De Galan, *Anal. Chem.*, 56 (1984) 971.
14 H. Cheng and R. Rao Gadde, *J. Chromatogr. Sci.*, 23 (1985) 227.

Journal of Chromatography, 410 (1987) 494–499
Elsevier Science Publishers B.V., Amsterdam — Printed in The Netherlands

CHROM. 20 036

Note

Determination of potassium nitrate and sodium monofluorophosphate in the presence of phosphate and sulfate by high-resolution ion chromatography

JOSEPH M. TALMAGE* and THOMAS A. BIEMER
Warner-Lambert Company, Consumer Products Division, 175 Tabor Road, Morris Plains, NJ 07950 (U.S.A.)
(Received September 3rd, 1987)

Prior to the advent of modern ion chromatography and electrochemical detection, the determination of potassium nitrate and sodium monofluorophosphate (MFP) in toothpaste was a formidable task. Methods for MFP included gas chromatography[1], colorimetry[2] and the use of specific ion electrodes[3]. These methods do not measure MFP directly, but involve either acid hydrolysis to fluoride for colorimetric or specific ion measurement, or derivitization for subsequent gas chromatography. Methods for potassium nitrate on the other hand included conversion of the nitrate to nitrite in a Jones reductor and subsequent colorimetry[4] and conversion to nitric acid with subsequent nitration of *m*-xylenol[5]. These methods are tedious, not directly stability indicating and require considerable skill and experience to perform in a quality control setting.

Recently, Chen *et al.*[6] described an ion chromatography procedure for the simultaneous determination of potassium nitrate and MFP in dentifrices. Potter *et al.*[7] described an ion chromatographic procedure for the determination of MFP and fluoride in toothpastes. Although these workers reported excellent analytical results, the quality of the chromatographic separations depicted exhibited low efficiency and resolution. Dentifrices commonly contain sulfate and phosphate in addition to the ions of interest. These excipient ions must be well separated from the analyte ions in order to assure consistent quantitation and allow for decreasing efficiency as columns age. Surprisingly, in the paper of Chen *et al.*[6] the chromatogram of a typical dentifrice indicates only a trace of sulfate, contrary to our experience with several commercial dentifrices. Potter *et al.*[7], on the other hand, indicate the expected amount of sulfate in a typical toothpaste, but the chromatograms show rather broad peaks for MFP and sulfate.

The method presented here is novel because it uses a high pH, weak carbonate mobile phase with a moderate-capacity (0.01–0.05 mequiv./g) anion-exchange column to separate rapidly and efficiently the peaks of interest. The PO_3F^{2-} and SO_4^{2-} exhibit baseline separation and phosphate, converted to PO_4^{3-} by the high pH, is well separated from the other peaks of interest. Fluoride and nitrate are well separated from each other and from the divalent ions. Fluoride, although eluting at V_0,

0021-9673/87/$03.50

can be used as a stability-indicating limit test of $<0.014\%$ F^- indicating less than 10% decomposition of PO_3F^{2-}

EXPERIMENTAL

Apparatus

The chromatograph was the Dionex 4000i chromatography module containing the pump and conductivity detector (Dionex, Sunnyvale, CA, U.S.A.). All samples were injected automatically using the Dionex autosampler. Separation of the analytes was performed on a Dionex HPLC AS4A column equipped with a AG4A guard column all at room temperature. The signal from the detector was fed to a Heath d.c. offset module EU-200-02 (Heath Schumberger, Benton Harbon, MI, U.S.A.) to offset the 100-mV baseline produced by the detector since that output was not compatible with the Sigma 10 data station (Perkin-Elmer, Norwalk, CT, U.S.A.) used to record and integrate peak areas. A Spectrum 921 filter set at 0.01 (Spectrum, Newark, DE, U.S.A.) was placed between the data station and amplifier to remove any high frequency noise. The following chromatography conditions were used: flow-rate, 1.2 ml/min; back pressure, *ca.* 1000 p.s.i., detector sensitivity, 300 μS; column temperature, 25°C; detector compensation temperature, 1.7°C; injection volume, 50 μl; chart speed, 5 mm/min.

Reagents

Except for the MFP, all reagents were analytical grade. The MFP was obtained from Ozark-Manhoning Div. of Pennwalt Corp. (Tulsa, OK, U.S.A.) and had an assay value of 93.7%. Water purified by a Milli-R04 system (Millipore, Bedford, MA, U.S.A.) and having a resistivity of 15 MΩ or greater, was used to prepare the mobile phase and regenerant solution used in the suppressor column. The mobile phase consisted of 100 mg sodium carbonate dissolved in a liter of water and adjusted to pH = 11.00 ± 0.05 using 1 *M* sodium hydroxide.

Standard preparation

A stock standard was prepared by dissolving 500 mg of potassium nitrate and 90 mg of MFP in 100 ml of distilled water. A 10-ml aliquot was then diluted to 100 ml to make the working standard.

Sample preparation

An amount of 5.0 ± 0.2 g of the sample toothpaste was weighed into a 500-ml volumetric flask. The flask was filled about halfway with water and shaken until the sample was fully dispersed. After diluting to volume with water, a portion was taken and filtered through a 0.45-μm nylon filter for analysis.

RESULTS AND DISCUSSION

The standard Dionex mobile phase for anion elution consists of sodium hydrogencarbonate (62.5 mg/l) and sodium carbonate (235 mg/l). A typical chromatogram of a toothpaste sample using this mobile phase is shown in Fig. 1. The chromatogram shows a skewed peak where the monofluorophosphate elutes. This skewed

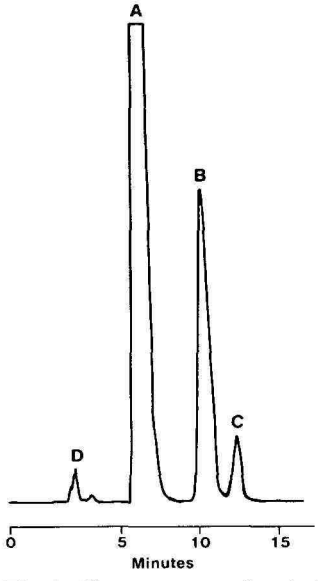

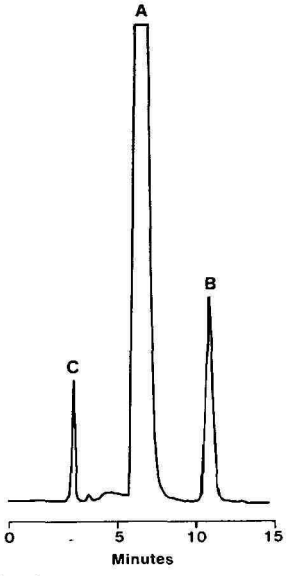

Fig. 1. Chromatogram of typical toothpaste using standard anion mobile phase. Peaks: A = nitrate; B = phosphate, monofluorophosphate; C = sulfate; D = fluoride.

Fig. 2. Chromatogram of standard using standard Dionex anion elution conditions. Peaks: A = nitrate; B = monofluorophosphate; C = fluoride.

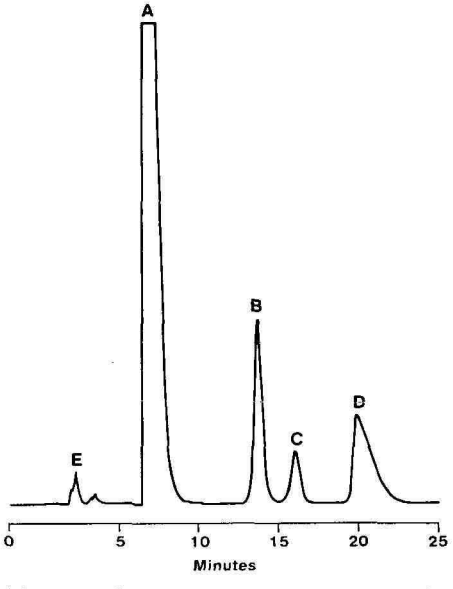

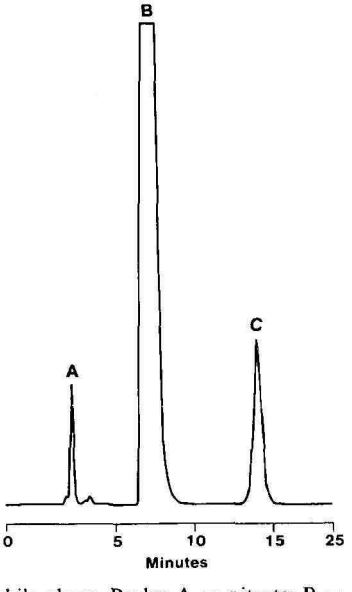

Fig. 3. Typical toothpaste chromatogram using modified anion mobile phase. Peaks: A = nitrate; B = monofluorophosphate; C = sulfate, D = phosphate; E = fluoride.

Fig. 4. Standard chromatogram using modified anion mobile phase. Peaks: A = fluoride; B = nitrate; C = monofluorophosphate.

TABLE I

LINEARITY

Sodium fluoride		*Potassium nitrate*		*Sodium monofluorophosphate*	
mg/100 ml	*Area*	*mg/100 ml*	*Area*	*mg/100 ml*	*Area*
0.128	24.60	25.13	1766.9	3.945	146.2
0.128	23.57	25.13	1734.4	3.945	147.5
0.257	58.91	50.26	3474.4	7.890	306.3
0.257	55.65	50.26	3498.5	7.890	316.2
0.386	91.09	75.39	4874.1	11.385	471.3
0.386	90.39	75.39	4883.9	11.385	470.3
R = 0.9993		R = 0.9979		R = 0.9997	
a = 0.00387		a = 0.0160		a = 0.024	
b = 0.035		b = −3.70		b = 0.353	
S.D. = 0.0048		S.D. = 1.61		S.D. = 0.094	

peak results from the coelution of phosphate (HPO_4^{2-}) with monofluorophosphate (PO_3F^{2-}). Compared to the chromatogram for the working standard (Fig. 2) the peak for PO_3F^{2-} is sharp and without any significant tailing.

To shift the HPO_4^{2-} peak away from the PO_3F^{2-} peak, the mobile phase pH was adjusted to 11.00. This pH change shifts the phosphate equilibrium towards the pK_{a3} giving the ion more affinity for the ion exchange sites. The result is complete resolution of PO_3F^{2-} from the peak due to phosphate. The sodium hydrogencarbonate was deleted from the mobile phase since at this pH, the predominate ion would be CO_3^{2-}. Reducing the CO_3^{2-} concentration helped achieve a larger resolution factor between PO_3F^{2-} and SO_4^{2-}. A typical toothpaste chromatogram with this mobile phase is shown in Fig. 3. The peaks for the analytes are sharp and well resolved. Experience with this system has shown that the CO_3^{2-} concentration should be adjusted up or down slightly depending upon the age of the column. While selectivity can be restored by flushing the column per the manufacturer's recommendations, in time, it will be necessary to weaken the CO_3^{2-} concentration to maintain baseline separation between PO_3F^{2-} and SO_4^{2-}

TABLE II

REPRODUCIBILITY

Trial	*(%) Sodium fluoride*	*(%) Potassium nitrate*	*(%) MFP*
1	0.0167	5.256	0.773
2	0.0164	5.254	0.769
3	0.0165	5.267	0.768
4	0.0167	5.275	0.769
5	0.0168	5.294	0.769
6	0.0165	5.253	0.770
Mean	0.0167	5.266	0.769
S.D.	0.0002	0.015	0.003
R.S.D. (%)	1.2	0.28	0.39

TABLE III

RECOVERY

Potassium nitrate			*Sodium monofluorophosphate*		
mg added	*mg found*	*(%) Recovery*	*mg added*	*mg found*	*(%) Recovery*
25.13	24.74	98.4	3.945	3.87	98.1
40.21	42.65	106.1	6.312	6.29	99.7
45.24	47.12	104.1	7.101	6.90	97.2
50.26	51.92	103.3	7.890	7.65	97.0
55.29	56.29	101.5	8.679	8.36	96.3
60.32	60.83	100.8	9.468	9.19	97.0
74.40	75.93	100.7	11.835	11.70	99.2
0	0	–	0	0	–
		Mean 102.1			Mean 97.8
		S.D. 2.5			S.D. 1.3

Fig. 4 shows a chromatogram of a working standard. The fluoride peak elutes almost at the column void volume. In this system, fluoride cannot be quantitated, but used only as a means of indicating stability of MFP in the formulation.

Linearity data for nitrate, fluoride and MFP are shown in Table I. These analytes show excellent correlation over the range tested. This technique has demonstrated ruggedness and reliability and has been in use for several months. The reproducibility was demonstrated by chromatographing a toothpaste sample several times during the course of a day (Table II). Recovery studies were conducted by spiking

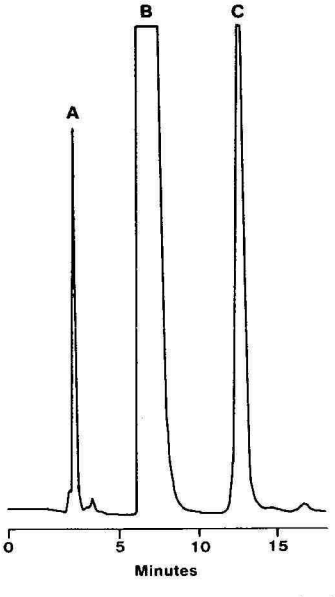

Fig. 5. Chromatogram of standard using modified anion mobile phase without suppressor flow. Peaks: A = fluoride; B = nitrate; C = monofluorophosphate.

a placebo toothpaste with potassium nitrate and monofluorophosphate at concentrations of 50% to 150% of that expected in a toothpaste sample (Table III).

As described previously, the method was developed using Dionex chromatography hardware exclusively. It is possible, however, to interface these columns to other chromatography systems using standard HPLC fittings. While the function of the regenerant flow is to reduce background conductivity, this system can be run without suppressor flow as shown in Fig. 5. This method could, therefore, be adapted to other ion chromatography systems. The weak carbonate mobile phase appears to contribute only a very low background signal.

REFERENCES

1 R. Black and H. J. Semmler, *Fresenius' Z. Anal. Chem.*, 320 (1967) 161.
2 L. Pickston, *N.Z. J. Technol.*, 1 (1985) 67.
3 P. A. Compagnon, *Sci. Tech. Pharm.*, 12 (1983) 495.
4 *Official Methods of Analysis*, Association of Official Analytical Chemists, Arlington, VA, 13th ed., 1980, 16.249–16.254.
5 *Official Methods of Analysis*, Association of Official Analytical Chemists, Arlington, VA, 13th ed., 1980, 24.038–24.040.
6 S. S. Chen, H. Lulla, F. J. Sena and V. Reynoso, *J. Chromatogr. Sci.*, 23 (1985) 355–359.
7 J. J. Potter, A. E. Hilliker and G. J. Breen, *J. Chromatogr.*, 367 (1986) 423–427.

Journal of Chromatography, 410 (1987) 500–503
Elsevier Science Publishers B.V., Amsterdam — Printed in The Netherlands

CHROM. 19 948

Note

Fast reversed-phase high-performance liquid chromatographic determination of ^{14}C- or ^{3}H-labelled S-adenosylmethionine in reaction mixtures

JANA VOČKOVÁ* and VRATISLAV SVOBODA
Institute for Research, Production and Application of Radioisotopes, Radiová 1, 102 27 Prague 10 (Czechoslovakia)
(Received August 7th, 1987)

S-Adenosyl-L-methionine (SAM) acts as a donor of a methyl group in various biochemical reactions changing the biological activity of a number of chemical compounds. SAM, labelled at the methyl group by the radioisotopes ^{14}C or ^{3}H, is prepared by the enzymatic reaction of [^{14}C]- or [^{3}H]-L-methionine with adenosine 5'-triphosphate (ATP). The need for an analytical method, enabling the determination of SAM in these reaction mixtures, to study the course of the enzymatic reaction and to find the optimum conditions for the preparation of SAM has thus arisen.

The chemical stability of SAM strongly depends on the pH and the temperature. At neutral or basic pH values as well as at elevated temperatures, decomposition of SAM occurs. Therefore it is necessary to work at a low pH and at the laboratory temperature. At low pH, the amino groups of SAM are positively charged and therefore the chromatographic methods used for its determination include cation-exchange[1–9], reversed-phase[7] and at present mostly ion-pair reversed-phase liquid chromatography. On C_{18} columns, heptanesulphonic acid[10,11] or octanesulphonic acid[12,13] were used for the ion-pair formation.

As found previously[7], we have shown that SAM is only slightly retained on a C_{18} reversed phase. To avoid interferences from other compounds eluted close to the void volume, the use of an ion-pair method was necessary. In this note we report a fast isocratic ion-pair reversed-phase liquid chromatographic method using sodium dodecyl sulphate (SDS) as the ion-pairing agent for the quantitation of SAM in reaction mixture after enzymatic synthesis.

EXPERIMENTAL

Chemicals

S-Adenosyl-L-methionine (SAM) was obtained from Boehringer (Mannheim, F.R.G.), S-adenosyl-L-homocysteine (SAH) from Sigma (St. Louis, MO, U.S.A.), L-methionine and acetonitrile for high-performance liquid chromatography (HPLC) from E. Merck (Darmstadt, F.R.G.) and sodium dodecyl sulphate puriss. from Fluka (Buchs, Switzerland). Methanol, sodium dihydrogenphosphate, phosphoric acid and sulphuric acid were analytical grade products from Lachema (Brno, Czechoslovakia). Water was twice distilled.

0021-9673/87/$03.50

The SAM stock solution (stored at −20°C), 10 mg/ml, was prepared by dissolving the compound in an aqueous sulphuric acid solution pH 2.00.

Apparatus

A Spectra Physics (San Jose, CA, U.S.A.) liquid chromatograph SP 8100 was equipped with an SP 8440 UV detector set to monitor absorbance at 254 nm and a SP 4200 computing integrator. Samples were injected manually by means of a Valco sample injector with a 25-μl injection loop. Glass analytical columns CGC 6802 (150 mm × 3.2 mm I.D.) from Laboratory Instruments (Prague, Czechoslovakia) packed with reversed-phase Separon SIX C 18 (particle size 5 μm) were used for the separation. The flow-rate was 0.5 ml/min and columns were thermostated at 25 ± 0.5°C in a jacket connected to a water-bath. For measurement of radioactive samples, a radioactivity detector constructed in our laboratory and packed with scintillation glass YG-30 (ÚVVVR, Prague, Czechoslovakia) was connected in front of the UV detector. Its signal was processed by a coincidence apparatus (Canberra, Meriden, U.S.A.) and recorded by a line recorder TZ 21 S (Laboratory Instruments).

RESULTS AND DISCUSSION

The initial reaction mixture for the preparation of SAM consisted mainly of ATP, L-methionine and inorganic salts, but the composition of the resulting mixture after the enzymatic synthesis was not known. The presence of such compounds as SAH, 5'-methylthioadenosine or decarboxylated SAM was expected. To ascertain the composition of the reaction mixture, its gradient analysis was performed according to ref. 12, because the increasing acetonitrile concentration made probable the elution of even more strongly retained compounds, *e.g.*, decarboxylated SAM. As SDS was used instead of octanesulphonic acid in the eluent, the retention times were longer than those obtained previously[12]. It was found that no SAH was formed during the reaction and that SAM was eluted last.

To find the optimum conditions for the preparation of SAM and to follow the reaction kinetics, tens of analyses of the reaction mixtures have to be performed. Therefore it was desirable to restrict the analysis time to the order of minutes. To achieve this, isocratic elution was preferred to gradient elution.

Using the dynamic cation exchanger, the elution behaviour of SAM can be affected by changes in the pairing ion concentration and the ionic strength, the pH and the temperature of the eluent. Considering the stability of SAM, we worked at the laboratory temperature and at acidic pH. The expensive acetonitrile was replaced by methanol. Both increasing ionic strength of the eluent and increasing methanol concentration result in a decrease in the elution time of SAM. A decrease in the concentration of SDS has a similar effect and in addition the column efficiency decreases. The eluent composition had to be chosen so that SAM could be fully separated from other components of the reaction mixture and that the analysis time was less than 15 min. The chromatographic conditions chosen were: $8 \cdot 10^{-4}$ *M* SDS, 550 ml of 0.1 *M* sodium dihydrogenphosphate, 450 ml methanol, pH 3.00 adjusted by the addition of phosphoric acid; flow-rate 0.5 ml/min.

Chromatograms of the standard solution of SAM (from Boehringer) and of a non-radioactive reaction mixture for the preparation of SAM, analyzed under

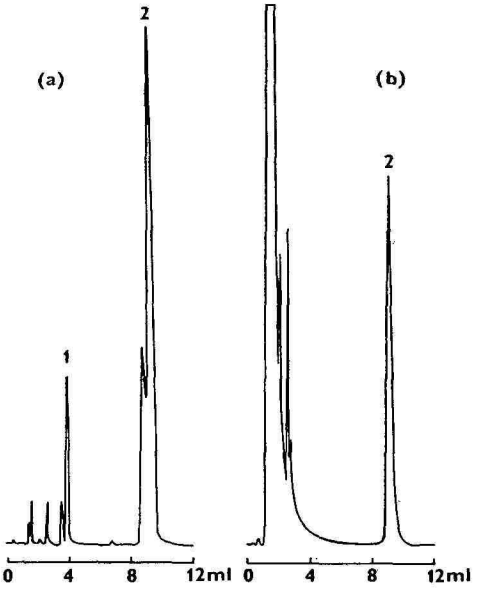

Fig. 1. Chromatograms of a partly decomposed standard solution of SAM (a) and of a non-radioactive reaction mixture for the preparation of SAM (b). Peaks: 1 = SAH; 2 = SAM. UV detection at 254 nm. For other chromatographic conditions see the text.

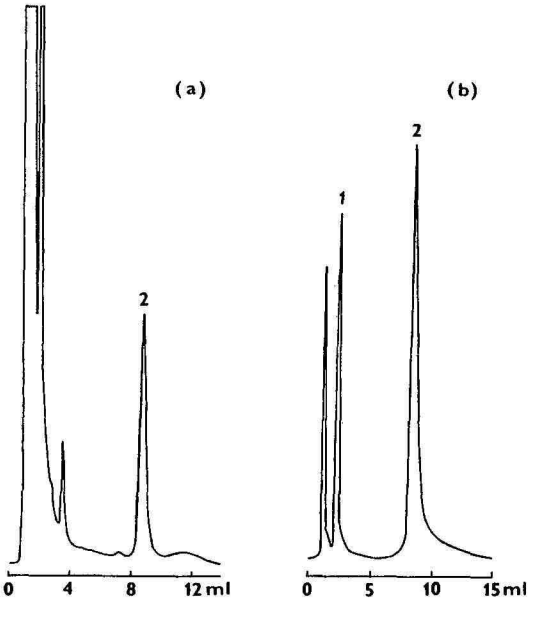

Fig. 2. Chromatograms of the radioactive reaction mixture for the preparation of [^{14}C]SAM obtained by (a) UV detection and (b) radioactivity detection. Peaks: 1 = [^{14}C]L-methionine; 2 = [^{14}C]SAM. For chromatographic conditions see Fig. 1.

identical conditions, are illustrated in Fig. 1a and b. The chromatograms of a reaction mixture monitored with an UV and a radioactivity detector are shown in Fig. 2a and b. The peak of non-reacted [^{14}C]methionine can be seen in the radioactivity record, but is undetected in the UV record at 254 nm.

The pressure on the column slowly increased with time and the retention time of SAM slowly decreased. This was caused probably by the sorption of enzyme residues on the column packing. Slow washing by methanol overnight regenerated the column for further use.

The method reported has been used for the qualitative and quantitative analyses of reaction mixtures for the preparation of SAM. A calibration curve was constructed by dilution of the standard solution of SAM from Boehringer in the concentration range from 0.68 to 174 μg/ml. The lower limit of this concentration range is approximately equal to the detection limit with the UV detector. The detection limits with the radioactivity detector are 1 kBq for [^{14}C]SAM and 10 kBq for [^{3}H]SAM; this is quite satisfactory for production samples.

REFERENCES

1 J. Hoffman, *Anal. Biochem.*, 68 (1975) 522.
2 T. O. Eloranta, E. O. Kajander and A. M. Raina, *Biochem. J.*, 1960 (1976) 287.
3 T. P. Zimmerman, R. D. Deeprose, G. Wolberg and G. S. Duncan, *Biochem. Biophys. Res. Commun.*, 91 (1979) 997.
4 L. Shughart, *J. Chromatogr.*, 174 (1979) 250.
5 V. Zappia, P. Galletti, M. Porcelli, C. Manna and F. Della Ragione, *J. Chromatogr.*, 189 (1980) 399.
6 H. Hibasami, J. L. Hoffman, A. E. Pegg, *J. Biol. Chem.*, 255 (1980) 6675.
7 F. Della Ragione, M. Vartenì-Farina, M. Porcelli, G. Cacciapuoti and V. Zappia, *J. Chromatogr.*, 226 (1981) 243.
8 R. I. Glaser and A. L. Peale, *Anal. Biochem.*, 91 (1981) 516.
9 B.-G. Chun, W. K. Paik and S. Kim, *J. Chromatogr.*, 264 (1983) 321.
10 B. E. Chabannes, J. N. Bidard, N. N. Sarda and L. A. Cronenberger, *J. Chromatogr.*, 170 (1979) 430.
11 W. J. Burke, *Anal. Biochem.*, 122 (1982) 258.
12 J. Wagner, Ch. Danzin and P. Mamont, *J. Chromatogr.*, 227 (1982) 349.
13 J. Wagner, Ch. Danzin, S. Huot-Olivier, N. Claverie and M. G. Palfreyman, *J. Chromatogr.*, 290 (1984) 247.

Journal of Chromatography, 410 (1987) 504–508
Elsevier Science Publishers B.V., Amsterdam — Printed in The Netherlands

CHROM. 19 944

Note

Quantitative high-performance liquid chromatographic determination of the amino acid spinacine in blood and chow of rats

M. ANASTASIA, D. COLOMBO* and A. FIECCHI
Department of Medical Chemistry and Biochemistry, University of Milan, Via Saldini 50, 20133 Milan (Italy)
(Received June 21st, 1987)

Spinacine (4,5,6,7-tetrahydro-1*H*-imidazo[4,5-*c*]pyridine-6-carboxylic acid) (1) is a cyclic amino acid homologue of histidine showing neither histamine-like nor antihistamine activity[1]. It was first synthesized by Wellisch[2] by heating histidine with aqueous formaldehyde, and it was first found in the shark liver by Ackermann and Mohr[3] and then in other animals[4]. More recently Fiecchi *et al.*[5] have shown that a spinacine residue is formed in the caseine of milk treated with formaldehyde. Spinacine is the reaction product of the histidine present as N-terminal amino acid in γ_2-caseine with formaldehyde. This is a rapid reaction; in fact spinacine was even formed on a chromatographic paper by cyclocondensation of histidine and formaldehyde present in the laboratory atmosphere[6]. Despite its easy formation, little has been reported concerning its toxicity[7].

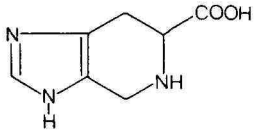

1

The study of the toxicity of spinacine requires a simple and fast method for its quantitative detection both in the food of treated animals and in their blood. A rapid quantitative analytical procedure and validation data suitable for the determination of spinacine added to chow and present in the rat blood are reported here. The results obtained, using standard instrumentation for high-performance liquid chromatography (HPLC), are close to the expected values in the case of chow and to that obtained by a radioisotopic measurement in the case of the blood of rats fed with [5-^{14}C]spinacine.

EXPERIMENTAL

Equipment, column and eluents

The HPLC system consisted of a Twincle pump (Jasco, Tokyo, Japan), a

0021-9673/87/$03.50

VL614 variable loop injector with a 200-μl sample loop, an Uvidec 100 II and a fluorescence detector Model FP-210 (Jasco, Japan). Excitation was through a 330-nm bandpass filter and the emission filter had a 530-nm cut-off. The recorder was a Shimadzu C-R3A Chromatopac. A number of chromatographic solvent systems were tried. The solvent system finally used was: (A) 0.1 *M* phosphate buffer, pH 4.8 and (B) acetonitrile. The Dns-amino acids were separated by reversed-phase liquid chromatography on a 25 cm × 40 mm I.D. column packed with 7-μm LiChrosorb RP-18. Initial conditions for the chromatography were 80% solvent A and 20% solvent B. A gradient was initiated 10 min after the injection of the sample; the concentration of solvent B was increased linearly from 20 to 30% over a period of 10 min. The flow-rate was 1.0 ml/min.

Materials

The chow was of Type 4RF25 of Italiana Mangimi, containing 24.30% proteins and 4.60% lipids. Dns-amino acids were obtained from Sigma, L-[guanido-^{14}C]arginine monohydrochloride and [^{14}C]formaldehyde from Amersham (U.K.). L-Arginine monohydrochloride was obtained from Merck. L-Spinacine was synthesized according to Vitali *et al.*[8] and showed m.p. 273–276°C; $[\alpha]_D^{20} = -85°$ (c = 1, water); ^{1}H NMR (^2H_2O) 3.20–3.40 (m, 2 H), 4.35 (m, 2H), 8.30 (s, 1 H); mass spectrum, *m/e* 167 (M^+), 122, 94. Found: C, 41.13; H, 4.96; N, 20.49; $C_7H_{10}O_2N_3Cl$ requires C, 41.29; H, 4.91; N, 20.64. All physico-chemical properties are in agreement with those reported[2,8,9].

Dns derivatization of L-arginine and of L-spinacine was carried out under conditions similar to those reported by Tapuhi *et al.*[10] and Oray *et al.*[11]. Ion-exchange chromatography was performed on Dowex AG-50W-X 8(H^+), 200–400 mesh (Bio-Rad), eluting with hydrochloric acid and then with ammonia.

Preparation of analytical solutions

Procedure for chow. Samples used for checking the linearity of the integrated detector response and for the analyses were prepared starting with the same quantity of chow (1 g). In the first case, spinacine and arginine were added in appropriate quantities (see Results and discussion). To the samples used for the analyses only arginine was added.

In each case the chow was mixed with purified sea sand (3 g, Merck) and eluted from a glass column with hot water (10 ml). The eluate was filtered over neutral alumina (1 g) and lyophilized to a standard volume (1 ml). With [5-^{14}C]spinacine obtained by reaction with [^{14}C]formaldehyde, it was observed that all spinacine was completely eluted and recovered in this way and that the recovery was constant between 0.06 and 20 mg/g. The solution was added to lithium carbonate (2 ml of a 40 m*M* solution) and Dns-chloride (5 molar excess in 1.5 ml of acetonitrile) and was heated at 45°C for 30 min.

Procedure for serum. To 2 g of serum of Sprague-Dawley male rats (Charles River, body weight 130–150 g) were added spinacine and arginine in appropriate quantities. To the samples used for the analysis only arginine was added and they were derived from similar rats which given chow containing [5-^{14}C]spinacine for 7 days before the blood was collected. Serum was reacted with Dns-chloride (5 molar excess in acetonitrile) after addition of lithium carbonate (2 ml of a 40 m*M* solution).

From the same serum (2 g), [5-^{14}C]spinacine was separated and detected by radioisotopic measurement.

RESULTS AND DISCUSSION

The analysis of Dns-amino acid derivatives using HPLC is suitable for the evaluation of spinacine in rat chow and in rat blood. In order to obtain results corrected for any loss or degradation during the sample preparation, arginine was added to the samples as an internal standard before the extraction and derivatization of the spinacine. Arginine was chosen because it was eluted from the chow similarly to spinacine. We found that [5-^{14}C]spinacine and L-[guanido-^{14}C]arginine were completely eluted from the chow (1 g) by the same quantity of water (10 ml). In addition, arginine afforded the Dns derivative in the same reaction time as that for spinacine, complete reaction being observed after 30 min at 45°C[10]. Finally Dns-arginine is

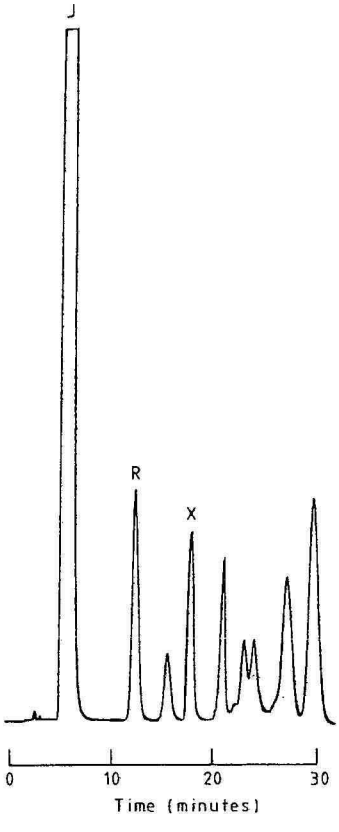

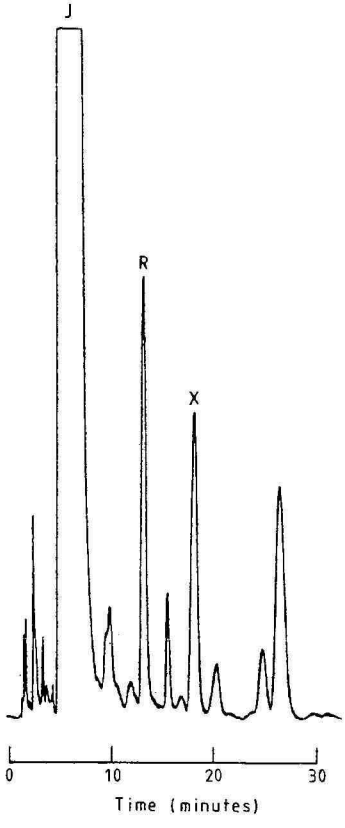

Fig. 1. Separation of Dns-spinacine (X) and Dns-arginine (R) in chow according to the conditions described in the text. J = Dns-sulphonic acid. The other peaks and J represent the profile of the HPLC chromatogram in the absence of X and R.

Fig. 2. Separation of Dns-spinacine (X) and Dns-arginine (R) in blood serum according to the conditions described in the text. Other details as in Fig. 1.

TABLE I

DETERMINATION OF SPINACINE CONTENT IN CHOW AND BLOOD

*Method**	*Amount added to chow (mg/100 g)*			*Amount added to blood (mg/100 g)*
	40	*100*	*500*	
Present	39.8 ± 0.57	99.7 ± 1.46	498.6 ± 7.16	3.5 ± 0.06
Ion-exchange purification and radioisotopic measurement	39.5 ± 0.8	98.6 ± 1.46	490.5 ± 8.3	3.5 ± 0.1

* Mean of seven determinations, ± e.s., for chow and four determinations, ± e.s., for blood, using HPLC of Dns derivative of [5-^{14}C]spinacine with Dns-arginine as the internal standard.

perfectly separated and eluted before Dns-spinacine but fairly close to the latter (Figs. 1 and 2). The Dns-amino acids were stable under the reaction conditions, as reported[12,13] for Dns-arginine which was found to be stable for 60 min at 110°C in the presence of hydrochloric acid. Thus, the samples were routinely derivatized by reaction at 45°C for 30 min. The relative standard deviations of the integrated area ratios for Dns-arginine and Dns-spinacine formed by reaction of the amino acids and Dns-chloride for 20, 30, 40 and 50 min were less than 2.1%.

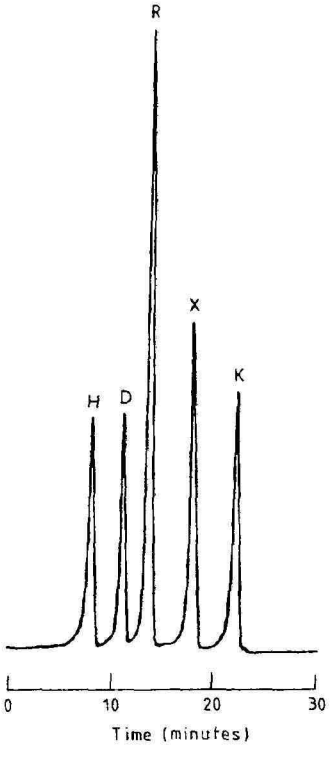

Fig. 3. HPLC elution profile of spinacine (X), histidine (H), arginine (R), aspartic acid (D) and lysine (K) as their Dns derivatives according to the conditions described in the text.

Using arginine as the internal standard, the linearity of the integrated detector response for Dns-arginine and Dns-spinacine was measured over three different concentration ranges for the chow and over one concentration range for the blood. HPLC analyses were performed on Dns derivatives of extracts obtained after addition of arginine and increasing amounts of spinacine to samples (1 g) of rat chow or of rat blood (2 ml). The linearity was checked in the blood using arginine (100 μg) and spinacine (0, 60, 80, 100, 150, 200 μg), and in the chow using arginine (300 μg; 1 mg; 10 mg) and spinacine (0, 200, 400, 500, 600, 800 μg; 0, 1, 2, 3 4, 5 mg; 0, 6, 8, 10, 15, 20 mg). The correlation coefficients (linearity of response for each concentration range) were 0.997, 0.996, 0.999 in the chow and 0.998 in the blood. Since arginine was added before any manipulation and derivatization, the observed linearity is related to the extraction procedure, to the derivatization and to the HPLC analysis. The relative standard deviation of the spinacine content from a repetitive analysis of a single sample was ± 2.1%. The detection of spinacine in three groups of seven samples, each group corresponding to a different content of spinacine in chow, always showed a relative standard deviation less than ± 4.0% (3.8, 3.9, 3.8%), while in four samples of blood it was ± 4.0%.

The results obtained (Table I) are near to the calculated values for chow and are comparable with those obtained by detecting [5-^{14}C]spinacine added to the chow or present in the blood by radioisotopic measurement after separation on a cation exchange column. In conclusion this procedure is simple and rapid both in terms of chromatographic separation time and of sample preparation. It permits the determination of spinacine without purification of extracts even when present in small amounts.

The method can be used to detect spinacine also in the presence of complex amino acid mixtures, since under the same chromatographic conditions the Dns-spinacine peak is separated from those of other common amino acid derivatives (Fig. 3).

REFERENCES

1 A. Braibanti, F. Dallavalle, E. Leporati and G. Mori, *J. Chem. Soc., Dalton Trans.*, (1973) 323.
2 J. Wellisch, *Biochem. Z.*, 49 (1913) 173.
3 D. Ackermann and M. Mohr, *Z. Biol. (Munich)*, 98 (1937) 37.
4 E. Mueller, in G. Hoppe-Seyler and H. Thierfelder (Editors), *Handbuch der physiologische und patologische chemischen Analyse*, Vol. II, Springer Verlag, Berlin, 1985, Ch. 3, p. 1185.
5 A. Fiecchi, C. Galli and P. Resmini, unpublished results.
6 S. Hrnčir, J. Kopoldova, K. Veres, V. Dedkova, V. Hanus and P. Sedmera, *J. Labelled Compd. Radiopharm.*, 15 (1978) 47.
7 D. Ackermann, *Hoppe-Seyler's Z. Physiol. Chem.*, 276 (1942) 268.
8 T. Vitali, F. Mossini and G. Bertaccini, *Gazz. Chim. Ital.*, 94 (1964) 296.
9 Y. Kitamoto and H. Maeda, *J. Biochem. (Tokyo)*, 87 (1980) 1519.
10 Y. Tapuhi, N. Miller and B. L. Karger, *J. Chromatogr.*, 205 (1981) 325.
11 B. Oray, H. S. Lu and R. W. Gracy, *J. Chromatogr.*, 270 (1983) 253.
12 C. De Jong, G. J. Hughes, E. Van Wieringen and K. J. Wilson, *J. Chromatogr.*, 241 (1982) 345.
13 R. Y. Chen, *Arch. Biochem. Biophys.*, 120 (1967) 609.

Journal of Chromatography, 410 (1987) 509–510
Elsevier Science Publishers B.V., Amsterdam — Printed in The Netherlands

CHROM. 19 955

Letter to the Editor

Letter symbols in the chemistry of glyceridic fats and oils

Sir,

I would like to draw the attention of the scientific community to a deficiency in the system of using letter symbols in the chemistry of glyceridic fats and oils.

The full names of fatty acids are often replaced by letter symbols in order to shorten communications, and this frequently leads to confusion. For example, the symbol S is used to stand for both stearic acid and for "saturated". Thus it is sometimes very difficult to read and comprehend a publication in which both unsaturation and stearic acid are discussed, even when the symbol S is used for only one of these concepts. I myself, however, have seen at least one (commercial) publication where the symbol S was given for both meanings. Sometimes a third symbol is used, G (gesättigt-saturated), taken from German. This confusion over the symbol S can be found in the scientific, patent and other commercial literature.

To a lesser extent, some authors use their own letter symbols, which sometimes are not even defined. It is thus possible to find L and Lo as symbols for linoleic acid, Ln and Le as symbols for linolenic acid, and E as a symbol for elaidic acid (normally used for erucic acid). One of these publications appeared as recently as 1984.

In my opinion it is easy to avoid these complications by using the following letter symbols proposed by Litchfield on p. 6 of his book *Analysis of Triglycerides*[1]:

P = Palmitic acid (C16:0)
St = Stearic acid (C18:0)
O = Oleic acid (C18:1; 9*c*)
L = Linoleic acid (C18:2; 9, 12*c*)
Ln = Linolenic acid (C18:3; 9, 12, 15*c*)
El = Elaidic acid (C18:1; 9*t*)
E = Erucic acid (C22:1; 13*c*)
S = "saturated"

No G is needed!

It can be said of course, that we also use the term ECN (equivalent carbon number) as a symbol for a different concept than most other workers today. In fact we proposed the term ECN as early as 1979[2]. Unfortunately we are not able to find another, adequate term for our purposes. If we could, we would use it instead.

Our definition of ECN is as follows: The ECN is the carbon number of a hypothetical saturated triglyceride, which would elute at the same retention time as the unsaturated triglyceride under study. This definition shows that there exists a relation between the hypothetical carbon number and the corresponding retention time.

The term ECN as it is used generally at present is only a new name (the eighth)

0021-9673/87/$03.50

for an old concept. The previous name was partition number (PN) (see the footnote on p. 86 in ref. 1). No relation with any other parameter can be found here — PPP, PPO, POO, OOO, PStL and other triglycerides all have PN (ECN) = 48, but widely different retention times. PN nowadays seems to be too coarse a concept, which indicates "critical pairs" where none any longer exist, but cannot predict experimental "critical pairs", such as StOO/PPP, which can occur with present-day techniques.

Karlshamns AB, S-29200 Karlshamn (Sweden) OLDRICH PODLAHA

1 C. Litchfield, *Analysis of Triglycerides*, Academic Press, New York and London, 1972.
2 B. Herslöf, O. Podlaha and B. Töregård, *J. Am. Oil Chem. Soc.*, 56 (1979) 864.

(Received August 11th, 1987)

Journal of Chromatography, 410 (1987) 511–512
Elsevier Science Publishers B.V., Amsterdam — Printed in The Netherlands

CHROM. 20 058

Book Review

Preparative liquid chromatography (*Journal of Chromatography Library*, Vol. 38), edited by B. A. Bidlingmeyer, Elsevier, Amsterdam, Oxford, New York, Tokyo, 1987, XIV + 341 pp., price Dfl. 200.00, ISBN 0-444-42832-1.

This is the third book on preparative chromatography to have appeared within a short time. This seems to indicate a strong interest in this field, which also manifests itself by the existence of two series of annual symposia on preparative chromatography.

However, the term "preparative" has become rather vague, as modern techniques of thin-layer chromatography, high-performance liquid chromatography (HPLC) and gas chromatography usually separate micro-amounts in analytical work. For some it seems to mean milligram amounts, enough to do spectra, analyses and melting points; to others it means gram quantities for biological work etc., and again others think only of producing kilogram amounts. It is generally ignored that the "renaissance" of chromatography in 1931 was essentially the separation of milligram amounts, enough to do structural work on isolated natural products. Workers in the field would do well to leaf through the book by Zechmeister and Cholnoky before announcing "new advances".

The present volume is a multi-author camera-ready book. Essentially it deals with the problems of choosing best adsorbents, etc. for "preparative HPLC columns", *i.e.* columns several centimeters in diameter.

The first chapter by McDonald and Bidlingmeyer is very well produced and presents some interesting facets more as a publicity pamphlet; however, it is not certain whether it will be very useful for workers in the field, who will not find anything new in it.

The second chapter on "Preparative Thin-Layer Chromatography", by Sherma and Fried, discusses separations "up to 20 mg", which is hardly news to workers who have separated gram quantities by paper chromatography.

Chapter 3, by Wankat, deals with the efficiency of "very large packed bed chromatographic separations". This from the point of view of a chemical engineer. The first paragraph reviews older work but not very effectively; also Spedding's name is spelt Speeding in the reference list.

The final section on "other methods for large-scale chromatography" is succint but incomplete.

The following sections are on applications to various fields. The chapter for the synthetic chemist has a section on computer simulation, "the real world" and practical matters, but boasts of only five references.

There is an excellent chapter on the resolution of enantiomers by Pirkle and Hamper. Although its title says that it is on direct preparative resolution, it is rather general, but does not mention the work on the separation of enantiomeric Co(III)

complexes and the reference list would have benefited from the attentions of a proof reader.

For a worker already in possession of one of the previous books on preparative chromatography, or who has attended one of the symposia, this book might seem superfluous; for others, it may prove a useful introduction to the field.

Journal of Chromatography, 410 (1987) 513
Elsevier Science Publishers B.V., Amsterdam — Printed in The Netherlands

CHROM. 20 079

Book Review

HRGC–FTIR: capillary gas chromatography–Fourier transform infrared spectroscopy — Theory and applications, by W. Herres, Hüthig, Heidelberg, New York, 1987, VIII + 212 pp., price DM 84.00, US$ 46.00, ISBN 3-7785-1061-4.

This book attempts to review a rather diverse subject and presents an overview of the theory and applications of gas chromatography (GC)–Fourier-transform infrared (FT-IR) spectrometry. The book begins with a rather disjointed explanation of the theory of FT-IR spectrometry. Brief mention is made of the advantages of FT-IR spectrometry over dispersive IR spectrometry. Here it is stated that there is a Jacquinôt (or throughput) advantage in FT-IR spectrometry because the spectrometer has no slits; unfortunately, this is a common misrepresentation of the Jacquinôt advantage. There are other basic errors or shortcomings; for example, a definition for resolution (*e.g.* the Rayleigh criterion) was not given when resolution was discussed. Furthermore, there is some confusion between the discrete and fast Fourier transforms (DFT and FFT). Despite these shortcomings there are many positive aspects and correct statements about GC–FT-IR spectrometry.

The preface acknowledgement for the book was written in February 1987 and published by August of that year. (Hüthig should be congratulated for such rapid publishing.) Nonetheless, references were restricted to 1985 or before. If the references had been up to date through 1986, many important developments would have been included. More serious than this shortcoming is that fact that figures and applications are largely restricted to data from one GC–FT-IR spectrometer manufacturer. There is rarely mention of developments in the field by other spectrometer manufacturers. Regrettably, much important data and some applications are therefore missing. Although this is a comprehensive text, one must wonder why data are restricted ostensibly to one system.

The book is concise and rather short, yet there is a good section on applications. There are only 179 pages of text, which includes 117 figures, many of which occupy a half page or more. The book contains a collection of terpene GC–FT-IR spectra. As these spectra are not available elsewhere this is a very useful addition to the small collection of GC–FT-IR spectra available to the public. As far as the printing is concerned, the number of grammatical errors is small and only one typographical error was found.

Athens, GA (U.S.A.) J. A. de HASETH

Journal of Chromatography, 410 (1987) 514
Elsevier Science Publishers B.V., Amsterdam — Printed in The Netherlands

CHROM. 19 997

Book Review

Methods in protein sequence analysis 1986, edited by Kenneth A. Walsh, Humana Press, Clifton, NJ, 1987, XXXV + 658 pp., price US$ 79.50, ISBN 0-89603-118-7.

The speed of development of new technologies for protein and DNA sequencing during the last 10–20 years has been amazing and, as these proceedings of the *Sixth International Conference on Methods in Protein Sequence Analysis* show, the impact of engineering on biochemistry has been profound. No longer does the biochemist work alone on research in the field of protein/DNA chemistry, but a whole industry of instrument makers is now involved. On page 11, one of the authors states, "While only the expert may be expected to fully understand these sophisticated instruments, their benefits to the sequence analyst have already been convincingly demonstrated...". Further, on page 39, another author is convinced that, "it is our belief that the development of new instrumentation and approaches for biological research will change science over the next 10 years as much as during the past decade". One could pose the question of where all this may end: the biochemist as a slave of technologies, who merely feeds in and takes out data from computers? On the other hand, the possibilities provided by the new technologies seem limitless. The total characterization of the human genome is now within reach. Other challenging problems such as the prediction of the three-dimensional structures of proteins from their amino acid sequence, the molecular mechanism of development and structure–activity relationships will be easier to solve with the rapid accumulation of data provided by the new technologies.

One of the highlights of the meeting was the growing awareness of the role of mass spectrometry in protein structure determination. Through the development of ionization techniques such as fast atom bombardment (FAB) and plasma desorption (PD), the structure determination of proteins of up to 14 500 daltons (with FAB) and of up to 25 000 daltons (with PD) have become possible.

Other papers concern the acquisition of sequence information from small amounts of protein, so as to construct corresponding oligonucleotides that can be sequenced and manipulated. Higher protein yields are therefore necessary. One advance in this direction is the electroblotting methods (direct transfer of proteins from chromatographic/electrophoretic layers or columns to modified glass-fibre papers for sequence analysis in gas-phase sequenators).

Another interesting item is the optimization of peptide synthesis; peptides of up to 140 residues can nowadays be synthesized within 12 days! The impact of the rapid synthesis of peptides (side to side with recombinant DNA techniques) on structure–function analysis hardly needs further elaboration.

The book has been produced with an increasingly popular technique, namely by the direct printing of camera-ready manuscripts provided by the authors themselves. Happily, in contrast to some other books produced in this way, the quality of this publication is outstanding and shows clearly the high quality of the proof reading, both of the text and of the well printed and clearly presented figures.

Lausanne (Switzerland) ALFRED KUHN

Author Index

Erratum

J. Chromatogr., 389 (1987) 339–344
Page 340, 4th line of *HPLC analysis* and page 341, 2nd line of the legend to Fig. 1, "0.52 μM" should read "0.26 M".

Corrected
ch. 9.
28 Feb. 98

PUBLICATION SCHEDULE FOR 1987

Journal of Chromatography and Journal of Chromatography, Biomedical Applications

MONTH	J	F	M	A	M	J	J	A	S	O	N	D
Journal of Chromatography	384 385 386 387	388/1 388/2 389/1	389/2 390/1 390/2 391/1	391/2 392 393/1 393/2	393/3 394/1 394/2 394/3	395 396 397	398 399 400 402	403 404/1	404/2 405	406 407	408 409 410/1	410/2 411
Bibliography Section		412/1		412/2		412/3		412/4		412/5		412/6
Cumulative Indexes, Vols. 351–400												401
Biomedical Applications	413	414/1	414/2 415/1	415/2 416/1	416/2	417/1	417/2 418	419	420/1 420/2	421/1 421/2	422	423

INFORMATION FOR AUTHORS

(Detailed *Instructions to Authors* were published in Vol. 396, pp. 451–454. A free reprint can be obtained by application to the publisher, Elsevier Science Publishers B.V., P.O. Box 330, 1000 AH Amsterdam, The Netherlands.)

Types of Contributions. The following types of papers are published in the *Journal of Chromatography* and the section on *Biomedical Applications:* Regular research papers (Full-length papers), Notes, Review articles and Letters to the Editor. Notes are usually descriptions of short investigations and reflect the same quality of research as Full-length papers, but should preferably not exceed six printed pages. Letters to the Editor can comment on (parts of) previously published articles, or they can report minor technical improvements of previously published procedures; they should preferably not exceed two printed pages. For review articles, see inside front cover under Submission of Papers.

Submission. Every paper must be accompanied by a letter from the senior author, stating that he is submitting the paper for publication in the *Journal of Chromatography.* Please do not send a letter signed by the director of the institute or the professor unless he is one of the authors.

Manuscripts. Manuscripts should be typed in double spacing on consecutively numbered pages of uniform size. The manuscript should be preceded by a sheet of manuscript paper carrying the title of the paper and the name and full postal address of the person to whom the proofs are to be sent. Authors of papers in French or German are requested to supply an English translation of the title of the paper. As a rule, papers should be divided into sections, headed by a caption (*e.g.,* Summary, Introduction, Experimental, Results, Discussion, etc.). All illustrations, photographs, tables, etc., should be on separate sheets.

Introduction. Every paper must have a concise introduction mentioning what has been done before on the topic described, and stating clearly what is new in the paper now submitted.

Summary. Full-length papers and Review articles should have a summary of 50–100 words which clearly and briefly indicates what is new, different and significant. In the case of French or German articles an additional summary in English, headed by an English translation of the title, should also be provided. (Notes and Letters to the Editor are published without a summary.)

Illustrations. The figures should be submitted in a form suitable for reproduction, drawn in Indian ink on drawing or tracing paper. Each illustration should have a legend, all the *legends* being typed (with double spacing) together on a *separate sheet.* If structures are given in the text, the original drawings should be supplied. Coloured illustrations are reproduced at the author's expense, the cost being determined by the number of pages and by the number of colours needed. The written permission of the author and publisher must be obtained for the use of any figure already published. Its source must be indicated in the legend.

References. References should be numbered in the order in which they are cited in the text, and listed in numerical sequence on a separate sheet at the end of the article. Please check a recent issue for the layout of the reference list. Abbreviations for the titles of journals should follow the system used by *Chemical Abstracts.* Articles not yet published should be given as "in press" (journal should be specified), "submitted for publication" (journal should be specified), "in preparation" or "personal communication".

Dispatch. Before sending the manuscript to the Editor please check that the envelope contains three copies of the paper complete with references, legends and figures. One of the sets of figures must be the originals suitable for direct reproduction. Please also ensure that permission to publish has been obtained from your institute.

Proofs. One set of proofs will be sent to the author to be carefully checked for printer's errors. Corrections must be restricted to instances in which the proof is at variance with the manuscript. "Extra corrections" will be inserted at the author's expense.

Reprints. Fifty reprints of Full-length papers, Notes and Letters to the Editor will be supplied free of charge. Additional reprints can be ordered by the authors. An order form containing price quotations will be sent to the authors together with the proofs of their article.

Advertisements. Advertisement rates are available from the publisher on request. The Editors of the journal accept no responsibility for the contents of the advertisements.

Collect LC peaks in separate tubes

You don't have to choose between diluted peaks or collecting too many small fractions. Isco's peak separator operates with your present UV or other LC detector and fraction collector to put separate peaks into separate test tubes.

Drifting baselines or incomplete resolution are no problem because peaks are identified by their shape, not height. Short HPLC peaks or long prep LC peaks are cut with equal accuracy. A delay timer compensates for the time lag as the peak passes from the flow cell to the fraction collector, and another timer postpones collection until the void volume has eluted. An optional valve lets you collect only peaks, diverting the effluent between peaks to waste or collecting it in a single container for recycling. So isn't it time to stop playing hide and seek with every LC peak?

Phone toll free **(800)228-4250** or write for a complete catalog.

Isco, Inc.,
P.O. Box 5347
Lincoln, Nebraska 68505, USA

ISCO